



## ANALYSIS REPORT

Pressurized Water Reactor Steam Generator Internal Loading Following a  
Main Steam or Feedwater Line Break

---

William J. Krotiuk

May 2004

---

Office of Nuclear Regulatory Research  
SAFETY MARGINS AND SYSTEM ANALYSIS BRANCH

---



Pressurized Water Reactor Steam Generator Internal Loading Following a  
Main Steam or Feedwater Line Break

William J. Krotiuk

May 2004

Office of Nuclear Regulatory Research  
SAFETY MARGINS AND SYSTEM ANALYSIS BRANCH



## TABLE OF CONTENTS

EXECUTIVE SUMMARY. . . . .	v
1.0 INTRODUCTION. . . . .	1
2.0 LITERATURE SEARCH. . . . .	3
<u>2.1 Steam Generator Internal Load Assessment Studies.</u> . . . .	3
<u>2.2 Acoustic Dominated Pressure Transient Tests, Calculations, and Modeling.</u> . . . .	5
2.2.1 Pipe Break Tests and Modeling. . . . .	5
2.2.2 PWR Water Hammer. . . . .	5
2.2.3 SRV Analyses and Tests. . . . .	6
2.2.4 RELAP5 Test Prediction Comparisons. . . . .	6
2.2.5 Wave Superposition and Method of Characteristics References. . . . .	7
2.2.6 Blowdown Tests and Calculations. . . . .	7
3.0 VERIFICATION OF THE TRAC-M COMPUTER CODE. . . . .	9
<u>3.1 Edwards Pipe Blowdown Experiment.</u> . . . .	9
3.1.1 References. . . . .	10
<u>3.2 LOFT Semiscale Blowdown Test.</u> . . . .	25
3.2.1 LOFT Semiscale Experiment Description. . . . .	25
3.2.2 TRAC-M Model of the LOFT Semiscale Blowdown Test. . . . .	26
3.2.3 Comparison of Test Data and Analytical Results. . . . .	26
3.2.4 Summary. . . . .	27
3.2.5 References. . . . .	28
4.0 STEAM GENERATOR ANALYSIS USING THE TRAC-M. . . . .	39
<u>4.1 Short-Term Steam Generator Analyses Using the TRAC-M.</u> . . . .	39
4.1.1 References. . . . .	51
<u>4.2 Long-Term Steam Generator Analysis Using the TRAC-M Code.</u> . . . .	74
5.0 CONSERVATIVE BOUNDING CALCULATION. . . . .	79
<u>5.1 Introduction.</u> . . . .	79
<u>5.2 Depressurization Phenomena.</u> . . . .	80
5.2.1 Blowdown Calculations for the Westinghouse Model 51 Steam Generator. . . . .	81
<u>5.3 References.</u> . . . .	87
APPENDIX A - TRAC-M Input Files. . . . .	93
<u>A.1 Input File for 4.6ft<sup>2</sup> MSLB with Steam Generator at Hot Standby.</u> . . . .	94
<u>A.2 Input File for FWLB with Steam Generator at 100-Percent Power.</u> . . . .	125
APPENDIX B - TRAC-M Assessment of GE Vessel Blowdown Tests. . . . .	155
APPENDIX C - TRAC-M Simulations of Westinghouse MB-2 Tests. . . . .	157



# PRESSURIZED WATER REACTOR STEAM GENERATOR INTERNAL LOADING FOLLOWING A MAIN STEAM OR FEEDWATER LINE BREAK

## EXECUTIVE SUMMARY

This document responds to Generic Safety Issue (GSI) 188, "Steam Generator Tube Leaks or Ruptures Concurrent with Containment Bypass from Main Steam Line or Feedwater Line Breaches". The objectives of this study are summarized in the following tasks:

- (1.) Perform thermal-hydraulic calculations and sensitivity studies using the three-dimensional (3-D) hydraulic components of TRAC-M to assess the loads on the tube support plates (TSPs) and steam generator tubes during a main steam line break (MSLB). Perform sensitivity studies on code and model parameters including numerics. Develop a conservative estimate of loads, and evaluate against similar analyses.
- (2.) Perform a thermal-hydraulic assessment of flow-induced vibrations during an MSLB. Using the thermal-hydraulic conditions calculated during the transient, generate a conservative estimate of flow-induced vibration displacement and frequency assuming steady state behavior.
- (3.) Perform additional sensitivity studies, as needed.

Specifically, this report provides the steam generator internal loadings following a main steam line break (MSLB) or a feedwater line break (FWLB), which can affect the structural integrity of the primary tubes. The loadings developed by this analysis will be used in a structural assessment of the primary tubes of the steam generator to determine the potential for a line breach which would increase tube leakage. The pressure loadings on the tube support plates (TSPs) in a Westinghouse Model 51 steam generator were calculated using the TRAC-M, recently renamed TRACE, computer code. The cases analyzed for this study include a guillotine MSLB near the steam generator nozzle, a flow restrictor-limited MSLB near the steam generator nozzle, and a guillotine FWLB near the steam generator nozzle. The loads calculated using the TRAC-M code are compared to similar calculations contained in the August 1996 Westinghouse report WCAP-14707, **Model 51 Steam Generator Limited Tube Support Plate Displacement Analysis for Dented or Packed Tube to Tube Support Plate Crevices**. Additionally, the TRAC-M results are compared to the results of a manual hand calculation performed using the Moody choked-flow method combined with calculations to follow the transport of the depressurization wave originating at the break location. The TRAC-M computer code is also verified against the results of the Edwards Pipe Blowdown Experiment and the Loss-of-Fluid (LOFT) Semiscale Blowdown Test, which follow the transmission of a depressurization wave resulting from a pipe rupture in a tank that initially contained subcooled water. TRAC-M calculations are also compared to measurements from General Electric Vessel Blowdown Tests which address pool swell phenomena following a pipe break, and Westinghouse Model Steam Generator Model Boiler (MB-2) Tests which directly address steam generator phenomena following a pipe break.

The current TRAC-M analysis, the Westinghouse analysis, and the Moody/acoustic manual hand calculation all conclude that a guillotine rupture of the steam line at hot standby conditions produces the largest loadings on the TSPs. The peak loadings on the upper TSPs, calculated using TRAC-M, are close in value to those calculated using the Moody/acoustic method. The

TRAC-M results are also close to the results of the TRANFLO and RELAP5 analyses presented in the Westinghouse report.

This report also presents the calculated loadings on the primary tubes at the bottom of the steam generator and at the primary tube bend location following a pipe break. Pressure differentials are also presented for the cylindrical shroud, which separates the primary boiling flow region around the primary tubes from the surrounding annular area through which feedwater flows. These additional loads can affect the integrity of the primary tubes either directly or indirectly. The primary tube forces are a direct contributor. The TSPs are supported by the cylindrical shroud; therefore, loads on the shroud may be transmitted to the primary tubes.

The TRAC-M analysis indicates that the loadings from an FWLB are substantially lower than those resulting from an MSLB. Therefore, an FWLB does not present a design case loading.

In addition to the verification provided by the comparison of the TRAC-M calculation with the Moody/acoustic manual hand calculation, the TRAC-M computer code has been used to analyze the Edwards Pipe Blowdown Experiment and the LOFT Semiscale Blowdown Test. Results from the TRAC-M analysis of these two tests agree well with experimental measurements. The modeling for these experiments provides guidance regarding the node size and analytical solution scheme used to perform the TRAC-M steam generator analysis.

The assessment of the steam generator analyses using the TRAC-M computer code and the manual hand calculation using the Moody/acoustic method revealed that the primary loads are developed by the short-term thermal-hydraulic and acoustic effects occurring in the first few seconds following the break. This study indicated that flow-induced vibration loading, developed as the result of quasi-steady flow present after the completion of the short-term effects, produced smaller loads than the short-term loads. Consequently, a comprehensive long-term analysis was not performed, and will only be considered if the short-term structural analysis indicates the need to develop long-term loadings on the steam generator internals.

The following tables summarize the results of the TRAC-M analysis of the Westinghouse Model 51 steam generator following a guillotine or flow restrictor-limited MSLB and a guillotine FWLB. It is recommended that a 1.2 multiplier be applied to the results calculated by the TRAC-M model to account for the lack of a two-phase pressure drop multiplier for the irreversible form loss calculation in the current version of TRAC-M. (The two-phase form loss pressure drop multiplier is scheduled to be added to the TRAC-M code in the future.) The loadings calculated by the TRAC-M code will be used in a structural assessment of the primary tubes in order to determine whether the calculated TSP loadings are acceptable.



**Table 1: TSP Peak Pressure Differentials<sup>a</sup> Using TRAC-M**

	<u>Initial Hot Standby Conditions</u>		
	<b>Guillotine 4.6 ft<sup>2</sup> MSLB</b>	<b>Flow Restrictor-Limited 1.4 ft<sup>2</sup> MSLB</b>	<b>Guillotine 1.12 ft<sup>2</sup> FWLB</b>
TSP 7 (top)	8.57 psi	2.68 psi	0.050 psi
TSP 6	5.06 psi	1.70 psi	0.041 psi
TSP 5	3.84 psi	1.23 psi	0.034 psi
TSP 4	2.63 psi	0.87 psi	0.030 psi
TSP 3	1.16 psi	0.43 psi	0.026 psi
TSP 2	0.15 psi	0.08 psi	0.022 psi
TSP 1 (bottom)	-0.33 psi	-0.057 psi	0.021 psi

	<u>Initial 100-Percent Power Condition</u>		
	<b>Guillotine 4.6 ft<sup>2</sup> MSLB</b>	<b>Flow Restrictor-Limited 1.4 ft<sup>2</sup> MSLB</b>	<b>Guillotine 1.12 ft<sup>2</sup> FWLB</b>
TSP 7 (top)	6.82 psi	1.49 psi	0.42 psi
TSP 6	5.41 psi	1.27 psi	0.36 psi
TSP 5	4.34 psi	1.09 psi	0.31 psi
TSP 4	3.20 psi	0.87 psi	0.27 psi
TSP 3	1.91 psi	0.61 psi	0.23 psi
TSP 2	0.79 psi	0.33 psi	0.19 psi
TSP 1 (bottom)	0.16 psi	0.21 psi	0.20 psi

<sup>a</sup> An upward-directed pressure differential is defined as positive.

**Table 2: Primary Tubing Peak Pressure Differentials Using TRAC-M**

	<u>Initial Hot Standby Conditions</u>		
	<b>Guillotine 4.6 ft<sup>2</sup> MSLB</b>	<b>Flow Restrictor-Limited 1.4 ft<sup>2</sup> MSLB</b>	<b>Guillotine 1.12 ft<sup>2</sup> FWLB</b>
At SG Bottom <sup>1</sup>	-0.28 psi	-0.07 psi	-0.004 psi
At Primary Tube Bend <sup>2</sup>	1.05 psi	0.33 psi	0.029 psi

	<u>Initial 100-Percent Power Condition</u>		
	<b>Guillotine 4.6 ft<sup>2</sup> MSLB</b>	<b>Flow Restrictor-Limited 1.4 ft<sup>2</sup> MSLB</b>	<b>Guillotine 1.12 ft<sup>2</sup> FWLB</b>
At SG Bottom <sup>a</sup>	-0.13 psi	0.037 psi	0.058 psi
At Primary Tube Bend <sup>b</sup>	0.71 psi	0.13 psi	0.043 psi

<sup>a</sup> A horizontal, radially directed inward force is defined as positive.

<sup>b</sup> An upward force is defined as positive.

**Table 3: Peak Pressure Differentials<sup>a</sup> Across the Cylindrical Shroud Using TRAC-M**

	<u>Initial Hot Standby Conditions</u>		
	<u>Guillotine</u>	<u>Flow Restrictor-Limited</u>	<u>Guillotine</u>
	<u>4.6 ft<sup>2</sup> MSLB</u>	<u>1.4 ft<sup>2</sup> MSLB</u>	<u>1.12 ft<sup>2</sup> FWLB</u>
	Min. / Max.	Min. / Max.	Maximum
Above TSP 7 (top)	-1.42 / 50.5 psi	-0.78 / 13.8 psi	1.88 psi
Between TSP 6 & TSP 7	-0.60 / 50.0 psi	-0.69 / 13.3 psi	1.56 psi
Between TSP 5 & TSP 6	-0.48 / 45.4 psi	-0.81 / 12.8 psi	1.34 psi
Between TSP 4 & TSP 5	-0.47 / 39.4 psi	-0.84 / 11.7 psi	1.17 psi
Between TSP 3 & TSP 4	-0.37 / 33.4 psi	-0.90 / 10.0 psi	0.97 psi
Between TSP 2 & TSP 3	-0.28 / 27.1 psi	-0.79 / 7.89 psi	0.73 psi
Between TSP 1 & TSP 2	-0.20 / 20.0 psi	-0.31 / 5.44 psi	0.45 psi
Below TSP 1 (bottom)	-0.16 / 15.2 psi	-0.18 / 3.61 psi	0.22 psi

	<u>Initial 100-Percent Power Condition</u>		
	<u>Guillotine</u>	<u>Flow Restrictor-Limited</u>	<u>Guillotine</u>
	<u>4.6 ft<sup>2</sup> MSLB</u>	<u>1.4 ft<sup>2</sup> MSLB</u>	<u>1.12 ft<sup>2</sup> FWLB</u>
	Min. / Max.	Min. / Max.	Min. / Max.
Above TSP 7 (top)	-2.40 / 38.5 psi	-0.38 / 7.24 psi	-3.41 / 2.05 psi
Between TSP6 & TSP7	-2.83 / 38.1 psi	8.76 psi	-1.65 / 4.29 psi
Between TSP5 & TSP6	-3.07 / 35.5 psi	8.17 psi	-1.91 / 3.78 psi
Between TSP4 & TSP5	-2.91 / 31.8 psi	7.30 psi	-1.93 / 2.99 psi
Between TSP3 & TSP4	-2.59 / 26.9 psi	6.18 psi	-1.77 / 2.22 psi
Between TSP2 & TSP3	-1.90 / 21.1 psi	4.94 psi	-1.58 / 1.75 psi
Between TSP1 & TSP2	-1.09 / 14.0 psi	3.54 psi	-1.01 / 1.43 psi
Below TSP1 (bottom)	-0.51 / 6.67 psi	2.14 psi	1.39 psi

<sup>a</sup> Note, pressure radially out is defined positive.

## 1.0 INTRODUCTION

This document responds to Generic Safety Issue (GSI) 188, “Steam Generator Tube Leaks or Ruptures Concurrent with Containment Bypass from Main Steam Line or Feedwater Line Breaches”. Specifically, the objectives of this study are summarized in the following tasks:

- (1.) Perform thermal-hydraulic calculations and sensitivity studies using the three-dimensional (3-D) hydraulic components of TRAC-M to assess the loads on the tube support plates (TSPs) and steam generator tubes during a main steam line break (MSLB). Perform sensitivity studies on code and model parameters including numerics. Develop a conservative estimate of loads, and evaluate against similar analyses.
- (2.) Perform a thermal-hydraulic assessment of flow-induced vibrations during an MSLB. Using the thermal-hydraulic conditions calculated during the transient, generate a conservative estimate of flow-induced vibration displacement and frequency assuming steady state behavior.
- (3.) Perform additional sensitivity studies, as needed.

The purpose of this study is to determine the hydraulic loadings on the internal components of a steam generator in a pressurized water reactor (PWR) following an MSLB or FWLB.

Assessments were made for MSLBs with 100-percent of the steam line break flow area and with the break area limited by the flow restrictor, as well as an FWLB with 100-percent of the feedwater line flow area. This study was divided into a number of activities, as follows:

- (1.) A literature search was performed to determine whether similar analyses have previously been conducted and to identify any previously developed conservative, simplified methods for determining loadings on the steam generator internals for the assumed breaks. (See Section 2.0 of this report for additional details.)
- (2.) The ability of the TRAC-M computer code’s ability to analyze the steam generator blowdown was verified against test data, but additional verification of TRAC-M is proceeding. The TRAC-M computer code has been and will continue to be used to analyze previously performed experiments, which address the phenomena present in the steam generator following a line break. Specifically, the Edwards Pipe Blowdown Experiment and the Loss-of-Fluid Test (LOFT) Semiscale Blowdown Test were modeled to assess the ability of the code to analyze a subcooled blowdown, and to follow the travel and behavior of a depressurization wave in a vessel. This report presents comparisons between the TRAC-M predictions and the Edwards Blowdown Test results. This report also presents the TRAC-M analysis of the Semiscale Blowdown Test, and comparisons between TRAC-M predictions for that test and predictions from the WHAMMOCH method-of-characteristics (MOC) computer code. The TRAC-M code has also been used to model the Westinghouse Steam Generator Model Boiler (MB-2) Tests and the General Electric (GE) Vessel Blowdown Tests. These test predictions will verify the ability of the code to model other phenomena such as flashing, interfacial drag, flow regime determination and void fraction distribution.
- (3.) The TRAC-M computer code was used to analyze a steam generator following MSLBs and FWLBs. For this task a short-term, one-dimensional TRAC-M model of the Westinghouse Model 51 steam generator was developed to calculate the loads on the

internal steam generator components following a flow restrictor-limited and 100-percent guillotine MSLB, and a 100-percent guillotine FWLB. A postprocessor methodology was developed to convert thermal-hydraulic conditions to component loads. After the structural integrity analysis of the steam generator primary tubing is completed using the short-term model results, an assessment will be conducted to assess the need to develop a long-term model to provide temperature gradients and oscillatory pressure loads on the steam generator internals. If required, a more detailed 3-D model of the steam generator will be developed and analyzed using the TRAC-M code at a future time.

- (4.) The critical steam generator internals that would be subjected to pressure loading following a line break have been identified and conservative, bounding manual hand calculations have been performed for a Westinghouse Model 51 steam generator design to determine the magnitude of these loads. These calculations also provided an independent verification of the analyses performed using the TRAC-M computer code.
- (5.) This report provides a methodology to calculate the steam generator internal component loadings for other Westinghouse steam generator designs, as well as steam generator designs from Combustion Engineering and Babcock & Wilcox. This study reveals that analysis performed using the TRAC-M code, or the manual hand calculation method using the Moody/acoustic approach outlined in this report can be used to calculate loadings on steam generator internals.

## 2.0 LITERATURE SEARCH

The literature search involving the determination of internal steam generator loads following an MSLB or FWLB was divided into completed studies involving the same or similar occurrences, and the identification of calculational methods and tests that address the phenomena involved in determining steam generator loads. Sections 2.1 and 2.2 list the relevant documents referenced for this study, as they relate to previously completed studies, and calculational methods and tests, respectively,

### 2.1 Steam Generator Internal Load Assessment Studies

The following references describe studies performed to determine steam generator loadings.

(1) **“Structural Analysis of Steam Generator Internals Following Feedwater/Main Steam Line Break: DFL Approach,”** Bhasin, V., et al., Bhabha Atomic Research Center, Bombay, India, BARC/1993/E/026, 1993. This report provides complete information regarding the effects of an MSLB or FWLB on steam generator internals, which are the primary focus of the current study. Specifically, this report describes a stress analysis of a steam generator in a Canadian Deuterium Uranium (CANDU) reactor, which is very similar in design to a steam generator in a Westinghouse PWR, following a 100-percent FWLB at 100-percent power and a 100-percent MSLB at hot standby conditions (0-percent power). In particular, the report assesses the loadings on the steam generator shroud, steam generator components, feedwater header, plate drier assemblies, flow distribution plate, and primary system tubes. The thermal-hydraulic calculations are described in a separate report, which the staff of the U. S. Nuclear Regulatory Commission (NRC) has not been able to locate. This reference lists the maximum calculated axial forces on the primary system tubing as being 0.63 kgf per tube for an FWLB and 9.96 kgf per tube for an MSLB. This translates to maximum calculated stresses on three typical tubes of 9.3 kgf/sq. cm for the FWLB and 134 kgf/sq. cm for the MSLB, which are much smaller than the allowable limit of 5298.3 kgf/sq. cm.

(2) **“Evaluation of Steam Generator Tube, Tube Sheet and Divider Plate Under Combined Load LOCA Plus SSE Conditions,”** De Rosa, P., et al., Westinghouse Electric Corp., WCAP-7832-A, April 1978. This report deals primarily with the results of a primary system Loss-of-Coolant (LOCA) on the steam generator.

(3) **“Considerations for Structural Analysis and Evaluation of Nuclear Steam Generator Internals,”** Kumar, R., and N. Idvorian, (Atomic Energy of Canada, B&W Canada), *International Journal of Pressure Vessels and Piping*, Vol. 78, p. 359–364, 2001. This paper addresses the concerns of this study and outlines an analytical approach. However, it does not provide analytical results.

(4) **“Transient Simulation of PWR Secondary Systems,”** Baschiere, R., and B. Strong, *Fluid Transients and Acoustics in the Power Industry*, Winter Annual Meeting of the American Society of Mechanical Engineers (ASME), December 1978.

(5) **“Experimental Study of the Coupled Hydrodynamic-Structure Transient Response to Rarefaction Wave Propagation,”** Squarer, D., and D. Green, *Fluid Transients and Acoustics in the Power Industry*, American Society of Mechanical Engineers Winter Annual Meeting, December 1978. This paper describes a Westinghouse program to obtain test data

from an experiment modeling the response of steam generator internals to a blowdown. The intent was to provide data that could be used for computer code verification. A 1:10 scale model of the preheater section of a steam generator was subjected to a simulated FWLB to obtain pressure differentials across simulated support, baffle, and divider plates. Unfortunately, the facility description and test results provided in the paper are not sufficiently detailed for use in computer code verification.

(6) **“Loss of Feed Flow, Steam Generator Tube Rupture and Steam Line Break Thermohydraulic Experiments,”** Westinghouse Electric Corp., NUREG/CR-4751, WCAP-11206, October 1986. The results from these experiments will be used to verify TRAC-M code predictions. A discussion of the verification study is presented in Section 3.0 of this report.

(7) **“Steam Generator Tube Failure,”** MacDonald, P. E., et al., Idaho National Engineering Laboratory, NUREG/CR-6365, April 1996. This report primarily discusses steam generator tube ruptures in PWRs, CANDU reactor systems, and VVER steam generators. The report also presents the results of analyses of the steam generator following a steam line break concurrent with one and fifteen tube failures.

(8) **“Model 51 Steam Generator Limited Tube Support Plate Displacement Analysis for Dented or Packed Tube to Tube Support Plate Crevices,”** Westinghouse, WCAP-14707, August 1996. This report describes an analysis of the Model 51 steam generator to provide support plate loadings attributable to a guillotine steam line break with and without the presence of the flow restrictor, and a structural analysis of the TSP. The thermal-hydraulic analysis was performed using the RELAP5 Mod3.2 and TRANFLO computer codes. Both the RELAP5 and TRANFLO computer codes employ a control volume approach to determine the thermal-hydraulic conditions in a flow transient. Loadings for conditions resulting from an MSLB at hot standby conditions were shown to be more limiting than for full-power conditions. Loadings calculated using RELAP5 are higher than those calculated using TRANFLO. In additions, this report presents an assessment of the potential for a tube crack to rupture.

(9) **“Model 51 Steam Generator Limited Tube Support Plate Displacement Analysis for Dented or Packed Tube to Tube Support Plate Crevices,”** Westinghouse, WCAP-14707, Revision 1, April 1997. This report updates the structural analysis presented in Revision 0 including additional analyses to assess the temperature effects on tube support plate loads.

(10) **“Technical Support for Implementing High-Voltage Alternate Repair Criteria at Hot Leg Limited Displacement TSP Inspections for South Texas Plant Unit 2, Model E Steam Generator,”** Westinghouse, WCAP-15163, Revision 1, March 1999. This report describes the results of RELAP5 thermal-hydraulic analyses of the steam generator to obtain TSP loadings, a structural analysis of the TSP and tubing, and an assessment of tube burst probability.

(11) **“South Texas Unit 2; 3V Alternate Repair Criteria Application of Bounding Analysis and Tube Expansion,”** Westinghouse, WCAP-15163 Addendum, Revision 1, January 2001. This report presents bounding thermal-hydraulic analyses to validate the use of the RELAP5 code for the determination of TSP loadings.

(12) **“A Determination of the 2-Dimensional Pressure Distribution on the Byron/Braidwood D4 SG Tube Support Plate During a MSLB,”** Commonwealth Edison,

PSA-B-97-07, March 1997. This report provides the results of a MATHCAD bounding calculation to determine the pressure differential across the upper TSP.

(13) **“Independent Verification of Byron/Braidwood D4 SG Tube Support Plate Differential Pressure During MSLB,”** Commonwealth Edison, PSA-B-95-15, September 1995. This report provides bounding calculations to estimate the upper tube support plate pressure differential following an MSLB and verify the results of more detailed analyses performed using the control volume-based TRANFLO and MOC-based MULTIFLEX computer codes.

(14) **“Calculation of Byron 1/Braidwood 1 D4 Steam Generator Tube Support Plate Loads with RELAP5M3,”** Commonwealth Edison, PSA-B-95-17, October 1995. This report documents the development of the tube support plate loads resulting from an MSLB in a steam generator at hot standby conditions using the RELAP5 computer code.

## **2.2 Acoustic Dominated Pressure Transient Tests, Calculations, and Modeling**

These references discuss phenomena which are important in the determination of internal loadings in a PWR steam generator.

### **2.2.1 Pipe Break Tests and Modeling**

(1) **“Hydrodynamics Describing Acoustic Phenomena During Reactor Coolant System Blowdown,”** Rose, R., et al., U. S. Atomic Energy Commission (AEC), IDO-17254, July 1967. This paper presents information on the LOFT Semiscale Blowdown Test, which was used to verify the TRAC-M computer code. The TRAC-M verification results are presented in Section 3.2 of this report.

### **2.2.2 PWR Water Hammer**

(1) **“An Investigation of Pressure Transient Propagation in Pressurized Water Reactor Feedwater Lines,”** Sutton, S., Lawrence Livermore National Laboratory, UCRL-52265, July 1977. This report describes a water hammer caused by the sudden collapse of a steam bubble in the feedwater feed ring in a steam generator following the injection of “cold” water through the feedwater line. Analyses of the water hammer phenomena in the feedwater line were analyzed using the WHAM and PTA computer codes. (WHAM uses the wave superposition method, whereas PTA employs the method of characteristics.) Transient line forces were also calculated using the fluid-thermal results obtained from WHAM and PTA. Both codes provide theoretical results to within 0.1-percent of the theoretical answer.

(2) **“An Evaluation of PWR Steam Generator Water Hammer - Final Technical Report,”** Block, J., et al., U. S. Nuclear Regulatory Commission (NRC), NUREG-0291, June 1977. This report discusses the causes and phenomena resulting from a water hammer attributable to the collapse of a vapor bubble in the feedwater line.

(3) **“Evaluation of Water Hammer Events in Light Water Reactor Plants,”** Uffer, R., et al., U. S. Nuclear Regulatory Commission, NUREG/CR-2781, July 1982. This document summarizes the experiences regarding hammer occurrences in boiling water reactors (BWRs) and PWRs for all but water hammer conditions originating in the steam generator. This reference is helpful for understanding the hammer phenomena in nuclear power systems.

### 2.2.3 SRV Analyses and Tests

The following references discuss analytical methods and test results for calculating conditions in a piping system downstream of an opening relief valve. This phenomenon is an acoustically dominated transient, which is similar to the phenomena that occur during a pipe break.

(1) **“Application of RELAP5/MOD1 for Calculation of Safety and Relief Valve Discharge Piping Hydrodynamic Loads,”** Intermountain Technologies, EPRI, NP-2479, 1982. This report documents test setups and results. This data will be used to verify the TRAC-M computer code, as documented in Section 3.0 of this report.

(2) **“Assessment of Analysis Methods for PWR Safety/Relief Valve Discharge Piping,”** Strong, B., and L. Metcalfe, Electric Power Research Institute, NP-80-9-LD, December 1980. This report compares analytical techniques for predicting the thermal-hydraulic response in SRV piping. The report recommends using finite difference codes, such as RELAP, to analyze the transient. It should be noted that no MOC codes with flashing capabilities were available at the time of the assessment.

(3) **“Steam Hammer Design Loads for Safety/Relief Valve Discharge Piping,”** Strong, B. and R. Baschiere, *Safety Relief Valves*, American Society of Mechanical Engineers, PVP-33, 1979. This paper discusses the use of RELAP to calculate forces in SRV downstream piping. The paper presents calculated piping force transients, but does not provide thermodynamic or flow conditions. Consequently, the information is only useful in providing methods to calculate forces attributable to a thermal-hydraulic transient.

(4) **“Measurement of Piping Forces in a Safety Relief Valve Discharge Line,”** Wheeler, A. and E. Siegel, American Society of Mechanical Engineers, Paper 82-WA/NE-8, 1982. This paper presents results of SRV testing performed as part of the EPRI SRV Test Program. This data will be used for TRAC-M verification is indicated in Section 3.0 of this report.

(5) **“Calculation of Safety Relief Valve Discharge Piping Hydrodynamic Loads Using RELAP5/MOD1,”** House, R., et al., American Society of Mechanical Engineers, Paper 83-NE-18, 1983. This paper compares RELAP5 predictions to test results from the EPRI SRV Test Program. The data is more fully described in Reference 1 of this section.

### 2.2.4 RELAP5 Test Prediction Comparisons

These references were obtained to provide information for comparing the TRAC-M calculated results against test data.

(1) **“The Application of RELAP5 to a Pipe Blowdown Experiment,”** Carlson, K., V. Ransom, and R. Wagner, American Society of Mechanical Engineers Nuclear Reactor Thermal-Hydraulic 1980 Topical Meeting, Conf. 801002-2, 1980. This paper compares RELAP5 predictions with the results from the Edwards Blowdown Experiment. The TRAC-M code predictions are compared with the Edwards test results in Section 3.1 of this report.

(2) **“Verification of RELAP5 Capabilities to Simulate Pressure Wave Propagation for Instantaneous Pipe Breaks,”** Wendel, M. and P. Williams, *American Nuclear Society Annual Meeting Proceedings*, Conf. 940602-5, June 1994. This paper addresses specific



concerns applicable to the steam generator study, but does not supply a sufficient description of the test setup for TRAC-M verification.

### 2.2.5 Wave Superposition and Method of Characteristics References

The references in this section describe methods for calculating acoustic transients, such as those attributable to a depressurization wave. The references also provide bases for test comparisons with the TRAC-M code.

(1) **“Computer Program WHAM for Calculation of Pressure, Velocity, and Force Transients in Liquid-Filled Piping Networks,”** Fabric, S., Kaiser Engineers, Report 67-49-R, November 1967. This report describes the WHAM computer code which solves acoustically dominated transients for liquid filled piping systems using the wave superposition method.

(2) ***Hydraulic Transients***, Streeter, V. and E. Wylie, McGraw-Hill, New York, 1967. This classic reference book describes the MOC approach for the solution of a water hammer.

(3) **“HAMOC: A Computer Program for Fluid Water Hammer,”** Johnson, H., Westinghouse Hanford, HEDL-TME 75-119, December 1975. This report describes the HAMOC computer code, which uses the MOC approach to solve acoustic transients in liquid-filled piping systems. The code includes the ability to calculate column separation effects, but cannot accommodate two-phase flow conditions.

(4) **“WHAMMOCII – A Computer Code for Performing One- or Two-Phase Water Hammer Analysis,”** Krotiuk, W., *Fluid Transients and Fluid-Structure Interaction*, American Society of Mechanical Engineers Pressure Vessel and Piping Conference, PVP-Vol. 64, 1982. The WHAMMOCII computer code is a MOC code that can follow acoustic transients in piping systems with one- or two-phase conditions. This MOC code can calculate transient conditions in a subcooled water system, which is subjected to a rapid depressurization blowdown transient. Results from this MOC code are compared to TRAC-M predictions in Section 3.2 of this report.

(5) **“A Method for Computing Transient Pressures and Forces in Safety Relief Valve Discharge Lines,”** Wheeler, A. and F. Moody, F., ***Safety Relief Valves***, American Society of Mechanical Engineers Third National Congress on Pressure Vessels and Piping, PVP-33, 1979. This paper describes a MOC approach for calculating conditions in a line downstream of an opening SRV. The paper also presents compressible manual hand calculation methods, which are compared to the MOC results. Modification of the manual hand calculation results should provide insight regarding methods to calculate depressurization conditions in a piping system.

(6) **“A Method to Determine Forces Developed During a Time Dependent Opening of a Relief Valve Discharging a Two-Phase Mixture,”** Hsiao, W., P. Valandani, and F. Moody, American Society of Mechanical Engineers Paper 81-WA/NE-15, 1981. This paper provides the results of a MOC analysis of the piping downstream of an SRV discharge.

### 2.2.6 Blowdown Tests and Calculations

(1) **“Prediction of Blowdown Thrust and Jet Forces,”** Moody, F., American Society of Mechanical Engineers Paper 69-HT-31, 1969. This paper presents a manual hand method for

calculating the forces attributable to saturated steam and water blowdown jets. The paper does not present methods for calculating conditions upstream of the break location.

(2) **"Time-Dependent Pipe Forces Caused by Blowdown and Flow Stoppage,"** Moody, F., American Society of Mechanical Engineers Paper 73-FE-23, 1973. This paper presents methods for calculating transient conditions in a pipe upstream of a depressurization caused by a rapid blowdown.

(3) **"Maximum Flow Rate of a Single Component, Two-Phase Mixture,"** Moody, F. J., *Journal of Heat Transfer*, Vol. 86, American Society of Mechanical Engineers, February 1965.

(4) **"Maximum Two-Phase Blowdown from Pipes,"** Moody, F. J., *Journal of Heat Transfer*, Vol. 87, American Society of Mechanical Engineers, August 1966.

(5) **"A Pressure Pulse Model for Two-Phase Critical Flow and Sonic Velocity,"** Moody, F. J. *Journal of Heat Transfer*, Vol. 91, American Society of Mechanical Engineers, August 1969.

(6) ***The Thermal-Hydraulics of a Boiling Water Nuclear Reactor***, Lahey, R. T. and F. J. Moody, Chapter 9, American Nuclear Society, 1993.

References 3, 4, 5, and 6 (above) provide methods for performing manual hand calculations to determine critical flow and break discharge pressure for flow exiting a two-phase tank at a pipe rupture.

### 3.0 VERIFICATION OF THE TRAC-M COMPUTER CODE

TRAC-M, recently renamed TRACE, is an advanced, best-estimate, thermal-hydraulic computer code being developed at the NRC. TRAC-M can perform steady-state and transient analyses of nuclear power plant systems. Consequently, TRAC-M is proposed for use in analyzing the PWR steam generator to calculate conditions following an MSLB or FWLB.

TRAC-M incorporates four-component (liquid water, liquid solute, water vapor, and noncondensable gas), nonequilibrium two-fluid (liquid-gas) modeling of thermal-hydraulic processes. The partial differential equations that describe the fluid flow conservation equations and heat transfer processes are solved by finite-difference techniques. Two semi-implicit numerical solution schemes are available in TRAC-M. The timestep used with the one step semi-implicit scheme is limited by the Courant stability criteria. This method is appropriate for use in solving problems in which it is important to track pressure wave propagation is important, such as for steam generator conditions immediately following a pipe break. The two-step, semi-implicit method relaxes the restriction on timestep size and is appropriate for solving long-term or other problems where the effects of pressure wave propagation is negligible, such as steam generator conditions present several seconds after the occurrence of a pipe break.

In order to verify the acceptability of TRAC-M calculations, it is desirable to compare TRAC-M predictions with experimental measurements, especially from tests of systems experiencing rapid depressurization. Specifically, this study proposes to compare TRAC-M predictions with results from the following experiments:

- Edwards Pipe Blowdown Experiment (see Section 3.1)
- LOFT Semiscale Blowdown Test (see Section 3.2)
- GE Vessel Blowdown Test (see Appendix B)
- Westinghouse Steam Generator Model Boiler (MB-2) Test (see Appendix C)

The following subsections present TRAC-M comparisons with the Edwards Pipe Blowdown Experiment and the LOFT Semiscale Blowdown Test, respectively. These results include TRAC-M predictions using the one-step and two-step semi-implicit solution schemes. TRAC-M comparisons with the GE Vessel Blowdown Test and the Westinghouse Steam Generator Model Boiler (MB-2) Test are presented in Appendices B and C.

#### **3.1 Edwards Pipe Blowdown Experiment**

This experiment studied depressurization in a horizontal pipe initially filled with subcooled water. The depressurization resulted from the rupture of a glass disk located at one end of the pipe. The other end of the pipe was permanently sealed. Table 3.1-1 describes the characteristics of the test facility.

**Table 3.1-1: Test Facility Characteristics for the Edwards Pipe Blowdown Experiment**

Pipe Length	4.096 m
Pipe ID	0.073152 m
Glass Rupture Disk Flow Area	$3.6566 \times 10^{-3} \text{ m}^2$ (best estimate)
Glass Rupture Disk Thickness	0.0127 m
Initial System Pressure	$7.0995 \times 10^6 \text{ Pa}$
Initial System Temperature	$\sim 505^\circ\text{K}$

Pressure measurements were taken at seven points along the pipe length. One temperature and one void fraction measurement were taken near the pipe center. Table 3.1-2 identifies the measurement locations.

**Table 3.1-2: Edwards Blowdown Test Measurement Locations**

<b>Measurement</b>	<b>Distance from Closed End</b>
Closed End	0.0 m
GS-7 Pressure (nearest closed end)	0.079 m
GS-6 Pressure	0.914 m
GS-5 Pressure, Temperature, and Void Fraction	1.469 m
GS-4 Pressure	2.024 m
GS-3 Pressure	2.935 m
GS-2 Pressure	3.770 m
GS-1 Pressure (nearest break)	3.928 m
Break Location	4.096 m

Version 3782 of the TRAC-M code was used to analyze the Edwards Experiment. Two TRAC-M models of the experiment were constructed. In one model, the pipe was divided into 37 nodes of 0.1107-m each. A more detailed model of 161 nodes of 0.02544-m was also constructed. Additionally, two numerical solution schemes were employed. One used a one-step semi-implicit solution scheme (nosets=1); the other used a methodology which permitted the solution to exceed the Courant limit at certain times during the calculation (nosets=0). Figures 3.1-1 through 3.1-9 show the results of these calculations. The calculated results for the two different node sizes and two different numerical solution techniques provide slightly different results, at a given time, for each measured parameter. All calculated results follow the trends of the measured data; however, the results for the smaller node size (0.02544-m) using the solution scheme with nosets=0 produced results closest to the actual measurements.

It appears that models developed with smaller node sizes produce the best predictions. However, the diameter of the pipe used in the Edwards Blowdown Experiment is much smaller than a typical steam generator or its attached lines. Consequently, a relationship between the best node size and the line diameter must be developed to provide a guideline for optimal node size for a TRAC-M model of a steam generator. In order to make this assessment, a third model of the Edwards Experiment with 74 nodes and a node size of 0.05535-m was executed. Figures 3.1-10 through 3.1-14 compare the calculated pressures, temperatures, and void fractions at GS-5 for this model with predictions from the more detailed model. These graphs indicate no noticeable difference in the results of these two models. Consequently, a node size of 0.05535-m, which is comparative to the pipe diameter of 0.073152-m, provides acceptable predictions of test results. This comparison suggests that the node size for a TRAC-M model must be equal to or smaller than the pipe diameter in order to be able to predict an acoustic transient, such as the travel of a depressurization wave.

### 3.1.1 References

- (1) "Studies of Phenomena Connected with the Depressurization of Water Reactors," Edwards, A. R. and T. P. O'Brien, T. P., *Journal of the British Nuclear Energy Society*, Volume 9, 1970.

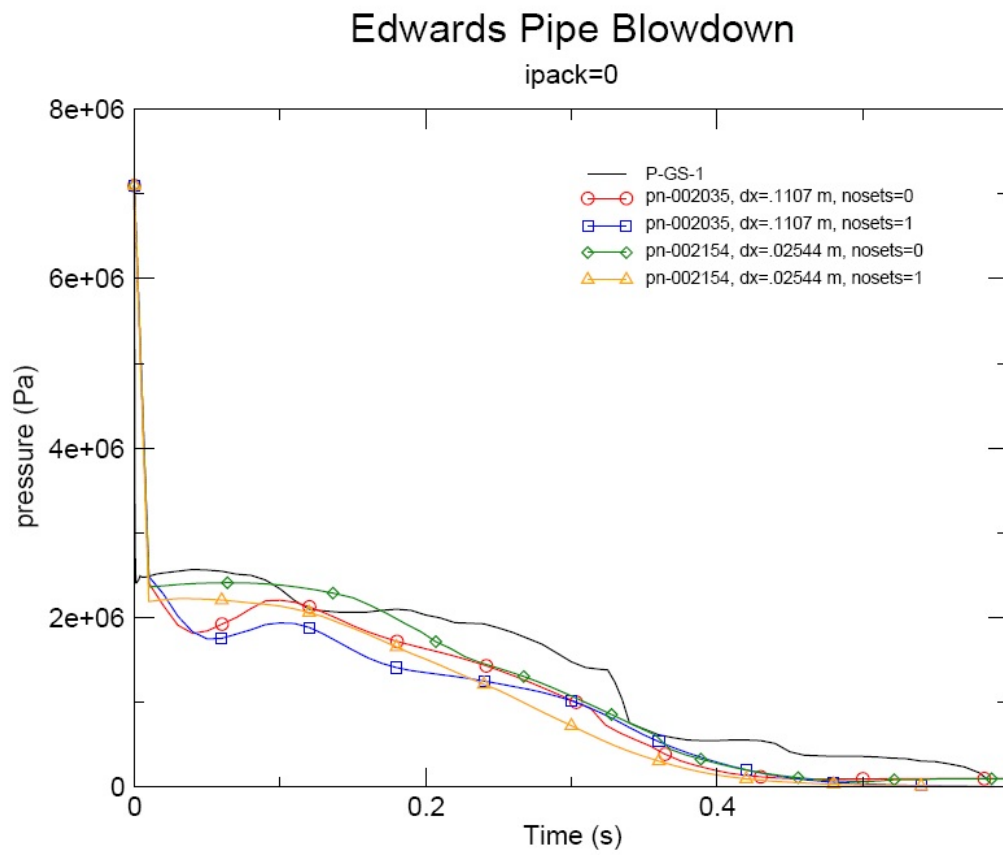


**Figure 3.1-1: Edwards Blowdown Experiment (Pressure at GS-1)**

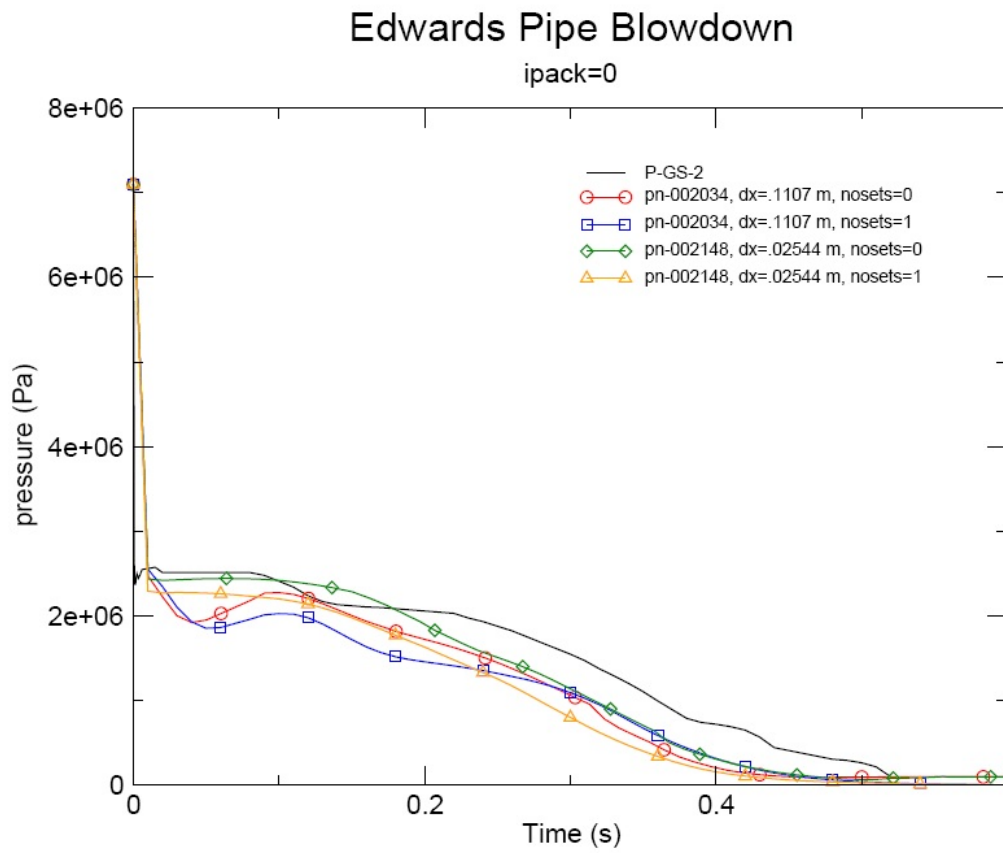


**Figure 3.1-2: Edwards Blowdown Experiment (Pressure at GS-2)**

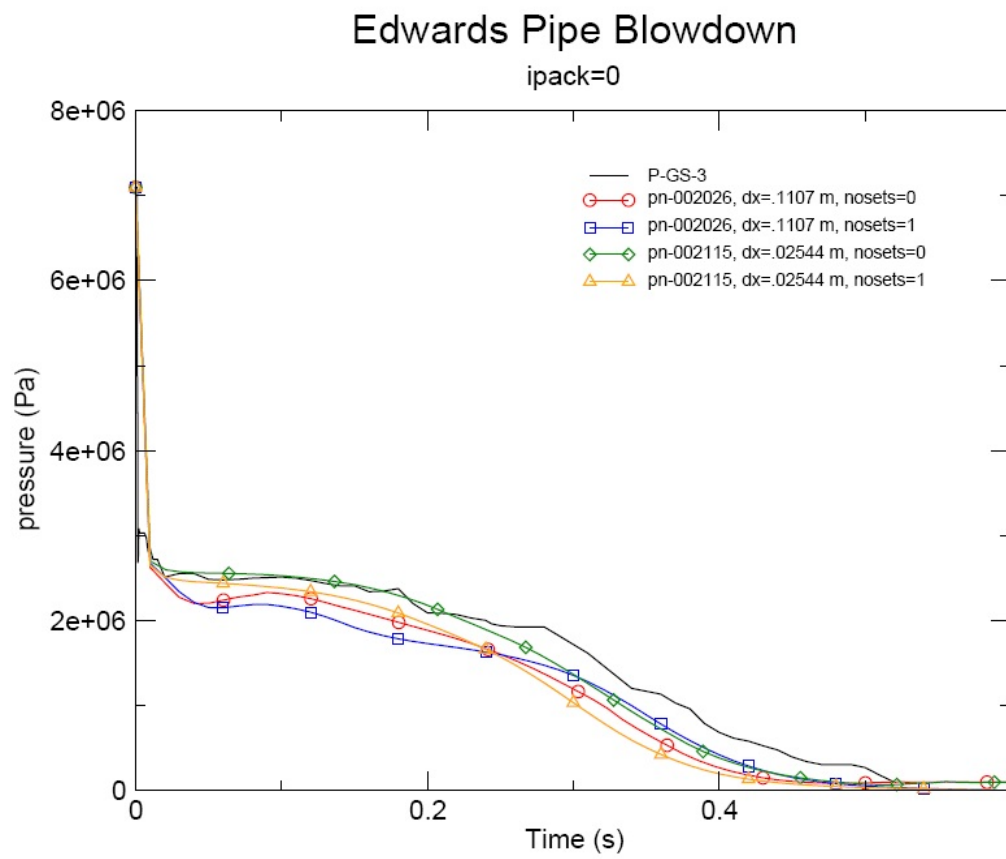


**Figure 3.1-3: Edwards Blowdown Experiment (Pressure at GS-3)**

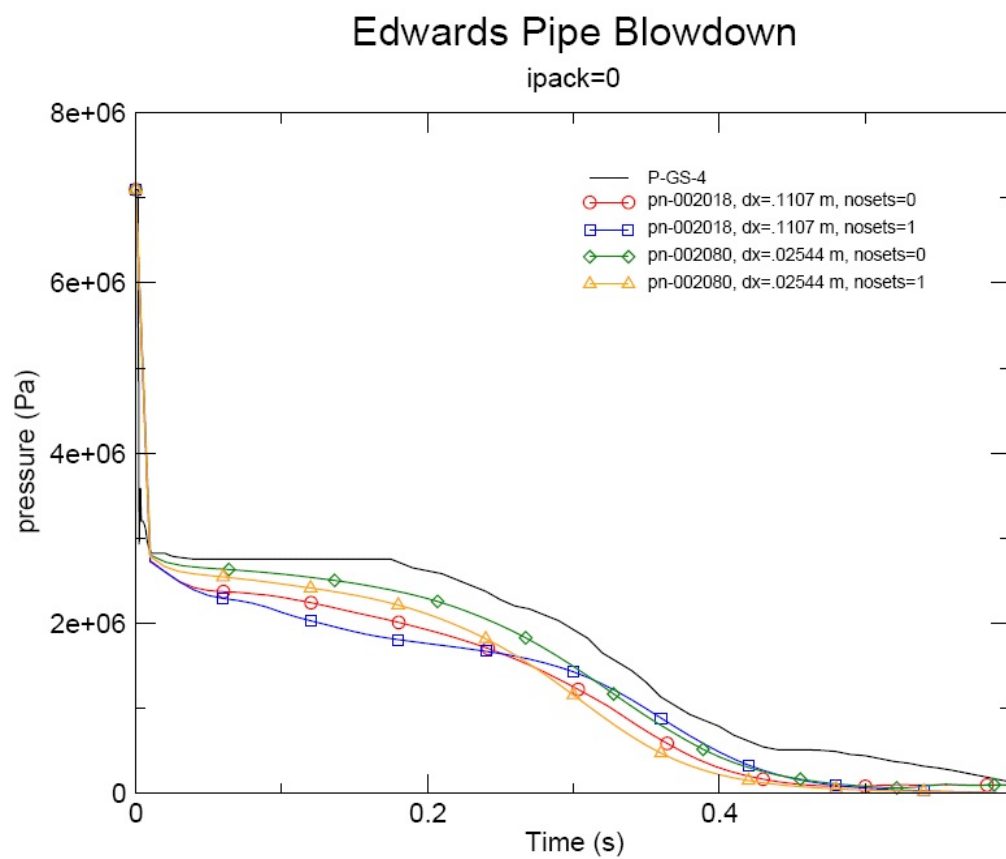


**Figure 3.1-4: Edwards Blowdown Experiment (Pressure at GS-4)**



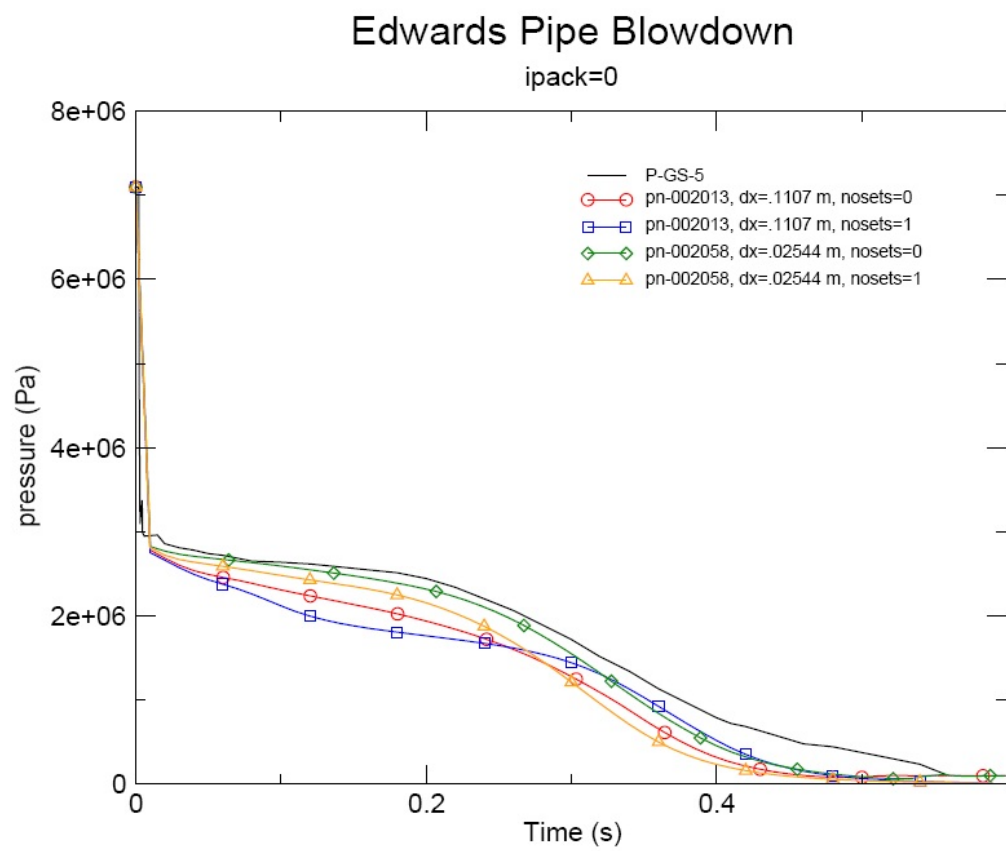


**Figure 3.1-5: Edwards Blowdown Experiment (Pressure at GS-5)**

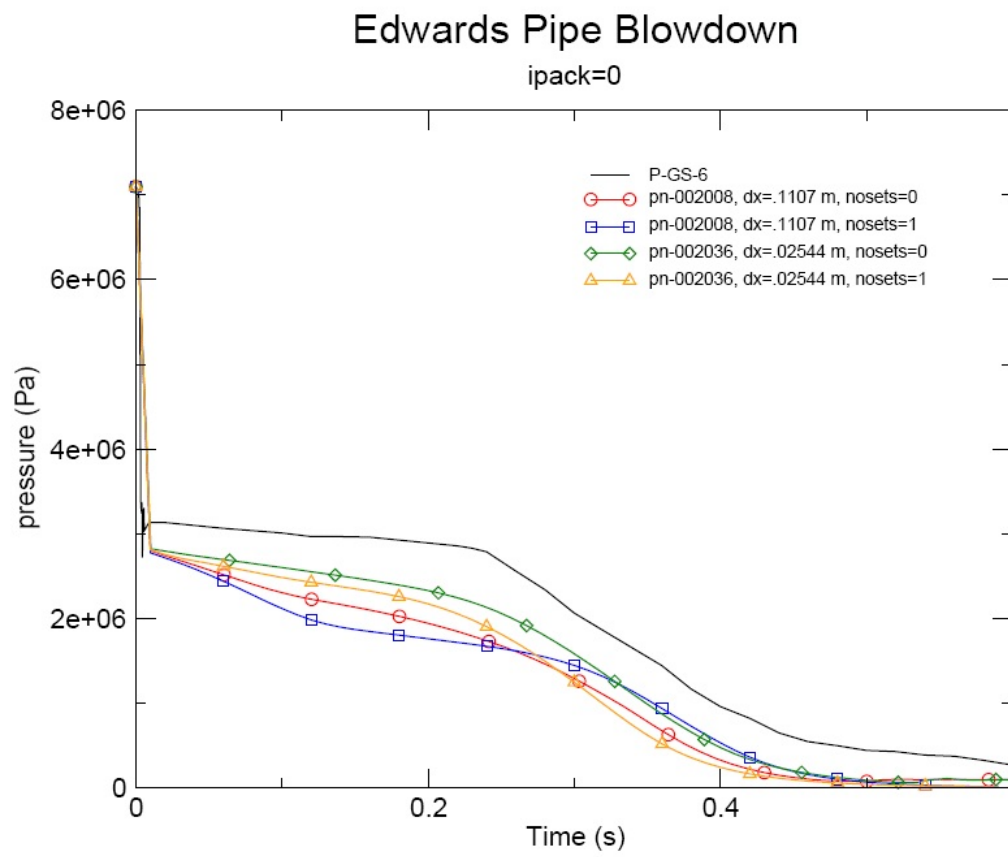


**Figure 3.1-6: Edwards Blowdown Experiment (Pressure at GS-6)**

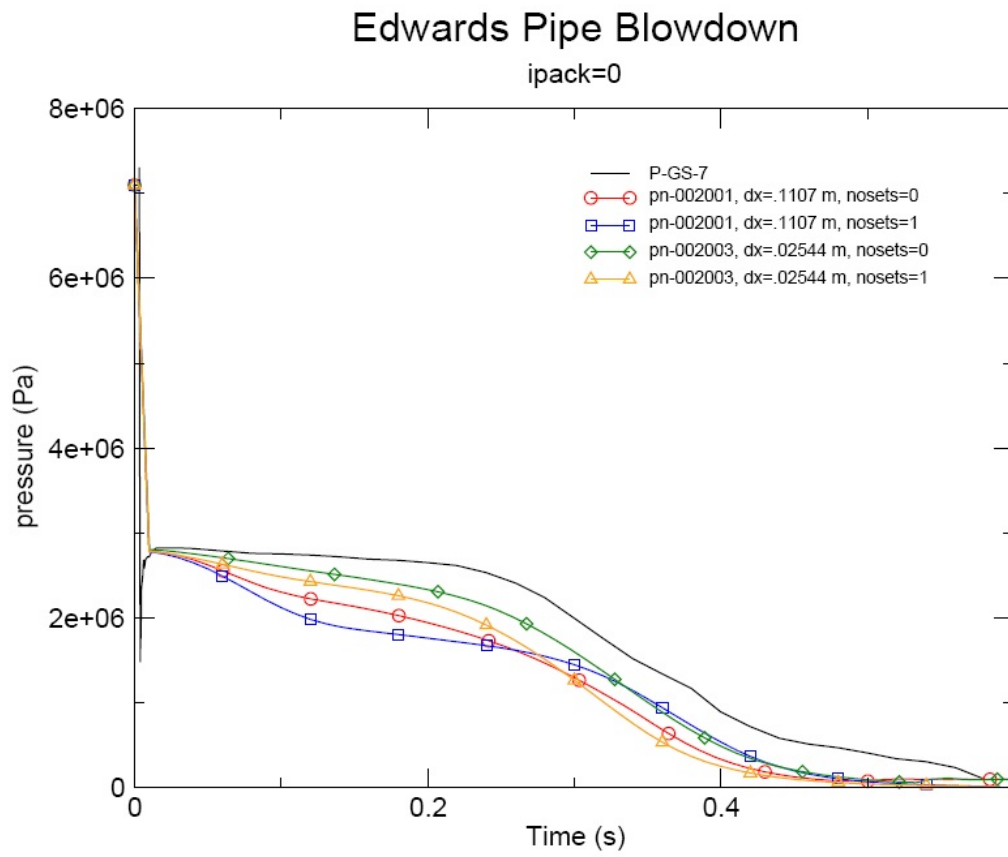


**Figure 3.1-7: Edwards Blowdown Experiment (Pressure at GS-7)**

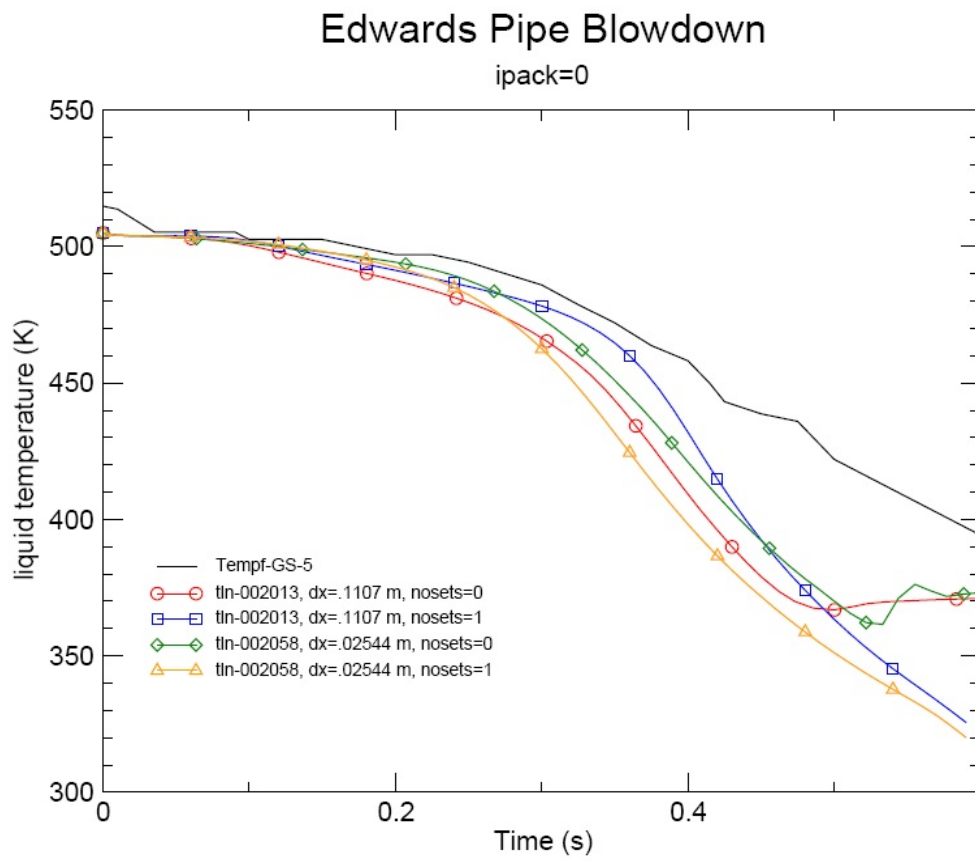


**Figure 3.1-8: Edwards Blowdown Experiment (Temperature at GS-5)**

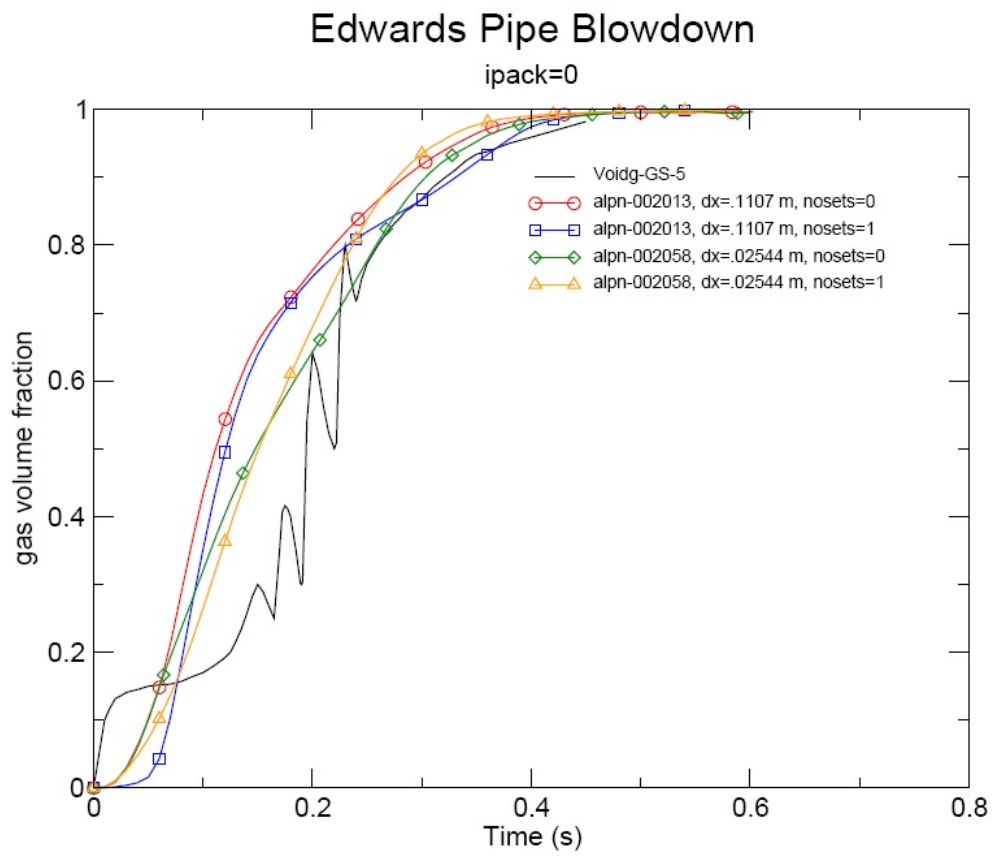


**Figure 3.1-9: Edwards Blowdown Experiment (Void Fraction at GS-5)**

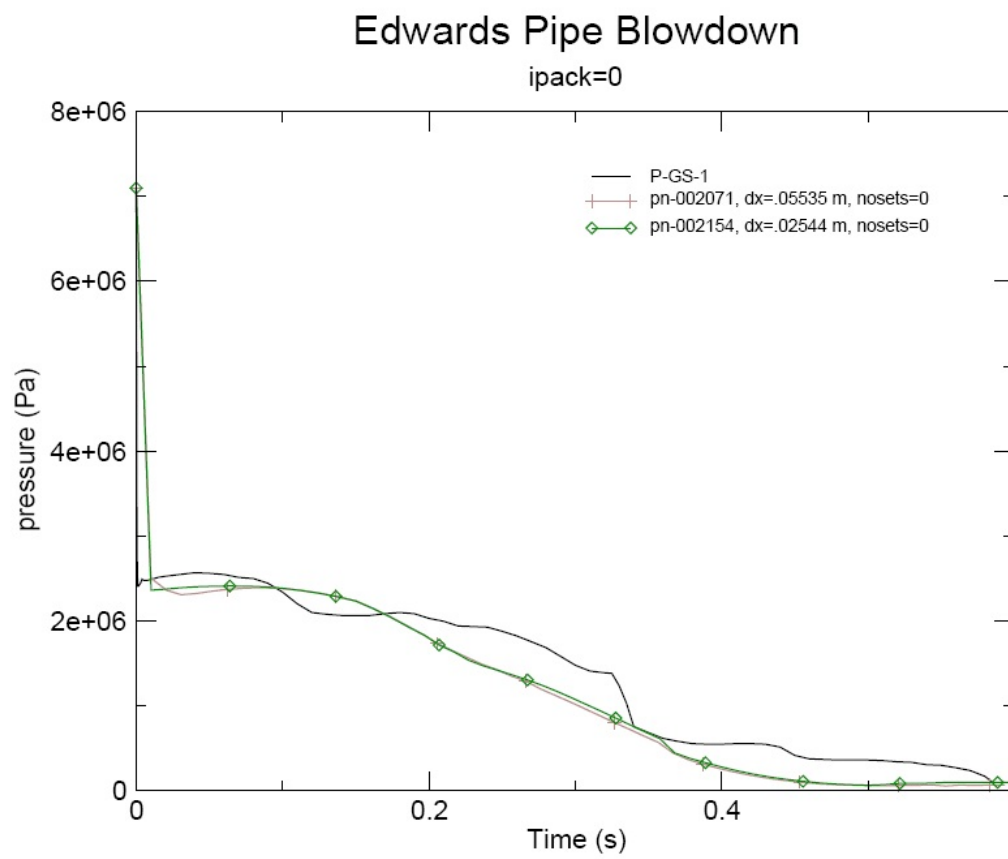


**Figure 3.1-10: Edwards Blowdown Experiment (Pressure at GS-1)**

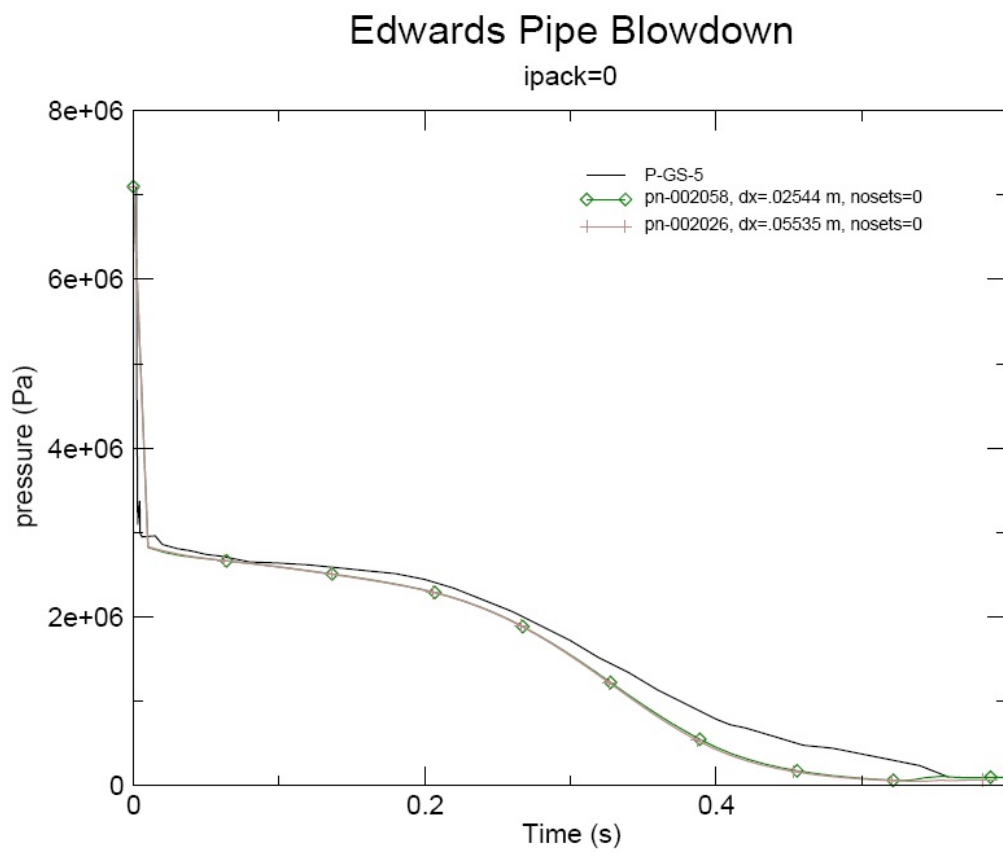


**Figure 3.1-11: Edwards Blowdown Experiment (Pressure at GS-5)**

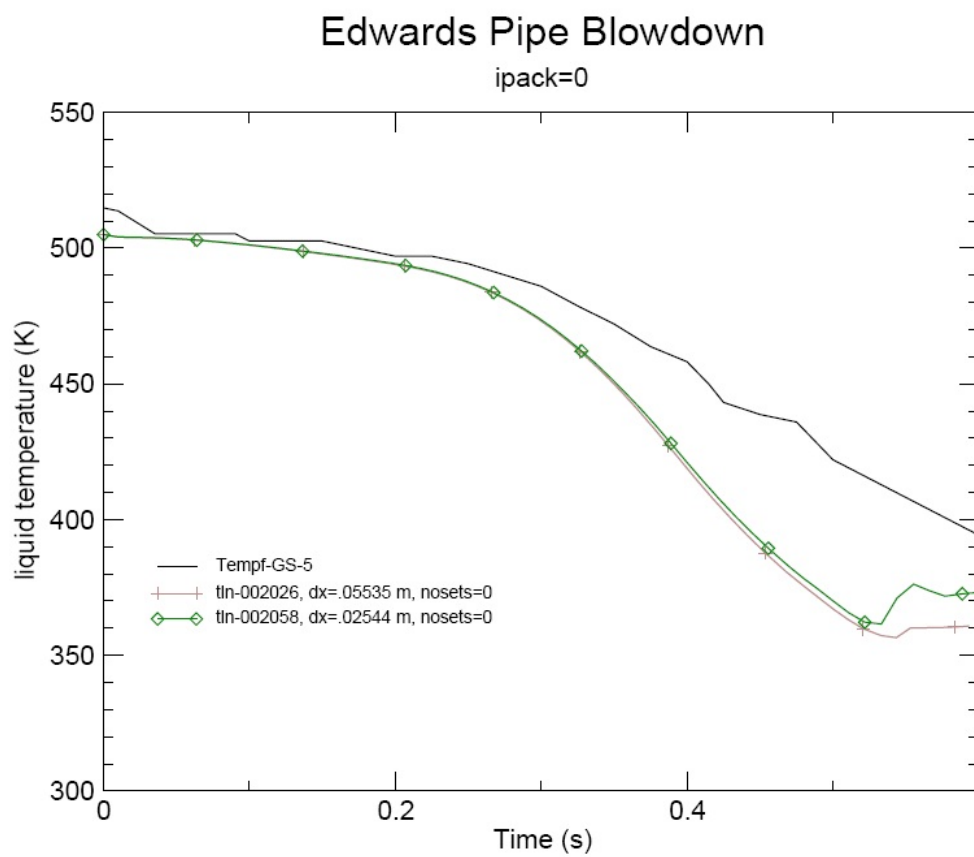


**Figure 3.1-12: Edwards Blowdown Experiment (Temperature at GS-5)**



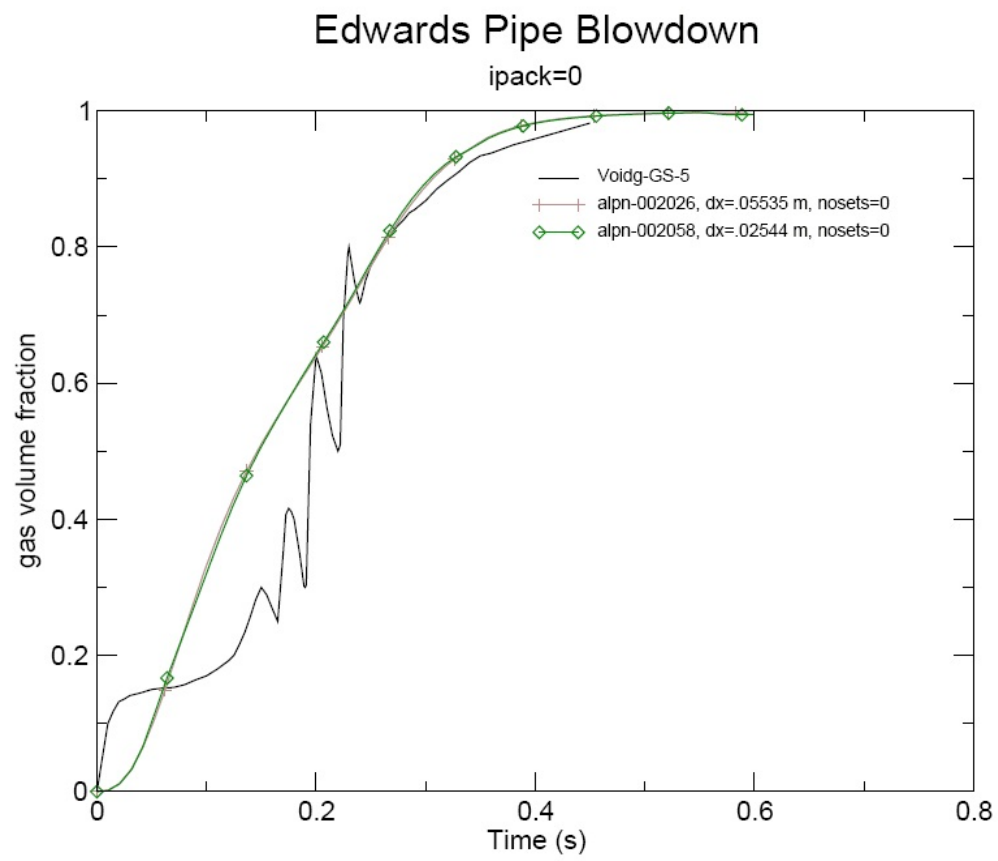


**Figure 3.1-13: Edwards Blowdown Experiment (Void Fraction at GS-5)**

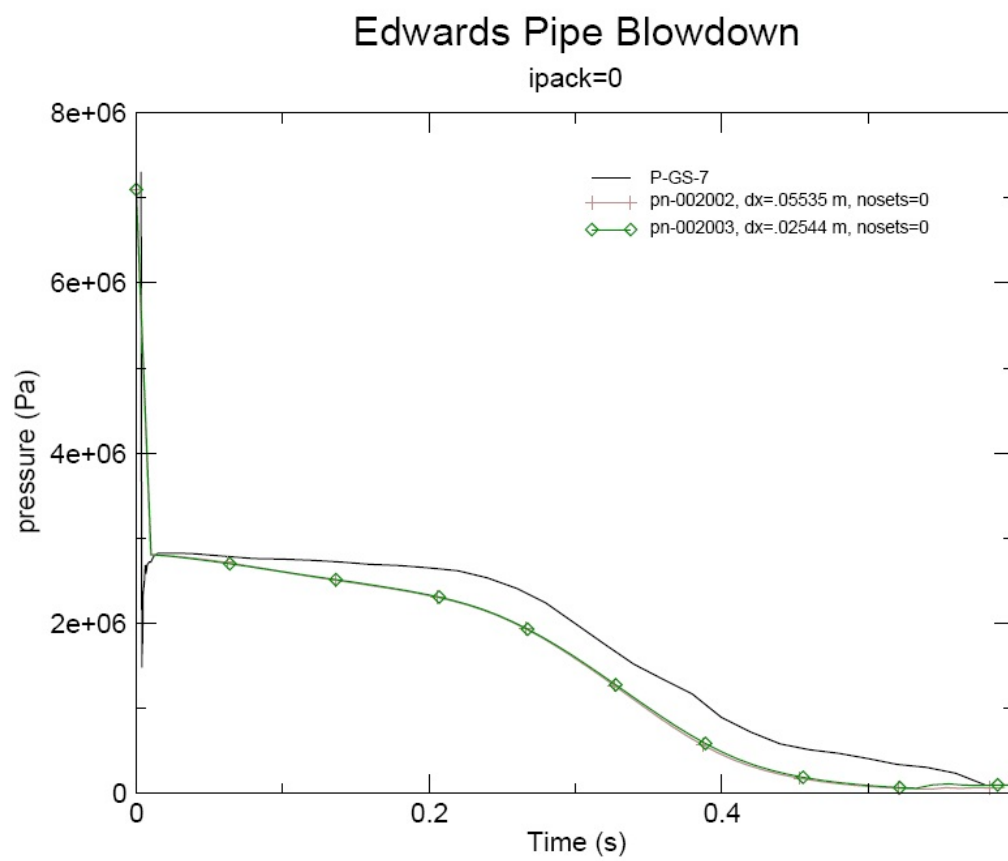


**Figure 3.1-14: Edwards Blowdown Experiment (Pressure at GS-7)**

### 3.2 LOFT Semiscale Blowdown Test

This experiment provides test results from the blowdown from a vessel containing subcooled water at high pressure. The blowdown is initiated by a quick-opening rupture disk. The blowdown initiates a depressurization wave in the vessel. Pressure measurements are provided for two points. These measurements show the travel of the acoustic wave by recording pressure variations.

Using this experiment to assess the TRAC-M code has a twofold purpose. The first objective is to verify the ability of the TRAC-M code to predict experimental results. The second objective is to compare the TRAC-M results with calculations from a MOC solution for the experiment. The MOC method has historically been used to analyze thermal-hydraulic transients, which are dominated by the travel of an acoustic wave. Other finite-difference computer codes have been shown to be able to predict acoustically-dominated thermal-hydraulic transients if properly modeled. Consequently, TRAC-M predictions for this test were compared with test data and calculations from the WHAMMOCII computer code, in order to verify the ability of the TRAC-M code to predict acoustically dominated thermal-hydraulic transients.

#### 3.2.1 LOFT Semiscale Experiment Description

Figure 3.2-1 shows the geometry for the Semiscale Blowdown Experiment. The facility consisted of a vertical 12-inch tank with two horizontal pipe connections. Table 3.2-1 lists the initial test conditions and the dimensions of the test facility. This test, which has been used for comparison with TRAC-M, is a subcooled liquid blowdown experiment. The initial system pressure was 2,300 psig with a best-estimate liquid temperature of 525°F. The blowdown was initiated by the bursting of a rupture disk near the exit of the 4-inch discharge pipe. A 1-inch diameter orifice is located upstream of the rupture disk. The experiment description assumes a pressure-time history at the rupture disk defined by the following equation postulates that the decompression time for the rupture disk is 300-microseconds.

$$P = 2300 \text{ psig} \qquad t = 0 \text{ sec.}$$

$$P = 2300 \left( \frac{1 + \cos(\pi t / \tau)}{2} \right) \qquad 0 \leq t \leq \tau$$

$$P = 0 \text{ psig} \qquad t > \tau$$

where

- P = break pressure (psig)
- t = time (sec.)
- $\tau$  = rupture disk decompression time = 300 microseconds

Pressure transducers were located at positions P-1 and P-2, as shown on Figure 3.2-1. The pressure transducer in the 4-1/16-inch inner diameter (ID) discharge line at P-2 is located just upstream from the 1-inch diameter orifice. The pressure transducer at P-1 is located at the end of the 4-1/16-inch ID line connected to the end of the vessel furthest from the break.

**Table 3.2-1: Test Facility Characteristics for the LOFT Semiscale Blowdown Test**

Vertical Tank Length (not including hemispherical heads)	118 inches (2.997 m)
Vertical Tank ID	12 inches (0.3048 m)
Upper Pipe Length (approximate)	42 inches (1.0668 m)
Upper Pipe ID	4 1/16 inches (0.10319 m)
Lower Pipe Length (approximate)	12 inches (0.3048 m)
Lower Pipe ID	4 1/16 inches (0.10319 m)
Orifice Diameter	1 inch (0.0254 m)
Initial System Pressure (assumed at rupture disk)	2300 psig (15.9593 x 10 <sup>6</sup> Pa abs.)
Initial System Temperature (best estimate)	525°F (547°K)
Rupture Disk Decompression Time (best estimate)	300 x 10 <sup>-6</sup> sec.

### **3.2.2 TRAC-M Model of the LOFT Semiscale Blowdown Test**

Two TRAC-M models of the LOFT Semiscale Blowdown Test were developed. In one model, the experiment was modeled using control volumes with a 2-inch length; the second model used control volumes with a 4-inch length. Figure 3.2-2 shows a schematic of the model using the 2-inch long volumes. Figure 3.2-3 presents the schematic of the 4-inch TRAC-M model. The two models were run with the TRAC-M code using two numerical solution options, NOSETS=1 and NOSETS=0. With NOSETS=1, the TRAC-M solution is limited by the numerical stability criteria; with NOSETS=0, TRAC-M uses a numerical solution scheme, which permits the code to use timesteps larger than dictated by stability considerations. Version 3.1011 of the TRAC-M code was used to perform the analysis of the LOFT Semiscale Blowdown Test.

### **3.2.3 Comparison of Test Data and Analytical Results**

Figures 3.2-4 and 3.2-5 show the measured and calculated pressures at P-1 and P-2. Following initial decompression, the pressure at P-2 rises to approximately 2,500 psig. This pressure increase is attributable to the reflections of the acoustic wave originating from the break location. When the initial decompression wave reaches the area change at the vessel, the wave is partially reflected as a compression wave. When this returning compression wave encounters the area reduction at the orifice, it is partially reflected as another compression wave. This double recompression results in pressures at P-2 that are larger than the initial pressure. The delay in pressure response at transducer P-1 is attributable to the travel time for the initial decompression wave originating at the break to reach P-1. The decompression at P-1 occurs somewhat in steps. The pressure variances at P-1 result from the initial decompression and recompression waves emanating from the break location. The 2-msec between the first minimum and maximum pressure at P-1 represents the round trip travel time of the acoustic waves in the break line. Subsequent pressure variances at P-1 result from the successive transmitted and reflected waves. The overall system decompression can be observed in the plot of the P-1 pressure response.

Figures 3.2-4 and 3.2-5 also plot the TRAC-M calculated pressures for the 2-inch and 4-inch models with NOSETS equal to 1 and 2. The differences between the calculated pressures from the 2-inch and 4-inch models with NOSETS equal to 1 are small. Both of these results follow the trends of the measured pressures; however, the code calculations show larger pressure losses than the measured data. The results of the 2-inch and 4-inch TRAC-M models with

NOSETS equal to 0 show an even larger pressure damping than observed with NOSETS equal to 1. These observations lead to the conclusion that the 4-inch model provides adequate results as long as NOSETS is set equal to 1, which permits the calculated timestep to be controlled by the stability criteria.

Figures 3.2-6 and 3.2-7 compare the measured pressures at P-2 and P-1 to the results from the 4-inch TRAC-M model and the WHAMMOCII MOC computer model of this experiment provided in Reference 2. Figure 3.2-6 illustrates the differences between pressure measurements and predictions at P-2. This comparative plot indicates that the TRAC-M finite-difference computer code and the WHAMMOCII MOC computer code yield predictions that possess different strengths and weaknesses. The pressure peaks predicted by the TRAC-M code occur slightly later than the measurements indicate. This indicates that the sound speed calculated by TRAC-M is slightly slower than in test data. By comparison, the WHAMMOCII computer code predicts the time for the first two pressure peaks more accurately; however, because the last two pressure peaks are predicted later than the test data, WHAMMOCII underpredicts the sound speed for the latter part of the transient. The magnitude of the first depressurization is overpredicted by both TRAC-M and WHAMMOCII. The magnitudes of the first two pressure peaks predicted by the TRAC-M code somewhat agree with the test data, while the WHAMMOCII code overpredicts the magnitudes of the first two pressure peaks. Consequently, the WHAMMOCII code underpredicts pressure damping for about half the transient. The TRAC-M code calculates larger pressure damping than the WHAMMOCII code. Therefore, both TRAC-M and WHAMMOCII provide acceptable predictions of pressure conditions at P-2.

Figure 3.2-7 indicates that TRAC-M and WHAMMOCII predict acceptable pressure responses at P-1. Both codes predict the magnitude and timing of the initial depressurization. The TRAC-M code, however, does appear to overpredict pressure damping at the end of the transient. The WHAMMOCII code does not appear to accurately predict the timing and, therefore, the sound speed during the latter part of the transient.

Figures 3.2-8, 3.2-9, and 3.2-10 provide other interesting results from the TRAC-M analysis of the LOFT Semiscale Blowdown Test. Figure 3.2-8 shows that even though the pressure upstream of the orifice at P-2 remains high and shows pressure variations attributable to acoustic wave travel, the pressure downstream of the orifice decompresses within 0.002-seconds after the rupture disk bursts. Figure 3.2-9 shows the calculated variations between flow through the orifice and out the break location during the early part of the calculation. Consistent with Figure 3.2-8, this curve indicates that the volume between the orifice and break quickly loses mass as a result of the large break flow at the beginning of the transient. Finally, Figure 3.2-10 shows that the volume between the orifice and the break quickly becomes two-phase, while the volume upstream of the orifice remains one-phase for the duration of the calculated transient.

### **3.2.4 Summary**

Test predictions of the LOFT Semiscale Blowdown Test using the TRAC-M code and the WHAMMOCII MOC code indicate that both codes and methods predict acceptable results when correctly modeled. Consistent with the conclusion obtained from the TRAC-M calculations for the Edwards Pipe Blowdown Experiment, it is recommended that an acceptable TRAC-M model should possess a node length comparative to the pipe diameter. Therefore, it is recommended

that the node size for a TRAC-M model must be equal to or smaller than the pipe diameter in order to be able to predict an acoustic transient, such as the travel of a depressurization wave.

### 3.2.5 References

- (1) **“Hydrodynamics Describing Acoustic Phenomena During Reactor Coolant System Blowdown,”** Rose, R. P., G. H. Hanson and G. A. Jayne, U. S. Atomic Energy Commission, Idaho Operations Office, IDO-17254, July 1967.
- (1) **“WHAMMOII – A Computer Code for Performing One or Two-Phase Water Hammer Analysis,”** Krotiuk, W., *Fluid Transients and Fluid-Structure Interaction*, American Society of Mechanical Engineers Pressure Vessel and Piping Conference, PVP-Vol. 64, 1982.

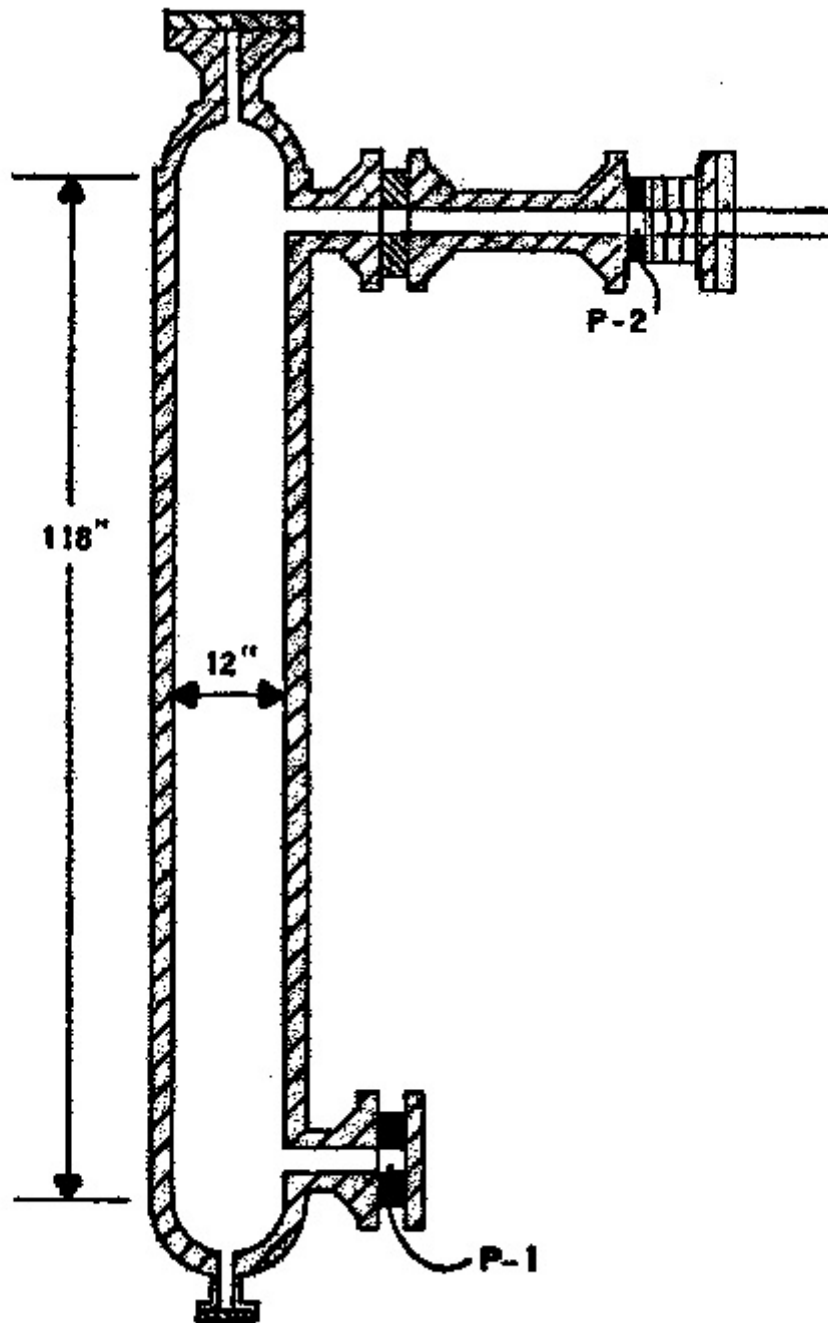
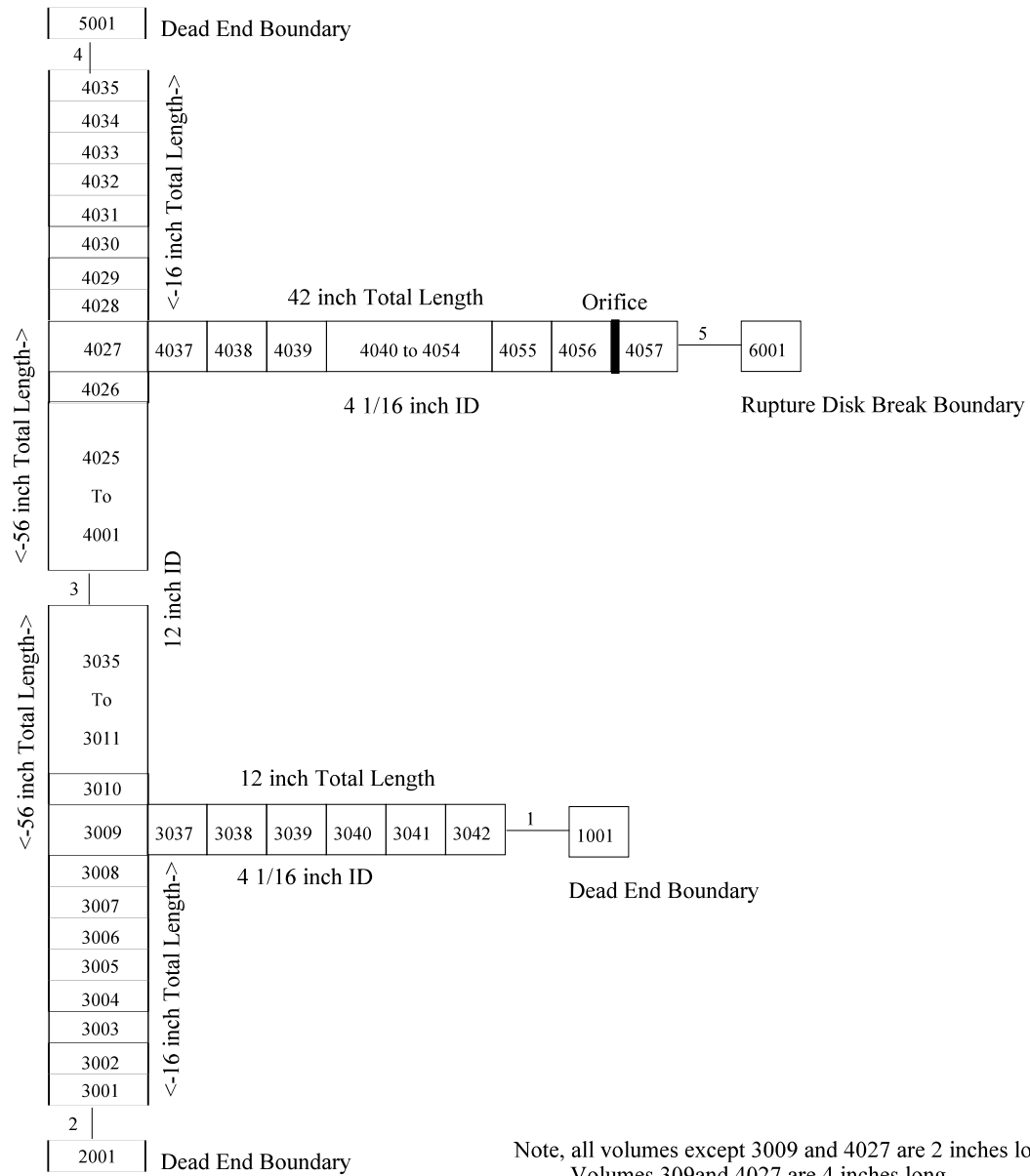
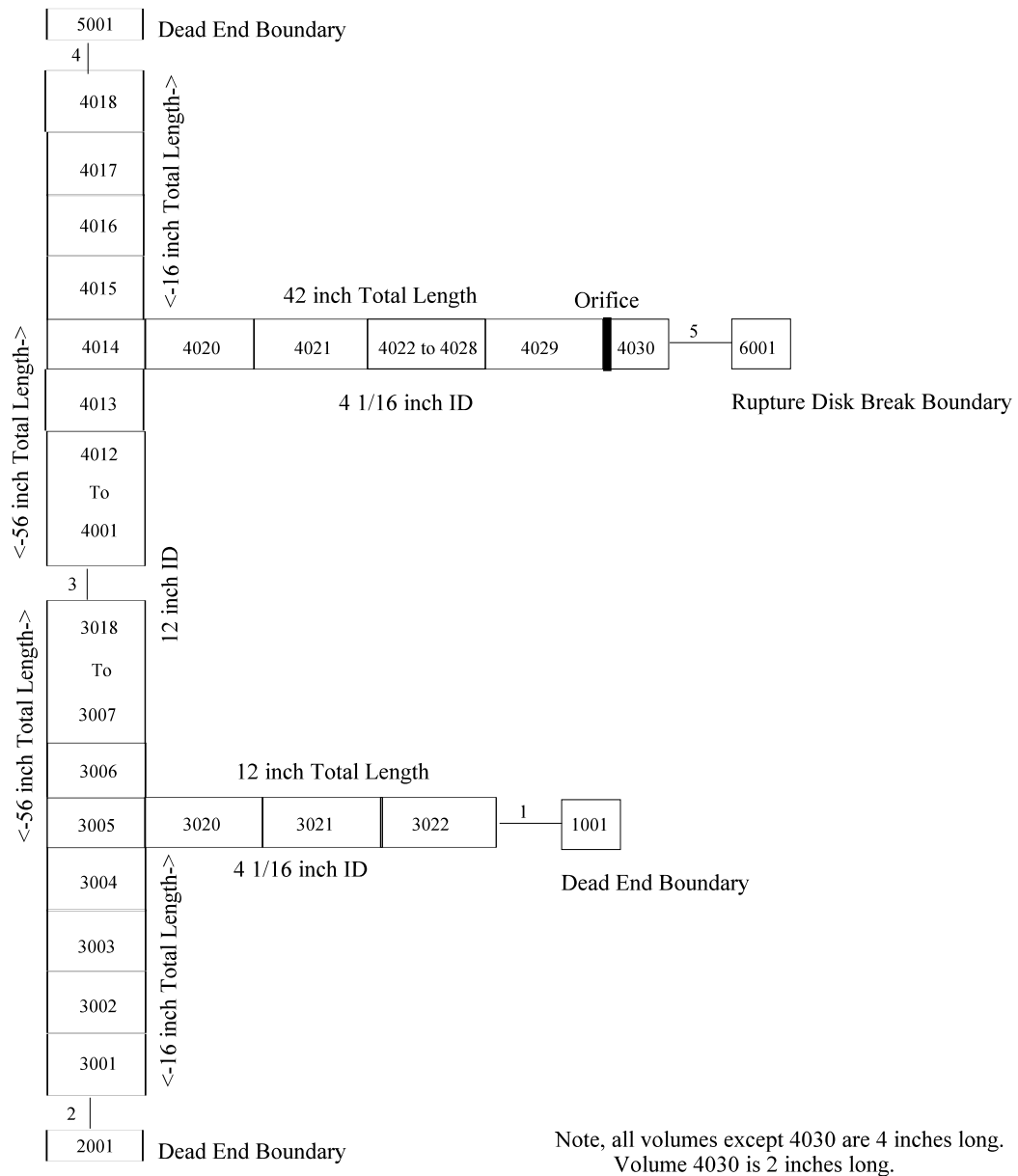


Figure 3.2-1: LOFT Semiscale Blowdown Apparatus (Top Break Configuration)



**Figure 3.2-2: TRAC-M Model of the LOFT Semiscale Blowdown Test with 2-inch Volumes**





**Figure 3.2-3: TRAC-M Model of the LOFT Semiscale Blowdown Test With 4-inch Volumes**

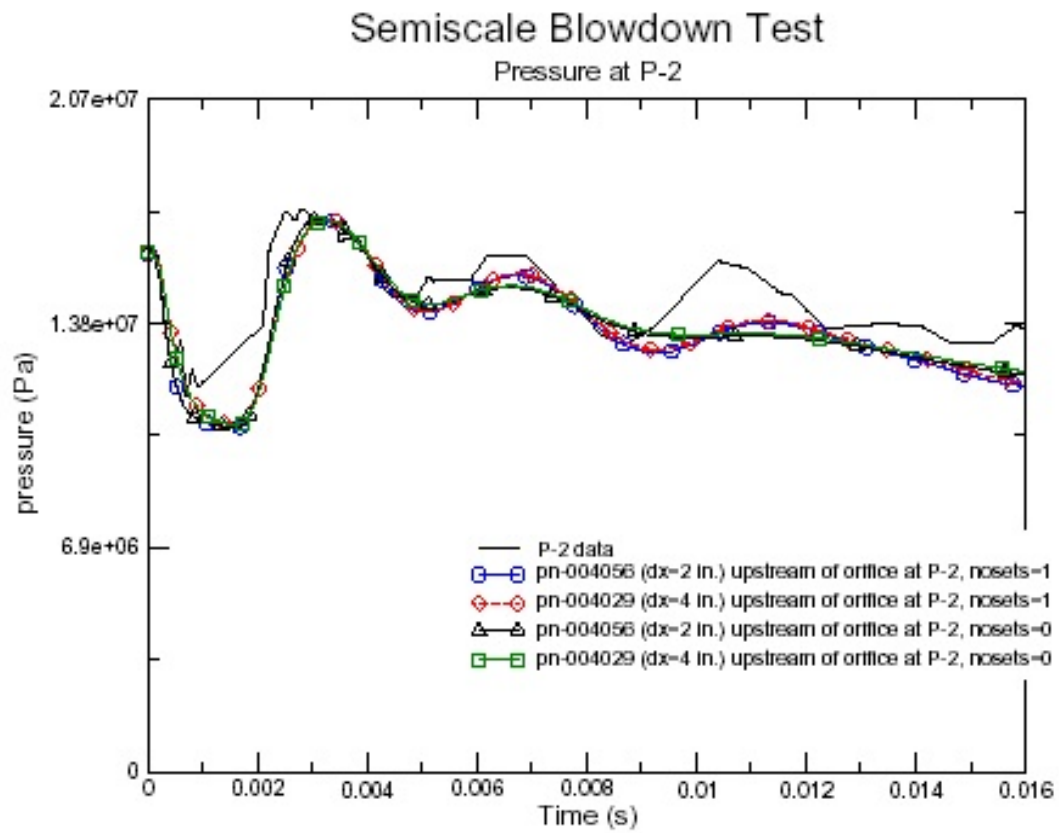


Figure 3.2-4: LOFT Semiscale Blowdown Measurements and TRAC-M Predictions at P-2

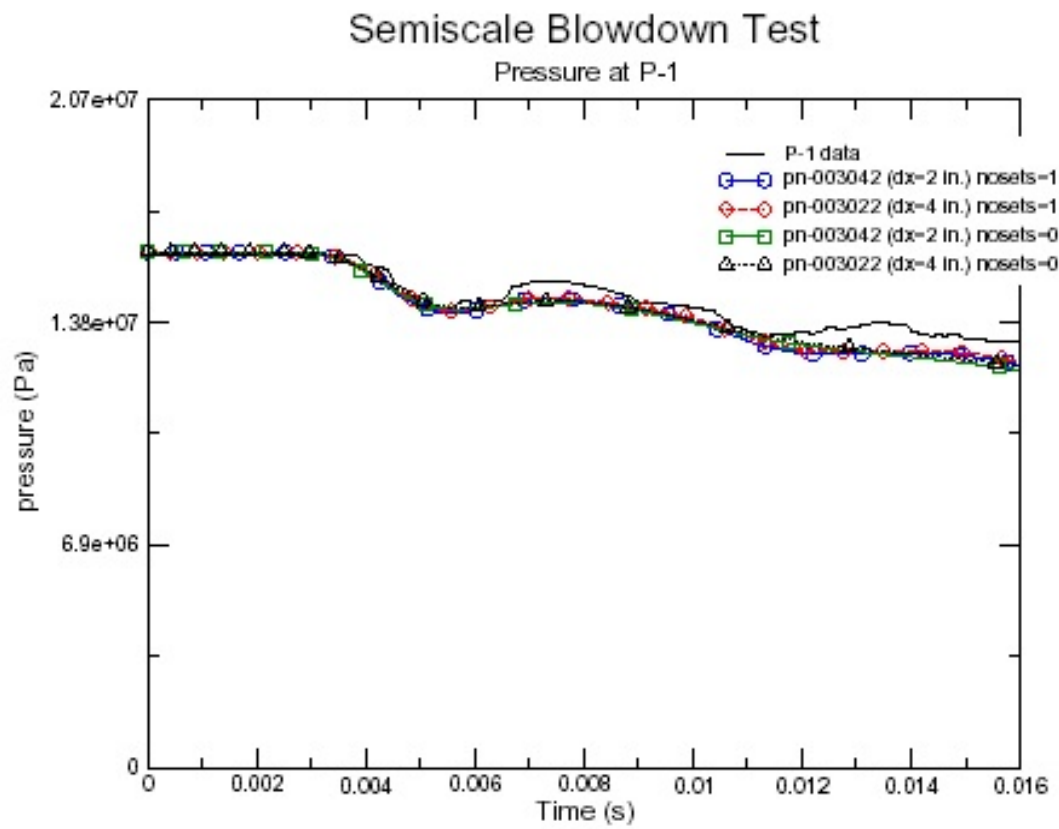
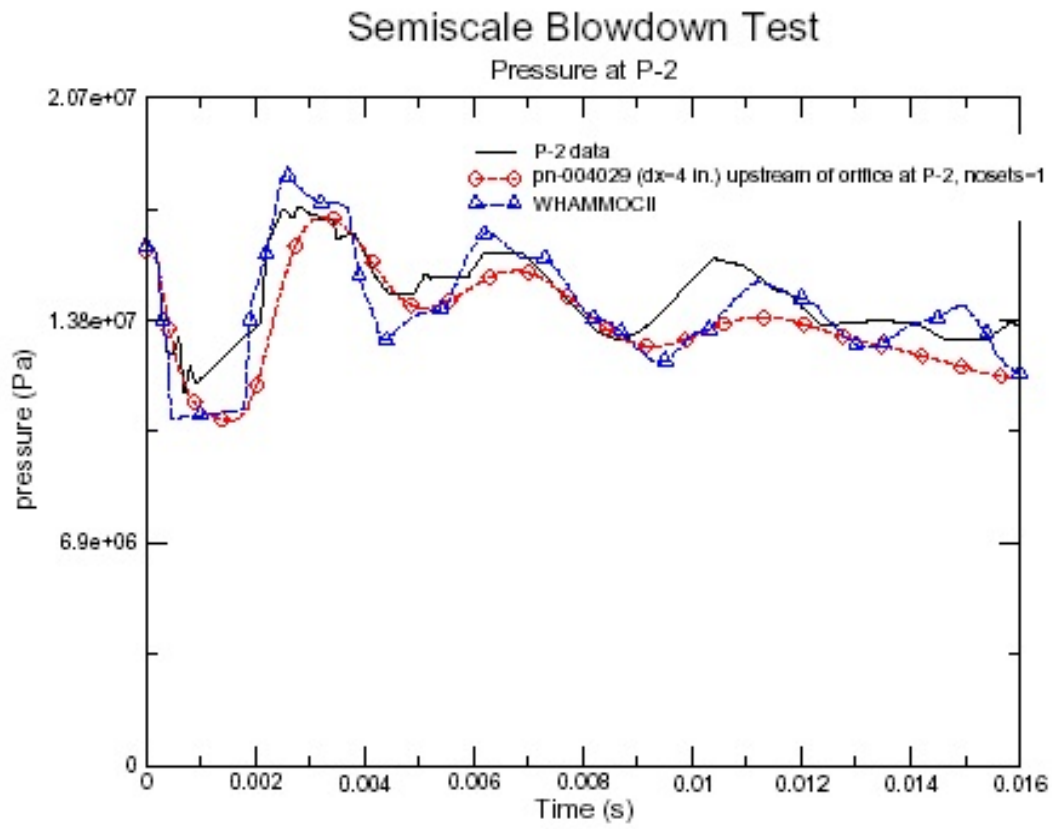
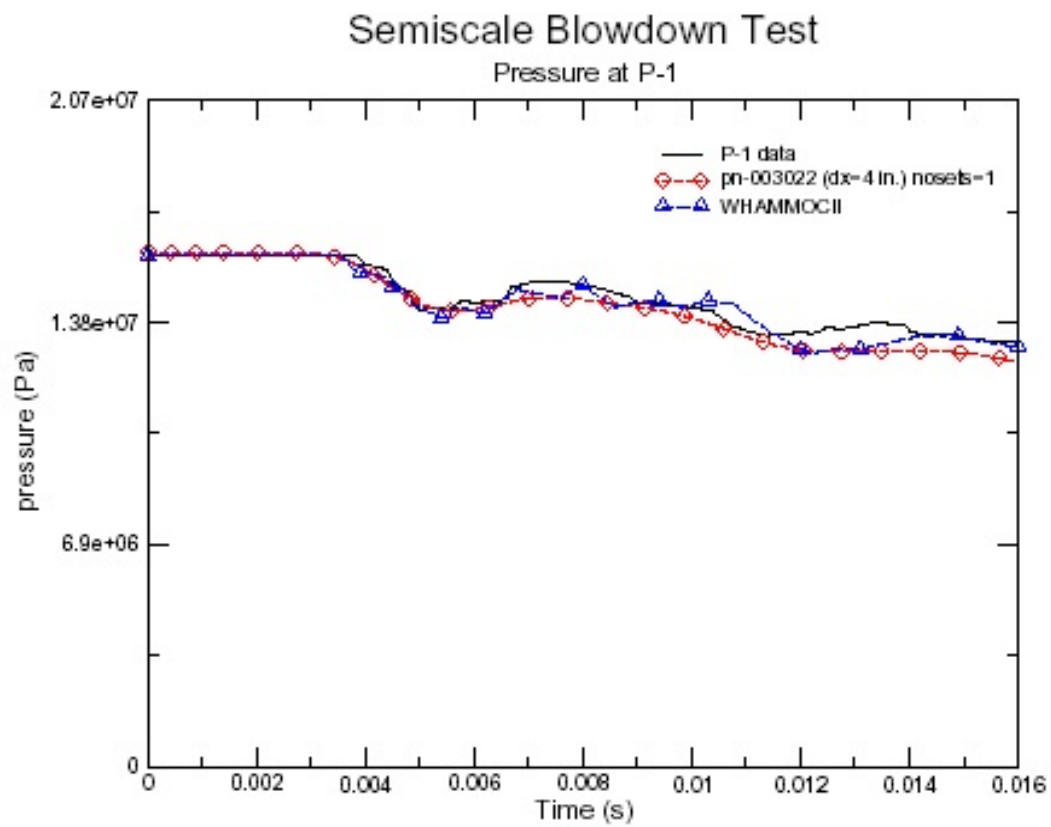


Figure 3.2-5: LOFT Semiscale Blowdown Measurements and TRAC-M Predictions at P-1



**Figure 3.2-6: LOFT Semiscale Blowdown Measurements and Analysis Predictions at P-2**



**Figure 3.2-7: LOFT Semiscale Blowdown Measurements and Analysis Predictions at P-1**

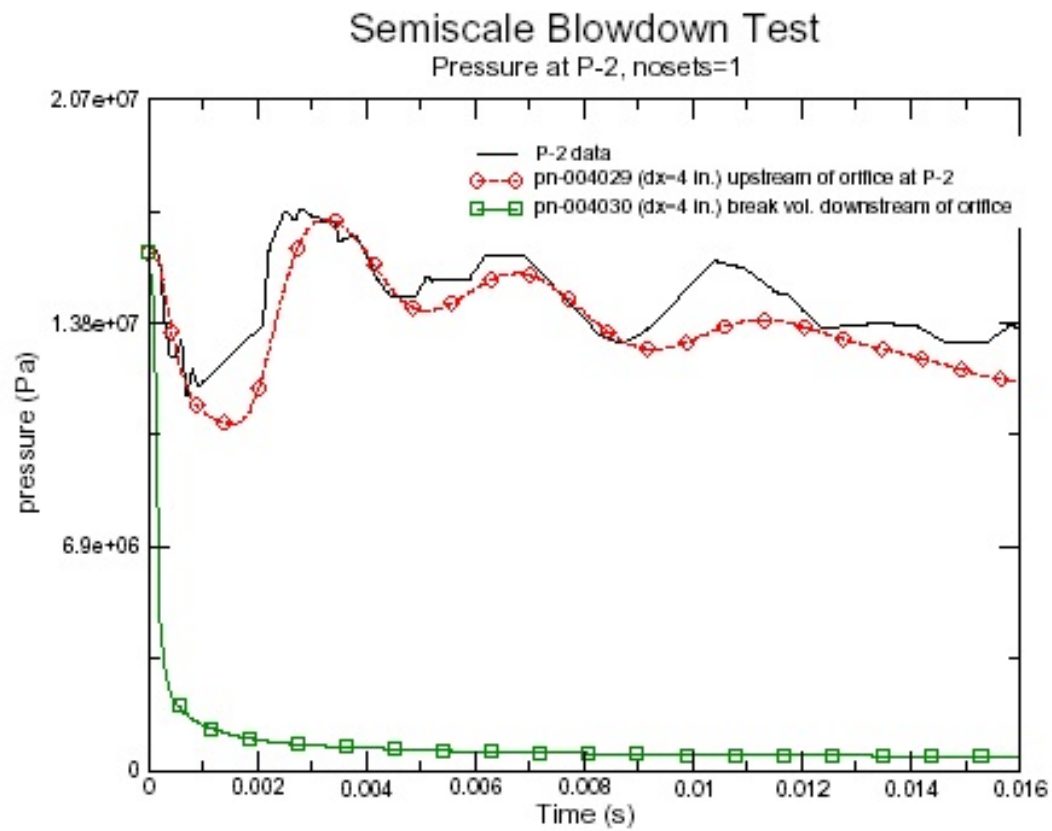
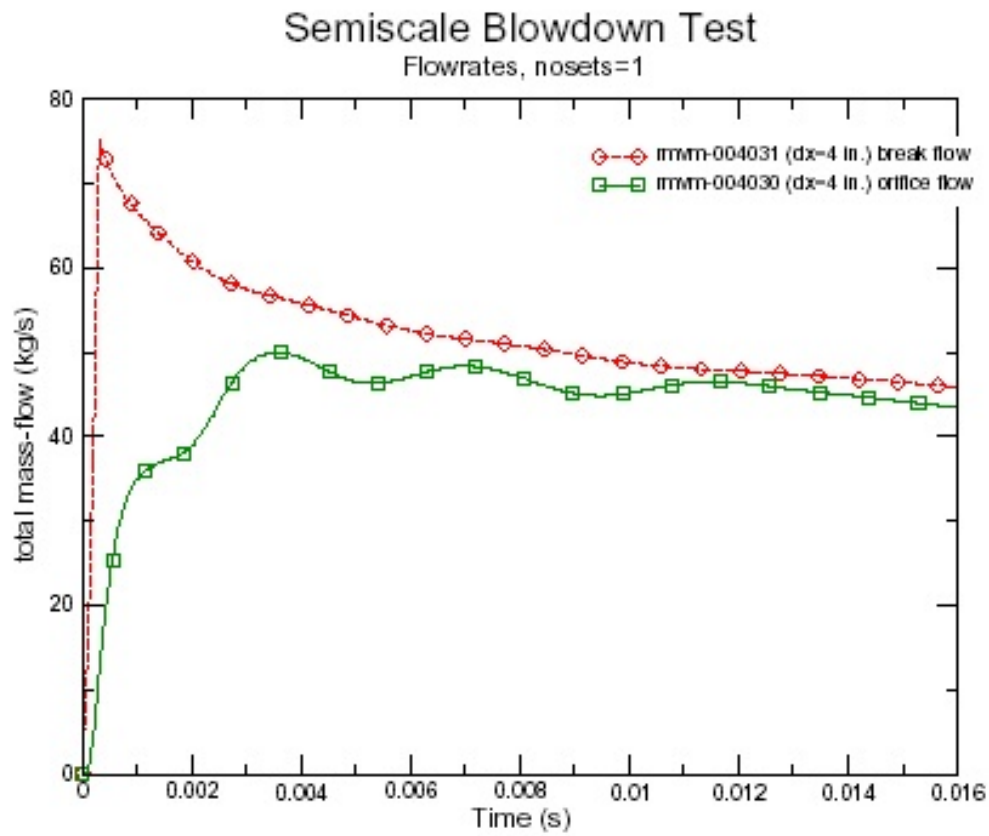
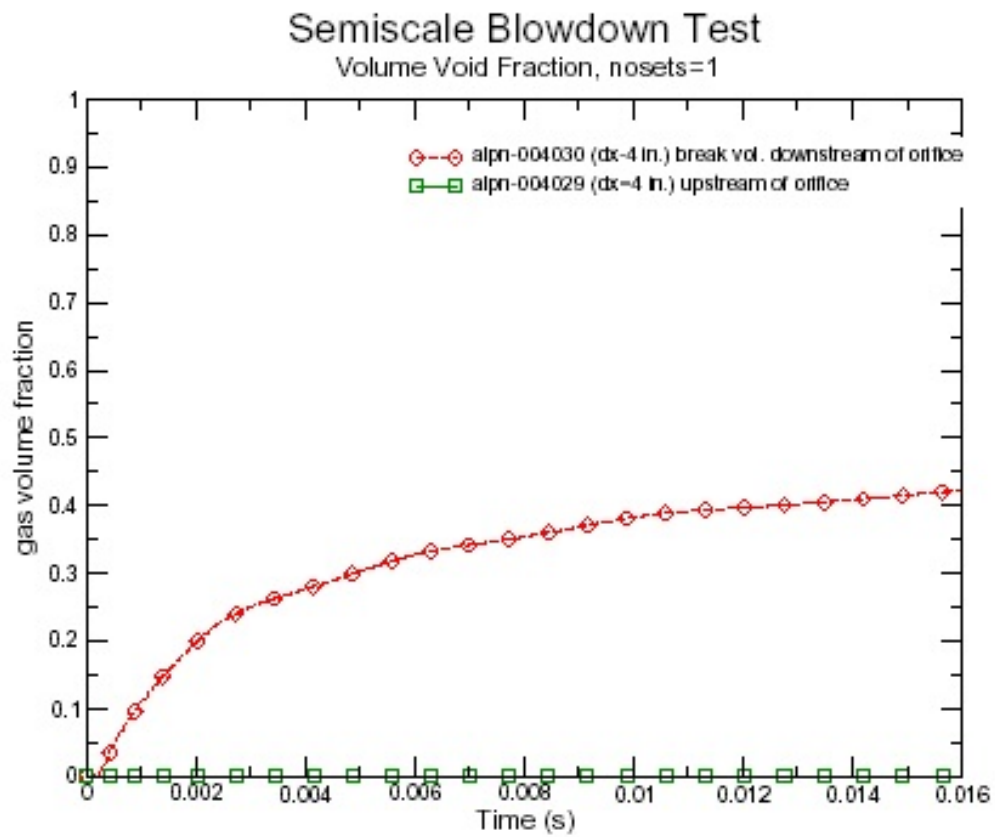


Figure 3.2-8: TRAC-M Pressure Predictions for the LOFT Semiscale Blowdown Test



**Figure 3.2-9: TRAC-M Flowrate Predictions for the LOFT Semiscale Blowdown Test**



**Figure 3.2-10: TRAC-M Void Fraction Predictions  
for the LOFT Semiscale Blowdown Test**



## 4.0 STEAM GENERATOR ANALYSIS USING THE TRAC-M CODE

Version 3.1011 of the TRAC-M computer code has been used to predict the thermal-hydraulic behavior of the Westinghouse Model 51 steam generator following an MSLB and an FWLB. The analysis can be divided into two time periods, including a short time period lasting a few seconds during which the peak internal loading on the TSPs and primary system tubing are generated, and a long time period during which the temperature gradients and oscillatory pressure loads are developed in the steam generator internals.

Separate TRAC-M models would need to be developed to handle the short-term and long-term analyses. A “simple” model, with only the primary system tube wall modeled as a heat transfer structure, has been used for the short-term analyses during which heat transfer effects can be neglected. This “simple” model divides the steam generator into one-dimensional flow paths and cannot predict radial flow conditions around the primary system tubing. The long-term model must be more detailed and must contain internal steam generator structures in order to predict temperature gradients of steam generator internals and the effects of hot structures in developing pressure loadings caused by liquid flashing. The long-term model must also possess three-dimensional flow modeling to be able to predict cross-flow conditions around the steam generator primary system tubing, as well as the ability to calculate temperature gradients and oscillatory pressure loads on the TSPs.

The following section presents the results of the short-term TRAC-M analyses of the steam generator following MSLBs and FWLBs.

### **4.1 Short-Term Steam Generator Analyses Using the TRAC-M Code**

This section presents the results of a “simplified” TRAC-M model of the Westinghouse Model 51 steam generator following a 4.6 ft<sup>2</sup> guillotine break of the main steam line at the steam generator nozzle, an MSLB limited by the 1.4 ft<sup>2</sup> flow restrictor, and a guillotine break of the feedwater line entering the steam generator. The Westinghouse analyses in References 1 and 2 presented results for a guillotine MSLB with a 1.4 ft<sup>2</sup> flow restrictor calculated using the Westinghouse-developed TRANFLO computer code, and 4.6 ft<sup>2</sup> and 1.4 ft<sup>2</sup> MSLBs determined using the RELAP5 computer code. A TRANFLO analysis for a full 4.6 ft<sup>2</sup> area MSLB without the presence of a flow restrictor was not provided in the Westinghouse report. The steam generator was assumed to be initially in a hot standby condition or at 100-percent power before the break. The analyses of the Westinghouse Model 51 steam generator, References 1 and 2, have shown that a guillotine MSLB at the hot standby initial condition produces the most severe loading on the TSPs. Table 4.1-1 compares the analysis conditions used in the current TRAC-M analysis, as well as the TRANFLO and RELAP5 analyses described in References 1 and 2. The TRANFLO and RELAP5 analyses described in References 1 and 2 included heat transfer structures; however, the short-term TRAC-M computer model shown in Figures 4.1-1 and 4.1-2 included heat transfer modeling of only the primary system tubing.

In order to obtain the steam generator initial conditions at hot standby or 100-percent power, a steady-state analysis was performed using the TRAC-M model prior to performing the transient MSLB or FWLB analyses. The steady-state TRAC-M-developed conditions were then used as the initial conditions for the transient analyses. The guillotine 4.6 ft<sup>2</sup> and flow area-limited 1.4 ft<sup>2</sup> MSLBs were assumed to occur near the steam generator nozzle. Specifically, these breaks were assumed to occur at the end of the first steam line volume 4001 (see Figure 4.1-2). The appropriate flow area was specified at this location. The guillotine FWLB was assumed to

occur near the steam generator feedwater nozzle. Specifically, this break was assumed to occur at the end of feedwater line volume 9005 (see Figure 4.1-2).

A pressure drop loss coefficient of 1.1 for flow through the TSPs was used in all analyses. Reference 1 indicates that this is the “best-estimate” value obtained using a correlation based on Westinghouse test data. For comparison, Reference 3 was used to obtain the loss coefficient for flow through a thick, perforated plate. Figures 4.1-3 and 4.1-4 compare the two correlations. Figure 4.1-3 shows the loss coefficient comparisons using the TSP flow area as the reference. Figure 4.1-4 shows the same comparisons using the flow area upstream of the TSP as a reference; The loss coefficient value of 0.96 calculated for the Model 51 TSP using Reference 3 is close to, but slightly lower than, the value of 1.1 obtained from the Westinghouse correlation. Consequently, the Westinghouse loss coefficient value was used in the TRAC-M analyses.



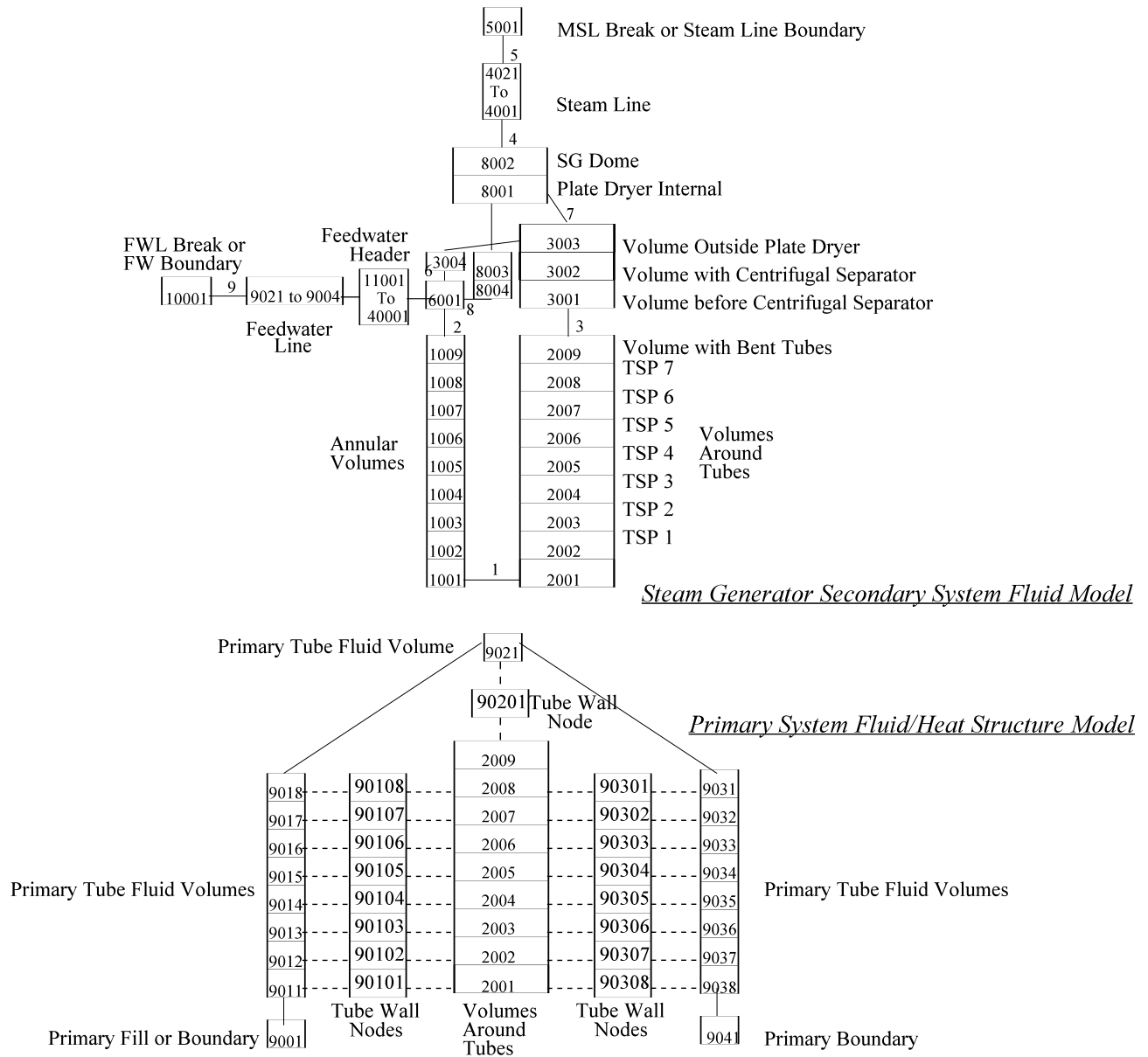


**Figure 4.1-2: TRAC-M Steam Generator Schematic Model (1 of 2)**

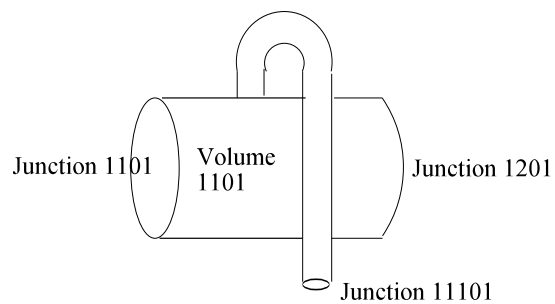
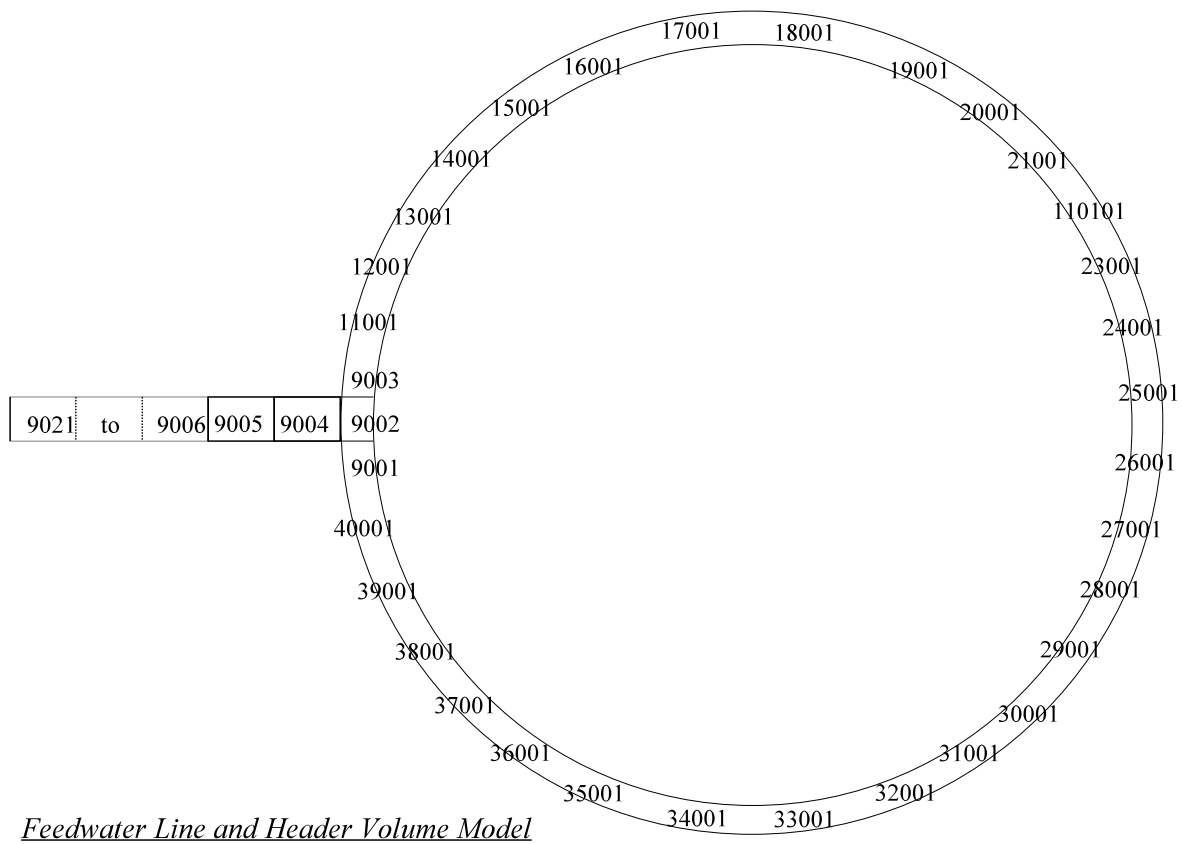


**Figure 4.1-2: TRAC-M Steam Generator Schematic Model (2 of 2)**

**Table 4.1-1: Computer Modeling and Initial Conditions Used in Analyses**

	<b>TRANFLO Reference 1</b>	<b>RELAP5 Reference 1</b>	<b>TRAC-M</b>
<b><u>Steam Generator Secondary System</u></b>			
100% Power per Steam Generator	886.67 MW	886.67 MW	878.0 <sup>a</sup> MW
Steam Generator Steam Pressure	793 psia	793 psia	793 psia 5.4675x10 <sup>6</sup> Pa
Hot Standby Steam Temperature	547°F	547°F	517.2°F 542.7°K
Steam Temperature at 100% Power	518.3°F <sup>#</sup>	518.3°F <sup>#</sup>	517.2°F 542.7°K
Feedwater Temperature	437.3°F	437.3°F	437.3°F 498.3°K
Hot Standby Water Level (Above Tubesheet)	490.5 inches	490.5 inches	~477.3 <sup>b</sup> inches
Water Level at 100% Power (Above Tubesheet)	506 inches	506 inches	~499.4 <sup>b</sup> inches
Feedwater Header Centerline (Above Tubesheet)	463.2 inches	463.2 inches	463.2 inches
FW Flow at 100% Power	3.87x10 <sup>6</sup> lb./hr <sup>c</sup>	3.87x10 <sup>6</sup> lb./hr <sup>c</sup>	3.87x10 <sup>6</sup> lb./hr <sup>c</sup> 487.6 kg/sec
TSP Δp Loss Coefficient (Using TSP Flow Area)	1.1	1.1	1.1
TSP Flow area	23.77 <sup>d</sup> ft <sup>2</sup>	23.77 <sup>d</sup> ft <sup>2</sup>	23.77 <sup>d</sup> ft <sup>2</sup> 2.2083 m <sup>2</sup>
Circulation Ratio at 100% Power	5.1	5.1	5.4
Break Opening Time	Instantaneous	Not specified	Instantaneous
MSLB Break Areas			
Guillotine Break	Full area guillotine not analyzed	4.6 ft <sup>2</sup>	4.6 ft <sup>2</sup> 0.4274 m <sup>2</sup>
Flow Restrictor-Limited Break	Guillotine break with 1.4 ft <sup>2</sup> restrictor	1.4 ft <sup>2</sup>	1.4 ft <sup>2</sup> 0.1301 m <sup>2</sup>
FW Guillotine Break	Not Analyzed	Not Analyzed	1.12 ft <sup>2</sup> 0.1038 m <sup>2</sup>
<b><u>Primary System Tubing</u></b>			
Primary Inlet Temperature	613.7°F	613.7°F	613.7°F 596.3K
Primary System Pressure	2250 psia	2250 psia	2250 psia 15.5132x10 <sup>6</sup> Pa
Primary Flow at 100% Power	88500 gpm	88500 gpm	88500 gpm 3747.4 kg/sec

<sup>a</sup> Calculated from TRAC-M steady-state conditions.

<sup>b</sup> The water level can only be approximated from the TRAC-M steady-state output, especially for the 100-Percent power case, because several steam generator volumes are two-phase.

<sup>c</sup> Obtained from "Steam Generator Standard Information Package," Westinghouse, January 4, 1982.

<sup>d</sup> Value provided by D. Merkovsky of Westinghouse in an e-mail message dated April 29, 2002.

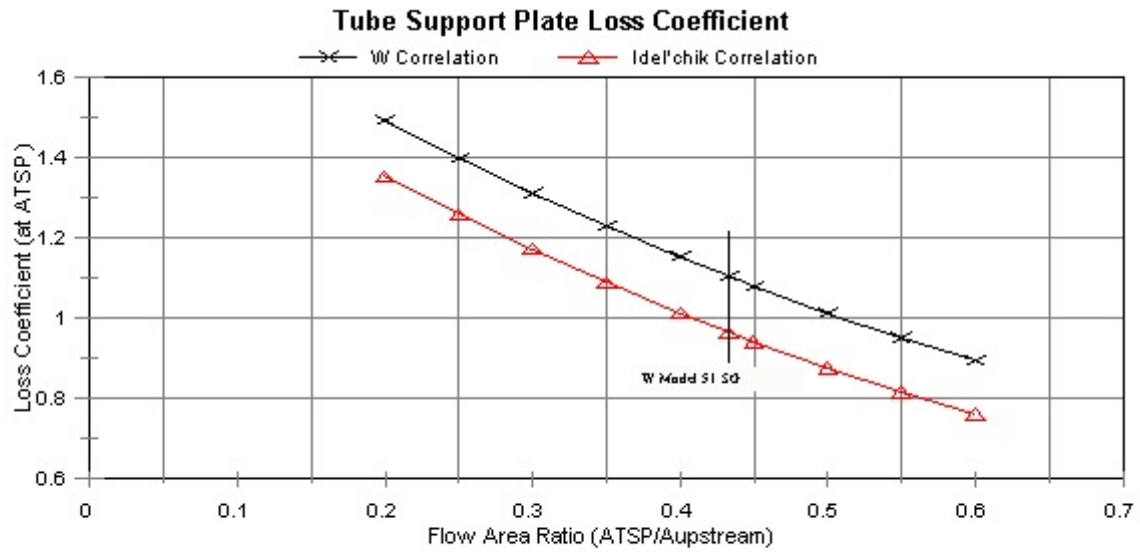


**Figure 4.1-3: Comparison of TSP Loss Coefficient Values Using the TSP Flow Area as a Reference**

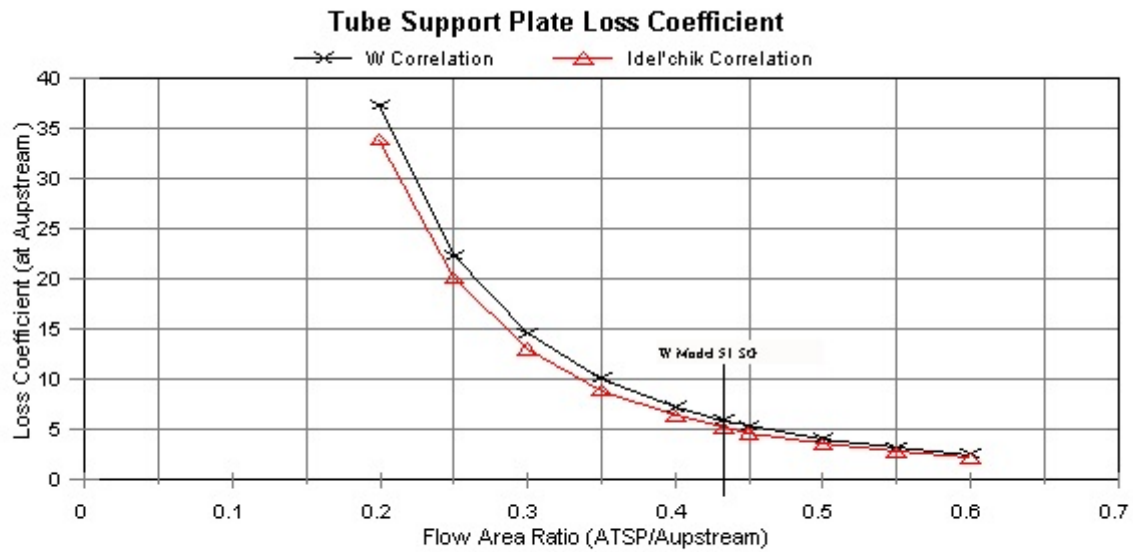


**Figure 4.1-4: Comparison of TSP Loss Coefficient Values Using the Flow Area Upstream of the TSP as a Reference**

The loading on each TSP and on the primary system tubing can be determined from the thermal-hydraulic conditions calculated using the TRAC-M code. Specifically, it can be shown that the pressure differential across a TSP or primary system tube can be calculated using the following equation. The pressure drop attributable to friction loss is the primary contributor to the pressure drop calculation. (Note that the subscript -1 indicates the previous timestep.)

$$\Delta p = \Delta p(\text{friction loss}) + \Delta p(\text{gravity head}) + \Delta p(\text{fluid acceleration})$$

$$\Delta p = K \frac{\rho_l v_l^2}{2} (1 - \alpha) + \rho_l g \Delta h (1 - \alpha) + \Delta h \frac{(\rho_l v_l (1 - \alpha) - (\rho_l v_l (1 - \alpha))_{-1})}{t - t_{-1}} + K \frac{\rho_v v_v^2}{2} \alpha + \rho_v g \Delta h \alpha + \Delta h \frac{(\rho_v v_v \alpha - (\rho_v v_v \alpha)_{-1})}{t - t_{-1}}$$

where  $\Delta p$  = pressure difference  
 $K$  = TSP irreversible loss coefficient  
 $v_l$  = liquid velocity through TSP  
 $\rho_l$  = liquid density  
 $\alpha$  = void fraction  
 $g$  = gravitational constant  
 $\Delta h$  = TSP thickness  
 $t$  = time  
 $v_v$  = vapor velocity through TSP  
 $\rho_v$  = vapor density

Subscripts

-1 = previous timestep

Table 4.1-2 compares the peak TSP differential pressures for initial hot standby conditions, calculated using TRANFLO and RELAP5 (as documented in Reference 1), and the TRAC-M computer code. These comparisons assumed that the steam generator was initially at hot standby because Reference 1 indicates that this condition provided the highest TSP loadings. In Reference 1, Westinghouse indicated that a multiplier of 1.5 should be applied to calculated nominal loads to account for uncertainties.

The peak loadings for the guillotine MSLB calculated using the TRAC-M code are close to the RELAP5 values. However, the RELAP5 results are larger than those calculated using the TRAC-M code. As previously stated, an analysis for a full guillotine MSLB using the TRANFLO code was not provided in Reference 1. For the limited-area MSLB, the TRAC-M results are close to the calculated TRANFLO results, but lower than the TRANFLO results with an uncertainty multiplier of 1.5. For the limited-area case, the TRAC-M results are comparable to or lower than the results calculated using RELAP5.

TRAC-M is a "best-estimate" computer code currently under development at the NRC, which can be applied to small- and large-break transients in both PWR and BWR designs. The TRAC-M code includes the latest available thermal-hydraulic model correlations applicable to PWR and BWR designs.

RELAP5 may also be classified as a "best-estimate" computer code specifically applicable to the analysis of small-break PWR transients. Additionally, RELAP5 may not adequately calculate thermal-hydraulic conditions when a large slip exists between phases. Therefore,



RELAP5 would not necessarily be capable of accurately predicting steam generator thermal-hydraulic conditions for larger break flows and, consequently, may not accurately calculate forces on the steam generator TSPs.

The TRANFLO computer code uses an elemental one-dimensional control volume approach to determine thermal-hydraulic conditions in a steam-water system undergoing rapid transients.

It should be noted that Version 3.1031 of the TRAC-M code, which was used to perform the steam generator analyses, does not currently include a two-phase pressure drop correction for irreversible form losses such as the TSP loss coefficient. Consequently, the current TRAC-M-calculated TSP pressure drops are probably underestimated. Therefore, it is recommended that a multiplier of 1.2 be used for the TSP pressure differentials determined by TRAC-M.

**Table 4.1-2: Comparisons of the TSP Peak Differential Pressures<sup>a</sup> with the System Initially at Hot Standby**

	<b>4.6 ft<sup>2</sup> MSLB TRANFLO</b>	<b>4.6 ft<sup>2</sup> MSLB RELAP5 Case LB2<sup>c</sup></b>	<b>4.6 ft<sup>2</sup> MSLB TRAC-M</b>
TSP 7 (top)	Not analyzed	9.6 psi	8.57 psi
TSP 6	Not analyzed	8.1 psi	5.06 psi
TSP 5	Not analyzed	6.1 psi	3.84 psi
TSP 4	Not analyzed	4.5 psi	2.63 psi
TSP 3	Not analyzed	3.2 psi	1.16 psi
TSP 2	Not analyzed	2.0 psi	0.15 psi
TSP 1 (bottom)	Not analyzed	1.9 psi	-0.33 psi
	<b>1.4 ft<sup>2</sup> MSLB TRANFLO Case 1<sup>c</sup></b>	<b>1.4 ft<sup>2</sup> MSLB RELAP5 Case SB2<sup>c</sup></b>	<b>1.4 ft<sup>2</sup> MSLB TRAC-M</b>
TSP 7 (top)	2.46 psi (3.69 <sup>b</sup> psi)	2.26 psi	2.68 psi
TSP 6	1.82 psi (2.73 <sup>b</sup> psi)	2.14 psi	1.70 psi
TSP 5	1.25 psi (1.88 <sup>b</sup> psi)	1.56 psi	1.23 psi
TSP 4	0.91 psi (1.37 <sup>b</sup> psi)	1.35 psi	0.87 psi
TSP 3	0.58 psi (0.87 <sup>b</sup> psi)	1.23 psi	0.43 psi
TSP 2	0.31 psi (0.47 <sup>b</sup> psi)	1.25 psi	0.08 psi
TSP 1 (bottom)	-0.12 psi (-0.18 <sup>b</sup> psi)	1.12 psi	-0.06 psi

<sup>a</sup> An upward directed pressure differential is defined as positive.

<sup>b</sup> TRANFLO values with Westinghouse recommended uncertainty multiplier of 1.5.

<sup>c</sup> Identifier from Westinghouse report, Reference 1.

The steam generator analyses using TRAC-M were performed for a larger number of conditions than reported in the Westinghouse report. Specifically, the following six cases were analyzed:

- (1) Guillotine (4.6 ft<sup>2</sup>) MSLB at Hot Standby Conditions
- (2) Flow Restrictor-Limited (1.4 ft<sup>2</sup>) MSLB at Hot Standby Conditions
- (3) Guillotine (1.12 ft<sup>2</sup>) FWLB at Hot Standby Conditions
- (4) Guillotine (4.6 ft<sup>2</sup>) MSLB at 100-Percent Power Conditions
- (5) Flow Restrictor-Limited (1.4 ft<sup>2</sup>) MSLB at 100-Percent Power Conditions
- (6) Guillotine (1.12 ft<sup>2</sup>) FWLB at 100-Percent Power Conditions

Table 4.1-3 presents the TRAC-M-calculated peak pressure differential loadings across the TSPs for each of the six cases analyzed. The results indicate that the peak TSP loadings result from an MSLB with the steam generator initially at hot standby conditions. As expected, the TSP loadings resulting from a guillotine MSLB are larger than those resulting from an MSLB with the break area limited by the steam line flow restrictor. The peak TSP loadings resulting from an FWLB occur when the steam generator is initially at 100-percent power, and are substantially lower than those resulting from an MSLB.

It should be noted that the TRAC-M calculations include the effects of steam generator “pool swell”. Specifically, the TRAC-M results include the effects of flow increases through the TSPs caused by the “swelling” of the fluid in the tube bundle region, which result from water flashing following the pressure decrease.

**Table 4.1-3: TSP Peak Pressure Differentials<sup>a</sup> Calculated Using TRAC-M**

	<u>Initial Hot Standby Conditions</u>		
	<b>4.6 ft<sup>2</sup> MSLB</b>	<b>1.4 ft<sup>2</sup> MSLB</b>	<b>1.12 ft<sup>2</sup> FWLB</b>
TSP 7 (top)	8.57 psi	2.68 psi	0.050 psi
TSP 6	5.06 psi	1.70 psi	0.041 psi
TSP 5	3.84 psi	1.23 psi	0.034 psi
TSP 4	2.63 psi	0.87 psi	0.030 psi
TSP 3	1.16 psi	0.43 psi	0.026 psi
TSP 2	0.15 psi	0.08 psi	0.022 psi
TSP 1 (bottom)	-0.33 psi	-0.06 psi	0.021 psi
	<u>Initial 100-Percent Power Condition</u>		
	<b>4.6 ft<sup>2</sup> MSLB</b>	<b>1.4 ft<sup>2</sup> MSLB</b>	<b>1.12 ft<sup>2</sup> FWLB</b>
TSP 7 (top)	6.82 psi	1.49 psi	0.42 psi
TSP 6	5.41 psi	1.27 psi	0.36 psi
TSP 5	4.34 psi	1.09 psi	0.31 psi
TSP 4	3.20 psi	0.87 psi	0.27 psi
TSP 3	1.91 psi	0.61 psi	0.23 psi
TSP 2	0.79 psi	0.33 psi	0.19 psi
TSP 1 (bottom)	0.16 psi	0.21 psi	0.20 psi

<sup>a</sup> An upward-directed pressure differential is defined as positive.

Because the purpose of generating the TSP loadings is to provide input into a structural assessment of the primary tubing, it was considered appropriate to calculate the peak forces on the primary tube resulting from cross-flow across the tubes at the steam generator bottom, and from flow across the tubes where the tubes bend. Peak forces across the tubes were determined using the same pressure drop equation used in calculating the TSP pressure differentials. The irreversible loss coefficient for a single primary tube at each considered location has been calculated using the appropriate geometries used in a correlation from Reference 3. Table 4.1-4 lists the maximum pressure differentials across a single primary tube at the two locations for the six analyzed cases. Because the primary tubing pressure differentials are calculated using an irreversible loss coefficient, it is recommended that a multiplier of 1.2 be used to account for the lack of a two-phase pressure drop multiplier in the current version of the TRAC-M code. (A 20-percent margin is recommended because this value is the generally accepted accuracy of two-phase flow pressure drop correlations.)

**Table 4.1-4: Primary Tubing Peak Pressure Differentials Calculated Using the TRAC-M Code**

	<b>Initial Hot Standby Conditions</b>		
	<b>4.6 ft<sup>2</sup> MSLB</b>	<b>1.4 ft<sup>2</sup> MSLB</b>	<b>1.12 ft<sup>2</sup> FWLB</b>
At SG Bottom <sup>a</sup>	-0.28 psi	-0.08 psi	-0.004 psi
At Primary Tube Bend <sup>b</sup>	1.05 psi	0.33 psi	0.029 psi
	<b>Initial 100-Percent Power Condition</b>		
	<b>4.6 ft<sup>2</sup> MSLB</b>	<b>1.4 ft<sup>2</sup> MSLB</b>	<b>1.12 ft<sup>2</sup> FWLB</b>
At SG Bottom <sup>a</sup>	-0.13 psi	0.04 psi	0.058 psi
At Primary Tube Bend <sup>b</sup>	0.71 psi	0.13 psi	0.043 psi

<sup>a</sup> A horizontal, radially directed inward force is defined as positive.

<sup>b</sup> An upward force is defined as positive.

The TSPs are supported by the cylindrical shroud between the steam generator central region containing the primary tubes and the surrounding annular flow area through which feedwater flows. Consequently, the pressure drop loadings on this cylindrical shroud have also been determined for the six analyzed cases. These pressure differentials are determined by subtracting the transient pressure in the annular region from the pressure inside the cylindrical shroud at eight vertical elevations, consistent with the center points of the associated eight vertical volumes (see Figures 4.1-1 and 4.1-2). As shown in Table 4.1-5, the pressure drop loadings on this structure following a line break are significant.

**Table 4.1-5: Peak Pressure Differentials<sup>a</sup> Across the Cylindrical Shroud Calculated Using the TRAC-M Code**

	<b>Initial Hot Standby Conditions</b>		
	<b>4.6 ft<sup>2</sup> MSLB</b>	<b>1.4 ft<sup>2</sup> MSLB</b>	<b>1.12 ft<sup>2</sup> FWLB</b>
	<b>Min. / Max.</b>	<b>Min. / Max.</b>	<b>Maximum</b>
p2009-p1009 (top)	-1.42 / 50.5 psi	-0.78 / 13.8 psi	1.87 psi
p2008-p1008	-0.60 / 50.0 psi	-0.69 / 13.3 psi	1.56 psi
p2007-p1007	-0.48 / 45.4 psi	-0.81 / 12.8 psi	1.34 psi
p2006-p1006	-0.47 / 39.4 psi	-0.84 / 11.7 psi	1.17 psi
p2005-p1005	-0.37 / 33.4 psi	-0.90 / 10.0 psi	0.97 psi
p2004-p1004	-0.28 / 27.1 psi	-0.79 / 7.89 psi	0.73 psi
p2003-p1003	-0.20 / 20.0 psi	-0.31 / 5.44 psi	0.45 psi
p2002-p1002 (bottom)	-0.16 / 15.2 psi	-0.18 / 3.61 psi	0.22 psi
	<b>Initial 100-Percent Power Condition</b>		
	<b>4.6 ft<sup>2</sup> MSLB</b>	<b>1.4 ft<sup>2</sup> MSLB</b>	<b>1.12 ft<sup>2</sup> FWLB</b>
	<b>Min. / Max.</b>	<b>Min. / Max.</b>	<b>Min. / Max.</b>
p2009-p1009 (top)	-2.40 / 38.5 psi	-0.38 / 7.24 psi	-3.41 / 2.05 psi
p2008-p1008	-2.83 / 38.1 psi	8.76 psi	-1.65 / 4.29 psi
p2007-p1007	-3.07 / 35.5 psi	8.17 psi	-1.91 / 3.78 psi
p2006-p1006	-2.91 / 31.8 psi	7.30 psi	-1.93 / 2.99 psi
p2005-p1005	-2.59 / 26.9 psi	6.18 psi	-1.77 / 2.22 psi
p2004-p1004	-1.90 / 21.1 psi	4.94 psi	-1.58 / 1.75 psi
p2003-p1003	-1.09 / 14.0 psi	3.54 psi	-1.01 / 1.43 psi
p2002-p1002 (bottom)	-0.51 / 6.67 psi	2.14 psi	1.39 psi

<sup>a</sup> Radially outward pressure is defined as positive.

In order to determine the effects of a line break on the integrity of the steam generator primary tubing, it is essential to consider all forces that can be transmitted to the primary tubing. Therefore, as a minimum, a structural assessment of the primary tubing following a line break should consider the effects of the following three forces:

- (1) fluid forces on the TSP which are transmitted to the primary tubing
- (2) fluid forces acting directly on the primary tubing
- (3) the effect of the cylindrical shroud loading on the support of the TSP

Figures 4.1-5 through 4.1-22 plot the considered steam generator loadings following an MSLB or FWLB, calculated using the TRAC-M computer code. These figures provide transient plots of the TSP pressure differentials, pressure differentials across the primary system tubing at the steam generator bottom and at the upper tube bending area, and pressure differentials across the cylinder shroud separating the annular area and the steam generator tube volumes.

Figures 4.1-23 and 4.1-24 show the steam generator pressure response and flowrate transient following the 4.6 ft<sup>2</sup> MSLB at hot standby conditions, which results in the largest TSP loadings.

Figure 4.1-23 plots the break flow, and the flows at the top of the tube bundle region and the top of the annular feedwater region. This figure indicates that the largest flowrate increase occurs during the first second following the pipe break. Figure 4.1-24 demonstrates the pressure response at the top and bottom of the tube bundle region and the annular feedwater region, and at the break volume. The pressure response plot shows that the largest pressure increase and the greatest pressure differentials occur during the first second following the pipe break. (Refer to Figures 4.1-1 and 4.1-2 for help identifying the locations of the plotted parameters.)

As previously indicated, all TRAC-M analyses considered the effects of fluid “swelling” in the tube bundle region. In order to illustrate this effect, Figure 4.1-25 shows the void fraction calculated by the TRAC-M code for the break case that supplied the largest TSP loadings, namely the 4.6 ft<sup>2</sup> MSLB at hot standby conditions. This figure plots the calculated void fraction transients for volumes 2001 through 2009 (identified in Figures 4.1-1 and 4.1-2) for the first 10-seconds following the break. Note that the largest TSP loads occurred less than 1-second after initiation of the break. Figure 4.1-26 plots the TRAC-M-calculated void fractions in the annular feedwater region surrounding the cylindrical shroud. These figures indicate that, especially during the first second following the pipe break, significant amounts of liquid flash into steam as the steam generator pressure decreases.

Again, note that the largest pressure drops and differentials, the largest flowrate increase, and the largest void fraction increase rates in the tube bundle region occur within the first second following a pipe break. This is also the time period for the occurrence of the largest loading on the TSPs. These observances suggest that the largest loadings on the TSPs are attributable to the travel of the depressurization wave at acoustic velocity, which occurs during the first few seconds following the pipe break. The fluid “swelling” effect appears to be a secondary contributor to the TSP loadings. The depressurization wave travel effects addressed in the next section provide insights regarding the importance of the acoustic effects on steam generator internals following a pipe break.

#### 4.1.1 References

- (1) “**Model 51 Steam Generator Limited Tube Support Plate Displacement Analysis for Dented or Packed Tube to Tube Support Plate Crevices,**” Westinghouse, WCAP-14707, August 1996.
- (2) **Model 51 Steam Generator Limited Tube Support Plate Displacement Analysis for Dented or Packed Tube to Tube Support Plate Crevices,** Westinghouse, WCAP-14707, Revision 1, April 1997.
- (3) **Handbook of Hydraulic Resistance,** Idel’chek, I. E., U. S. Department of Commerce, AEC-TR-6630, 1966.

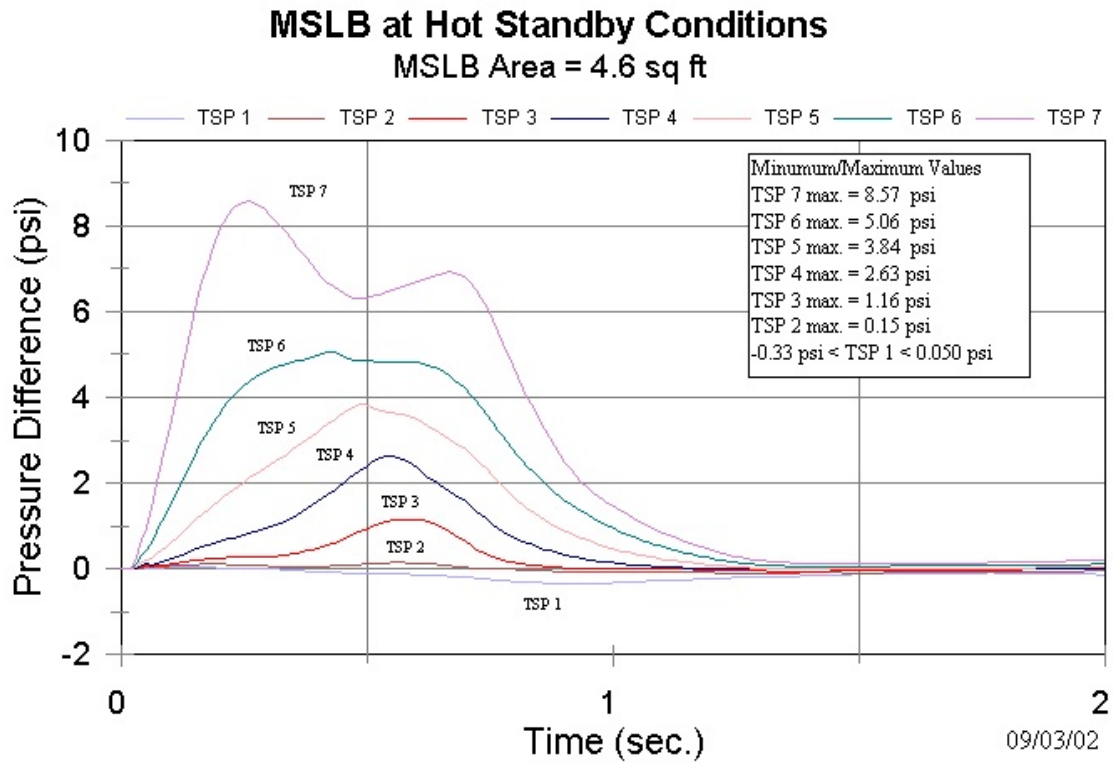


**Figure 4.1-5: TSP Pressure Differentials Following a Guillotine MSLB at Hot Standby**

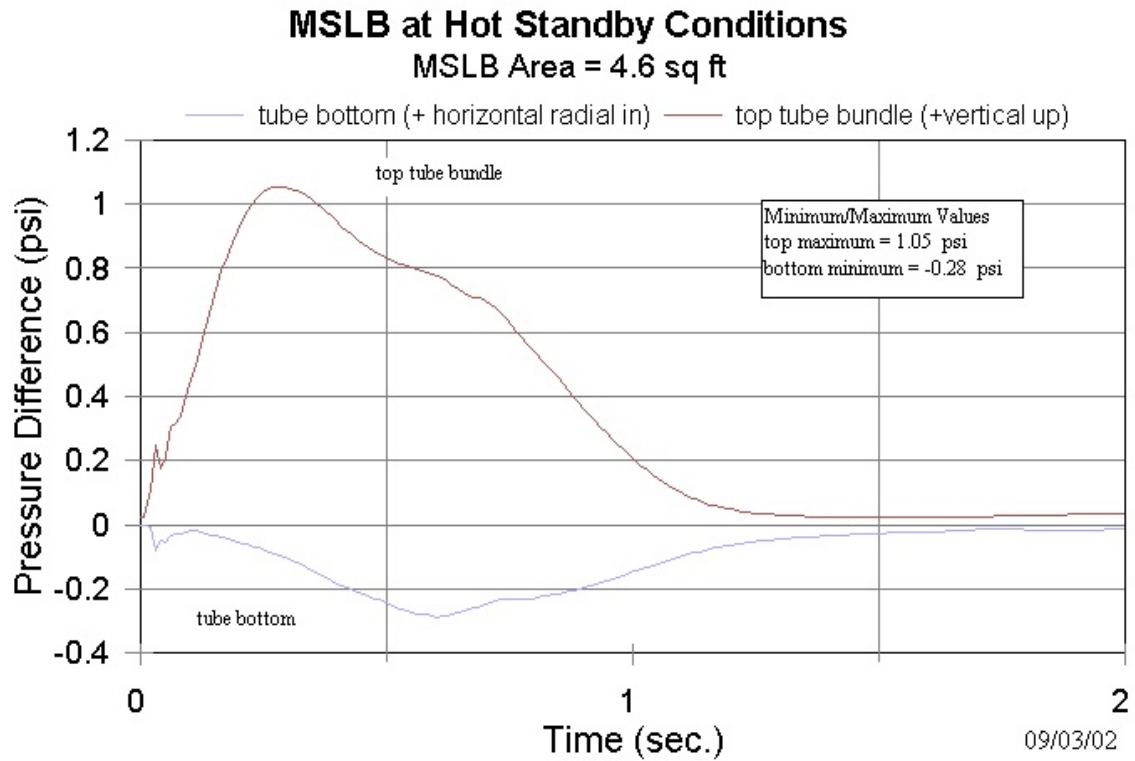


**Figure 4.1-6: Primary Tube Pressure Differentials Following a Guillotine MSLB at Hot Standby**

## MSLB at Hot Standby Conditions

MSLB Area = 4.6 sq ft

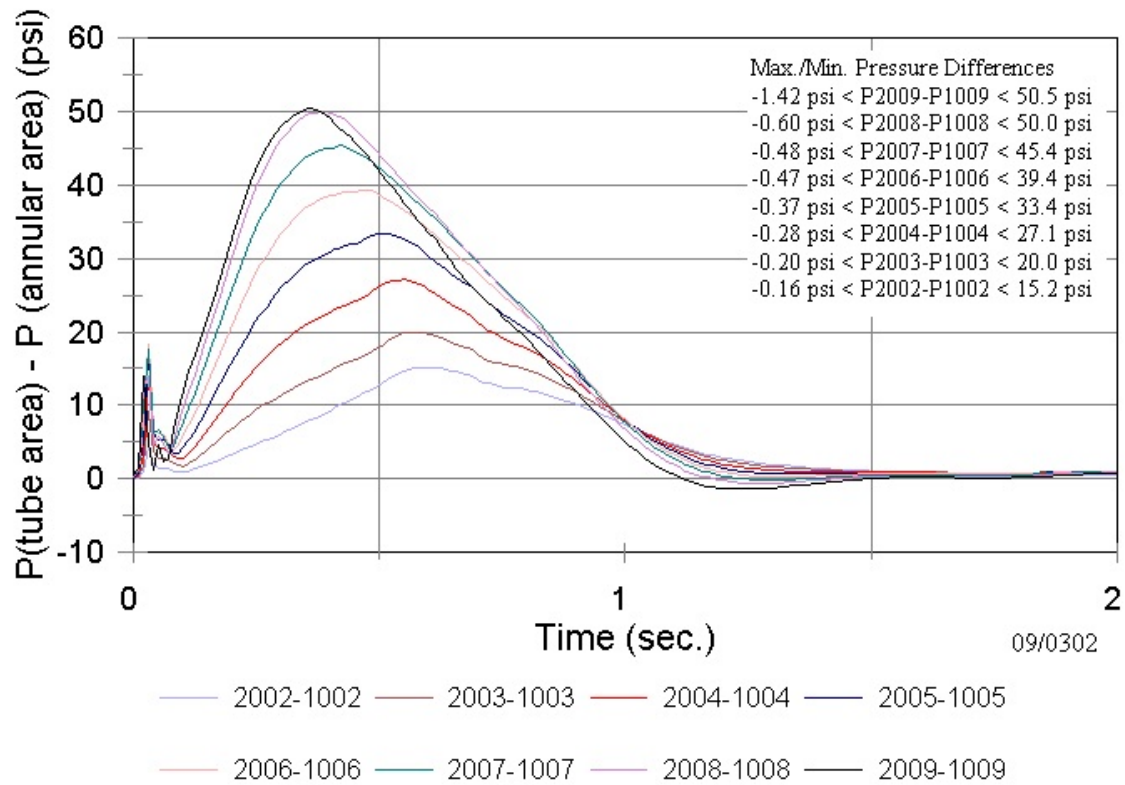


**Figure 4.1-7: Steam Generator Cylinder Pressure Differentials Following a Guillotine MSLB at Hot Standby**



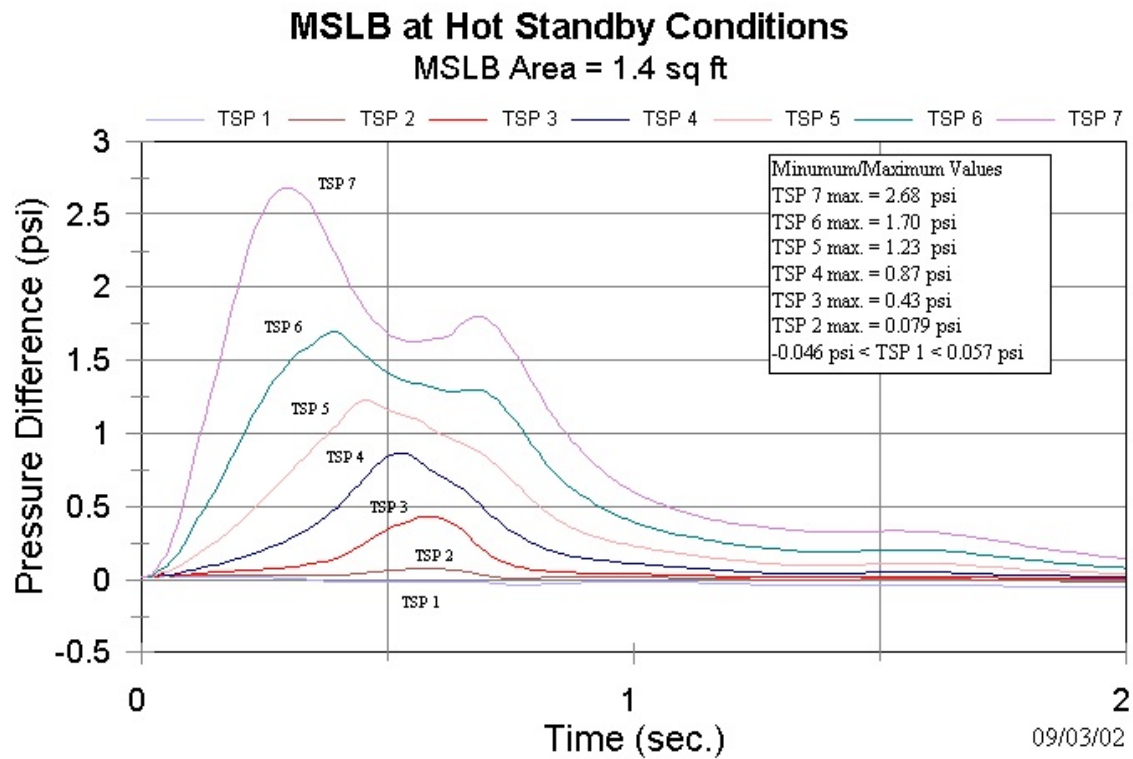
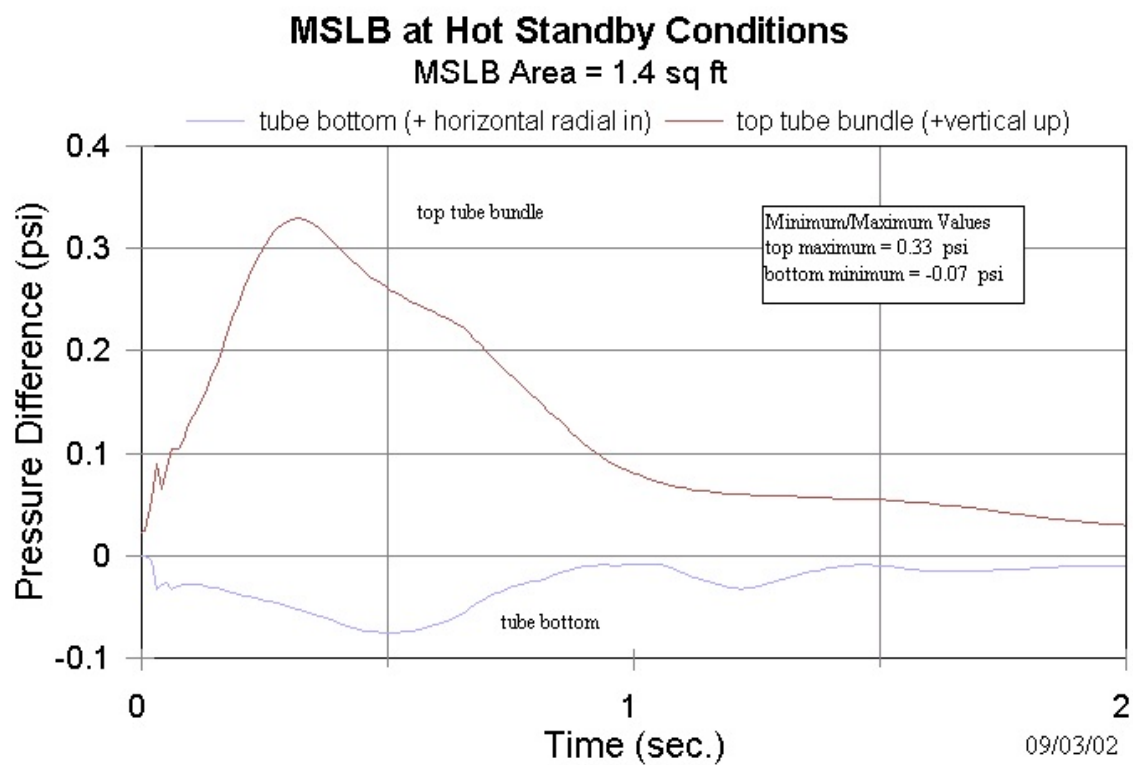


Figure 4.1-8: TSP Pressure Differentials for a Restrictor-Limited MSLB at Hot Standby



**Figure 4.1-9: Primary Tube Pressure Differentials for a Restrictor-Limited MSLB at Hot Standby**

## MSLB at Hot Standby Conditions

MSLB Area = 1.4 sq ft

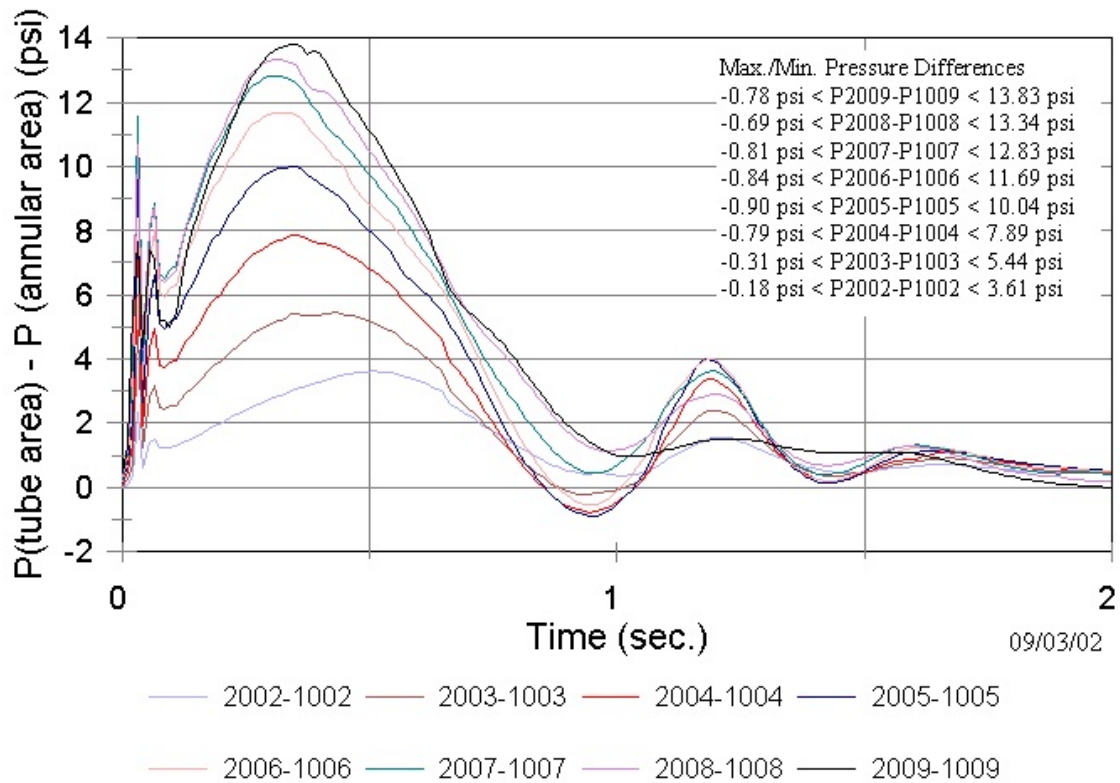


**Figure 4.1-10: Steam Generator Cylinder Pressure Differentials for a Restrictor-Limited MSLB at Hot Standby**

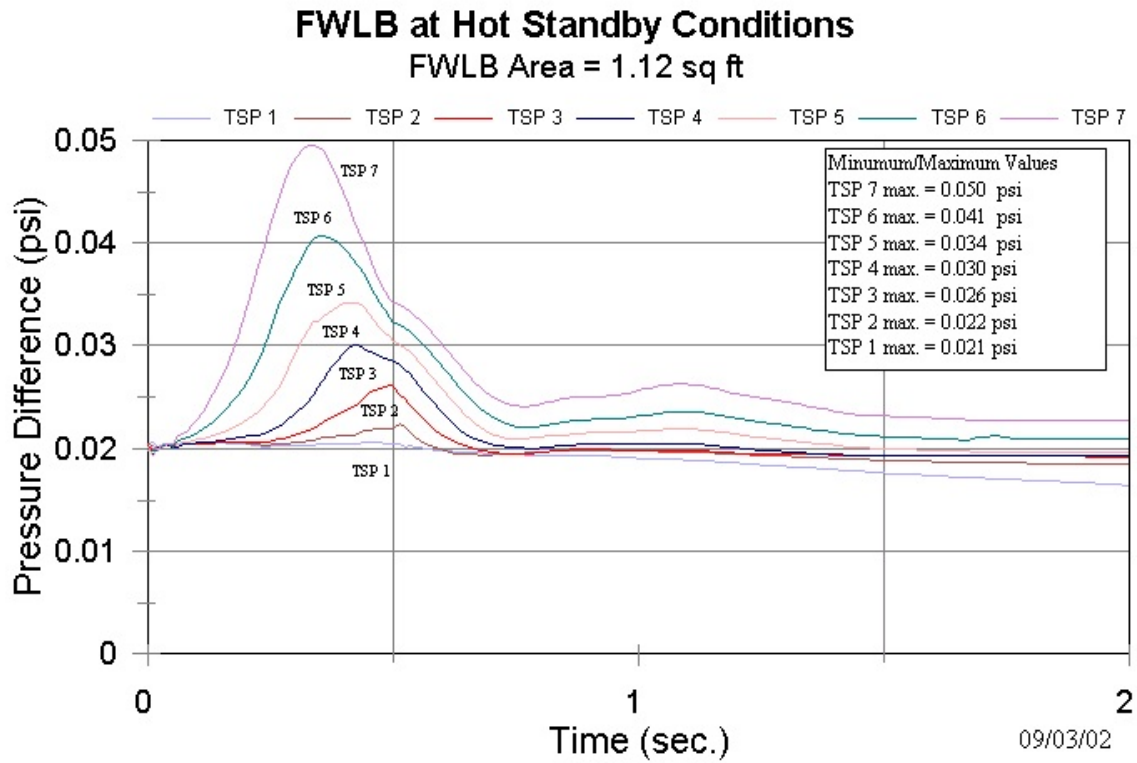
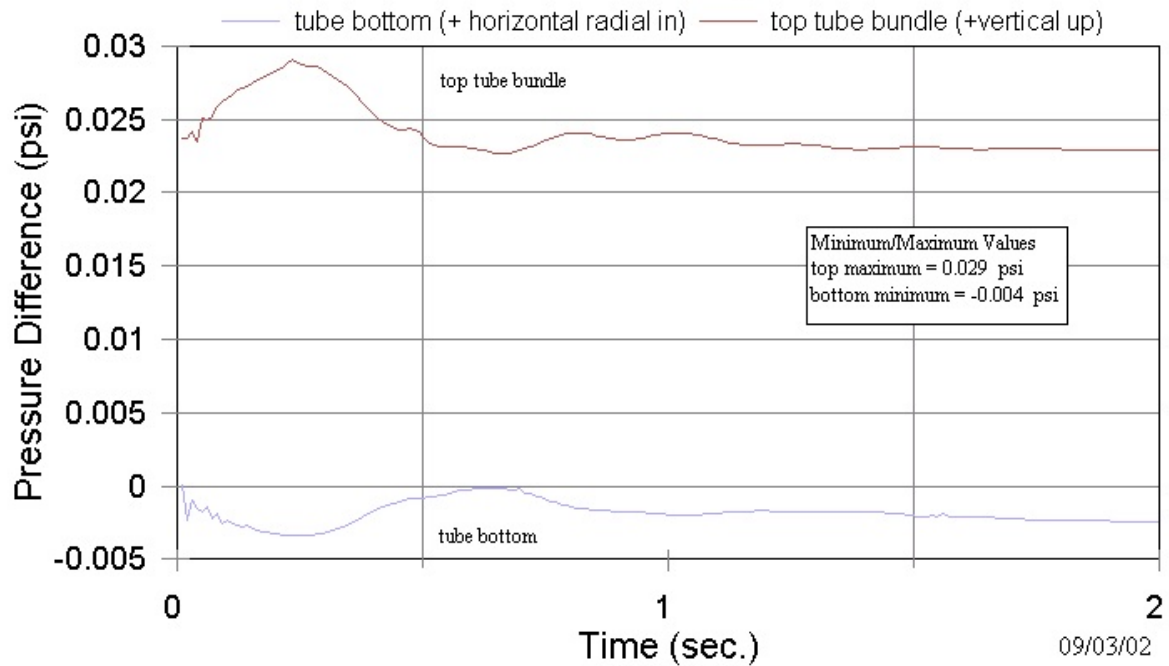


Figure 4.1-11: TSP Pressure Differentials Following a Guillotine FWLB at Hot Standby

## FWLB at Hot Standby Conditions

FWLB Area = 1.12 sq ft



**Figure 4.1-12: Primary Tube Pressure Differentials Following a Guillotine FWLB at Hot Standby**

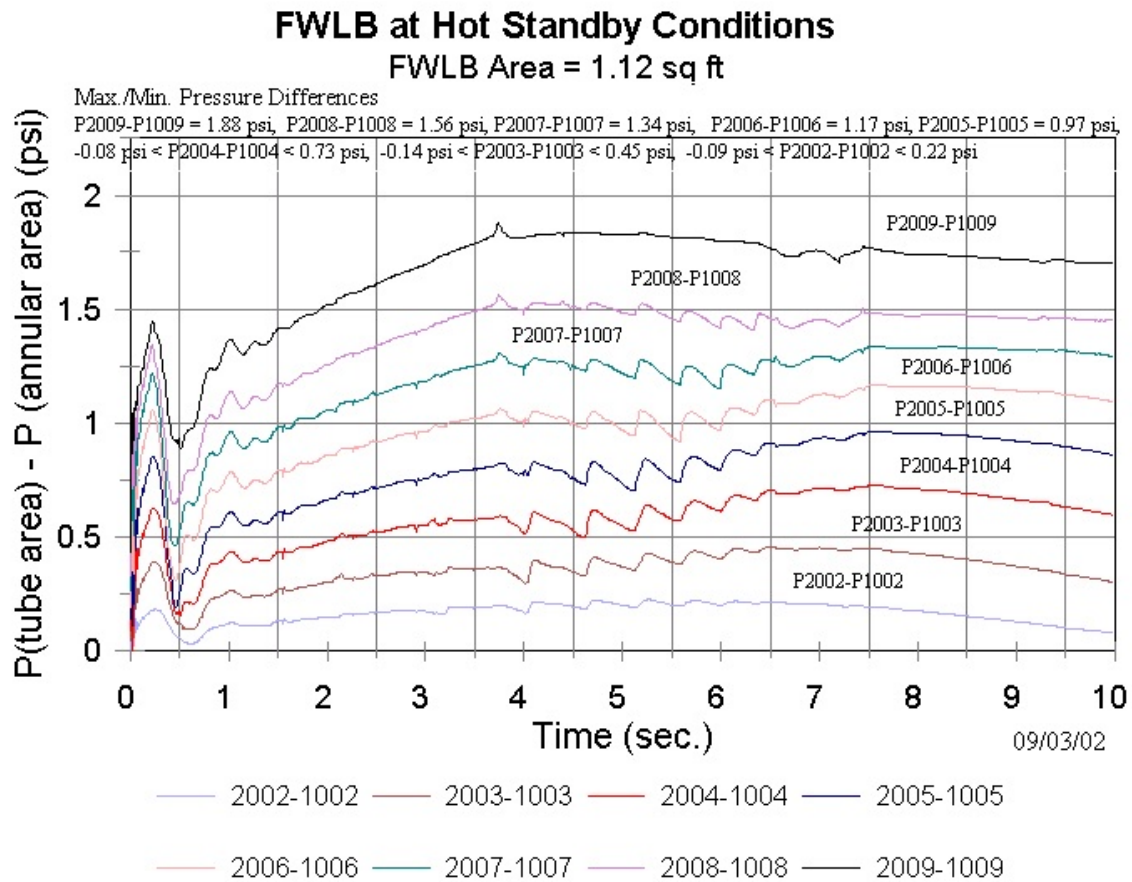


**Figure 4.1-13: Steam Generator Cylinder Pressure Differentials Following a Guillotine FWLB at Hot Standby**

## MSLB at 100% Power Conditions

MSLB Area = 4.6 sq ft

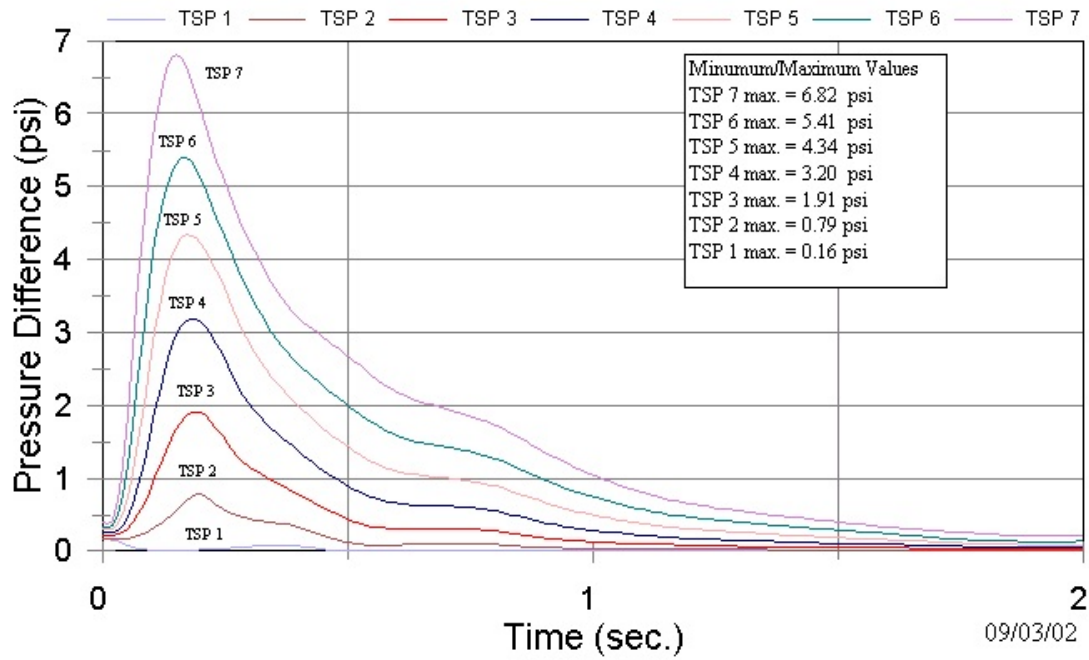
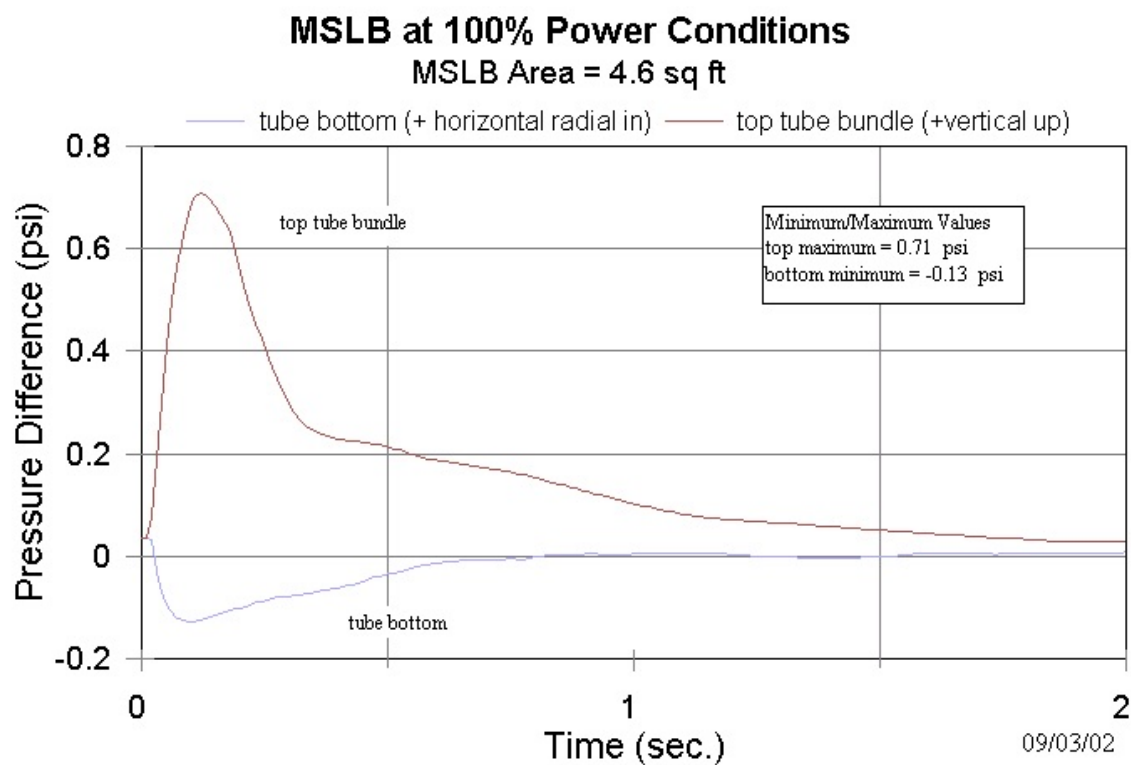


Figure 4.1-14: TSP Pressure Differentials Following a Guillotine MSLB at 100-Percent Power



**Figure 4.1-15: Primary Tube Pressure Differentials Following a Guillotine MSLB at 100-Percent Power**



## MSLB at 100% Power Conditions

MSLB Area = 4.6 sq ft

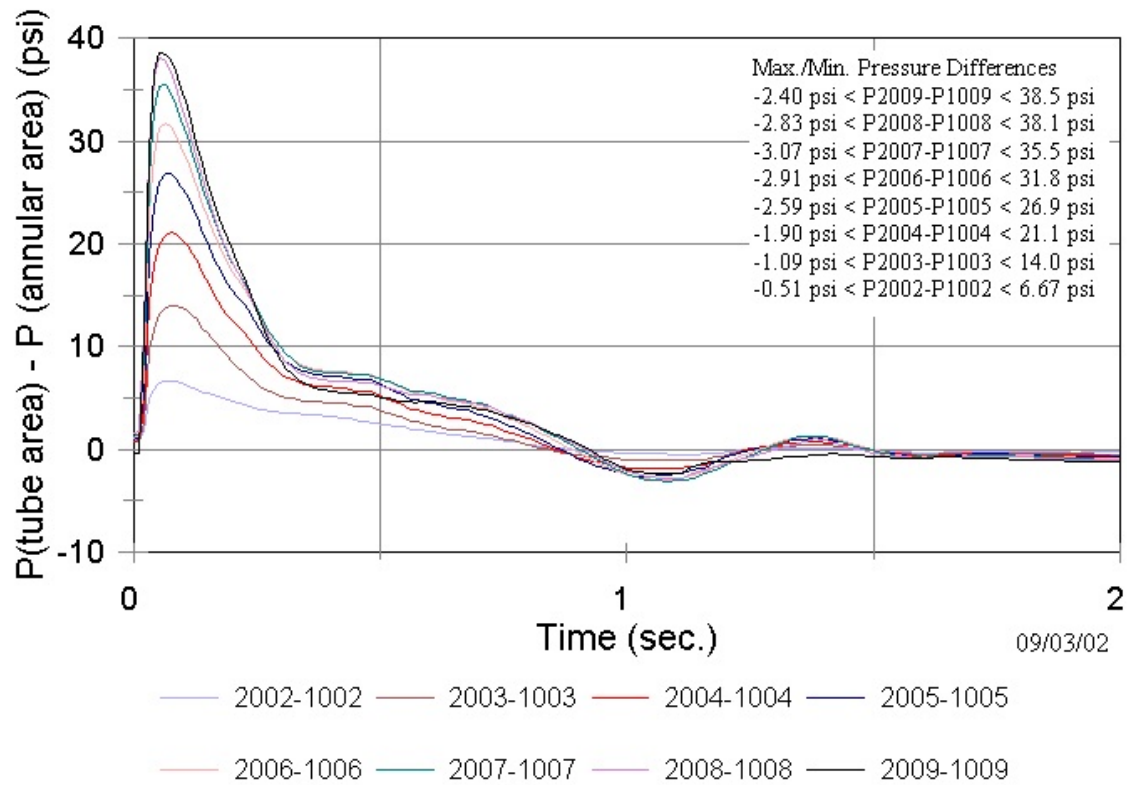


**Figure 4.1-16: Steam Generator Cylinder Pressure Differentials Following a Guillotine MSLB at 100-Percent Power**

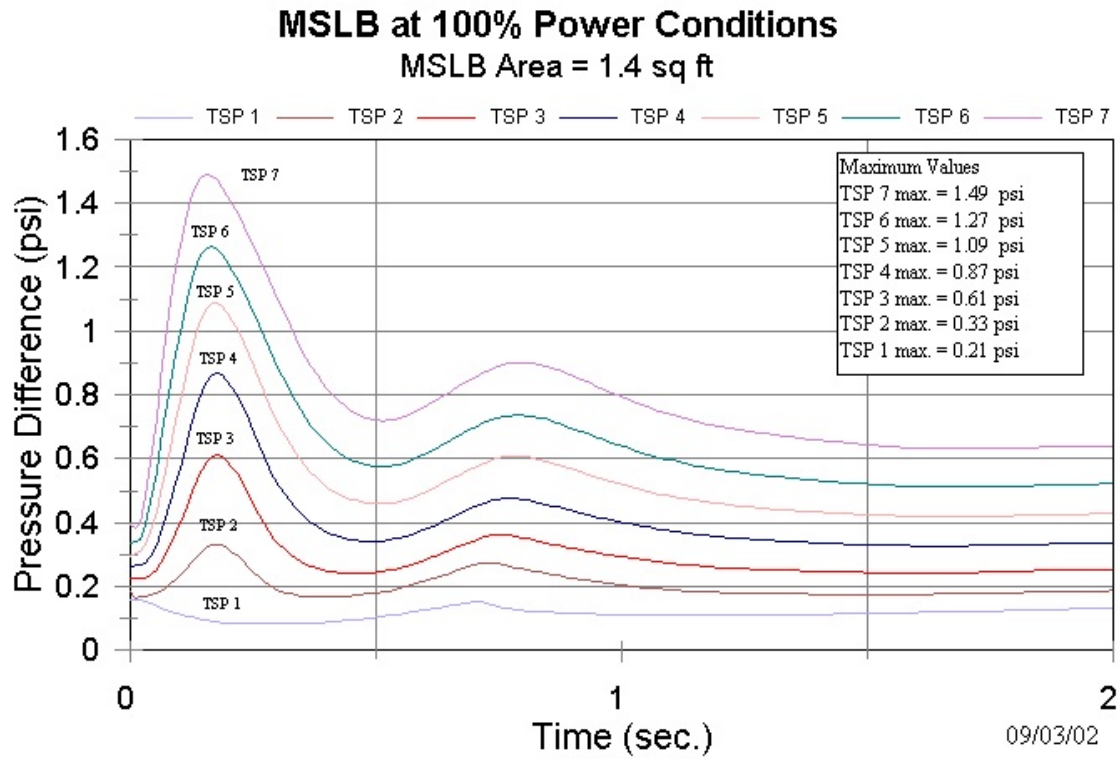


**Figure 4.1-17: TSP Pressure Differentials for a Restrictor-Limited MSLB at 100-Percent Power**

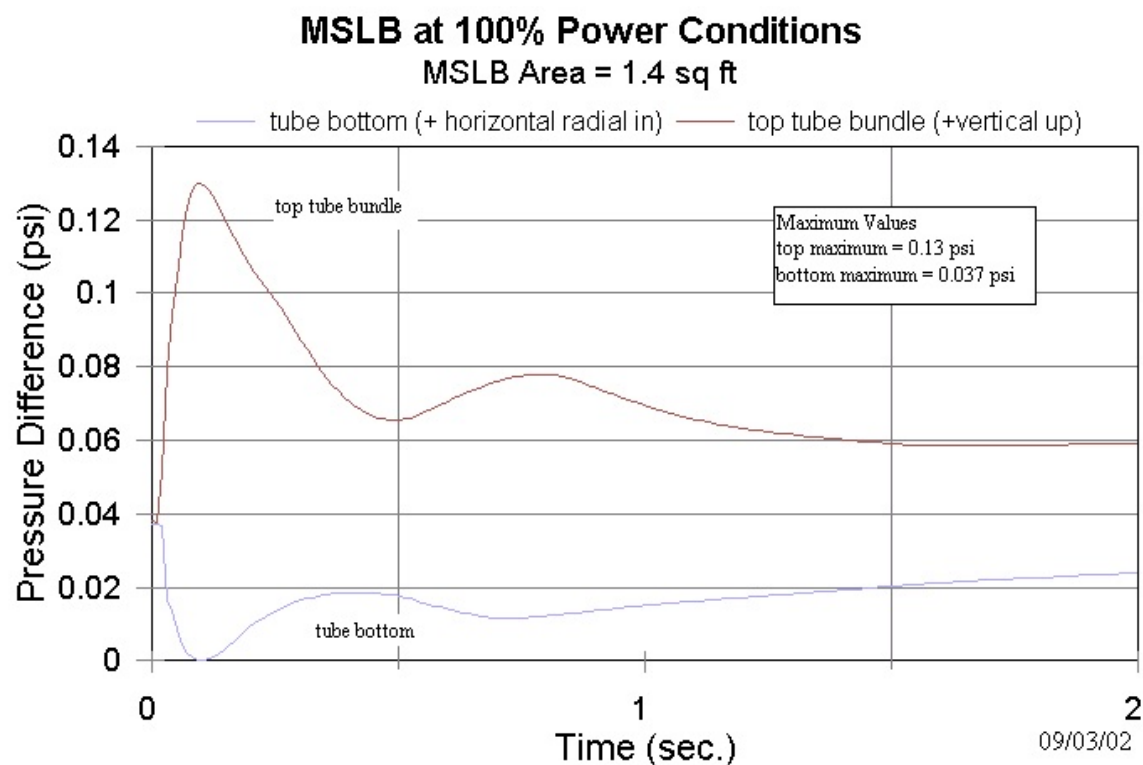


**Figure 4.1-18: Primary Tube Pressure Differentials for a Restrictor-Limited MSLB at 100-Percent Power**

## MSLB at 100% Power Conditions

MSLB Area = 1.4 sq ft

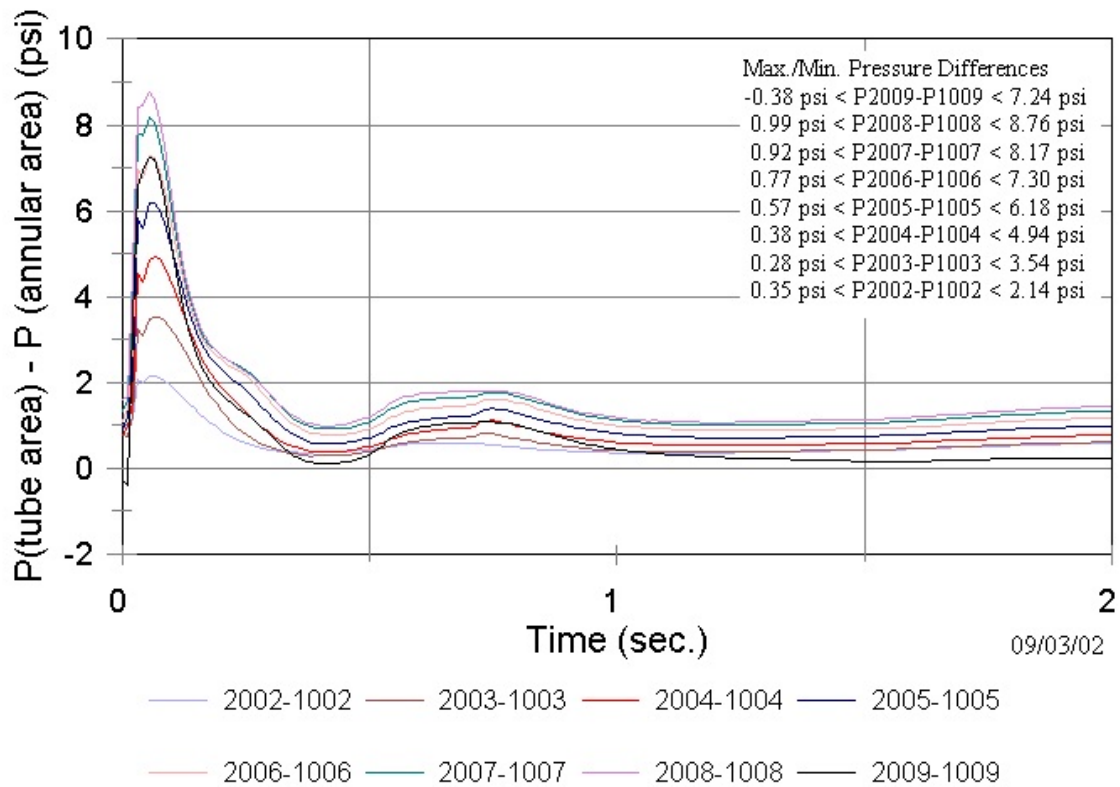


**Figure 4.1-19: Steam Generator Cylinder Pressure Differentials for a Restrictor-Limited MSLB at 100-Percent Power**

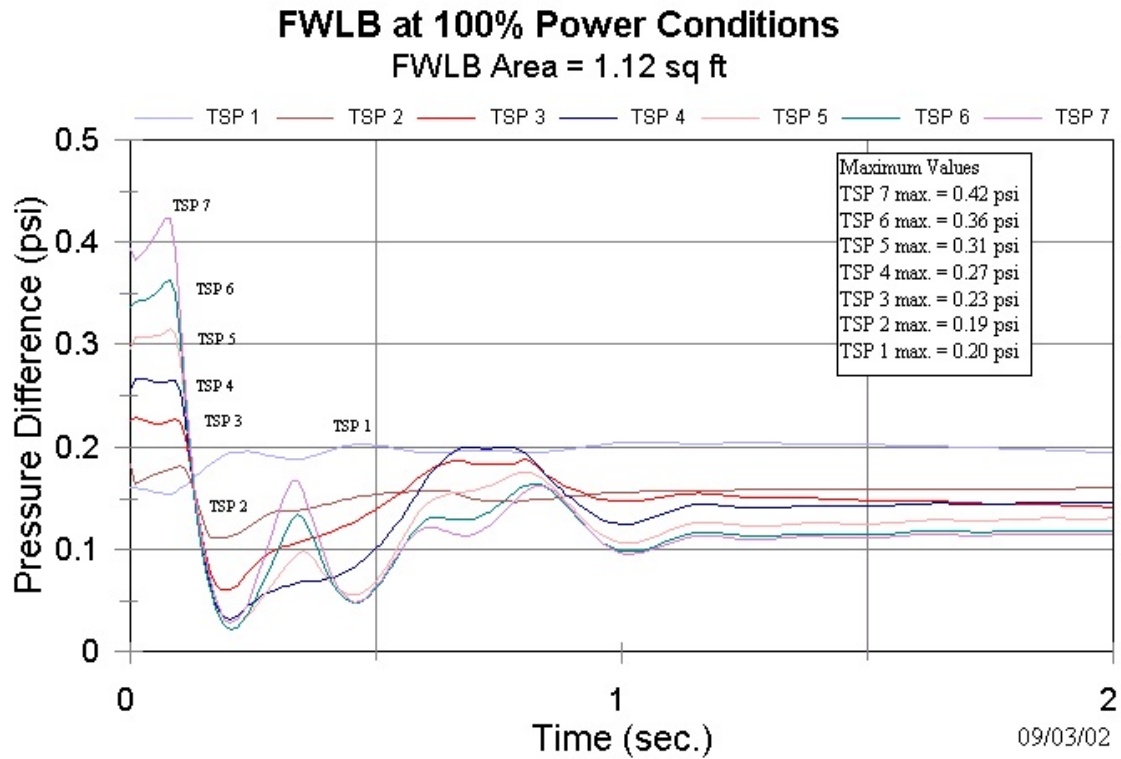


**Figure 4.1-20: TSP Pressure Differentials Following a Guillotine FWLB at 100-Percent Power**

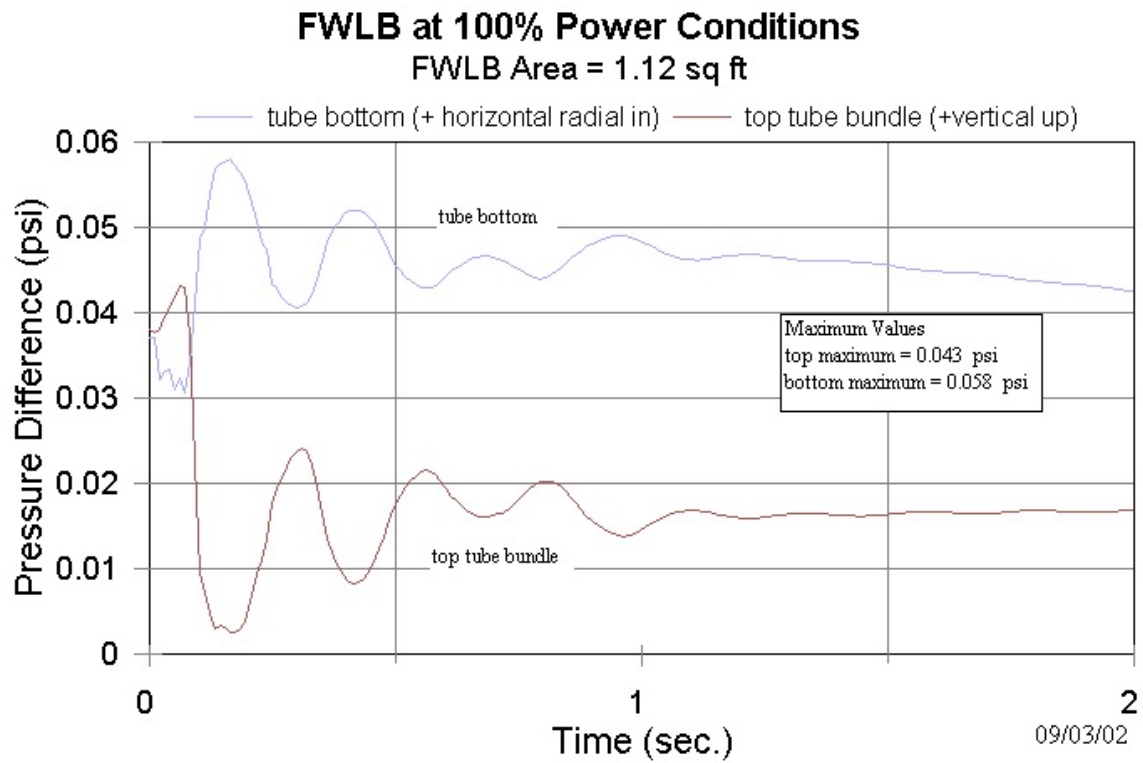


**Figure 4.1-21: Primary Tube Pressure Differentials Following a Guillotine FWLB at 100-Percent Power**

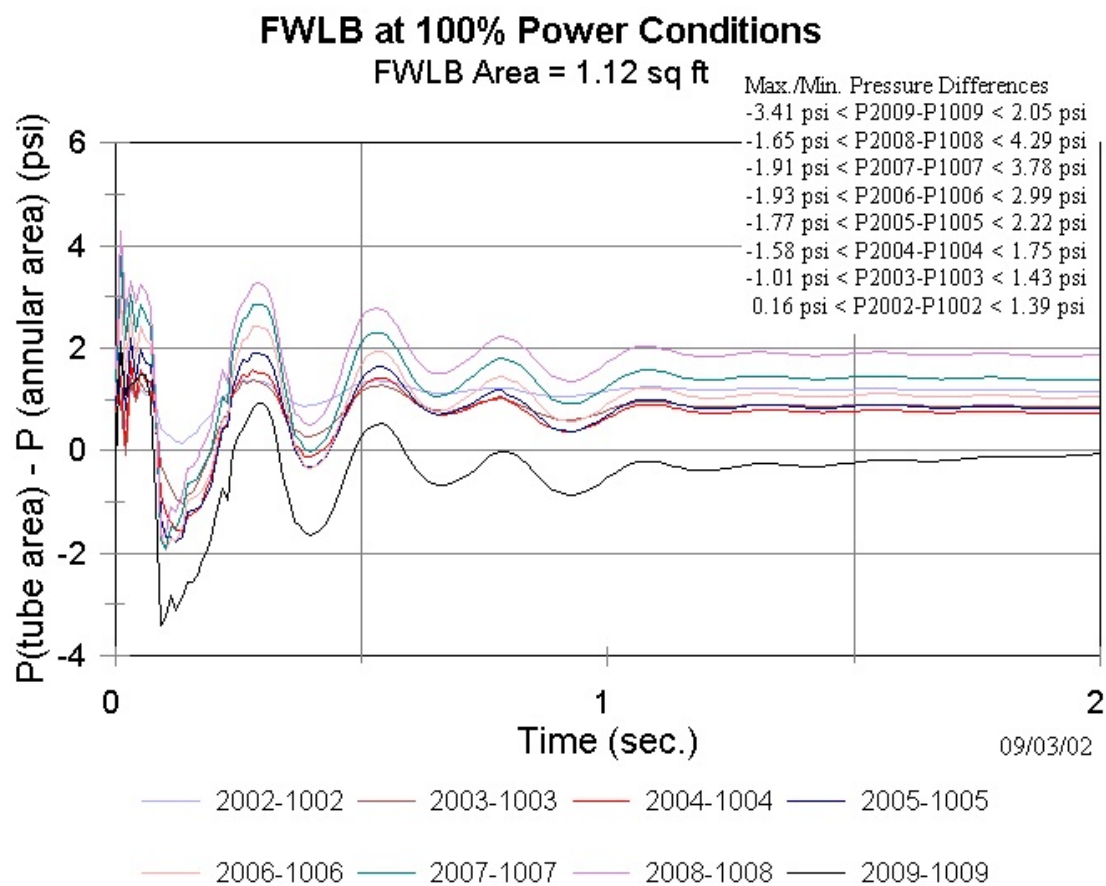


**Figure 4.1-22: Steam Generator Cylinder Pressure Differentials Following a Guillotine FWLB at 100-Percent Power**

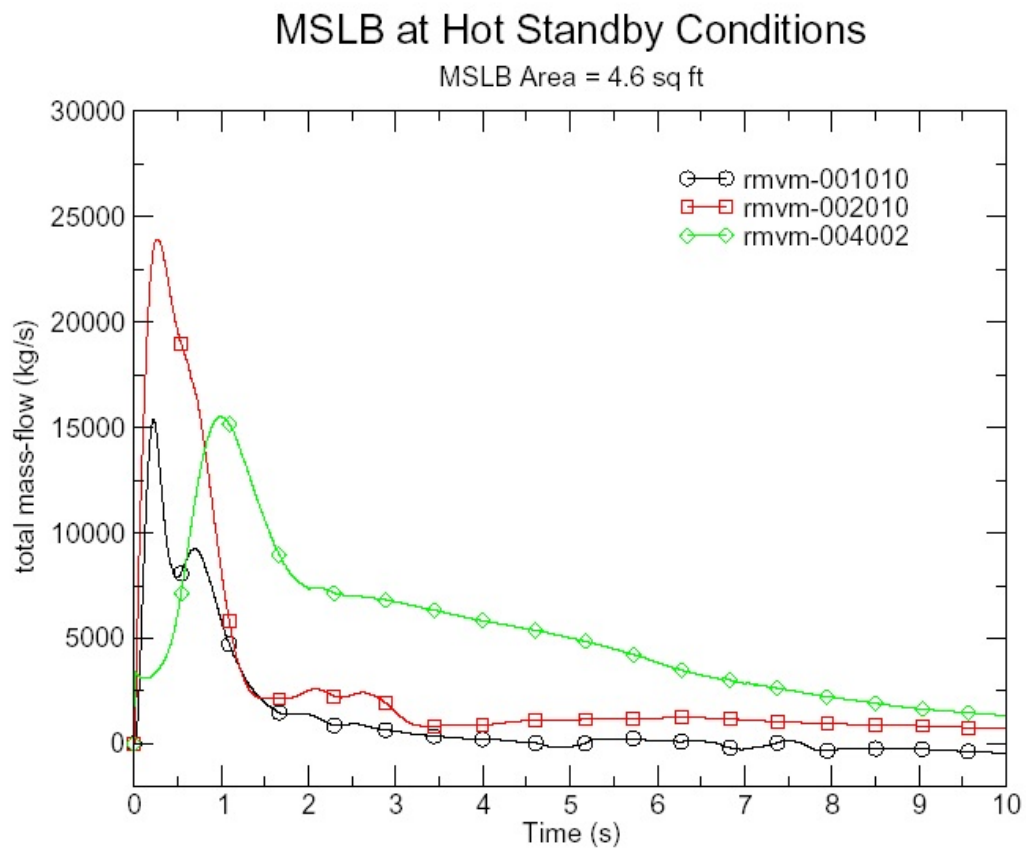


**Figure 4.1-23: Steam Generator Transient Flowrates Following a Guillotine MSLB at Hot Standby**



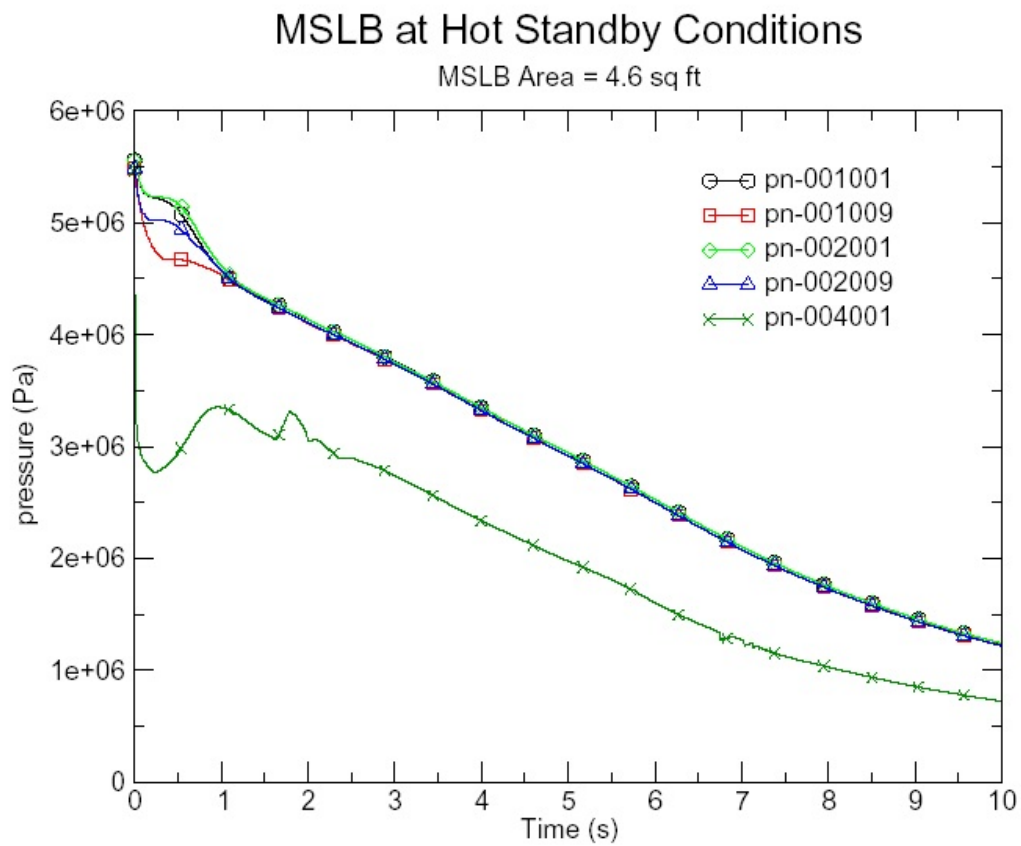


**Figure 4.1-24: Steam Generator Pressure Response Following a Guillotine MSLB at Hot Standby**

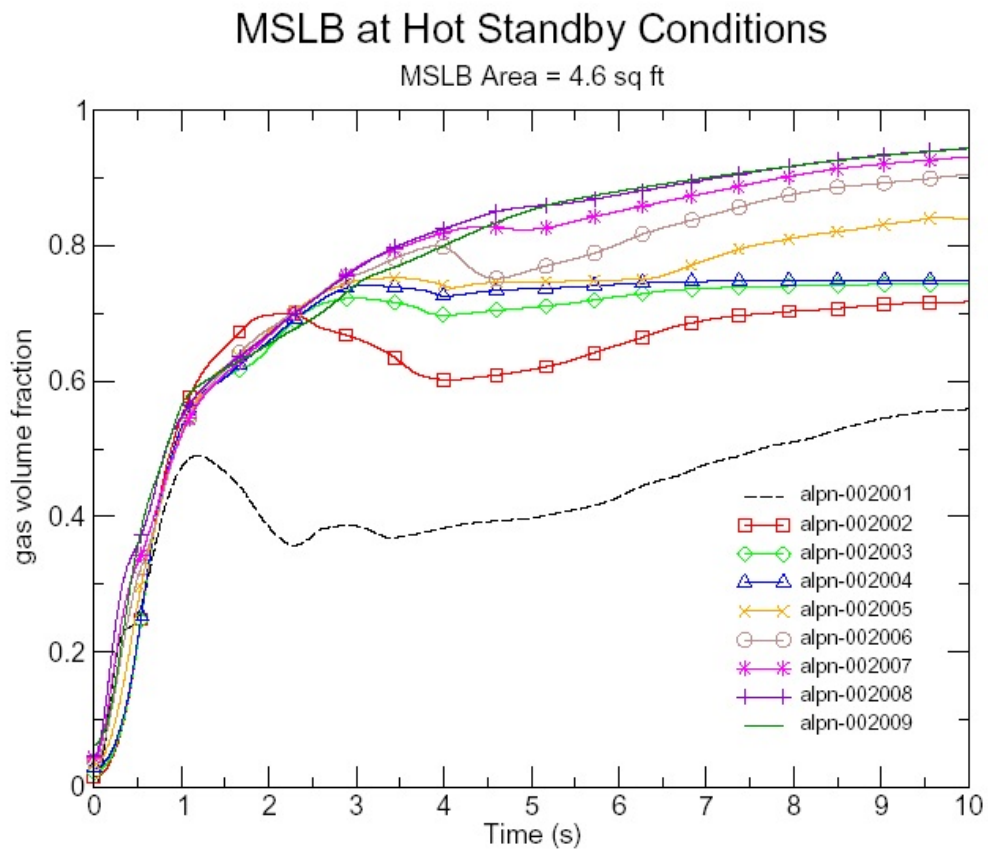


**Figure 4.1-25: Void Fraction in Tube Bundle Region Following a Guillotine MSLB at Hot Standby**

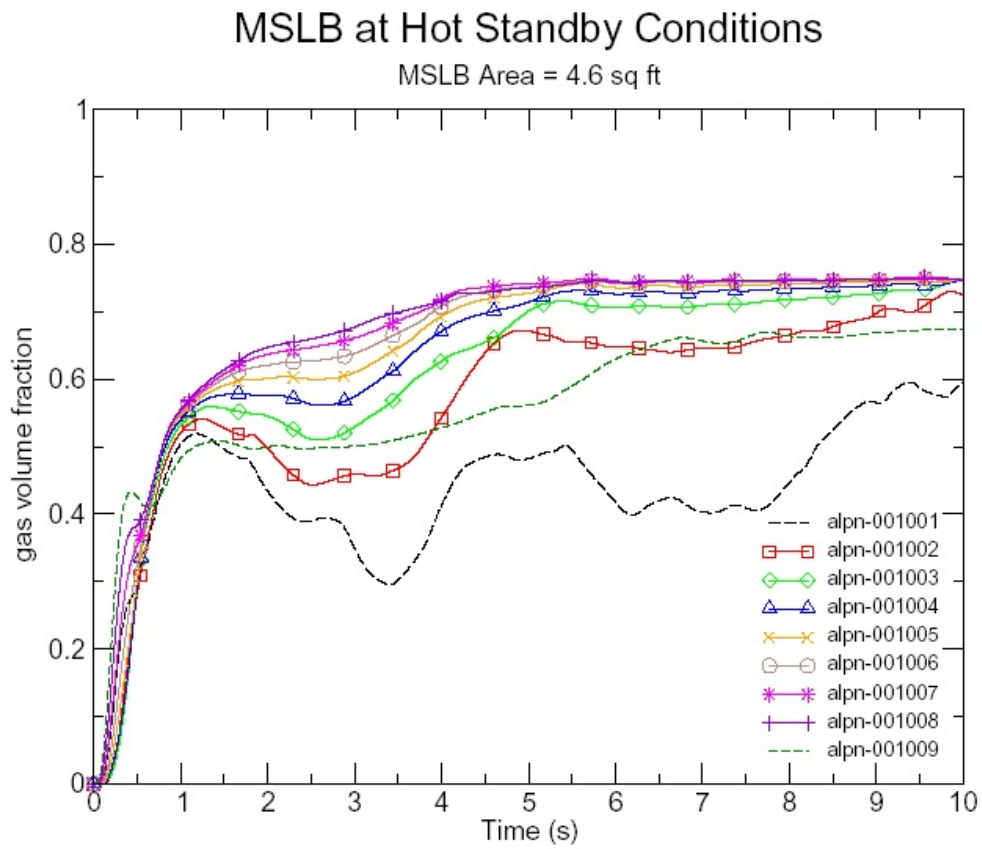


**Figure 4.1-26: Void Fraction in Steam Generator Annular Region Following a Guillotine MSLB at Hot Standby**

## **4.2 Long-Term Steam Generator Analysis Using the TRAC-M Code**

The loads developed using the short-term TRAC-M analyses will be used to assess the integrity of the steam generator primary tubing. If this assessment reveals the need to develop long-term temperature gradients for steam generator internals, the TRAC-M long-term steam generator analysis will be performed at a later time. A major concern of a long-term analysis is the evaluation of oscillatory pressure behavior in the lower part of the steam generator as the pressure drops. Such pressure oscillations could result from periodic vapor formation caused by flashing of the hot liquid as the steam generator pressure decreases. The pressure oscillations could result, in turn, in periodic loadings on the TSPs, the primary tubes, and the cylindrical shroud surrounding the tube bundle region.

In order to get a sense of the magnitude of this concern, a 60-second transient analysis, using the short-term TRAC-M model of the Westinghouse Model 51 steam generator, was performed for the break case that resulted in the largest loads, namely the guillotine MSLB at hot standby. This analysis provided only an approximate assessment of the magnitude of the long-term pressure oscillation effects because the effects of heat addition from hot steam generator internal structures were not included in the current model. Additional internal steam generator heat structures would need to be added to the existing TRAC-M model to allow a more accurate assessment of the boiling caused by the hot surfaces and the resultant pressure effects. Additionally, it would be appropriate to increase the number of control volumes in the tube bundle region by modeling this region using the 3-D fluid component model available in TRAC-M. The use of the 3-D fluid volume model would also allow assessment of the presence of cross-flow in the tube bundle region between the TSPs.

Figures 4.2-1 and 4.2-2 show the resultant loads on TSP 1 and TSP 6 developed using the results of the 60-second analysis using the short-term TRAC-M model. (Figures 4.1-1 and 4.1-2 illustrate the relationship between the steam generator geometry and the TRAC-M Model.) The long-term (between 2- and 60-seconds) loadings on the TSPs are small and, generally, smaller than the short-term (less than 2-seconds) loadings. Figures 4.2-3 and 4.2-4 illustrate the typical void fraction variation and pressure transient in the tube bundle control volumes. The void fraction variation may result from flashing within the volume, and flow entering and leaving the volume. The figures indicate that loadings on the TSPs can be present in the long-term period following an MSLB.

Questions remain, however, concerning the accuracy of the results shown in the long-term analysis figures, and the ability of any existing thermal-hydraulic computer code, including TRAC-M and RELAP5, to accurately predict the behavior of a low-pressure, boiling-liquid volume, such as that present at the bottom of the steam generator after about 16-seconds into the calculational transient. Various studies have demonstrated the inability of the RELAP5 code to adequately predict "pool boiling" thermal-hydraulic behavior under similar conditions. The void fraction variations indicated in Figure 4.2-3 may be attributable to numerical conditions originating from inaccuracies in the fluid-thermal correlations used in the TRAC-M model. Consequently, long-term oscillatory results, as demonstrated in the void fraction plot and reflected in the loadings on TSP 1 and, to a lesser degree, TSP 6 shown on Figures 4.2-1 and 4.2-2 may be the result of the unstable fluid-thermal relations. Consequently, any long-term analysis must verify the ability of a thermal-hydraulic code to correctly predict the long-term thermal-hydraulic steam generator behavior before accepting the accuracy of the predictions. Therefore, the appropriateness of the TRAC-M code for performing the long-term will be addressed, the detailed long-term model will be developed, and the subsequent transient

analysis will be performed only if the short-term assessment of the integrity of the primary tubing dictates the need for further long-term studies.

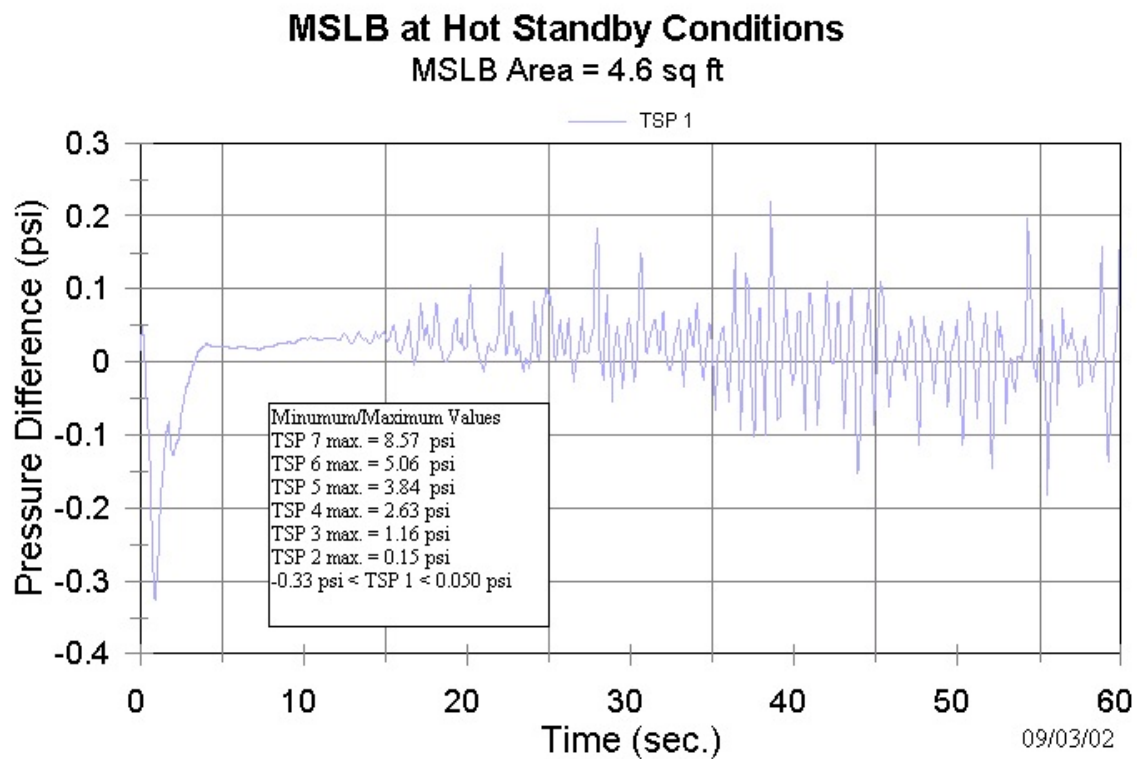


Figure 4.2-1: Long-Term Loading on TSP 1 Following a Guillotine MSLB at Hot Standby

## MSLB at Hot Standby Conditions

MSLB Area = 4.6 sq ft

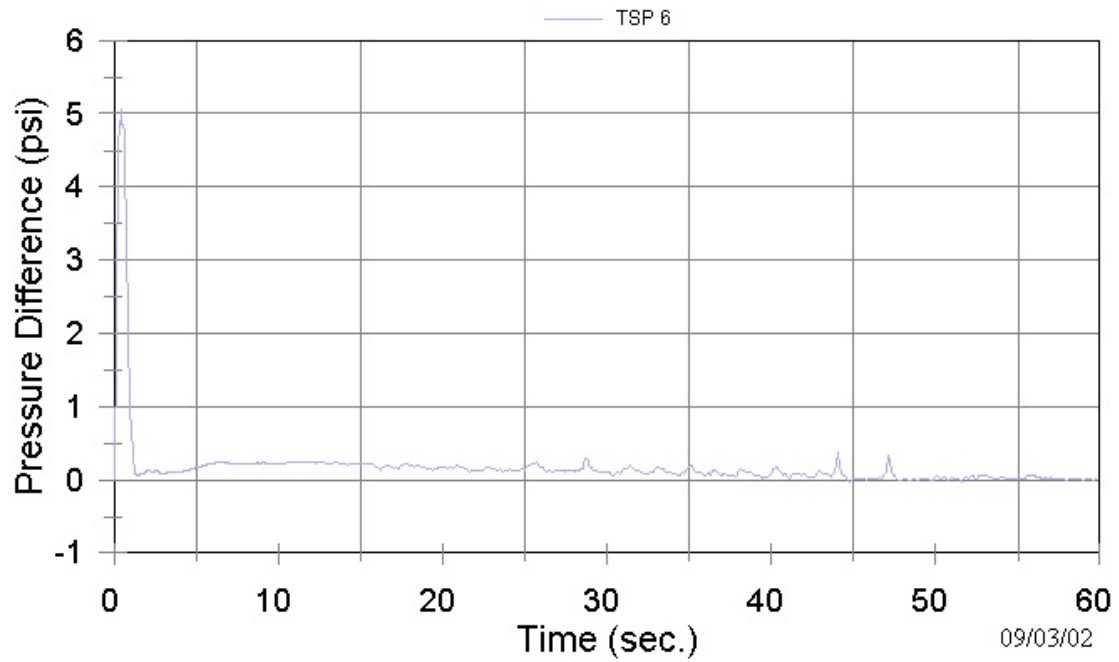
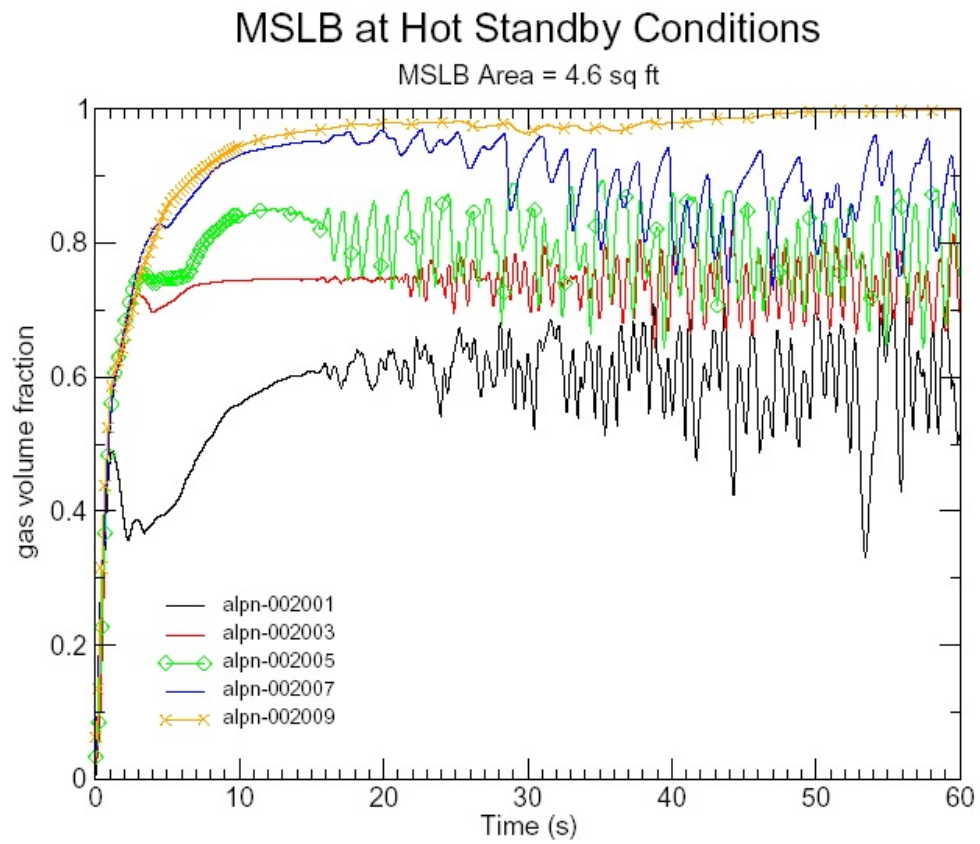
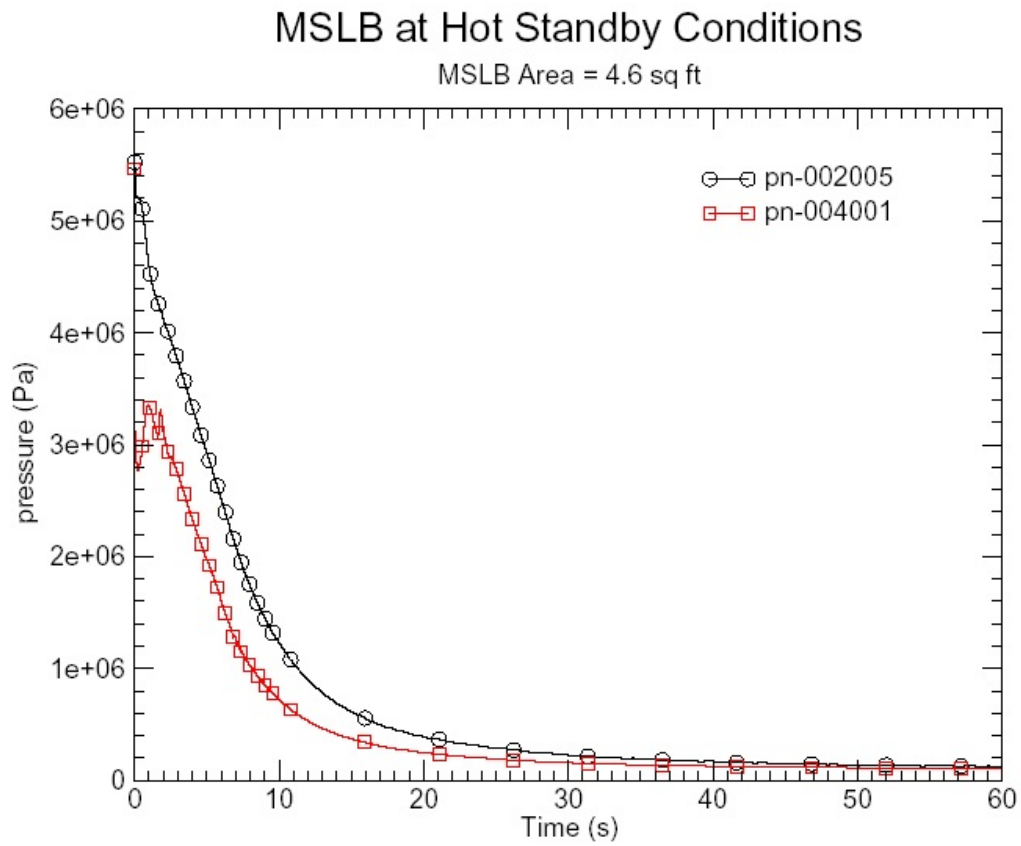


Figure 4.2-2: Long-Term Loading on TSP 6 Following a Guillotine MSLB at Hot Standby



**Figure 4.2-3: Long-Term Void Fraction in Tube Bundle Volumes Following a Guillotine MSLB at Hot Standby**



**Figure 4.2-4: Long-Term Pressure in Tube Bundle Volume 2005 and Break Volume Following a Guillotine MSLB at Hot Standby**



## 5.0 CONSERVATIVE BOUNDING CALCULATION

A major objective of this section is to provide an independent verification of the steam generator TSP forces calculated using the TRAC-M computer code with an independent methodology. Specifically, the TRAC-M predictions of the TSP loads for the Westinghouse Model 51 steam generator are compared to the results of a manual hand calculation performed using the Moody choked-flow method combined with calculations which follow the transport of the depressurization wave originating at the break location. A verified manual hand calculation methodology could also serve as the basis for a generic method for calculating TSP loadings for other Westinghouse steam generator designs, as well as steam generator designs from Combustion Engineering and Babcock & Wilcox.

### 5.1 Introduction

A pressurized PWR component, such as a steam generator, may initially contain subcooled or saturated water, steam, or a two-phase mixture. If the component is subjected to a sudden depressurization caused by a pipe rupture, different behaviors will occur in the component depending on the initial conditions.

- (1) If the fluid is initial saturated liquid and the break pressure is below the saturation pressure, the decompression will cause the liquid to flash, and a two-phase mixture will result.
- (2) If the fluid is initial saturated liquid and the break pressure is above the saturation pressure, non-flashing liquid flow will result.
- (3) If the fluid is initially subcooled liquid and the break pressure is below the saturation pressure, the liquid will flash to a two-phase mixture; this behavior similar to that of saturated liquid.
- (4) If the fluid is initially subcooled liquid and the break pressure is above the saturation pressure, non-flashing liquid flow will result.
- (5) If the fluid is initially saturated steam, an isentropic depressurization will produce “wet” steam. However, in the following calculations, steam will be approximated as an ideal gas for the short time period following a depressurization.
- (6) If the fluid is initially superheated steam and the break pressure is below the tank saturation pressure, the depressurization will initially produce “wet” steam.
- (7) If the fluid is initially superheated steam and the break pressure is above the saturation pressure, superheated flow will result.
- (8) If the fluid is initially a two-phase mixture, it will remain two-phase following depressurization and the liquid will further flash, thereby increasing the quality of the mixture.

Table 5.1-1 summarizes the possible outcomes listed above.

For normal PWR operating conditions, the secondary side steam generator fluid is subcooled liquid, saturated liquid, two-phase flow, or saturated steam, depending on location in the steam generator. The following procedure provides a simplified method to calculate the magnitude of

the depressurization wave entering the steam generator following either an MSLB or FWLB. The travel time for the depressurization wave can also be estimated based on the fluid (one or two-phase) condition.

**Table 5.1-1: Flow Conditions a Sudden Depressurization (Pipe Rupture)**

<b>Initial Tank Condition</b>	<b>Break Pressure</b>	<b>Upstream Condition Following Break</b>
Saturated liquid	Below tank saturation pressure	Flashing two-phase flow
Saturated liquid	Above tank saturation pressure	Non-flashing liquid flow
Subcooled liquid	Below tank saturation pressure	Flashing two-phase flow
Subcooled liquid	Above tank saturation pressure	Non-flashing liquid flow
Saturated steam	Below tank pressure	“Wet” steam
Superheated steam	Below tank saturation pressure	“Wet” steam
Superheated steam	Above tank saturation pressure	Superheated steam
Two-phase mixture	Below tank pressure	Two-phase flashing flow

## **5.2 Depressurization Phenomena**

A PWR steam generator is connected to the rest of the system by steam and feedwater piping. Following a postulated steam or feedwater line rupture, a depressurization wave propagates toward the steam generator. The depressurization wave travels at sonic speed through the piping until it arrives at the steam generator. At that point, part of the depressurization wave continues traveling into the steam generator, and a compression wave is reflected back toward the rupture. During this time period, structural forces are generated, primarily by the pressure differentials associated with the travel of the depressurization and pressurization waves. Successive wave transmissions and reflections, and the associated decay in fluid acceleration out the break eventually result in a steady discharge flow. At that point, system forces are primarily attributable to fluid friction or drag, except at the break location where thrust forces are present.

**Table 5.2-1: Initial Break Conditions at Steam Generator Operating Pressure**

	<b>0.0 Quality</b>	<b>0.5 Quality</b>	<b>1.0 Quality</b>
Initial Pressure	1085 psia	1085 psia	1085 psia
Initial Enthalpy	555.33 BTU/lbm	572.52 BTU/lbm	1189.7 BTU/lbm
Discharge Pressure	700 psia	690 psia	610 psia
Break Flux (fL/d=0)	8400 lbm/sec/ft <sup>2</sup>	3800 lbm/sec/ft <sup>2</sup>	2300 lbm/sec/ft <sup>2</sup>
Break Flux (fL/d=1)	7400 lbm/sec/ft <sup>2</sup>	3000 lbm/sec/ft <sup>2</sup>	1900 lbm/sec/ft <sup>2</sup>
Break Flux (fL/d=5)	4000 lbm/sec/ft <sup>2</sup>	1700 lbm/sec/ft <sup>2</sup>	1000 lbm/sec/ft <sup>2</sup>

The initial value of the depressurization wave can be determined using the derivations performed by F. J. Moody in References 1, 2, and 4. For example, using these references, Table 5.2-1 summarizes the initial conditions upstream of a break for saturated vapor and liquid at a tank pressure of 1,085 psia. These calculations conservatively assume an instantaneous

break opening time (<1-msec.). Mass fluxes out of the break are provided for different values of break line wall friction (fL/d) to represent the effect of the length of pipe present between the break and the tank. A double-ended break is assumed.

The initial pressures listed in the previous table present the value of the depressurization wave that travels upstream of the break following the start of choked sonic conditions at the break. For flashing saturated or subcooled liquid initial conditions, a depressurization wave travels back from the break location before flashing occurs at the break. However, water cannot exist for more than about 1-msec. in this metastable condition. When flashing occurs at the break, the small length that is initially depressurized repressurizes and choked sonic outflow begins.

When an acoustic wave reaches an area change, part of the wave is transmitted and part is reflected. The equations for the transmission and reflection of an acoustic wave are similar to the relations for electrical transmission line theory. Consequently, the reflection ratio for an acoustic wave at an area change is given by the following equations:

$$\text{Transmission Ratio} = \text{Reflection Ratio} + 1$$

$$\frac{P_{T-}}{P_i} = \frac{2 A_1 / A_2}{A_1 / A_2 + 1} = \frac{2 A_1}{A_1 + A_2}$$

$$\text{Reflection Ratio} = \text{Transmission Ratio} - 1$$

$$\frac{P_R}{P_i} = \frac{A_1 - A_2}{A_1 + A_2} = \frac{A_1 / A_2 - 1}{A_1 / A_2 + 1}$$

where  $P_T$  is the transmitted pressure change  
 $A_1$  is the flow area upstream of the area change  
 $A_2$  is the flow area downstream of the area change  
 $P_i$  is the incident pressure change  
 $P_R$  is the reflected pressure change

It is informative to derive the reflection and transmission ratios for the two limiting cases of a dead-ended pipe and an open-ended pipe.

For a dead end,  $A_2 = 0$ , the reflection ratio is 1, and the transmission ratio is 2. This means that the incident wave is completely reflected with the same sign. Consequently, a compression wave is reflected as a compression wave, thereby doubling the pressure at the dead end.

For an open end,  $A_2 = \infty$ , the reflection ratio is -1, and the transmission ratio is 0. This means that the incident wave is completely reflected with a change of sign and none of the pressure wave is transmitted. Consequently, an incident compression wave is reflected as a depressurization wave of equal magnitude.

### 5.2.1 Blowdown Calculations for the Westinghouse Model 51 Steam Generator

The calculation methods developed by F. J. Moody (see References) were intended to assess the conditions in a BWR vessel following a pipe break. Since the secondary side of a PWR steam generator operates at about the same conditions as a BWR, the methods developed by Moody are also applicable to steam generator blowdown phenomena. The Moody methods assume that the initial volume is a two-phase, liquid-vapor mixture at equilibrium. Although, this

assumption is not entirely correct for the steam generator, the bulk of the steam generator fluid is at equilibrium.

The Moody method uses the steam generator volume, initial mass, initial stagnation pressure, initial stagnation enthalpy, and break line diameter and area to calculate the choked flow and discharge pressure at the break in the ruptured line. The choked flow calculation assumes that the flow is at equilibrium. The choked flowrate and discharge pressure are also dependent on the break line wall friction (fL/d). For the 4.6 ft<sup>2</sup> guillotine MSLB, the wall friction is very small because the break is assumed to occur at the steam generator nozzle; therefore, an fL/d value of 0.0 was used. An fL/d value of 1.6 was used for the limited 1.4 ft<sup>2</sup> MSLB in order to account for the frictional loss contributed by the steam line flow restrictor. The first item assessed is the steam generator depressurization rate following an MSLB. The maximum choked flowrate is a necessary input into the depressurization rate determination.

$$\frac{dp}{dt} = \frac{w_{in}(h_{oin} - f_p) - w_{out}(h_{oout} - f_p)}{M F(p, V/M)}$$

where: dp/dt = pressure depressurization rate  
 $w_{in}$  = inlet flowrate = entering feedwater flow  
 $h_{oin}$  = inlet stagnation enthalpy = entering feedwater stagnation enthalpy  
 $f_p$  = Moody function (from Reference 4)  
 $w_{out}$  = exiting flowrate = choked flow at break  
 $h_{oout}$  = exiting stagnation enthalpy at break  
 $M$  = initial mass in steam generator  
 $F(p, V/M)$  = Moody function (from Reference 4)

Using the steam generator initial conditions indicated in Table 3.1-1 for hot standby and 100-percent power, the maximum choked flowrate, the discharge pressure at the steam line rupture, and the initial depressurization rate have been determined by the TRAC-M analyses discussed in Section 4 of this report and the Moody method. One set of values for the Moody calculation is reported in Table 5.2-2 because the calculational inputs for the hot standby and 100-percent power conditions are close in value; therefore, the Moody calculational method yields almost identical results for both conditions. Table 5.2-2 provides a comparison between the Moody calculations and the TRAC-M results described in section 4 of this report.

**Table 5.2-2: Steam Generator Depressurization Rate Comparison**

	<b>Moody Calculation</b>	<b>TRAC-M Results at Standby</b>	<b>TRAC-M Results at 100% Power</b>
Pressure	5.5 x 10 <sup>6</sup> Pa 800 psia	5.47 x 10 <sup>6</sup> Pa 793 psia <sup>a</sup>	5.47 x 10 <sup>6</sup> Pa 793 psia <sup>a</sup>
Saturation Temperature	542.7°K 517.2°F	542.7°K 517.2°F	542.7°K 517.2°F
<b>4.6 ft<sup>2</sup> Guillotine MSLB</b>	with fL/d = 0.0	at 0.9939943 sec.	at 0.31101373 sec.
Maximum Break Flow	12730 kg/sec. 28064 lbm/sec.	15489 kg/sec. 34146 lbm/sec.	13402 kg/sec. 29546 lbm/sec.
Discharge Pressure	520 psia 3.585 x 10 <sup>6</sup> Pa	486 psia 3.35 x 10 <sup>6</sup> Pa	446 psia 3.075 x 10 <sup>6</sup> Pa
Depressurization Rate		at 0.9939943 sec.	
Standby Conditions	-2.48 x 10 <sup>5</sup> Pa/sec.	-3.29 x 10 <sup>5</sup> Pa/sec.	—
(No feedwater flow)	-36 psi/sec.	-47.8 psi/sec.	—
		Avg. over 10 sec.	
		-4.28 x 10 <sup>5</sup> Pa/sec.	—
		62.1 psi/sec.	—
			at 0.31101373 sec.
100% Power	-2.68 x 10 <sup>5</sup> Pa/sec.	—	-1.34 x 10 <sup>5</sup> Pa/sec.
(With feedwater flow)	-38.9 psi/sec.	—	-19.4 psi/sec
			Avg. over 10 sec.
		—	-3.80 x 10 <sup>5</sup> Pa/sec.
		—	-55.1 psi/sec.
<b>1.4 ft<sup>2</sup> MSLB</b>	with fL/d = 1.6	at 3.207063 sec.	at 0.736579 sec.
Maximum Break Flow	3150 kg/sec. 6944 lbm/sec.	2373 kg/sec. 5231 lbm/sec.	2600 kg/sec. 5732 lbm/sec.
Discharge Pressure	688 psia 4.744 x 10 <sup>6</sup> Pa	644 psia 4.44 x 10 <sup>6</sup> Pa	751 psia 5.18 x 10 <sup>6</sup> Pa
Depressurization Rate		at 3.207063 sec.	
Standby Conditions	-6.13 x 10 <sup>4</sup> Pa/sec.	-1.41 x 10 <sup>5</sup> Pa/sec.	—
(No feedwater flow)	-8.9 psi/sec.	-20.4 psi/sec.	—
		Avg. over 10 sec.	
		-1.93 x 10 <sup>5</sup> Pa/sec.	—
		-28.1 psi/sec.	—
			at 0.736579 sec.
100% Power	-8.17 x 10 <sup>4</sup> Pa/sec.	—	-1.39 x 10 <sup>5</sup> Pa/sec.
(With feedwater flow)	-11.9 psi/sec.	—	-20.2 psi/sec.
		—	Avg. over 10 sec.
		—	-1.05 x 10 <sup>5</sup> Pa/sec.
		—	-15.2 psi/sec.

<sup>a</sup> Pressure at steam line. The pressures of the TRAC-M steam generator volumes vary and are slightly larger than 793 psia.

The TRAC-M parameters listed in Table 5.2-2 include the maximum calculated break choked flow, and the corresponding break line pressure and pressure decrease slope ( $dp/dt$ ) at the time of maximum choked flow. These values provide the best comparison with the Moody calculation, which is representative of the conditions at the time of the break. The choked break flowrates determined using the Moody method generally agree with the results calculated from the TRAC-M analyses in spite of the fact that the choking correlations used by the two methods are different. The discharge pressure calculated using the Moody method is also close in value to the TRAC-M calculated results. Because TRAC-M calculates a thermal-hydraulic transient, the values of choked flow, pressure and  $dp/dt$  vary during the transient. Figures 5.2-1 through 5.2-8 illustrate these effects for the four steam line breaks analyzed by TRAC-M and described in Section 4.1 of this report. Figure 5.2-1 illustrates the TRAC-M-calculated transient break flow, steam generator pressure (p8002), and steam line discharge pressure (p4001) for the 4.6ft<sup>2</sup> MSLB with the steam generator at hot standby. The maximum break flow occurs at about 1-second. Table 5.2-1 lists the break flow and discharge pressure at that time. Figure 5.2-2 plots the instantaneous  $dp/dt$  value for steam generator volume p8002. This plot shows that calculated  $dp/dt$  varies during the course of the transient as calculated by TRAC-M. However, the  $dp/dt$  value listed in Table 5.2-1 reflects the value at the time of maximum choked flowrate. The remaining Figures 5.2-3 through 5.2-8 indicate the behavior of the break flow, steam generator pressure, discharge pressure, and steam generator  $dp/dt$  for the three other MSLBs analyzed using TRAC-M and discussed in section 4.1 of this report.

The initial maximum pressure differential load across a TSP resulting from acoustic wave travel can be determined by calculating the attenuation of the depressurization wave traveling back from the break location to the TSP. This calculation uses the transmission ratio relation (discussed in Section 5.2.1 above), and the area changes in the steam generator from the break location to each TSP. Using this information, calculations show that about 0.032 of the depressurization wave originating from an MSLB near the steam generator nozzle is initially transmitted to the volume just above the uppermost TSP (TSP 7). Additionally, about 0.84 of the depressurization wave is transmitted across each TSP. Based on the calculated Moody discharge pressures for the two MSLBs listed in Table 5.2-1, Table 5.2-3 lists the resultant initial pressure differentials across each TSP and compares them to the TRAC-M calculated results discussed in Section 4 of this report. The maximum Moody/acoustic differential pressures across the TSPs are calculated assuming that the pressure above each TSP is lowered as a result of the depressurization wave, and the pressure below the TSP has not yet been affected by the depressurization wave and remains at 800-psia.

The TSP pressure differentials calculated using the Moody/acoustic method are larger than those calculated using the TRAC-M computer code. The following assumptions were used in the Moody/acoustic calculation:

- (1) The Moody/acoustic calculation is a conservative method, which ignores frictional losses inside the steam generator. The consideration of frictional losses is beyond the ability of a manual hand calculation, and its effect in the time frame for the travel of the initial depressurization wave is probably minimal.
- (2) Only the travel of the initial depressurization wave is considered; acoustic wave reflections are ignored. Following acoustic wave transmissions and reflections in a manual hand calculation is very tedious and difficult and, consequently, was conservatively ignored in assessing the travel of the initial depressurization wave.

- (3) Only the depressurization wave travel through the center area with the primary tubing is considered. The travel of the depressurization wave in the annular area surrounding the cylindrical center area is not considered. The inclusion of the depressurization wave travel through the annular region would reduce the pressure at the bottom of the steam generator more quickly than if only the central region is considered. Therefore, the inclusion of the annular region in the calculation would reduce the pressure differential of the lower TSPs, but would not affect the upper TSPs as significantly. This effect is illustrated by the difference between the values calculated using the Moody/acoustic method and the TRAC-M code. The TRAC-M model accounts for flow through the central steam generator region and the annular area. This effect reduces the lower TSP pressure differentials. However, the pressure differentials for the upper TSPs calculated using the Moody/acoustic method more closely match the TRAC-M-calculated values because the upper TSPs are less affected by the inclusion of the flow through the annular region.

**Table 5.2-3: TSP Peak Pressure Differentials<sup>a</sup>  
Using TRAC-M and Moody/Acoustic Calculation**

	<b>TRAC-M Hot Standby Condition</b>	<b>TRAC-M 100% Power Condition</b>	<b>Moody/Acoustic Calculation<sup>b</sup></b>
<b><u>4.6 ft<sup>2</sup> MSLB</u></b>			
			<u>P<sub>discharge</sub> = 520 psia</u>
TSP 7 (top)	8.57 psi	6.82 psi	9.0 psi
TSP 6	5.06 psi	5.41 psi	7.6 psi
TSP 5	3.84 psi	4.34 psi	6.4 psi
TSP 4	2.63 psi	3.20 psi	5.4 psi
TSP 3	1.16 psi	1.91 psi	4.6 psi
TSP 2	0.15 psi	0.79 psi	3.8 psi
TSP 1 (bottom)	-0.33 psi	0.16 psi	3.3 psi (1.6 <sup>c</sup> psi)
<b><u>1.4 ft<sup>2</sup> MSLB</u></b>			
			<u>P<sub>discharge</sub> = 688 psia</u>
TSP 7 (top)	2.68 psi	1.49 psi	3.6 psi
TSP 6	1.70 psi	1.27 psi	3.0 psi
TSP 5	1.23 psi	1.09 psi	2.6 psi
TSP 4	0.87 psi	0.87 psi	2.2 psi
TSP 3	0.43 psi	0.61 psi	1.8 psi
TSP 2	0.08 psi	0.33 psi	1.5 psi
TSP 1 (bottom)	-0.05 psi	0.21 psi	1.3 psi (0.7 <sup>c</sup> psi)

<sup>a</sup> An upward-directed pressure differential is defined as positive.

<sup>b</sup> Differential pressure is conservatively calculated, ignoring depressurization wave travel through the annular feedwater region.

<sup>c</sup> TSP 1 pressure differential is adjusted for depressurization wave travel through the annular feedwater region.

For comparison, Table 5.2-3 also indicates the pressure differential across the lowest tube support plate, TSP 1, when the pressure below that TSP is adjusted to include the effects of the depressurization wave travel from the break through the annular feedwater region surrounding the center area with the primary tubes. Calculation show that about 0.0057 of the depressurization wave originating from the break initially travels through the annular region to the central volume below TSP 1. The depressurization wave travels through the annular region faster than through the central primary tube region because the annular region is one-phase liquid, while the central region is two-phase. (The sonic speed through liquid is much faster than through a two-phase fluid.) Consequently, the pressure below TSP 1 has been reduced to reflect the effects of the depressurization wave. The listed pressure differential for TSP 1 is the difference of the pressure below TSP 1 (calculated by taking the effect of the depressurization wave travel through the annular region) and the pressure above TSP 1 (determined from the travel of the depressurization wave through the central region). The effects of the depressurization wave travel through the annular region is only indicated for TSP 1. It is expected that the lower TSPs would also be affected by the depressurization wave travel through the annular region; however, the assessment of the effects on the other TSPs would require tracking numerous wave interactions and reflections, and would be very tedious and difficult.

**Table 5.2-4: TSP Peak Pressure Differential<sup>a</sup> Comparisons a for 4.6 ft<sup>2</sup> MSLB with System Initially at Hot Standby**

	<b>TRANFLO</b>	<b>RELAP5</b>	<b>TRAC-M</b>	<b>Moody/Acoustic Calc.<sup>b</sup></b>
TSP 7 (top)	Not analyzed	9.6 psi	8.57 psi	9.0 psi
TSP 6	Not analyzed	8.1 psi	5.06 psi	7.6 psi
TSP 5	Not analyzed	6.1 psi	3.84 psi	6.4 psi
TSP 4	Not analyzed	4.5 psi	2.63 psi	5.4 psi
TSP 3	Not analyzed	3.2 psi	1.16 psi	4.6 psi
TSP 2	Not analyzed	2.0 psi	0.15 psi	3.8 psi
TSP 1 (bottom)	Not analyzed	1.9 psi	-0.33 psi	3.3 psi (1.6 <sup>c</sup> psi)

<sup>a</sup> An upward-directed pressure differential is defined as positive.

<sup>b</sup> Differential pressure is conservatively calculated, ignoring depressurization wave travel through annular feedwater region.

<sup>c</sup> TSP 1 pressure differential is adjusted for depressurization wave travel through the annular feedwater region.

The most important result obtained by comparing the Moody/acoustic wave calculation to the TRAC-M results is the code verification that this comparison affords. The pressure differentials for the upper TSPs, especially TSP 7, for the 4.6 ft<sup>2</sup> MSLB at hot standby are of the same magnitude. This verifies the ability of the TRAC-M code to calculate the results of acoustic phenomena that are close to the theoretical maximum value and, thus, validates the use of the computer code for this application. It also supports the conclusion that the major contributor to forces on the TSPs are attributable to the depressurization wave travel from the break location. The force contribution from the fluid "swell" in the tube bundle region appears to be a secondary, but not insignificant, contributor to the TSP forces. A comparison of the TSP loads calculated by Westinghouse and the TRAC-M code (from Table 4.1-2) with the Moody/acoustic



values are listed on Table 5.2-4. It is interesting to note that results calculated using RELAP5, TRAC-M, and the Moody/acoustic method are close in value, as indicated in Table 5.2-4.

A comparison of the TSP pressure differential loadings for a 1.4 ft<sup>2</sup> MSLB at hot standby calculated using TRANFLO, RELAP5, TRAC-M, and the Moody/acoustic method shown in Table 5.2-5 indicates that the Moody/acoustic calculation results in TSP loadings that are larger than those calculated using the TRANFLO, RELAP5, or TRAC-M computer codes. However, the TRANFLO, RELAP5 and TRAC-M TSP loading values are close to the Moody/acoustic values. The difference between the computer methods and the manual Moody/acoustic hand calculation may be attributable to the increase in importance of frictional losses and acoustic wave reflections with the smaller break size, especially with the slower depressurization rate, smaller mass flows, and smaller increases in flowrate for the smaller break. The computer calculations also reflect a decreased contribution from the fluid “swell” resulting from liquid flashing in the tube bundle region. Irrespective of the reason, the TRANFLO, RELAP5 and TRAC-M-calculated TSP pressure differential loadings are close to the Moody/acoustic calculated values.

**Table 5.2-5: TSP Peak Pressure Differential<sup>a</sup> Comparisons for 1.4 ft<sup>2</sup> MSLB with System Initially at Hot Standby**

	<b>1.4 ft<sup>2</sup> MSLB TRANFLO Case1<sup>d</sup></b>	<b>1.4 ft<sup>2</sup> MSLB RELAP5 Case SB2<sup>d</sup></b>	<b>1.4 ft<sup>2</sup> MSLB TRAC-M</b>	<b>Moody/Acoustic Calc.<sup>b</sup></b>
TSP 7 (top)	2.46 psi	2.26 psi	2.68 psi	3.6 psi
TSP 6	1.82 psi	2.14 psi	1.70 psi	3.0 psi
TSP 5	1.25 psi	1.56 psi	1.23 psi	2.6 psi
TSP 4	0.91 psi	1.35 psi	0.87 psi	2.2 psi
TSP 3	0.58 psi	1.23 psi	0.43 psi	1.8 psi
TSP 2	0.31 psi	1.25 psi	0.08 psi	1.5 psi
TSP 1 (bottom)	-0.12 psi	1.12 psi	-0.05 psi	1.3 psi (0.7 <sup>c</sup> psi)

<sup>a</sup> An upward-directed pressure differential is defined as positive.

<sup>b</sup> Differential pressure is conservatively calculated, ignoring depressurization wave travel through annular feedwater region.

<sup>c</sup> TSP 1 pressure differential is adjusted for depressurization wave travel through the annular feedwater region.

<sup>d</sup> Identifier from Westinghouse report, Reference 5.

### **5.3 References**

- (1) “**Maximum Flow Rate of a Single Component, Two-Phase Mixture**,” Moody, F. J., *Journal of Heat Transfer*, Vol. 86, American Society of Mechanical Engineers, February 1965.
- (2) “**Maximum Two-Phase Blowdown from Pipes**,” Moody, F. J., *Journal of Heat Transfer*, Vol. 87, American Society of Mechanical Engineers, August 1966.

- (3) **"A Pressure Pulse Model for Two-Phase Critical Flow and Sonic Velocity,"**  
Moody, F. J., *Journal of Heat Transfer*, Vol. 91, American Society of Mechanical Engineers, August 1969.
- (4) ***The Thermal-Hydraulics of a Boiling Water Nuclear Reactor***, Lahey, R. T. and F. J. Moody, Chapter 9, American Nuclear Society, 1993.
- (5) **"Model 51 Steam Generator Limited Tube Support Plate Displacement Analysis for Dented or Packed Tube to Tube Support Plate Crevices,"** Westinghouse, WCAP-14707, August 1996.

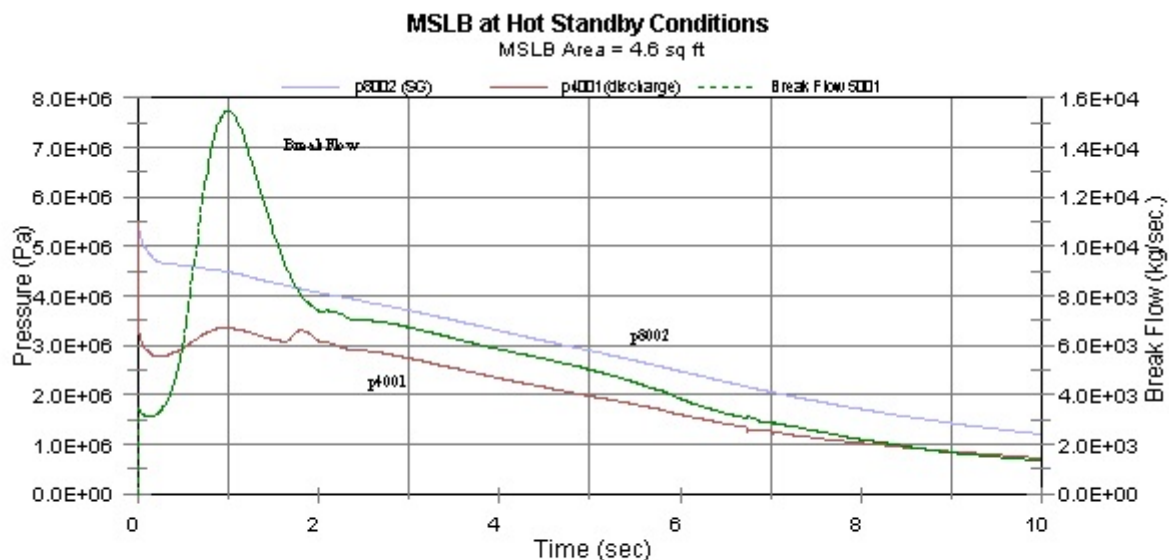


**Figure 5.2-1: TRAC-M-Calculated Conditions Following a 4.6ft<sup>2</sup> MSLB at Hot Standby**

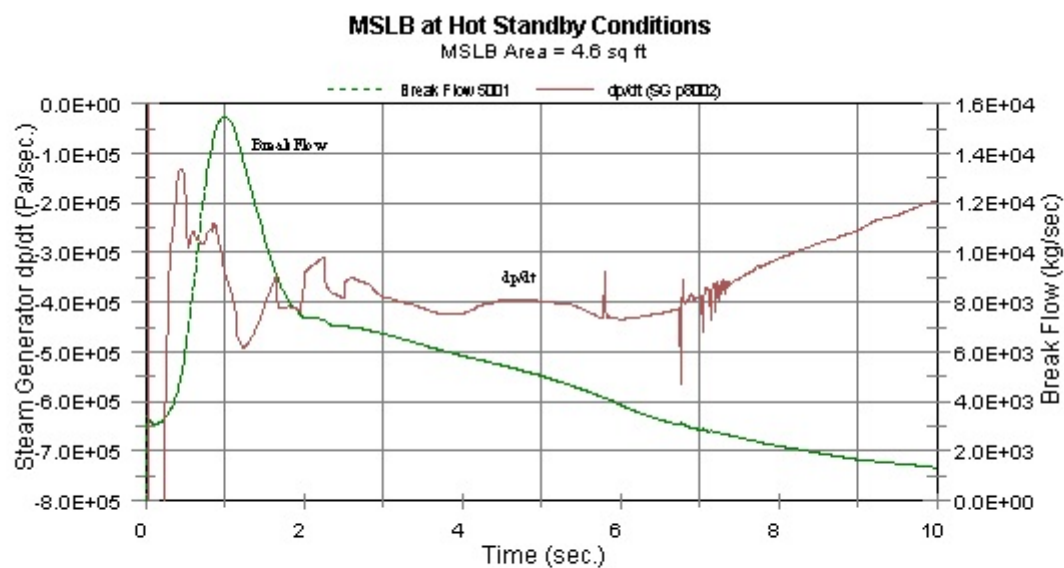


**Figure 5.2-2: TRAC-M-Calculated Conditions Following a 4.6ft<sup>2</sup> MSLB at Hot Standby**

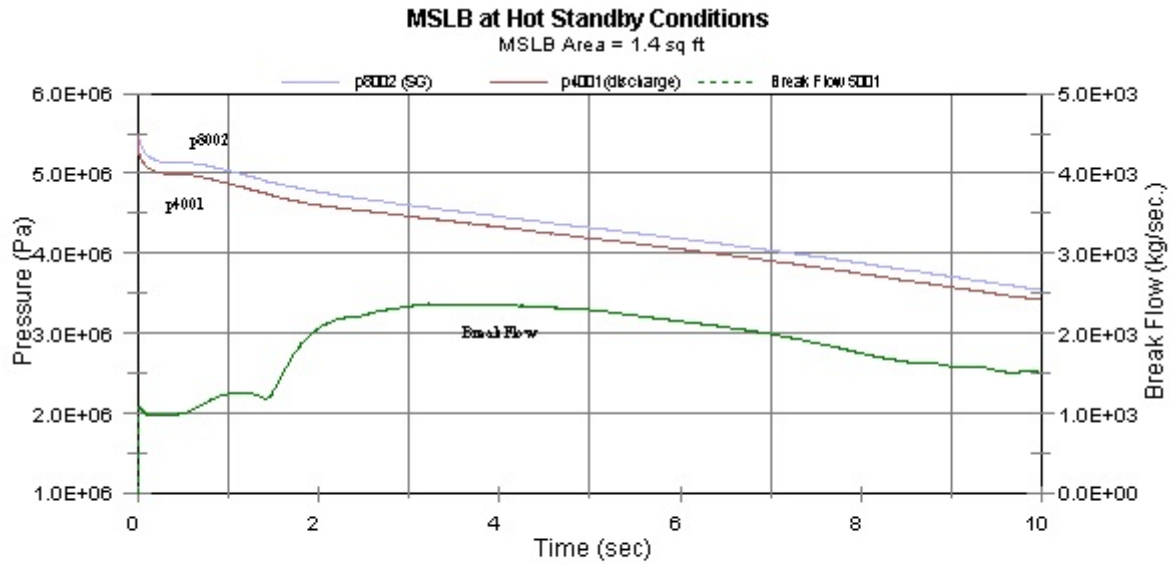


**Figure 5.2-3: TRAC-M-Calculated Conditions Following a 1.4ft<sup>2</sup> MSLB at Hot Standby**

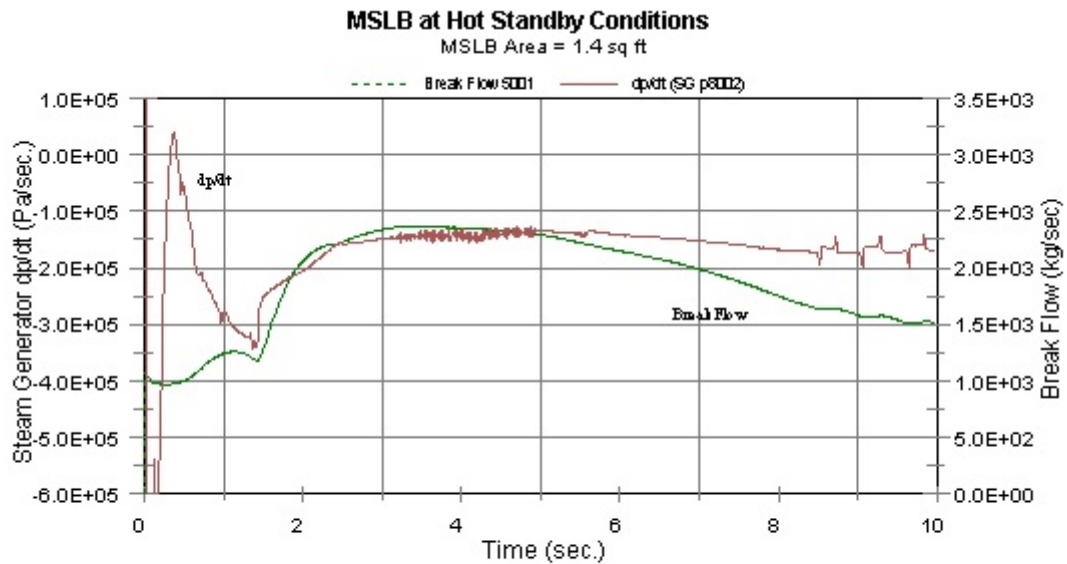


**Figure 5.2-4: TRAC-M-Calculated Conditions Following a 1.4ft<sup>2</sup> MSLB at Hot Standby**



**Figure 5.2-5: TRAC-M-Calculated Conditions Following a 4.6ft<sup>2</sup> MSLB at 100-Percent Power**

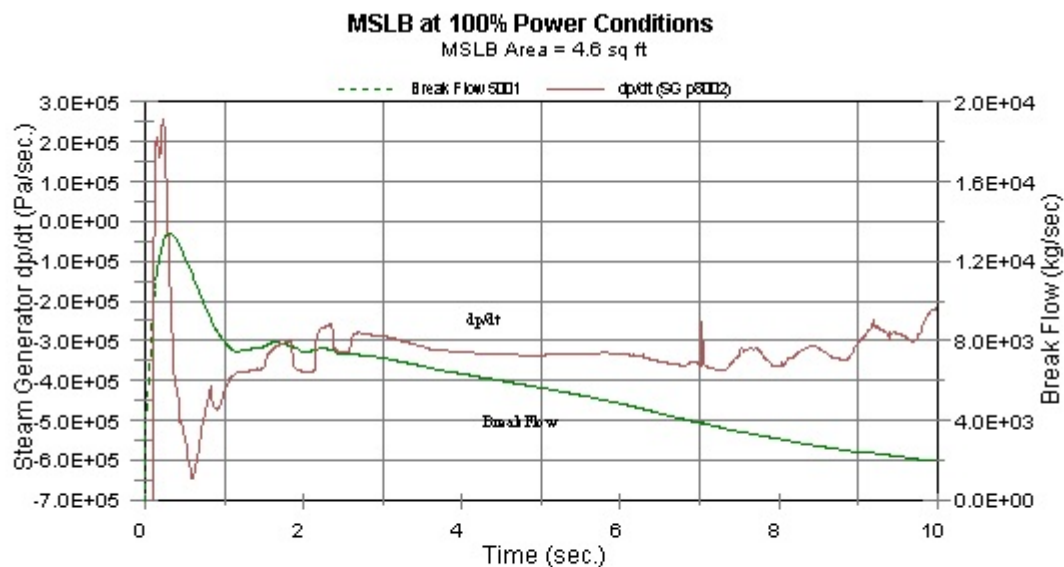


**Figure 5.2-6: TRAC-M-Calculated Conditions Following a 4.6ft<sup>2</sup> MSLB at 100-Percent Power**

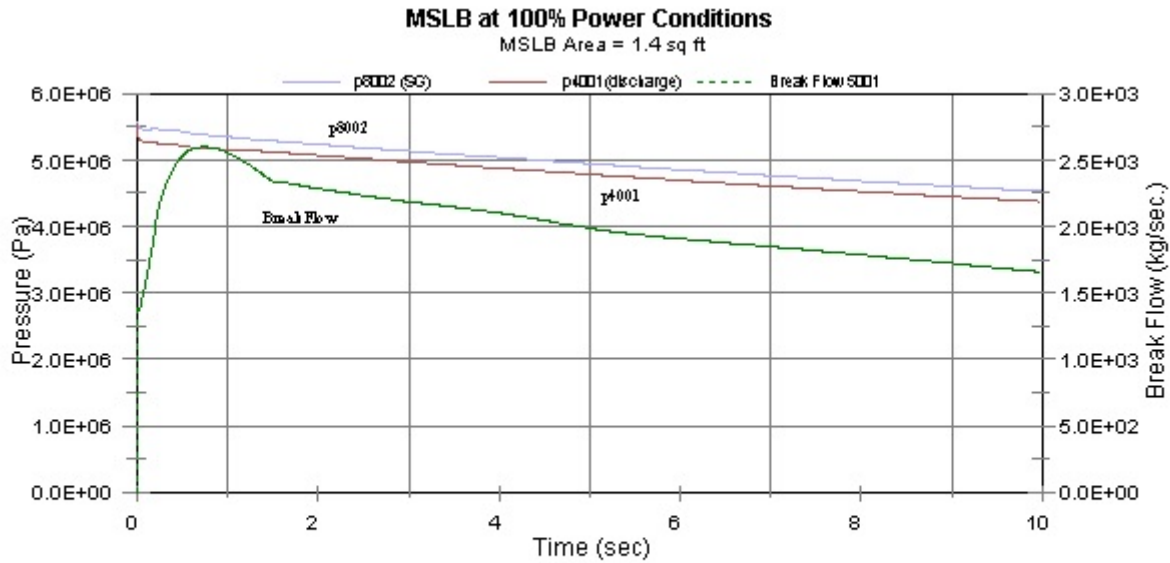


**Figure 5.2-7: TRAC-M-Calculated Conditions Following a 1.4ft<sup>2</sup> MSLB at 100-Percent Power**

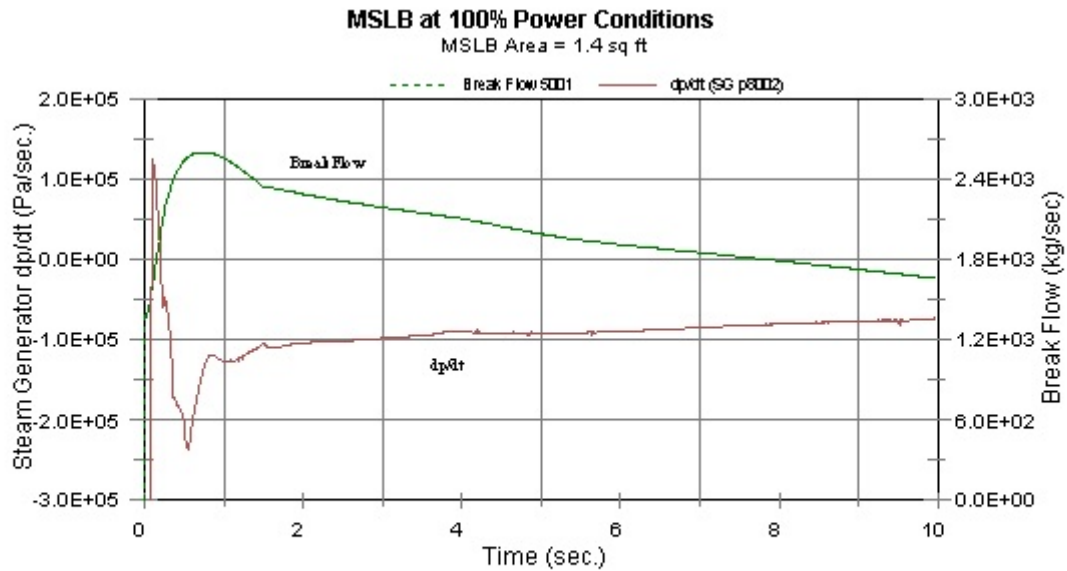


**Figure 5.2-8: TRAC-M-Calculated Conditions Following a 1.4ft<sup>2</sup> MSLB at 100-Percent Power**

## **APPENDIX A**

### **TRAC-M Input Files**





## A.1 Input File for 4.6 ft<sup>2</sup> MSLB with Steam Generator at Hot Standby

```

free format
*
*          numtcr          ieos          inopt          nmat
*              4              0              1              0
Simple W Model 51 Steam Generator
Eight Tube Sections 2 to 9
water packing off, ipack=0
choked flow option, icflow=2
*
&inopts
  icflow=2, iadded=20, ikfac=1, nosets=1, nhtstr=3, ithd=1
&end
*
*          dstep          timet
*              0              0.0
*
*          stdyst          transi          ncomp          njun          ipack
*              0              1              47              74              0
*
*          epso          epss
*      1.0e-08      1.0e-03
*
*          oitmax          sitmax          isolut          ncontr          nccfl
*              100              100              0              0              0
*
*          ntsv          ntcb          ntcf          ntrp          ntcp
*              0              0              0              0              1
*
* iorder      +              +              +              +              +
*              1              2              3              4              5s
*              6              8              9              10             11s
*              12             13             14             15             16s
*              17             18             19             20             21s
*              22             23             24             25             26s
*              27             28             29             30             31s
*              32             33             34             35             36s
*              37             38             39             40             900s
*              901            902            903            904            9010s
*              9020            9030e
*
*****
*
*                      component data
*
*****
*
*          type          num          id          ctitle
pipe          1          1          $1$ annulus
*
*          ncells          nodes          jun1          jun2          epsw
*              9              0              1              2          4.57e-5
*
*          ichf          iconc          iacc          ipow          npipes
*              1              0              0              0              1
*
*          radin          th          houtl          houtv          toutl
*      2.56800e+00      1.00000e-01          0.          0.          3.00000e+02
*
*          toutv          powin          powoff          rpowmx          powscl
*      3.00000e+02          0.          0.          0.          1.
*
*          +              +              +              +              +
* dx *          0.3556          0.9271 r6          1.2827          1.9543 e
* vol *          0.2568          0.6556 r6          0.9124          6.80 e
* fa * r9          0.722          6.627 e
* fric *          0.175 r7          0.          1.          1. e
* grav *          0. r9          1. e
* hd *          0.2678 r7          0.1430          0.36          0.64 e
* icflg *f          0 e
* nff * r8          1 r2          1 e
* alp * f          0.0 e

```

```

* vl * f 0.0 e
* vv * f 0.0 e
* + + + + +
* tl * 540.9 540.7 540.3 r3 540.1 540.3s
* tl * 540.4 540.5 e
* tv * 543.8 543.7 543.6 543.5 543.4s
* tv * 543.3 543.2 544.0 542.9 e
* p * 5.55649e+06 5.55162e+06 5.54321e+06 5.53345e+06 5.52369e+06s
* p * 5.51393e+06 5.50416e+06 5.49440e+06 5.48209e+06 e
* pa * f 0. e
*****
* type num id ctitle
pipe 2 2 $2$ tube sections
*
* ncells nodes jun1 jun2 epsw
9 0 1 3 4.57e-5
*
* ichf iconc iacc ipow npipes
1 0 0 0 1
*
* radin th hout1 houtv tout1
2.56800e+00 1.00000e-01 0. 0. 3.00000e+02
*
* toutv powin powoff rpowmx powsc1
3.00000e+02 0. 0. 0. 1.
*
* + + + + +
* dx * 0.3556 0.9271 r6 1.2827 1.9543 e
* vol * 1.785 4.655 r6 6.44 11.85 e
* fa * 0.722 r8 5.1 4.77 e
* fric * 0.175 0.0 r7 5.87 8.33 e
* grav * 0. r9 1. e
* hd * 0.2678 r8 0.0422 0.0817 e
* icflg * f 0 e
* nff * f 1 e
* alp * 0.005995 0.01477 0.02191 0.02796 0.03361s
* alp * 0.03889 0.04449 0.04679 0.06229 e
* vl * f 0.0 e
* vv * f 0.0 e
* + + + + +
* tl * 543.8 543.7 543.6 543.5 543.4s
* tl * 543.3 543.2 543.1 542.9 e
* tv * 543.8 543.7 543.6 543.5 543.4s
* tv * 543.3 543.2 543.1 542.9 e
* p * 5.55649e+06 5.55170e+06 5.54350e+06 5.53404e+06 5.52463e+06s
* p * 5.51527e+06 5.50596e+06 5.49668e+06 5.48510e+06 e
* pa * f 0. e
*****
* type num id ctitle
tee 3 3 $3$ sg top
*
* jcell nodes ichf cost epsw
3 0 1 1. 4.57e-5
*
* iconc1 ncell1 jun1 jun2 ipow
0 3 3 7 0
*
* radin1 th1 hout11 houtv1 tout11
2.56800e+00 1.00000e-01 0. 0. 3.00000e+02
*
* toutv1 pwin1 pwoff1 rpwmx1 pwsc11
3.00000e+02 0. 0. 0. 1.
*
* iconc2 ncell2 jun3 ipow2
0 1 6 0
*
* radin2 th2 hout12 houtv2 tout12
2.56800e+00 1.00000e-01 0. 0. 3.00000e+02
*
* toutv2 pwin2 pwoff2 rpwmx2 pwsc12
3.00000e+02 0. 0. 0. 1.

```

```

*
*      +      +      +      +      +
* dx      * r2      1.44      2.88 e
* vol      * r2      6.182      27.17 e
* fa      * r3      4.77      7.68 e
* fric      *      8.33      2.5      2.0      2.0 e
* grav      * r3      1.      0.74 e
* hd      *      0.0817      1.42      1.35      2.20 e
* icflg      * f      0 e
* nff      * f      1 e
* alp      *      0.02599      0.9165      1.0 e
* vl      * f      0.0 e
* vv      * f      0.0 e
*      +      +      +      +      +
* tl      *      542.8      542.7      542.7 e
* tv      *      542.8      542.7      542.7 e
* p      *      5.47283e+06      5.46688e+06      5.46585e+06 e
* pa      * f      0. e
*      +      +      +      +      +
* dx      * f      1.44 e
* vol      * f      13.495 e
* fa      *      9.49      9.49 e
* fric      *      15.9      15.9 e
* grav      * f      -1. e
* hd      *      1.47      1.35 e
* icflg      * f      0 e
* nff      * f      1 e
* alp      *      1.0 e
* vl      * f      0.0 e
* vv      * f      0.0 e
*      +      +      +      +      +
* tl      *      542.7 e
* tv      *      542.7 e
* p      *      5.46644e+06 e
* pa      * f      0. e
*****
*      type      num      id      ctitle
pipe      4      4      $4$ steam line
*
*      ncells      nodes      jun1      jun2      epsw
*      1      0      4      5      4.57e-5
*
*      ichf      iconc      iacc      ipow      npipes
*      1      0      0      0      1
*
*      radin      th      hout1      houtv      tout1
*      2.56800e+00      1.00000e-01      0.      0.      3.00000e+02
*
*      toutv      powin      powoff      rpowmx      powscl
*      3.00000e+02      0.      0.      0.      1.
*
*      +      +      +      +      +
* dx      *      0.5334 e
* vol      *      0.2280 e
* fa      * f      0.4274 e
* fric      *      0.5      1.0 e
* grav      * r2      1. e
* hd      *      2.96      0.7377 e
* icflg      *      1      1 e
* nff      * f      1 e
* alp      * f      1.0 e
* vl      * f      0.0 e
* vv      * f      0.0 e
*      +      +      +      +      +
* tl      * f      542.7 e
* tv      * f      542.7 e
* p      *      5.46453e+06 e
* pa      * f      0. e
*****
*      type      num      id      ctitle
break      5      5      $5$ pressure boundary

```

```

*
*      jun1      ibty      isat      ioff
*      5         0         0         1
*
*      dxin      volin      alpin      tin      pin
*      0.5334    0.2280    1.        373.15    1.0e+05
*
*      pain      concin      rbmx      poff      belv
*      0.        0.        0.        0.        0.
*
*****
*      type      num      id      ctitle
plenum          6         6      $6$ lower sg fw entry volume
*      mpljn      iconc      juns1      juns2
*      33         0         1         32
*
*      +      +      +      +      +
* junj *      2         6         8      111      112 s
* junj *      113      114      115      116      117 s
* junj *      118      119      120      121      122 s
* junj *      123      124      125      126      127 s
* junj *      128      129      130      131      132 s
* junj *      133      134      135      136      137 s
* junj *      138      139      140 e
* dx * f      1.44 e
* vol *      13.495 e
* elev *      0. e
* alp *      0.23031 e
* tl *      540.88 e
* tv *      542.76 e
* p *      5.47040e+06 e
* pa * f      0. e
*****
*      type      num      id      ctitle
tee            8         8      $8$ sg top
*      jcell      nodes      ichf      cost      epsw
*      1         0         1         1.        4.57e-5
*      iconc1      ncell1      jun1      jun2      ipow
*      0         2         7         4         0
*      radin1      th1      hout11      houtv1      tout11
*      2.56800e+00  1.00000e-01  0.        0.        3.00000e+02
*      toutv1      pwin1      pwoff1      rpwm1      pwsc11
*      3.00000e+02  0.        0.        0.        1.
*      iconc2      ncell2      jun3      ipow2
*      0         2         8         0
*      radin2      th2      hout12      houtv2      tout12
*      2.56800e+00  1.00000e-01  0.        0.        3.00000e+02
*      toutv2      pwin2      pwoff2      rpwm2      pwsc12
*      3.00000e+02  0.        0.        0.        1.
*
*      +      +      +      +      +
* dx *      2.134      1.606 e
* vol *      14.30      15.02 e
* fa *      7.68      14.4      0.4274 e
* fric *      2.0      2.0      0.5 e
* grav *      0.74      1.        1. e
* hd *      2.20      4.28      2.96 e
* icflg *r2      0         1 e
* nff * f      1 e
* alp *      1.0      0.9999 e
* vl * f      0.0 e
* vv * f      0.0 e
* tl *      542.7      542.7 e
* tv *      542.7      542.7 e
* p *      5.46533e+06  5.46482e+06 e
* pa * f      0. e
*
*      +      +      +      +
* dx *      2.186      1.12 e
* vol *      0.7062      0.3618 e
* fa * f      0.3231 e
* fric *      1.0      0.        1. e
* grav * f      -1. e
* hd * f      0.6414 e

```

```

* icflg *f          0 e
* nff  *f          1 e
* alp  *f          1.0 e
* vl   *f          0.0 e
* vv   *f          0.0 e
* tl   *          542.7      542.7 e
* tv   *          542.7      542.7 e
* p    *          5.46583e+06  5.46625e+06 e
* pa   *f          0. e
*****
*          type          num          id          ctitle
tee          9          9          $9$ fw tee
*          jcell          nodes          ichf          cost          epsw
          2          0          0          0.          4.57e-5
*          iconcl          ncell1          jun1          jun2          ipow
          0          3          41          11          0
*          radin1          th1          hout11          houtv1          tout11
2.56800e+00  1.00000e-01          0.          0.          3.00000e+02
*          toutv1          pwin1          pwoff1          rpwmx1          pwsc11
3.00000e+02          0.          0.          0.          1.
*          iconc2          ncell2          jun3          ipow2
          0          22          9          0
*          radin2          th2          hout12          houtv2          tout12
2.56800e+00  1.00000e-01          0.          0.          3.00000e+02
*          toutv2          pwin2          pwoff2          rpwmx2          pwsc12
3.00000e+02          0.          0.          0.          1.
*          +          +          +          +          +
* dx *f          0.4064 e
* vol *f          0.019576 e
* fa  *f          0.04817 e
* fric *          0.          0.2          0.2          0. e
* grav *f          0. e
* hd  *f          0.24765 e
* icflg *f          0 e
* nff  *f          1 e
* alp  *          0.006756          0.004192          0.006746 e
* vl   *f          0.0 e
* vv   *f          0.0 e
* tl   *          535.6          506.8          532.6 e
* tv   *          542.7          542.7          542.7 e
* p    *          5.46712e+06  5.46710e+06  5.46712e+06 e
* pa   *f          0. e
*          +          +          +          +
* dx *          0.3048          0.4826 r20          1.5 e
* vol *          0.033315          0.050094 r20          0.1557 e
* fa  *          0.1093          0.1038 r21          0.1038 e
* fric *          1.2          0. r21          0. e
* grav * r3          0. r8          -1. r12          0. e
* hd  *          0.3731          0.3814 r21          0.3635 e
* icflg *          0          0 r20          0          1 e
* nff  *          1          -1 r21          1 e
* alp  *f          0. e
* vl   *f          0.0 e
* vv   *f          0.0 e
* tl   *          500.3 r21          498.3 e
* tv   * r3          542.7          542.9          543.0          543.2          543.3s
* tv   *          543.4          543.6          543.7 r12          543.9e
* p    *          5.46706e+06  5.46705e+06  5.46705e+06  5.47938e+06  5.49170e+06s
* p    *          5.50403e+06  5.51636e+06  5.52869e+06  5.54101e+06  5.55334e+06s
* p    *          5.56567e+06  5.56566e+06  5.56566e+06  5.56565e+06  5.56564e+06s
* p    *          5.56564e+06  5.56563e+06  5.56563e+06  5.56563e+06  5.56562e+06s
* p    *          5.56562e+06  5.56562e+06 e
* pa   *f          0. e
*****
*          type          num          id          ctitle
fill          10          10          $10$ fw fill
*          jun1          ifty          ioff
          9          2          0
*          twtold          rfmix          concin          felv
          0.          1.e+6          0.          0.
*          dxin          volin          alpin          vlin          tlin

```

```

1.5      0.1557      0.      0.      498.3
*      pin      pain      flowin      vvin      tvin
5.46754e+06      0.      0.      0.      542.7
*****
*      type      num      id      ctitle
tee      11      11      $11$ fw tee
*      jcell      nodes      ichf      cost      epsw
1      0      0      0.      4.57e-5
*      iconcl      ncell1      jun1      jun2      ipow
0      1      11      12      0
*      radin1      th1      hout11      houtv1      tout11
2.56800e+00      1.00000e-01      0.      0.      3.00000e+02
*      toutv1      pwin1      pwoff1      rpwm1      pwsc11
3.00000e+02      0.      0.      0.      1.
*      iconc2      ncell2      jun3      ipow2
0      1      111      0
*      radin2      th2      hout12      houtv2      tout12
2.56800e+00      1.00000e-01      0.      0.      3.00000e+02
*      toutv2      pwin2      pwoff2      rpwm2      pwsc12
3.00000e+02      0.      0.      0.      1.
*      +      +      +      +      +
* dx * f      1.1887 e
* vol * f      0.05726 e
* fa * f      0.04817 e
* fric * f      0. e
* grav * f      0. e
* hd * f      0.24765 e
* icflg *f      0 e
* nff * f      1 e
* alp *      0.009053 e
* vl * f      0.0 e
* vv * f      0.0 e
* tl *      500.2 e
* tv *      542.7 e
* p *      5.46713e+06 e
* pa * f      0. e
*      +      +      +      +
* dx *      0.3048 e
* vol *      0.0005806 e
* fa * f      0.001905 e
* fric *      0.5      1. e
* grav *      1.      -1. e
* hd * f      0.04925 e
* icflg *f      0 e
* nff * f      1 e
* alp *      1. e
* vl * f      0.0 e
* vv * f      0.0 e
* tl *      542.7 e
* tv *      542.7 e
* p *      5.46616e+06 e
* pa * f      0. e
*****
*      type      num      id      ctitle
tee      12      12      $12$ fw tee
*      jcell      nodes      ichf      cost      epsw
1      0      0      0.      4.57e-5
*      iconcl      ncell1      jun1      jun2      ipow
0      1      12      13      0
*      radin1      th1      hout11      houtv1      tout11
2.56800e+00      1.00000e-01      0.      0.      3.00000e+02
*      toutv1      pwin1      pwoff1      rpwm1      pwsc11
3.00000e+02      0.      0.      0.      1.
*      iconc2      ncell2      jun3      ipow2
0      1      112      0
*      radin2      th2      hout12      houtv2      tout12
2.56800e+00      1.00000e-01      0.      0.      3.00000e+02
*      toutv2      pwin2      pwoff2      rpwm2      pwsc12
3.00000e+02      0.      0.      0.      1.
*      +      +      +      +      +
* dx * f      1.1887 e

```

```

* vol * f      0.05726 e
* fa  * f      0.04817 e
* fric * f      0. e
* grav * f      0. e
* hd  * f      0.24765 e
* icflg *f      0 e
* nff  * f      1 e
* alp  *      0.01067 e
* vl  * f      0.0 e
* vv  * f      0.0 e
* tl  * f      499.1 e
* tv  * f      542.7 e
* p   * f      5.46715e+06 e
* pa  * f      0. e
*      +      +      +      +
* dx  *      0.3048 e
* vol *      0.0005806 e
* fa  * f      0.001905 e
* fric *      0.5      1. e
* grav *      1.      -1. e
* hd  * f      0.04925 e
* icflg *f      0 e
* nff  * f      1 e
* alp  *      1. e
* vl  * f      0.0 e
* vv  * f      0.0 e
* tl  * f      542.7 e
* tv  * f      542.7 e
* p   * f      5.46617e+06 e
* pa  * f      0. e
*****
*      type      num      id      ctitle
tee      13      13      $13$ fw tee
*      jcell      nodes      ichf      cost      epsw
*      1      0      0      0.      4.57e-5
*      iconcl      ncell1      jun1      jun2      ipow
*      0      1      13      14      0
*      radin1      th1      houtl1      houtv1      toutl1
*      2.56800e+00      1.00000e-01      0.      0.      3.00000e+02
*      toutv1      pwin1      pwoff1      rpwmx1      pwscl1
*      3.00000e+02      0.      0.      0.      1.
*      iconc2      ncell2      jun3      ipow2
*      0      1      113      0
*      radin2      th2      houtl2      houtv2      toutl2
*      2.56800e+00      1.00000e-01      0.      0.      3.00000e+02
*      toutv2      pwin2      pwoff2      rpwmx2      pwscl2
*      3.00000e+02      0.      0.      0.      1.
*      +      +      +      +
* dx  * f      1.1887 e
* vol * f      0.05726 e
* fa  * f      0.04817 e
* fric * f      0. e
* grav * f      0. e
* hd  * f      0.24765 e
* icflg *f      0 e
* nff  * f      1 e
* alp  *      0.0165 e
* vl  * f      0.0 e
* vv  * f      0.0 e
* tl  * f      499.3 e
* tv  * f      542.7 e
* p   * f      5.46715e+06 e
* pa  * f      0. e
*      +      +      +      +
* dx  *      0.3048 e
* vol *      0.0005806 e
* fa  * f      0.001905 e
* fric *      0.5      1. e
* grav *      1.      -1. e
* hd  * f      0.04925 e
* icflg *f      0 e

```

```

* nff * f          1 e
* alp *          1. e
* vl  * f          0.0 e
* vv  * f          0.0 e
* tl  * f          542.7 e
* tv  * f          542.7 e
* p   * f  5.46618e+06 e
* pa  * f          0. e
*****
*      type          num          id          ctitle
tee          14          14          $14$ fw tee
*      jcell          nodes          ichf          cost          epsw
*      1          0          0          0.          4.57e-5
*      iconcl          ncell1          jun1          jun2          ipow
*      0          1          14          15          0
*      radin1          th1          hout11          houtv1          tout11
*      2.56800e+00  1.00000e-01          0.          0.          3.00000e+02
*      toutv1          pwin1          pwoff1          rpwmx1          pwsc11
*      3.00000e+02          0.          0.          0.          1.
*      iconc2          ncell2          jun3          ipow2
*      0          1          114          0
*      radin2          th2          hout12          houtv2          tout12
*      2.56800e+00  1.00000e-01          0.          0.          3.00000e+02
*      toutv2          pwin2          pwoff2          rpwmx2          pwsc12
*      3.00000e+02          0.          0.          0.          1.
*      +          +          +          +          +
* dx * f          1.1887 e
* vol * f          0.05726 e
* fa  * f          0.04817 e
* fric * f          0. e
* grav * f          0. e
* hd  * f          0.24765 e
* icflg *f          0 e
* nff * f          1 e
* alp *          0.01234 e
* vl  * f          0.0 e
* vv  * f          0.0 e
* tl  * f          499.2 e
* tv  * f          542.7 e
* p   * f  5.46716e+06 e
* pa  * f          0. e
*      +          +          +          +
* dx *          0.3048 e
* vol *          0.0005806 e
* fa  * f          0.001905 e
* fric *          0.5          1. e
* grav *          1.          -1. e
* hd  * f          0.04925 e
* icflg *f          0 e
* nff * f          1 e
* alp *          1. e
* vl  * f          0.0 e
* vv  * f          0.0 e
* tl  * f          542.7 e
* tv  * f          542.7 e
* p   * f  5.46619e+06 e
* pa  * f          0. e
*****
*      type          num          id          ctitle
tee          15          15          $15$ fw tee
*      jcell          nodes          ichf          cost          epsw
*      1          0          0          0.          4.57e-5
*      iconcl          ncell1          jun1          jun2          ipow
*      0          1          15          16          0
*      radin1          th1          hout11          houtv1          tout11
*      2.56800e+00  1.00000e-01          0.          0.          3.00000e+02
*      toutv1          pwin1          pwoff1          rpwmx1          pwsc11
*      3.00000e+02          0.          0.          0.          1.
*      iconc2          ncell2          jun3          ipow2
*      0          1          115          0
*      radin2          th2          hout12          houtv2          tout12

```



```

2.56800e+00 1.00000e-01 0. 0. 3.00000e+02
* toutv2 pwin2 pwoff2 rpwmx2 pwsc12
3.00000e+02 0. 0. 0. 1.
* + + + +
* dx * f 1.1887 e
* vol * f 0.05726 e
* fa * f 0.04817 e
* fric * f 0. e
* grav * f 0. e
* hd * f 0.24765 e
* icflg * f 0 e
* nff * f 1 e
* alp * 0.01284 e
* vl * f 0.0 e
* vv * f 0.0 e
* tl * f 499.1 e
* tv * f 542.7 e
* p * f 5.46717e+06 e
* pa * f 0. e
* + + + +
* dx * 0.3048 e
* vol * 0.0005806 e
* fa * f 0.001905 e
* fric * 0.5 1. e
* grav * 1. -1. e
* hd * f 0.04925 e
* icflg * f 0 e
* nff * f 1 e
* alp * 1. e
* vl * f 0.0 e
* vv * f 0.0 e
* tl * f 542.7 e
* tv * f 542.7 e
* p * f 5.46619e+06 e
* pa * f 0. e
*****
* type num id ctitle
tee 16 16 $16$ fw tee
* jcell nodes ichf cost epsw
1 0 0 0. 4.57e-5
* iconc1 ncell1 jun1 jun2 ipow
0 1 16 17 0
* radin1 th1 hout11 houtv1 tout11
2.56800e+00 1.00000e-01 0. 0. 3.00000e+02
* toutv1 pwin1 pwoff1 rpwmx1 pwsc11
3.00000e+02 0. 0. 0. 1.
* iconc2 ncell2 jun3 ipow2
0 1 116 0
* radin2 th2 hout12 houtv2 tout12
2.56800e+00 1.00000e-01 0. 0. 3.00000e+02
* toutv2 pwin2 pwoff2 rpwmx2 pwsc12
3.00000e+02 0. 0. 0. 1.
* + + + +
* dx * f 1.1887 e
* vol * f 0.05726 e
* fa * f 0.04817 e
* fric * f 0. e
* grav * f 0. e
* hd * f 0.24765 e
* icflg * f 0 e
* nff * f 1 e
* alp * 0.01323 e
* vl * f 0.0 e
* vv * f 0.0 e
* tl * f 499.1 e
* tv * f 542.7 e
* p * f 5.46717e+06 e
* pa * f 0. e
* + + + +
* dx * 0.3048 e
* vol * 0.0005806 e

```

```

* fa * f 0.001905 e
* fric * 0.5 1. e
* grav * 1. -1. e
* hd * f 0.04925 e
* icflg * f 0 e
* nff * f 1 e
* alp * 1. e
* vl * f 0.0 e
* vv * f 0.0 e
* tl * f 542.7 e
* tv * f 542.7 e
* p * f 5.46620e+06 e
* pa * f 0. e
*****
* type num id ctitle
tee 17 17 $17$ fw tee
* jcell nodes ichf cost epsw
1 0 0 0. 4.57e-5
* iconcl ncell1 jun1 jun2 ipow
0 1 17 18 0
* radin1 th1 hout11 houtv1 tout11
2.56800e+00 1.00000e-01 0. 0. 3.00000e+02
* toutv1 pwin1 pwoff1 rpwmx1 pwsc11
3.00000e+02 0. 0. 0. 1.
* iconc2 ncell2 jun3 ipow2
0 1 117 0
* radin2 th2 hout12 houtv2 tout12
2.56800e+00 1.00000e-01 0. 0. 3.00000e+02
* toutv2 pwin2 pwoff2 rpwmx2 pwsc12
3.00000e+02 0. 0. 0. 1.
* + + + +
* dx * f 1.1887 e
* vol * f 0.05726 e
* fa * f 0.04817 e
* fric * f 0. e
* grav * f 0. e
* hd * f 0.24765 e
* icflg * f 0 e
* nff * f 1 e
* alp * 0.01353 e
* vl * f 0.0 e
* vv * f 0.0 e
* tl * f 499.1 e
* tv * f 542.7 e
* p * f 5.46717e+06 e
* pa * f 0. e
* + + + +
* dx * 0.3048 e
* vol * 0.0005806 e
* fa * f 0.001905 e
* fric * 0.5 1. e
* grav * 1. -1. e
* hd * f 0.04925 e
* icflg * f 0 e
* nff * f 1 e
* alp * 1. e
* vl * f 0.0 e
* vv * f 0.0 e
* tl * f 542.7 e
* tv * f 542.7 e
* p * f 5.46620e+06 e
* pa * f 0. e
*****
* type num id ctitle
tee 18 18 $18$ fw tee
* jcell nodes ichf cost epsw
1 0 0 0. 4.57e-5
* iconcl ncell1 jun1 jun2 ipow
0 1 18 19 0
* radin1 th1 hout11 houtv1 tout11
2.56800e+00 1.00000e-01 0. 0. 3.00000e+02

```

```

*      toutv1      pwin1      pwoff1      rpwmx1      pwsc11
3.00000e+02      0.      0.      0.      1.
*      iconc2      ncell2      jun3      ipow2
0      1      118      0
*      radin2      th2      houtl2      houtv2      toutl2
2.56800e+00      1.00000e-01      0.      0.      3.00000e+02
*      toutv2      pwin2      pwoff2      rpwmx2      pwsc12
3.00000e+02      0.      0.      0.      1.
*      +      +      +      +      +
* dx * f      1.1887 e
* vol * f      0.05726 e
* fa * f      0.04817 e
* fric * f      0. e
* grav * f      0. e
* hd * f      0.24765 e
* icflg *f      0 e
* nff * f      1 e
* alp *      0.01376 e
* vl * f      0.0 e
* vv * f      0.0 e
* tl * f      499.0 e
* tv * f      542.7 e
* p * f      5.46718e+06 e
* pa * f      0. e
*      +      +      +      +
* dx *      0.3048 e
* vol *      0.0005806 e
* fa * f      0.001905 e
* fric *      0.5      1. e
* grav *      1.      -1. e
* hd * f      0.04925 e
* icflg *f      0 e
* nff * f      1 e
* alp *      1. e
* vl * f      0.0 e
* vv * f      0.0 e
* tl * f      542.7 e
* tv * f      542.7 e
* p * f      5.46620e+06 e
* pa * f      0. e
*****
*      type      num      id      ctitle
tee      19      19      $19$ fw tee
*      jcell      nodes      ichf      cost      epsw
1      0      0      0.      4.57e-5
*      iconc1      ncell1      jun1      jun2      ipow
0      1      19      20      0
*      radin1      th1      houtl1      houtv1      toutl1
2.56800e+00      1.00000e-01      0.      0.      3.00000e+02
*      toutv1      pwin1      pwoff1      rpwmx1      pwsc11
3.00000e+02      0.      0.      0.      1.
*      iconc2      ncell2      jun3      ipow2
0      1      119      0
*      radin2      th2      houtl2      houtv2      toutl2
2.56800e+00      1.00000e-01      0.      0.      3.00000e+02
*      toutv2      pwin2      pwoff2      rpwmx2      pwsc12
3.00000e+02      0.      0.      0.      1.
*      +      +      +      +      +
* dx * f      1.1887 e
* vol * f      0.05726 e
* fa * f      0.04817 e
* fric * f      0. e
* grav * f      0. e
* hd * f      0.24765 e
* icflg *f      0 e
* nff * f      1 e
* alp *      0.01396 e
* vl * f      0.0 e
* vv * f      0.0 e
* tl * f      499.0 e
* tv * f      542.7 e

```

```

* p      * f  5.46718e+06 e
* pa     * f      0. e
*      +      +      +      +
* dx     *      0.3048 e
* vol    *      0.0005806 e
* fa     * f      0.001905 e
* fric   *      0.5      1. e
* grav   *      1.      -1. e
* hd     * f      0.04925 e
* icflg  *f      0 e
* nff    * f      1 e
* alp    *      1. e
* vl     * f      0.0 e
* vv     * f      0.0 e
* tl     * f      542.7 e
* tv     * f      542.7 e
* p      * f  5.46620e+06 e
* pa     * f      0. e
*****
*      type      num      id      ctitle
tee      20      20      $20$ fw tee
*      jcell      nodes      ichf      cost      epsw
*      1      0      0      0.      4.57e-5
*      iconcl1      ncell1      jun1      jun2      ipow
*      0      1      20      21      0
*      radin1      th1      houtl1      houtv1      toutl1
*      2.56800e+00      1.00000e-01      0.      0.      3.00000e+02
*      toutv1      pwin1      pwoff1      rpwmx1      pwsc11
*      3.00000e+02      0.      0.      0.      1.
*      iconc2      ncell2      jun3      ipow2
*      0      1      120      0
*      radin2      th2      houtl2      houtv2      toutl2
*      2.56800e+00      1.00000e-01      0.      0.      3.00000e+02
*      toutv2      pwin2      pwoff2      rpwmx2      pwsc12
*      3.00000e+02      0.      0.      0.      1.
*      +      +      +      +      +
* dx     * f      1.1887 e
* vol    * f      0.05726 e
* fa     * f      0.04817 e
* fric   * f      0. e
* grav   * f      0. e
* hd     * f      0.24765 e
* icflg  *f      0 e
* nff    * f      1 e
* alp    *      0.01413 e
* vl     * f      0.0 e
* vv     * f      0.0 e
* tl     * f      499.0 e
* tv     * f      542.7 e
* p      * f  5.46718e+06 e
* pa     * f      0. e
*      +      +      +      +
* dx     *      0.3048 e
* vol    *      0.0005806 e
* fa     * f      0.001905 e
* fric   *      0.5      1. e
* grav   *      1.      -1. e
* hd     * f      0.04925 e
* icflg  *f      0 e
* nff    * f      1 e
* alp    *      1. e
* vl     * f      0.0 e
* vv     * f      0.0 e
* tl     * f      542.7 e
* tv     * f      542.7 e
* p      * f  5.46621e+06 e
* pa     * f      0. e
*****
*      type      num      id      ctitle
tee      21      21      $21$ fw tee
*      jcell      nodes      ichf      cost      epsw

```

```

*      1      0      0      0.      4.57e-5
*      iconc1      ncell1      jun1      jun2      ipow
*      0      1      21      22      0
*      radin1      th1      hout11      houtv1      tout11
*      2.56800e+00      1.00000e-01      0.      0.      3.00000e+02
*      toutv1      pwin1      pwoff1      rpwmx1      pwsc11
*      3.00000e+02      0.      0.      0.      1.
*      iconc2      ncell2      jun3      ipow2
*      0      1      121      0
*      radin2      th2      hout12      houtv2      tout12
*      2.56800e+00      1.00000e-01      0.      0.      3.00000e+02
*      toutv2      pwin2      pwoff2      rpwmx2      pwsc12
*      3.00000e+02      0.      0.      0.      1.
*      +      +      +      +      +
*      dx * f      1.1887 e
*      vol * f      0.05726 e
*      fa * f      0.04817 e
*      fric * f      0. e
*      grav * f      0. e
*      hd * f      0.24765 e
*      icflg *f      0 e
*      nff * f      1 e
*      alp *      0.01424 e
*      vl * f      0.0 e
*      vv * f      0.0 e
*      tl * f      499.0 e
*      tv * f      542.7 e
*      p * f      5.46718e+06 e
*      pa * f      0. e
*      +      +      +      +
*      dx *      0.3048 e
*      vol *      0.0005806 e
*      fa * f      0.001905 e
*      fric *      0.5      1. e
*      grav *      1.      -1. e
*      hd * f      0.04925 e
*      icflg *f      0 e
*      nff * f      1 e
*      alp *      1. e
*      vl * f      0.0 e
*      vv * f      0.0 e
*      tl * f      542.7 e
*      tv * f      542.7 e
*      p * f      5.46621e+06 e
*      pa * f      0. e
*****
*      type      num      id      ctitle
tee      22      22      $22$ fw tee
*      jcell      nodes      ichf      cost      epsw
*      1      0      0      0.      4.57e-5
*      iconc1      ncell1      jun1      jun2      ipow
*      0      1      22      23      0
*      radin1      th1      hout11      houtv1      tout11
*      2.56800e+00      1.00000e-01      0.      0.      3.00000e+02
*      toutv1      pwin1      pwoff1      rpwmx1      pwsc11
*      3.00000e+02      0.      0.      0.      1.
*      iconc2      ncell2      jun3      ipow2
*      0      1      122      0
*      radin2      th2      hout12      houtv2      tout12
*      2.56800e+00      1.00000e-01      0.      0.      3.00000e+02
*      toutv2      pwin2      pwoff2      rpwmx2      pwsc12
*      3.00000e+02      0.      0.      0.      1.
*      +      +      +      +      +
*      dx * f      1.1887 e
*      vol * f      0.05726 e
*      fa * f      0.04817 e
*      fric * f      0. e
*      grav * f      0. e
*      hd * f      0.24765 e
*      icflg *f      0 e
*      nff * f      1 e

```

```

* alp * 0.01431 e
* vl * f 0.0 e
* vv * f 0.0 e
* tl * f 499.0 e
* tv * f 542.7 e
* p * f 5.46718e+06 e
* pa * f 0. e
* + + + +
* dx * 0.3048 e
* vol * 0.0005806 e
* fa * f 0.001905 e
* fric * 0.5 1. e
* grav * 1. -1. e
* hd * f 0.04925 e
* icflg * f 0 e
* nff * f 1 e
* alp * 1. e
* vl * f 0.0 e
* vv * f 0.0 e
* tl * f 542.7 e
* tv * f 542.7 e
* p * f 5.46621e+06 e
* pa * f 0. e
*****
* type num id ctitle
tee 23 23 $23$ fw tee
* jcell nodes ichf cost epsw
1 0 0 0. 4.57e-5
* iconcl ncell1 jun1 jun2 ipow
0 1 23 24 0
* radin1 th1 hout11 houtv1 tout11
2.56800e+00 1.00000e-01 0. 0. 3.00000e+02
* toutv1 pwin1 pwoff1 rpwmx1 pwsc11
3.00000e+02 0. 0. 0. 1.
* iconc2 ncell2 jun3 ipow2
0 1 123 0
* radin2 th2 hout12 houtv2 tout12
2.56800e+00 1.00000e-01 0. 0. 3.00000e+02
* toutv2 pwin2 pwoff2 rpwmx2 pwsc12
3.00000e+02 0. 0. 0. 1.
* + + + +
* dx * f 1.1887 e
* vol * f 0.05726 e
* fa * f 0.04817 e
* fric * f 0. e
* grav * f 0. e
* hd * f 0.24765 e
* icflg * f 0 e
* nff * f 1 e
* alp * 0.01435 e
* vl * f 0.0 e
* vv * f 0.0 e
* tl * f 499.0 e
* tv * f 542.7 e
* p * f 5.46719e+06 e
* pa * f 0. e
* + + + +
* dx * 0.3048 e
* vol * 0.0005806 e
* fa * f 0.001905 e
* fric * 0.5 1. e
* grav * 1. -1. e
* hd * f 0.04925 e
* icflg * f 0 e
* nff * f 1 e
* alp * 1. e
* vl * f 0.0 e
* vv * f 0.0 e
* tl * f 542.7 e
* tv * f 542.7 e
* p * f 5.46621e+06 e

```

```

* pa      * f      0. e
*****
*          type          num          id          ctitle
tee          24          24          $24$ fw tee
*          jcell          nodes          ichf          cost          epsw
*          1          0          0          0.          4.57e-5
*          iconcl          ncell1          jun1          jun2          ipow
*          0          1          24          25          0
*          radin1          th1          hout11          houtv1          tout11
*          2.56800e+00          1.00000e-01          0.          0.          3.00000e+02
*          toutv1          pwin1          pwoff1          rpwmx1          pwsc11
*          3.00000e+02          0.          0.          0.          1.
*          iconc2          ncell2          jun3          ipow2
*          0          1          124          0
*          radin2          th2          hout12          houtv2          tout12
*          2.56800e+00          1.00000e-01          0.          0.          3.00000e+02
*          toutv2          pwin2          pwoff2          rpwmx2          pwsc12
*          3.00000e+02          0.          0.          0.          1.
*          +          +          +          +          +
* dx * f      1.1887 e
* vol * f      0.05726 e
* fa * f      0.04817 e
* fric * f      0. e
* grav * f      0. e
* hd * f      0.24765 e
* icflg * f      0 e
* nff * f      1 e
* alp * f      0.01438 e
* vl * f      0.0 e
* vv * f      0.0 e
* tl * f      499.0 e
* tv * f      542.7 e
* p * f      5.46719e+06 e
* pa * f      0. e
*          +          +          +          +
* dx * f      0.3048 e
* vol * f      0.0005806 e
* fa * f      0.001905 e
* fric * f      0.5          1. e
* grav * f      1.          -1. e
* hd * f      0.04925 e
* icflg * f      0 e
* nff * f      1 e
* alp * f      1. e
* vl * f      0.0 e
* vv * f      0.0 e
* tl * f      542.7 e
* tv * f      542.7 e
* p * f      5.46621e+06 e
* pa * f      0. e
*****
*          type          num          id          ctitle
tee          25          25          $25$ fw tee
*          jcell          nodes          ichf          cost          epsw
*          1          0          0          0.          4.57e-5
*          iconcl          ncell1          jun1          jun2          ipow
*          0          1          25          26          0
*          radin1          th1          hout11          houtv1          tout11
*          2.56800e+00          1.00000e-01          0.          0.          3.00000e+02
*          toutv1          pwin1          pwoff1          rpwmx1          pwsc11
*          3.00000e+02          0.          0.          0.          1.
*          iconc2          ncell2          jun3          ipow2
*          0          1          125          0
*          radin2          th2          hout12          houtv2          tout12
*          2.56800e+00          1.00000e-01          0.          0.          3.00000e+02
*          toutv2          pwin2          pwoff2          rpwmx2          pwsc12
*          3.00000e+02          0.          0.          0.          1.
*          +          +          +          +          +
* dx * f      1.1887 e
* vol * f      0.05726 e
* fa * f      0.04817 e

```

```

* fric * f          0. e
* grav * f          0. e
* hd * f          0.24765 e
* icflg *f          0 e
* nff * f          1 e
* alp * f          0.01443 e
* vl * f          0.0 e
* vv * f          0.0 e
* tl * f          499.2 e
* tv * f          542.7 e
* p * f          5.46719e+06 e
* pa * f          0. e
*      +          +          +          +
* dx * f          0.3048 e
* vol * f          0.0005806 e
* fa * f          0.001905 e
* fric * f          0.5          1. e
* grav * f          1.          -1. e
* hd * f          0.04925 e
* icflg *f          0 e
* nff * f          1 e
* alp * f          1. e
* vl * f          0.0 e
* vv * f          0.0 e
* tl * f          542.7 e
* tv * f          542.7 e
* p * f          5.46621e+06 e
* pa * f          0. e
*****
*      type      num      id      ctitle
tee      26      26      $26$ fw tee
*      jcell      nodes      ichf      cost      epsw
      1      0      0      0.      4.57e-5
*      iconcl      ncell1      jun1      jun2      ipow
      0      1      26      27      0
*      radin1      th1      hout11      houtv1      tout11
2.56800e+00      1.00000e-01      0.      0.      3.00000e+02
*      toutv1      pwin1      pwoff1      rpwmx1      pwscl1
3.00000e+02      0.      0.      0.      1.
*      iconc2      ncell2      jun3      ipow2
      0      1      126      0
*      radin2      th2      hout12      houtv2      tout12
2.56800e+00      1.00000e-01      0.      0.      3.00000e+02
*      toutv2      pwin2      pwoff2      rpwmx2      pwscl2
3.00000e+02      0.      0.      0.      1.
*      +          +          +          +
* dx * f          1.1887 e
* vol * f          0.05726 e
* fa * f          0.04817 e
* fric * f          0. e
* grav * f          0. e
* hd * f          0.24765 e
* icflg *f          0 e
* nff * f          1 e
* alp * f          0.01447 e
* vl * f          0.0 e
* vv * f          0.0 e
* tl * f          499.0 e
* tv * f          542.7 e
* p * f          5.46719e+06 e
* pa * f          0. e
*      +          +          +          +
* dx * f          0.3048 e
* vol * f          0.0005806 e
* fa * f          0.001905 e
* fric * f          0.5          1. e
* grav * f          1.          -1. e
* hd * f          0.04925 e
* icflg *f          0 e
* nff * f          1 e
* alp * f          1. e

```



```

* vl * f 0.0 e
* vv * f 0.0 e
* tl * f 542.7 e
* tv * f 542.7 e
* p * f 5.46621e+06 e
* pa * f 0. e
*****
* type num id ctitle
tee 27 27 $27$ fw tee
* jcell nodes ichf cost epsw
1 0 0 0. 4.57e-5
* iconcl ncell1 jun1 jun2 ipow
0 1 27 28 0
* radin1 th1 houtl1 houtv1 toutl1
2.56800e+00 1.00000e-01 0. 0. 3.00000e+02
* toutv1 pwin1 pwoff1 rpwmx1 pwsc11
3.00000e+02 0. 0. 0. 1.
* iconc2 ncell2 jun3 ipow2
0 1 127 0
* radin2 th2 houtl2 houtv2 toutl2
2.56800e+00 1.00000e-01 0. 0. 3.00000e+02
* toutv2 pwin2 pwoff2 rpwmx2 pwsc12
3.00000e+02 0. 0. 0. 1.
* + + + + +
* dx * f 1.1887 e
* vol * f 0.05726 e
* fa * f 0.04817 e
* fric * f 0. e
* grav * f 0. e
* hd * f 0.24765 e
* icflg * f 0 e
* nff * f 1 e
* alp * 0.01450 e
* vl * f 0.0 e
* vv * f 0.0 e
* tl * f 499.0 e
* tv * f 542.7 e
* p * f 5.46719e+06 e
* pa * f 0. e
* + + + + +
* dx * 0.3048 e
* vol * 0.0005806 e
* fa * f 0.001905 e
* fric * 0.5 1. e
* grav * 1. -1. e
* hd * f 0.04925 e
* icflg * f 0 e
* nff * f 1 e
* alp * 1. e
* vl * f 0.0 e
* vv * f 0.0 e
* tl * f 542.7 e
* tv * f 542.7 e
* p * f 5.46621e+06 e
* pa * f 0. e
*****
* type num id ctitle
tee 28 28 $28$ fw tee
* jcell nodes ichf cost epsw
1 0 0 0. 4.57e-5
* iconcl ncell1 jun1 jun2 ipow
0 1 28 29 0
* radin1 th1 houtl1 houtv1 toutl1
2.56800e+00 1.00000e-01 0. 0. 3.00000e+02
* toutv1 pwin1 pwoff1 rpwmx1 pwsc11
3.00000e+02 0. 0. 0. 1.
* iconc2 ncell2 jun3 ipow2
0 1 128 0
* radin2 th2 houtl2 houtv2 toutl2
2.56800e+00 1.00000e-01 0. 0. 3.00000e+02
* toutv2 pwin2 pwoff2 rpwmx2 pwsc12

```

```

3.00000e+02      0.      0.      0.      1.
*   +   +   +   +   +
* dx * f      1.1887 e
* vol * f      0.05726 e
* fa * f      0.04817 e
* fric * f      0. e
* grav * f      0. e
* hd * f      0.24765 e
* icflg * f      0 e
* nff * f      1 e
* alp *      0.01453 e
* vl * f      0.0 e
* vv * f      0.0 e
* tl * f      499.0 e
* tv * f      542.7 e
* p * f      5.46719e+06 e
* pa * f      0. e
*   +   +   +   +
* dx *      0.3048 e
* vol *      0.0005806 e
* fa * f      0.001905 e
* fric *      0.5
* grav *      1.
* hd * f      0.04925 e
* icflg * f      0 e
* nff * f      1 e
* alp *      1. e
* vl * f      0.0 e
* vv * f      0.0 e
* tl * f      542.7 e
* tv * f      542.7 e
* p * f      5.46621e+06 e
* pa * f      0. e
*****
*          type          num          id          ctitle
tee          29          29          $29$ fw tee
*          jcell          nodes          ichf          cost          epsw
          1          0          0          0.          4.57e-5
*          iconcl          ncell1          jun1          jun2          ipow
          0          1          29          30          0
*          radin1          th1          hout11          houtv1          tout11
2.56800e+00  1.00000e-01          0.          0.          3.00000e+02
*          toutv1          pwin1          pwoff1          rpwmx1          pwsc11
3.00000e+02          0.          0.          0.          1.
*          iconc2          ncell2          jun3          ipow2
          0          1          129          0
*          radin2          th2          hout12          houtv2          tout12
2.56800e+00  1.00000e-01          0.          0.          3.00000e+02
*          toutv2          pwin2          pwoff2          rpwmx2          pwsc12
3.00000e+02          0.          0.          0.          1.
*   +   +   +   +
* dx * f      1.1887 e
* vol * f      0.05726 e
* fa * f      0.04817 e
* fric * f      0. e
* grav * f      0. e
* hd * f      0.24765 e
* icflg * f      0 e
* nff * f      1 e
* alp *      0.01452 e
* vl * f      0.0 e
* vv * f      0.0 e
* tl * f      499.0 e
* tv * f      542.7 e
* p * f      5.46719e+06 e
* pa * f      0. e
*   +   +   +   +
* dx *      0.3048 e
* vol *      0.0005806 e
* fa * f      0.001905 e
* fric *      0.5

```

```

* grav * 1. -1. e
* hd * f 0.04925 e
* icflg * f 0 e
* nff * f 1 e
* alp * 1. e
* vl * f 0.0 e
* vv * f 0.0 e
* tl * f 542.7 e
* tv * f 542.7 e
* p * f 5.46621e+06 e
* pa * f 0. e
*****
* type num id ctitle
tee 30 30 $30$ fw tee
* jcell nodes ichf cost epsw
1 0 0 0. 4.57e-5
* iconcl ncell1 jun1 jun2 ipow
0 1 30 31 0
* radin1 th1 hout11 houtv1 tout11
2.56800e+00 1.00000e-01 0. 0. 3.00000e+02
* toutv1 pwin1 pwoff1 rpwmx1 pwsc11
3.00000e+02 0. 0. 0. 1.
* iconc2 ncell2 jun3 ipow2
0 1 130 0
* radin2 th2 hout12 houtv2 tout12
2.56800e+00 1.00000e-01 0. 0. 3.00000e+02
* toutv2 pwin2 pwoff2 rpwmx2 pwsc12
3.00000e+02 0. 0. 0. 1.
* + + + + +
* dx * f 1.1887 e
* vol * f 0.05726 e
* fa * f 0.04817 e
* fric * f 0. e
* grav * f 0. e
* hd * f 0.24765 e
* icflg * f 0 e
* nff * f 1 e
* alp * 0.01450 e
* vl * f 0.0 e
* vv * f 0.0 e
* tl * f 499.0 e
* tv * f 542.7 e
* p * f 5.46719e+06 e
* pa * f 0. e
* + + + + +
* dx * 0.3048 e
* vol * 0.0005806 e
* fa * f 0.001905 e
* fric * 0.5 1. e
* grav * 1. -1. e
* hd * f 0.04925 e
* icflg * f 0 e
* nff * f 1 e
* alp * 1. e
* vl * f 0.0 e
* vv * f 0.0 e
* tl * f 542.7 e
* tv * f 542.7 e
* p * f 5.46621e+06 e
* pa * f 0. e
*****
* type num id ctitle
tee 31 31 $31$ fw tee
* jcell nodes ichf cost epsw
1 0 0 0. 4.57e-5
* iconcl ncell1 jun1 jun2 ipow
0 1 31 32 0
* radin1 th1 hout11 houtv1 tout11
2.56800e+00 1.00000e-01 0. 0. 3.00000e+02
* toutv1 pwin1 pwoff1 rpwmx1 pwsc11
3.00000e+02 0. 0. 0. 1.

```

```

*      iconc2      ncell2      jun3      ipow2
*      0          1          131          0
*      radin2      th2      houtl2      houtv2      toutl2
*      2.56800e+00  1.00000e-01  0.      0.      3.00000e+02
*      toutv2      pwin2      pwoff2      rpwmx2      pwsc12
*      3.00000e+02  0.      0.      0.      1.
*      +          +          +          +          +
*      dx * f      1.1887 e
*      vol * f      0.05726 e
*      fa * f      0.04817 e
*      fric * f      0. e
*      grav * f      0. e
*      hd * f      0.24765 e
*      icflg * f      0 e
*      nff * f      1 e
*      alp *      0.01445 e
*      vl * f      0.0 e
*      vv * f      0.0 e
*      tl * f      499.0 e
*      tv * f      542.7 e
*      p * f      5.46718e+06 e
*      pa * f      0. e
*      +          +          +          +          +
*      dx *      0.3048 e
*      vol *      0.0005806 e
*      fa * f      0.001905 e
*      fric *      0.5      1. e
*      grav *      1.      -1. e
*      hd * f      0.04925 e
*      icflg * f      0 e
*      nff * f      1 e
*      alp *      1. e
*      vl * f      0.0 e
*      vv * f      0.0 e
*      tl * f      542.7 e
*      tv * f      542.7 e
*      p * f      5.46621e+06 e
*      pa * f      0. e
*****
*      type      num      id      ctitle
tee      32      32      $32$ fw tee
*      jcell      nodes      ichf      cost      epsw
*      1          0          0          0.      4.57e-5
*      iconc1      ncell1      jun1      jun2      ipow
*      0          1          32      33      0
*      radin1      th1      houtl1      houtv1      toutl1
*      2.56800e+00  1.00000e-01  0.      0.      3.00000e+02
*      toutv1      pwin1      pwoff1      rpwmx1      pwsc11
*      3.00000e+02  0.      0.      0.      1.
*      iconc2      ncell2      jun3      ipow2
*      0          1          132      0
*      radin2      th2      houtl2      houtv2      toutl2
*      2.56800e+00  1.00000e-01  0.      0.      3.00000e+02
*      toutv2      pwin2      pwoff2      rpwmx2      pwsc12
*      3.00000e+02  0.      0.      0.      1.
*      +          +          +          +          +
*      dx * f      1.1887 e
*      vol * f      0.05726 e
*      fa * f      0.04817 e
*      fric * f      0. e
*      grav * f      0. e
*      hd * f      0.24765 e
*      icflg * f      0 e
*      nff * f      1 e
*      alp *      0.01435 e
*      vl * f      0.0 e
*      vv * f      0.0 e
*      tl * f      499.0 e
*      tv * f      542.7 e
*      p * f      5.46718e+06 e
*      pa * f      0. e

```

```

*      +      +      +      +      +
* dx *      0.3048 e
* vol *      0.0005806 e
* fa * f      0.001905 e
* fric *      0.5      1. e
* grav *      1.      -1. e
* hd * f      0.04925 e
* icflg *f      0 e
* nff * f      1 e
* alp *      1. e
* vl * f      0.0 e
* vv * f      0.0 e
* tl * f      542.7 e
* tv * f      542.7 e
* p * f      5.46621e+06 e
* pa * f      0. e
*****
*      type      num      id      ctitle
tee      33      33      $33$ fw tee
*      jcell      nodes      ichf      cost      epsw
*      1      0      0      0.      4.57e-5
*      iconcl      ncell1      jun1      jun2      ipow
*      0      1      33      34      0
*      radin1      th1      hout11      houtv1      tout11
*      2.56800e+00      1.00000e-01      0.      0.      3.00000e+02
*      toutv1      pwin1      pwoff1      rpwmx1      pwscl1
*      3.00000e+02      0.      0.      0.      1.
*      iconc2      ncell2      jun3      ipow2
*      0      1      133      0
*      radin2      th2      hout12      houtv2      tout12
*      2.56800e+00      1.00000e-01      0.      0.      3.00000e+02
*      toutv2      pwin2      pwoff2      rpwmx2      pwscl2
*      3.00000e+02      0.      0.      0.      1.
*      +      +      +      +      +
* dx * f      1.1887 e
* vol * f      0.05726 e
* fa * f      0.04817 e
* fric * f      0. e
* grav * f      0. e
* hd * f      0.24765 e
* icflg *f      0 e
* nff * f      1 e
* alp *      0.01418 e
* vl * f      0.0 e
* vv * f      0.0 e
* tl * f      499.1 e
* tv * f      542.7 e
* p * f      5.46718e+06 e
* pa * f      0. e
*      +      +      +      +
* dx *      0.3048 e
* vol *      0.0005806 e
* fa * f      0.001905 e
* fric *      0.5      1. e
* grav *      1.      -1. e
* hd * f      0.04925 e
* icflg *f      0 e
* nff * f      1 e
* alp *      1. e
* vl * f      0.0 e
* vv * f      0.0 e
* tl * f      542.7 e
* tv * f      542.7 e
* p * f      5.46620e+06 e
* pa * f      0. e
*****
*      type      num      id      ctitle
tee      34      34      $34$ fw tee
*      jcell      nodes      ichf      cost      epsw
*      1      0      0      0.      4.57e-5
*      iconcl      ncell1      jun1      jun2      ipow

```

```

*      0      1      34      35      0
*      radin1      th1      houtl1      houtv1      toutl1
* 2.56800e+00 1.00000e-01      0.      0.      3.00000e+02
*      toutv1      pwin1      pwoff1      rpwmx1      pwsc11
* 3.00000e+02      0.      0.      0.      1.
*      iconc2      ncell2      jun3      ipow2
*      0      1      134      0
*      radin2      th2      houtl2      houtv2      toutl2
* 2.56800e+00 1.00000e-01      0.      0.      3.00000e+02
*      toutv2      pwin2      pwoff2      rpwmx2      pwsc12
* 3.00000e+02      0.      0.      0.      1.
*      +      +      +      +      +
* dx * f      1.1887 e
* vol * f      0.05726 e
* fa * f      0.04817 e
* fric * f      0. e
* grav * f      0. e
* hd * f      0.24765 e
* icflg * f      0 e
* nff * f      1 e
* alp *      0.01394 e
* vl * f      0.0 e
* vv * f      0.0 e
* tl * f      499.1 e
* tv * f      542.7 e
* p * f      5.46718e+06 e
* pa * f      0. e
*      +      +      +      +
* dx *      0.3048 e
* vol *      0.0005806 e
* fa * f      0.001905 e
* fric *      0.5      1. e
* grav *      1.      -1. e
* hd * f      0.04925 e
* icflg * f      0 e
* nff * f      1 e
* alp *      1. e
* vl * f      0.0 e
* vv * f      0.0 e
* tl * f      542.7 e
* tv * f      542.7 e
* p * f      5.46620e+06 e
* pa * f      0. e
*****
*      type      num      id      ctitle
tee      35      35      $35$ fw tee
*      jcell      nodes      ichf      cost      epsw
*      1      0      0      0.      4.57e-5
*      iconc1      ncell1      jun1      jun2      ipow
*      0      1      35      36      0
*      radin1      th1      houtl1      houtv1      toutl1
* 2.56800e+00 1.00000e-01      0.      0.      3.00000e+02
*      toutv1      pwin1      pwoff1      rpwmx1      pwsc11
* 3.00000e+02      0.      0.      0.      1.
*      iconc2      ncell2      jun3      ipow2
*      0      1      135      0
*      radin2      th2      houtl2      houtv2      toutl2
* 2.56800e+00 1.00000e-01      0.      0.      3.00000e+02
*      toutv2      pwin2      pwoff2      rpwmx2      pwsc12
* 3.00000e+02      0.      0.      0.      1.
*      +      +      +      +      +
* dx * f      1.1887 e
* vol * f      0.05726 e
* fa * f      0.04817 e
* fric * f      0. e
* grav * f      0. e
* hd * f      0.24765 e
* icflg * f      0 e
* nff * f      1 e
* alp *      0.01361 e
* vl * f      0.0 e

```

```

* vv * f 0.0 e
* tl * f 499.1 e
* tv * f 542.7 e
* p * f 5.46717e+06 e
* pa * f 0. e
* + + + +
* dx * 0.3048 e
* vol * 0.0005806 e
* fa * f 0.001905 e
* fric * 0.5 1. e
* grav * 1. -1. e
* hd * f 0.04925 e
* icflg * f 0 e
* nff * f 1 e
* alp * 1. e
* vl * f 0.0 e
* vv * f 0.0 e
* tl * f 542.7 e
* tv * f 542.7 e
* p * f 5.46620e+06 e
* pa * f 0. e
*****
* type num id ctitle
tee 36 36 $36$ fw tee
* jcell nodes ichf cost epsw
1 0 0 0. 4.57e-5
* iconcl ncell1 jun1 jun2 ipow
0 1 36 37 0
* radin1 th1 hout11 houtv1 tout11
2.56800e+00 1.00000e-01 0. 0. 3.00000e+02
* toutv1 pwin1 pwoff1 rpwm1 pwsc11
3.00000e+02 0. 0. 0. 1.
* iconc2 ncell2 jun3 ipow2
0 1 136 0
* radin2 th2 hout12 houtv2 tout12
2.56800e+00 1.00000e-01 0. 0. 3.00000e+02
* toutv2 pwin2 pwoff2 rpwm2 pwsc12
3.00000e+02 0. 0. 0. 1.
* + + + +
* dx * f 1.1887 e
* vol * f 0.05726 e
* fa * f 0.04817 e
* fric * f 0. e
* grav * f 0. e
* hd * f 0.24765 e
* icflg * f 0 e
* nff * f 1 e
* alp * 0.01318 e
* vl * f 0.0 e
* vv * f 0.0 e
* tl * f 499.2 e
* tv * f 542.7 e
* p * f 5.46717e+06 e
* pa * f 0. e
* + + + +
* dx * 0.3048 e
* vol * 0.0005806 e
* fa * f 0.001905 e
* fric * 0.5 1. e
* grav * 1. -1. e
* hd * f 0.04925 e
* icflg * f 0 e
* nff * f 1 e
* alp * 1. e
* vl * f 0.0 e
* vv * f 0.0 e
* tl * f 542.7 e
* tv * f 542.7 e
* p * f 5.46619e+06 e
* pa * f 0. e
*****

```

```

*          type          num          id          ctitle
tee          37          37          $37$ fw tee
*          jcell          nodes          ichf          cost          epsw
          1          0          0          0.          4.57e-5
*          iconc1          ncell1          jun1          jun2          ipow
          0          1          37          38          0
*          radin1          th1          hout11          houtv1          tout11
2.56800e+00  1.00000e-01  0.          0.          3.00000e+02
*          toutv1          pwin1          pwoff1          rpwmx1          pwsc11
3.00000e+02  0.          0.          0.          1.
*          iconc2          ncell2          jun3          ipow2
          0          1          137          0
*          radin2          th2          hout12          houtv2          tout12
2.56800e+00  1.00000e-01  0.          0.          3.00000e+02
*          toutv2          pwin2          pwoff2          rpwmx2          pwsc12
3.00000e+02  0.          0.          0.          1.
*          +          +          +          +          +
* dx * f          1.1887 e
* vol * f          0.05726 e
* fa * f          0.04817 e
* fric * f          0. e
* grav * f          0. e
* hd * f          0.24765 e
* icflg *f          0 e
* nff * f          1 e
* alp *          0.01261 e
* vl * f          0.0 e
* vv * f          0.0 e
* tl * f          499.2 e
* tv * f          542.7 e
* p * f          5.46716e+06 e
* pa * f          0. e
*          +          +          +          +
* dx *          0.3048 e
* vol *          0.0005806 e
* fa * f          0.001905 e
* fric *          0.5          1. e
* grav *          1.          -1. e
* hd * f          0.04925 e
* icflg *f          0 e
* nff * f          1 e
* alp *          1. e
* vl * f          0.0 e
* vv * f          0.0 e
* tl * f          542.7 e
* tv * f          542.7 e
* p * f          5.46619e+06 e
* pa * f          0. e
*****
*          type          num          id          ctitle
tee          38          38          $38$ fw tee
*          jcell          nodes          ichf          cost          epsw
          1          0          0          0.          4.57e-5
*          iconc1          ncell1          jun1          jun2          ipow
          0          1          38          39          0
*          radin1          th1          hout11          houtv1          tout11
2.56800e+00  1.00000e-01  0.          0.          3.00000e+02
*          toutv1          pwin1          pwoff1          rpwmx1          pwsc11
3.00000e+02  0.          0.          0.          1.
*          iconc2          ncell2          jun3          ipow2
          0          1          138          0
*          radin2          th2          hout12          houtv2          tout12
2.56800e+00  1.00000e-01  0.          0.          3.00000e+02
*          toutv2          pwin2          pwoff2          rpwmx2          pwsc12
3.00000e+02  0.          0.          0.          1.
*          +          +          +          +          +
* dx * f          1.1887 e
* vol * f          0.05726 e
* fa * f          0.04817 e
* fric * f          0. e
* grav * f          0. e

```



```

* hd * f 0.24765 e
* icflg *f 0 e
* nff * f 1 e
* alp * 0.01186 e
* vl * f 0.0 e
* vv * f 0.0 e
* tl * f 499.3 e
* tv * f 542.7 e
* p * f 5.46715e+06 e
* pa * f 0. e
* + + + +
* dx * 0.3048 e
* vol * 0.0005806 e
* fa * f 0.001905 e
* fric * 0.5 1. e
* grav * 1. -1. e
* hd * f 0.04925 e
* icflg *f 0 e
* nff * f 1 e
* alp * 1. e
* vl * f 0.0 e
* vv * f 0.0 e
* tl * f 542.7 e
* tv * f 542.7 e
* p * f 5.46618e+06 e
* pa * f 0. e
*****
* type num id ctitle
tee 39 39 $39$ fw tee
* jcell nodes ichf cost epsw
1 0 0 0. 4.57e-5
* iconcl ncell1 jun1 jun2 ipow
0 1 39 40 0
* radin1 th1 hout11 houtv1 tout11
2.56800e+00 1.00000e-01 0. 0. 3.00000e+02
* toutv1 pwin1 pwoff1 rpwmx1 pwsc11
3.00000e+02 0. 0. 0. 1.
* iconc2 ncell2 jun3 ipow2
0 1 139 0
* radin2 th2 hout12 houtv2 tout12
2.56800e+00 1.00000e-01 0. 0. 3.00000e+02
* toutv2 pwin2 pwoff2 rpwmx2 pwsc12
3.00000e+02 0. 0. 0. 1.
* + + + +
* dx * f 1.1887 e
* vol * f 0.05726 e
* fa * f 0.04817 e
* fric * f 0. e
* grav * f 0. e
* hd * f 0.24765 e
* icflg *f 0 e
* nff * f 1 e
* alp * 0.01079 e
* vl * f 0.0 e
* vv * f 0.0 e
* tl * f 499.2 e
* tv * f 542.7 e
* p * f 5.46715e+06 e
* pa * f 0. e
* + + + +
* dx * 0.3048 e
* vol * 0.0005806 e
* fa * f 0.001905 e
* fric * 0.5 1. e
* grav * 1. -1. e
* hd * f 0.04925 e
* icflg *f 0 e
* nff * f 1 e
* alp * 1. e
* vl * f 0.0 e
* vv * f 0.0 e

```

```

* tl * f      542.7 e
* tv * f      542.7 e
* p  * f  5.46617e+06 e
* pa * f      0. e
*****
*      type      num      id      ctitle
tee      40      40      $40$ fw tee
*      jcell      nodes      ichf      cost      epsw
*      1      0      0      0.      4.57e-5
*      iconcl      ncell1      jun1      jun2      ipow
*      0      1      40      41      0
*      radin1      th1      hout11      houtv1      tout11
*      2.56800e+00      1.00000e-01      0.      0.      3.00000e+02
*      toutv1      pwin1      pwoff1      rpwmx1      pwscl1
*      3.00000e+02      0.      0.      0.      1.
*      iconc2      ncell2      jun3      ipow2
*      0      1      140      0
*      radin2      th2      hout12      houtv2      tout12
*      2.56800e+00      1.00000e-01      0.      0.      3.00000e+02
*      toutv2      pwin2      pwoff2      rpwmx2      pwscl2
*      3.00000e+02      0.      0.      0.      1.
*      +      +      +      +      +
* dx * f      1.1887 e
* vol * f      0.05726 e
* fa * f      0.04817 e
* fric * f      0. e
* grav * f      0. e
* hd * f      0.24765 e
* icflg * f      0 e
* nff * f      1 e
* alp * f      0.009087 e
* vl * f      0.0 e
* vv * f      0.0 e
* tl * f      501.6 e
* tv * f      542.7 e
* p * f      5.46713e+06 e
* pa * f      0. e
*      +      +      +      +
* dx * f      0.3048 e
* vol * f      0.0005806 e
* fa * f      0.001905 e
* fric * f      0.5      1. e
* grav * f      1.      -1. e
* hd * f      0.04925 e
* icflg * f      0 e
* nff * f      1 e
* alp * f      1. e
* vl * f      0.0 e
* vv * f      0.0 e
* tl * f      542.7 e
* tv * f      542.7 e
* p * f      5.46616e+06 e
* pa * f      0. e
*****
*      type      num      id      ctitle
break      900      900      $900$ pressure boundary
*      jun1      ibty      isat      ioff
*      900      0      0      1
*      dxin      volin      alpin      tin      pin
*      0.3556      0.3667      0.      596.3      15.5132e+06
*      pain      concin      rbmx      poff      belv
*      0.      0.      0.      0.      0.
*****
*      type      num      id      ctitle
pipe      901      901      $901$ primary tube inlet
*      ncells      nodes      jun1      jun2      epsw
*      8      0      900      901      4.57e-5
*      ichf      iconc      iacc      ipow      npipes
*      1      0      0      0      1
*      radin      th      hout1      houtv      tout1
*      2.56800e+00      1.00000e-01      0.      0.      3.00000e+02

```

```

*      toutv      powin      powoff      rpowmx      powscl
3.00000e+02      0.      0.      0.      1.
*      +      +      +      +      +
* dx *      0.3556      0.9271 r6      1.2827 e
* vol *      0.3667      0.9559 r6      1.3226 e
* fa * f      1.0311 e
* fric * f      0. e
* grav * f      1. e
* hd * f      0.019685 e
* icflg * f      0 e
* nff * f      1 e
* alp * f      0. e
* vl * f      0.0 e
* vv * f      0.0 e
*      +      +      +      +      +
* tl *      579.7      563.6      557.3      557.7      555.4 s
* tl *      555.1      554.7      554.0 e
* tv *      618.0      617.9      617.9      617.8      617.8 s
* tv *      617.7      617.7      617.6 e
* p *      15.5108e+06      15.5062e+06      15.4980e+06      15.4885e+06      15.4789e+06 s
* p *      15.4693e+06      15.4597e+06      15.4501e+06 e
* pa * f      0. e
*****
*      type      num      id      ctitle
pipe      902      902      $902$ primary tube bend
*      ncells      nodes      jun1      jun2      epsw
*      1      0      901      902      4.57e-5
*      ichf      iconc      iacc      ipow      npipes
*      1      0      0      0      1
*      radin      th      houtl      houtv      toutl
2.56800e+00      1.00000e-01      0.      0.      3.00000e+02
*      toutv      powin      powoff      rpowmx      powscl
3.00000e+02      0.      0.      0.      1.
*      +      +      +      +      +
* dx * f      2.2678 e
* vol * f      2.3383 e
* fa * f      1.0311 e
* fric * f      0. e
* grav *      -1. e
* hd * f      0.019685 e
* icflg * f      0 e
* nff * f      1 e
* alp *      0. e
* vl * f      0.0 e
* vv * f      0.0 e
*      +      +      +      +      +
* tl *      547.7 e
* tv *      617.6 e
* p *      15.4367e+06 e
* pa * f      0. e
*****
*      type      num      id      ctitle
pipe      903      903      $903$ primary tube outlet
*      ncells      nodes      jun1      jun2      epsw
*      8      0      902      903      4.57e-5
*      ichf      iconc      iacc      ipow      npipes
*      1      0      0      0      1
*      radin      th      houtl      houtv      toutl
2.56800e+00      1.00000e-01      0.      0.      3.00000e+02
*      toutv      powin      powoff      rpowmx      powscl
3.00000e+02      0.      0.      0.      1.
*      +      +      +      +      +
* dx * r6      1.2827      0.9271      0.3556 e
* vol * r6      1.3226      0.9559      0.3667 e
* fa * f      1.0311 e
* fric * f      0. e
* grav * f      -1. e
* hd * f      0.019685 e
* icflg * f      0 e
* nff * f      1 e
* alp * f      0. e

```

```

* vl * f 0.0 e
* vv * f 0.0 e
* + + + + +
* tl * 552.1 552.2 552.0 551.7 551.3 s
* tl * 550.9 550.7 549.3 e
* tv * 617.6 617.7 617.7 617.8 617.8 s
* tv * 617.9 617.9 618.0 e
* p * 15.4501e+06 15.4598e+06 15.4694e+06 15.4791e+06 15.4888e+06 s
* p * 15.4985e+06 15.5068e+06 15.5117e+06 e
* pa * f 0. e
*****
* type num id ctitle
fill 904 904 $904$ primary system fill
* jun1 ifty iooff
903 2 0
* twtold rfmz concin felv
0. 1.e+6 0. 0.
* dxin volin alpin vlin tlin
0.3556 0.3667 0. 596.3
* pin pain flowin vvin tvin
15.5132e+06 0. 0. 0. 596.3
*****
* type num id ctitle
htstr 9010 9010 $9010$ ht surface at tube inlet
* nzhtstr ittc hscyl ichf
8 0 0
* nopowr plane liqlev iaxcnd
1 3 0 0
* nmwrx nfci nfcil hdri hdro
0 0 0 0.019685 0.04224
* width
236.555
* nhot nodes irftr nzmax irftr2
0 3 0 8 0
* dtxht(1) dtxht(2) dznht hgapo
1000. 1000. 1000. 1000.
* + + + + +
*idbcin* f 2 e
*idbcon* f 2 e
* hcomin hcelii hcelji hcelki
901 1 0 0 e
901 2 0 0 e
901 3 0 0 e
901 4 0 0 e
901 5 0 0 e
901 6 0 0 e
901 7 0 0 e
901 8 0 0 e
* hcomon hcelio hceljo hcelko
2 1 0 0 e
2 2 0 0 e
2 3 0 0 e
2 4 0 0 e
2 5 0 0 e
2 6 0 0 e
2 7 0 0 e
2 8 0 0 e
*dhtstrz* 0.3556 0.9271 r6 1.2827 e
* rdx * 1. e
* radrd* 0. 0.000635 0.00127 e
* matrd* f 12 e
* nfax * f 0 e
* rftn * 567.52 567.47 567.43 557.13 557.11s
* rftn * 557.08 552.88 552.86 552.85 551.82s
* rftn * 551.81 551.79 551.57 551.56 551.54s
* rftn * 551.37 551.35 551.34 551.02 551.00s
* rftn * 550.99 550.55 550.53 550.52 e
*****
* type num id ctitle
htstr 9020 9020 $9020$ ht surface at tube bend area
* nzhtstr ittc hscyl ichf

```

```

      1      0      0      0
*   nopowr   plane   liqlev   iaxcnd
      1      3      0      0
*   nmwrwx   nfci    nfcil    hdri    hdro
      0      0      0    0.019685    0.00893
*   width
236.555
*   nhot      nodes      irftr      nzmax      irftr2
      0      3      0      8      0
*   dtxht(1)   dtxht(2)   dznht      hgapo
      1000.    1000.    1000.    1000.
*   +      +      +      +      +
*idbcin* f      2 e
*idbcon* f      2 e
*
      hcomin      hcelii      hcelji      hcelki
      902      1      0      0 e
*
      hcomon      hcelio      hceljo      hcelko
      2      9      0      0 e
*dhtstrz*
*   rdx *      1. e
*   radrd*      0.      0.000635      0.00127 e
*   matrd* f      12 e
*   nfax * f      0 e
*   rftn *      544.45      544.44      544.43 e
*****
*   type      num      id      ctitle
htstr      9030      9030      $9030$ ht surface at tube outlet
*   nzhtstr      ittc      hscyl      ichf
      8      0      0      0
*   nopowr   plane   liqlev   iaxcnd
      1      3      0      0
*   nmwrwx   nfci    nfcil    hdri    hdro
      0      0      0    0.019685    0.04224
*   width
236.555
*   nhot      nodes      irftr      nzmax      irftr2
      0      3      0      8      0
*   dtxht(1)   dtxht(2)   dznht      hgapo
      1000.    1000.    1000.    1000.
*   +      +      +      +      +
*idbcin* f      2 e
*idbcon* f      2 e
*
      hcomin      hcelii      hcelji      hcelki
      903      1      0      0 e
      903      2      0      0 e
      903      3      0      0 e
      903      4      0      0 e
      903      5      0      0 e
      903      6      0      0 e
      903      7      0      0 e
      903      8      0      0 e
*
      hcomon      hcelio      hceljo      hcelko
      2      8      0      0 e
      2      7      0      0 e
      2      6      0      0 e
      2      5      0      0 e
      2      4      0      0 e
      2      3      0      0 e
      2      2      0      0 e
      2      1      0      0 e
*dhtstrz* r6      1.2827      0.9271      0.3556 e
*   rdx *      1. e
*   radrd*      0.      0.000635      0.00127 e
*   matrd* f      12 e
*   nfax * f      0 e
*   rftn *      549.25      549.24      549.22      549.36      549.34s
*   rftn *      549.33      549.24      549.23      549.22      549.06s
*   rftn *      549.05      549.04      548.85      548.84      548.83s
*   rftn *      548.62      548.61      548.61      548.49      548.48s
*   rftn *      548.47      547.59      547.58      547.57 e
*****

```

```

end
*
*****
*                               time step data                               *
*****
*
*      dtmin      dtmax      tend      trwfp
*      .00001      .01      10.      10.
*
*      edint      gfint      dmpint      sedint
*      2.      0.01      20.      1.e6
*      -1.0

```

## A.2 Input File for FWLB with Steam Generator at 100-Percent Power

```

free format
*
*          numtcr          ieos          inopt          nmat
*              4              0              1              0
Simple W Model 51 Steam Generator
Eight Tube Sections 2 to 9
water packing off, ipack=0
choked flow option, icflow=2
*
&inopts
  icflow=2, iadded=20, ikfac=1, nosets=1, nhtstr=3, ithd=1
&end
*
*          dstep          timet
*              0              0.0
*
*          stdyst          transi          ncomp          njun          ipack
*              0              1              47              74              0
*
*          epso          epss
*      1.0e-08      1.0e-03
*
*          oitmax          sitmax          isolut          ncontr          nccfl
*              100              100              0              0              0
*
*          ntsv          ntcb          ntcf          ntrp          ntcp
*              0              0              0              0              1
*
* iorder      +              +              +              +              +
*              1              2              3              4              5s
*              6              8              9              10             11s
*              12             13             14             15             16s
*              17             18             19             20             21s
*              22             23             24             25             26s
*              27             28             29             30             31s
*              32             33             34             35             36s
*              37             38             39             40             900s
*              901            902            903            904            9010s
*              9020            9030e
*
*****
*                                component data                                *
*****
*
*          type          num          id          ctitle
pipe          1          1          $1$ annulus
*
*          ncells          nodes          jun1          jun2          epsw
*              9              0              1              2          4.57e-5
*
*          ichf          iconc          iacc          ipow          npipes
*              1              0              0              0              1
*
*          radin          th          houtl          houtv          toutl
*      2.56800e+00      1.00000e-01          0.          0.          3.00000e+02
*
*          toutv          powin          powoff          rpowmx          powscl
*      3.00000e+02          0.          0.          0.          1.
*
*          +              +              +              +              +
* dx *          0.3556          0.9271 r6          1.2827          1.9543 e
* vol *          0.2568          0.6556 r6          0.9124          6.80 e
* fa * r9          0.722          6.627 e
* fric *          0.175 r7          0.          1.          1. e
* grav *          0. r9          1. e
* hd *          0.2678 r7          0.1430          0.36          0.64 e
* icflg *f          0 e
* nff * r8          1 r2          1 e

```

```

* alp * f 0.0 e
* vl * r9 -4.697 -0.5117 e
* vv * -4.691 r7 -4.694 -4.699 -0.5084 e
* + + + + +
* tl * r3 536.1 r6 536.0 e
* tv * 544.9 544.8 544.8 544.7 544.6s
* tv * 544.5 544.4 544.3 544.3 e
* p * 5.65557e+06 5.65085e+06 5.64348e+06 5.63480e+06 5.62612e+06s
* p * 5.61743e+06 5.60875e+06 5.60007e+06 5.60529e+06 e
* pa * f 0. e
*****
* type num id ctitle
pipe 2 2 $2$ tube sections
*
* ncells nodes jun1 jun2 epsw
* 9 0 1 3 4.57e-5
*
* ichf iconc iacc ipow npipes
* 1 0 0 0 1
*
* radin th hout1 houtv tout1
* 2.56800e+00 1.00000e-01 0. 0. 3.00000e+02
*
* toutv powin powoff rpowmx powsc1
* 3.00000e+02 0. 0. 0. 1.
*
* + + + + +
* dx * 0.3556 0.9271 r6 1.2827 1.9543 e
* vol * 1.785 4.655 r6 6.44 11.85 e
* fa * 0.722 r8 5.1 4.77 e
* fric * 0.175 0.0 r7 5.87 8.33 e
* grav * 0. r9 1. e
* hd * 0.2678 r8 0.0422 0.0817 e
* icflg * f 0 e
* nff * f 1 e
* alp * 0.0 0.0 0.1798 0.3348 0.4203s
* alp * 0.5009 0.5633 0.6153 0.6255 e
* vl * 4.697 0.6699 0.6768 0.8174 0.9894s
* vl * 1.113 1.267 1.417 1.573 1.686e
* vv * 4.691 0.6734 2.078 1.310 1.676s
* vv * 2.142 2.491 2.848 3.202 4.036e
* + + + + +
* tl * 539.3 543.6 545.0 545.0 544.9s
* tl * 544.8 544.7 544.6 544.5 e
* tv * 545.0 544.9 544.8 544.7 544.6s
* tv * 544.5 544.5 544.4 544.3 e
* p * 5.66234e+06 5.65742e+06 5.64886e+06 5.64025e+06 5.63237e+06s
* p * 5.62504e+06 5.61804e+06 5.61124e+06 5.60336e+06 e
* pa * f 0. e
*****
* type num id ctitle
tee 3 3 $3$ sg top
*
* jcell nodes ichf cost epsw
* 3 0 1 1. 4.57e-5
*
* iconc1 ncell1 jun1 jun2 ipow
* 0 3 3 7 0
*
* radin1 th1 hout11 houtv1 tout11
* 2.56800e+00 1.00000e-01 0. 0. 3.00000e+02
*
* toutv1 pw1n1 pwoff1 rpwm1x1 pwsc11
* 3.00000e+02 0. 0. 0. 1.
*
* iconc2 ncell2 jun3 ipow2
* 0 1 6 0
*
* radin2 th2 hout12 houtv2 tout12
* 2.56800e+00 1.00000e-01 0. 0. 3.00000e+02

```



```

*      toutv2      pwin2      pwoff2      rpwmx2      pwsc12
3.00000e+02      0.      0.      0.      1.
*
*      +      +      +      +      +
* dx * r2      1.44      2.88 e
* vol * r2      6.182      27.17 e
* fa * r3      4.77      7.68 e
* fric *      8.33      2.5      2.0      2.0 e
* grav * r3      1.      0.74 e
* hd *      0.0817      1.42      1.35      2.20 e
* icflg *f      0 e
* nff * f      1 e
* alp *      0.6477      0.6573      0.6987 e
* vl *      1.686      1.789      1.839      0.1432 e
* vv *      4.036      3.926      3.879      2.274 e
*      +      +      +      +      +
* tl *      544.2      544.1      544.0 e
* tv *      544.2      544.1      544.1 e
* p *      5.59324e+06      5.58771e+06      5.58115e+06 e
* pa * f      0. e
*      +      +      +      +      +
* dx * f      1.44 e
* vol * f      13.495 e
* fa *      9.49      9.49 e
* fric *      15.9      15.9 e
* grav * f      -1. e
* hd *      1.47      1.35 e
* icflg *f      0 e
* nff * f      1 e
* alp *      0.4730 e
* vl *      0.9355      0.5344 e
* vv *      -0.002851      -1.160 e
*      +      +      +      +      +
* tl *      544.1 e
* tv *      544.1 e
* p *      5.58537e+06 e
* pa * f      0. e
*****
*      type      num      id      ctitle
pipe      4      4      $4$ steam line
*
*      ncells      nodes      jun1      jun2      epsw
21      0      4      5      4.57e-5
*
*      ichf      iconc      iacc      ipow      npipes
1      0      0      0      1
*
*      radin      th      hout1      houtv      tout1
2.56800e+00      1.00000e-01      0.      0.      3.00000e+02
*
*      toutv      powin      powoff      rpowmx      powsc1
3.00000e+02      0.      0.      0.      1.
*
*      +      +      +      +      +
* dx *      0.5334 r20      1.5 e
* vol *      0.2280 r20      0.6411 e
* fa * f      0.4274 e
* fric *      0.5      5.26 r20      0.0 e
* grav * r2      1. r8      -1. r12      0.0 e
* hd *      2.96 r21      0.7377 e
* icflg *      1 r20      0      1 e
* nff * f      1 e
* alp *      0.9769      0.9834      0.9846      0.9850      0.9852s
* alp *      0.9854      0.9855      0.9855      0.9856      0.9855s
* alp *      0.9854      0.9853 r9      0.9852 e
* vl *      21.31      18.40      25.52      27.48      28.30s
* vl *      28.75      29.03      29.23      29.40      29.56s
* vl *      28.27      29.06      28.91      28.82      28.76s
* vl *      28.73      28.71 r4      28.70      28.83 e
* vv *      29.17      29.37      29.55 r8      29.54 r3      29.55s
* vv * r4      29.56 r4      29.57 e

```

```

*      +      +      +      +      +
*  tl  *      543.7      542.9 r14      542.8 r5      542.7 e      +
*  tv  *      543.5      542.2      542.4      542.5      542.6s
*  tv  * r4      542.7 r3      542.8 r9      542.7 e
*  p   *      5.54907e+06  5.47387e+06  5.47170e+06  5.47128e+06  5.47122e+06s
*  p   *      5.47127e+06  5.47137e+06  5.47150e+06  5.47163e+06  5.47177e+06s
*  p   *      5.47148e+06  5.47117e+06  5.47084e+06  5.47049e+06  5.47013e+06s
*  p   *      5.46977e+06  5.46939e+06  5.46902e+06  5.46864e+06  5.46826e+06s
*  p   *      5.46789e+06 e
*  pa  * f      0. e
*****
*      type      num      id      ctitle
fill      5      5      $5$ steam line end
*      jun1      ifty      ioff
*      5      2      0
*      twtold      rfmix      concin      felv
*      0.      1.e+6      0.      0.
*      dxin      volin      alpin      vlin      tlin
*      1.5      0.6411      1.      0.      543.3
*      pin      pain      flowin      vvin      tvin
*      5.46754e+06      0.      0.      0.      543.3
*****
*      type      num      id      ctitle
plenum      6      6      $6$ lower sg fw entry volume
*      mpljn      iconc      juns1      juns2
*      33      0      1      32
*      +      +      +      +      +
*  junj *      2      6      8      111      112 s
*  junj *      113      114      115      116      117 s
*  junj *      118      119      120      121      122 s
*  junj *      123      124      125      126      127 s
*  junj *      128      129      130      131      132 s
*  junj *      133      134      135      136      137 s
*  junj *      138      139      140 e
*  dx  * f      1.44 e
*  vol *      13.495 e
*  elev *      0. e
*  alp *      0.0 e
*  tl  *      536.04 e
*  tv  *      544.18 e
*  p   *      5.59271e+06 e
*  pa  * f      0. e
*****
*      type      num      id      ctitle
tee      8      8      $8$ sg top
*      jcell      nodes      ichf      cost      epsw
*      1      0      1      1.      4.57e-5
*      iconc1      ncell1      jun1      jun2      ipow
*      0      2      7      4      0
*      radin1      th1      hout11      houtv1      tout11
*      2.56800e+00  1.00000e-01  0.      0.      3.00000e+02
*      toutv1      pwin1      pwoff1      rpwmx1      pwscl1
*      3.00000e+02  0.      0.      0.      1.
*      iconc2      ncell2      jun3      ipow2
*      0      2      8      0
*      radin2      th2      hout12      houtv2      tout12
*      2.56800e+00  1.00000e-01  0.      0.      3.00000e+02
*      toutv2      pwin2      pwoff2      rpwmx2      pwscl2
*      3.00000e+02  0.      0.      0.      1.
*      +      +      +      +      +
*  dx  *      2.134      1.606 e
*  vol *      14.30      15.02 e
*  fa  *      7.68      14.4      0.4274 e
*  fric *      2.0      2.0      0.5 e
*  grav *      0.74      1.      1. e
*  hd  *      2.20      4.28      2.96 e
*  icflg *r2      0      1 e
*  nff  * f      1 e
*  alp *      0.6135      0.9801 e
*  vl  *      0.1432      0.03265      21.31 e
*  vv  *      2.274      1.382      29.17 e

```

```

*   tl   *           544.0           543.9 e
*   tv   *           544.0           543.9 e
*   p     *   5.57609e+06   5.57244e+06 e
*   pa   * f           0. e
*   +     +           +           +           +           +
*   dx   *           2.186           1.12 e
*   vol   *           0.7062          0.3618 e
*   fa   * f           0.3231 e
*   fric  *           1.0           0.           1. e
*   grav  * f          -1. e
*   hd   * f           0.6414 e
*   icflg *f           0 e
*   nff   * f           1 e
*   alp   *           0.7017          0.6258 e
*   vl   *           1.199           1.554           1.239 e
*   vv   *           0.003141          0.001485          -0.6975 e
*   tl   *           544.0           544.0 e
*   tv   *           544.0           544.1 e
*   p     *   5.58147e+06   5.58576e+06 e
*   pa   * f           0. e
*****
*           type           num           id           ctitle
tee           9           9           $9$ fw tee
*   jcell          nodes           ichf           cost           epsw
*   2           0           0           0.           4.57e-5
*   iconcl          ncell1          jun1           jun2           ipow
*   0           3           41           11           0
*   radin1          th1           hout11          houtv1          tout11
*   2.56800e+00   1.00000e-01          0.           0.           3.00000e+02
*   toutv1          pwin1          pwoff1          rpwmx1          pwsc11
*   3.00000e+02          0.           0.           0.           1.
*   iconc2          ncell2          jun3           ipow2
*   0           2           9           0
*   radin2          th2           hout12          houtv2          tout12
*   2.56800e+00   1.00000e-01          0.           0.           3.00000e+02
*   toutv2          pwin2          pwoff2          rpwmx2          pwsc12
*   3.00000e+02          0.           0.           0.           1.
*   +           +           +           +           +
*   dx   * f           0.4064 e
*   vol   * f           0.019576 e
*   fa   * f           0.04817 e
*   fric  *           0.           0.2           0.2           0. e
*   grav  * f           0. e
*   hd   * f           0.24765 e
*   icflg *f           0 e
*   nff   * f           1 e
*   alp   * f           0. e
*   vl   *           -6.035          -6.034           6.034           6.035 e
*   vv   *           -6.036          -6.050           6.050           6.036 e
*   tl   *           498.4           498.4           498.4 e
*   tv   *           545.5           546.3           545.5 e
*   p     *   5.71043e+06   5.77491e+06   5.71043e+06 e
*   pa   * f           0. e
*   +           +           +           +           +
*   dx   *           0.3048           0.4826 e
*   vol   *           0.033315          0.050094 e
*   fa   *           0.1093           0.1038           0.1038 e
*   fric  *           1.2           0.           1. e
*   grav  * r3          0. e
*   hd   *           0.3731           0.3814           0.3635 e
*   icflg *           0           0           1 e
*   nff   *           1           -1           1 e
*   alp   * f           0. e
*   vl   *           -5.319          -5.601           0. e
*   vv   *           -5.327          -5.599           0. e
*   tl   * f           498.4 e
*   tv   * f           546.4 e
*   p     *   5.78926e+06   5.78817e+06 e
*   pa   * f           0. e
*****
*           type           num           id           ctitle

```

```

break                10                10    $10$ pressure boundary
*      jun1          ibty              isat      ioff
*      9              0                0        1
*      dxin          volin             alpin      tin        pin
*      0.4826        0.050094          1.        373.15      1.0e+5
*      pain          concin            rbmx       poff       belv
*      0.            0.                0.        0.         0.
*****
*      type          num              id          ctitle
tee          11              11          $11$ fw tee
*      jcell         nodes           ichf         cost          epsw
*      1              0              0            0.          4.57e-5
*      iconc1        ncell1          jun1         jun2          ipow
*      0              1              11           12           0
*      radin1        th1             hout11        houtv1         tout11
*      2.56800e+00    1.00000e-01      0.           0.          3.00000e+02
*      toutv1        pwin1           pwoff1        rpwm1         pwsc11
*      3.00000e+02    0.             0.           0.           1.
*      iconc2        ncell2          jun3         ipow2
*      0              1              111          0
*      radin2        th2             hout12        houtv2         tout12
*      2.56800e+00    1.00000e-01      0.           0.          3.00000e+02
*      toutv2        pwin2           pwoff2        rpwm2         pwsc12
*      3.00000e+02    0.             0.           0.           1.
*      +              +              +            +            +
*      dx * f         1.1887 e
*      vol * f         0.05726 e
*      fa * f         0.04817 e
*      fric * f        0. e
*      grav * f        0. e
*      hd * f         0.24765 e
*      icflg * f       0 e
*      nff * f         1 e
*      alp * f         0. e
*      vl *           6.035          5.642 e
*      vv *           6.036          5.641 e
*      tl *           498.4 e
*      tv *           545.5 e
*      p *           5.70975e+06 e
*      pa * f         0. e
*      +              +              +            +            +
*      dx *           0.3048 e
*      vol *          0.0005806 e
*      fa * f         0.001905 e
*      fric *         0.5           1. e
*      grav *         1.           -1. e
*      hd * f         0.04925 e
*      icflg * f       0 e
*      nff * f         1 e
*      alp *          0. e
*      vl *           9.938          9.939 e
*      vv *           9.966          9.942 e
*      tl *           498.3 e
*      tv *           544.3 e
*      p *           5.59942e+06 e
*      pa * f         0. e
*****
*      type          num              id          ctitle
tee          12              12          $12$ fw tee
*      jcell         nodes           ichf         cost          epsw
*      1              0              0            0.          4.57e-5
*      iconc1        ncell1          jun1         jun2          ipow
*      0              1              12           13           0
*      radin1        th1             hout11        houtv1         tout11
*      2.56800e+00    1.00000e-01      0.           0.          3.00000e+02
*      toutv1        pwin1           pwoff1        rpwm1         pwsc11
*      3.00000e+02    0.             0.           0.           1.
*      iconc2        ncell2          jun3         ipow2
*      0              1              112          0
*      radin2        th2             hout12        houtv2         tout12
*      2.56800e+00    1.00000e-01      0.           0.          3.00000e+02

```

```

*      toutv2      pwin2      pwoff2      rpwmx2      pwsc12
3.00000e+02      0.      0.      0.      1.
*      +      +      +      +      +
* dx * f      1.1887 e
* vol * f      0.05726 e
* fa * f      0.04817 e
* fric * f      0. e
* grav * f      0. e
* hd * f      0.24765 e
* icflg * f      0 e
* nff * f      1 e
* alp * f      0. e
* vl *      5.642      5.247 e
* vv *      5.641      5.246 e
* tl * f      498.4 e
* tv * f      545.5 e
* p * f      5.71074e+06 e
* pa * f      0. e
*      +      +      +      +
* dx *      0.3048 e
* vol *      0.0005806 e
* fa * f      0.001905 e
* fric *      0.5      1. e
* grav *      1.      -1. e
* hd * f      0.04925 e
* icflg * f      0 e
* nff * f      1 e
* alp *      0. e
* vl *      9.978      9.979 e
* vv *      10.01      9.983 e
* tl * f      498.3 e
* tv * f      544.3 e
* p * f      5.59953e+06 e
* pa * f      0. e
*****
*      type      num      id      ctitle
tee      13      13      $13$ fw tee
*      jcell      nodes      ichf      cost      epsw
1      0      0      0      4.57e-5
*      iconcl      ncell1      jun1      jun2      ipow
0      1      13      14      0
*      radin1      th1      hout11      houtv1      tout11
2.56800e+00      1.00000e-01      0.      0.      3.00000e+02
*      toutv1      pwin1      pwoff1      rpwmx1      pwsc11
3.00000e+02      0.      0.      0.      1.
*      iconc2      ncell2      jun3      ipow2
0      1      113      0
*      radin2      th2      hout12      houtv2      tout12
2.56800e+00      1.00000e-01      0.      0.      3.00000e+02
*      toutv2      pwin2      pwoff2      rpwmx2      pwsc12
3.00000e+02      0.      0.      0.      1.
*      +      +      +      +      +
* dx * f      1.1887 e
* vol * f      0.05726 e
* fa * f      0.04817 e
* fric * f      0. e
* grav * f      0. e
* hd * f      0.24765 e
* icflg * f      0 e
* nff * f      1 e
* alp * f      0. e
* vl *      5.247      4.851 e
* vv *      5.246      4.850 e
* tl * f      498.4 e
* tv * f      545.5 e
* p * f      5.71171e+06 e
* pa * f      0. e
*      +      +      +      +
* dx *      0.3048 e
* vol *      0.0005806 e
* fa * f      0.001905 e

```

```

* fric *          0.5          1. e
* grav *          1.          -1. e
* hd * f          0.04925 e
* icflg * f          0 e
* nff * f          1 e
* alp *          0. e
* vl *          10.02          10.02 e
* vv *          10.05          10.02 e
* tl * f          498.3 e
* tv * f          544.3 e
* p * f          5.59963e+06 e
* pa * f          0. e
*****
*          type          num          id          ctitle
tee          14          14          $14$ fw tee
*          jcell          nodes          ichf          cost          epsw
          1          0          0          0.          4.57e-5
*          iconcl          ncell1          jun1          jun2          ipow
          0          1          14          15          0
*          radin1          th1          hout11          houtv1          tout11
2.56800e+00  1.00000e-01          0.          0.          3.00000e+02
*          toutv1          pwin1          pwoff1          rpwmx1          pwsc11
3.00000e+02          0.          0.          0.          1.
*          iconc2          ncell2          jun3          ipow2
          0          1          114          0
*          radin2          th2          hout12          houtv2          tout12
2.56800e+00  1.00000e-01          0.          0.          3.00000e+02
*          toutv2          pwin2          pwoff2          rpwmx2          pwsc12
3.00000e+02          0.          0.          0.          1.
*          +          +          +          +          +
* dx * f          1.1887 e
* vol * f          0.05726 e
* fa * f          0.04817 e
* fric * f          0. e
* grav * f          0. e
* hd * f          0.24765 e
* icflg * f          0 e
* nff * f          1 e
* alp * f          0. e
* vl *          4.851          4.453 e
* vv *          4.850          4.452 e
* tl * f          498.4 e
* tv * f          545.5 e
* p * f          5.71268e+06 e
* pa * f          0. e
*          +          +          +          +
* dx *          0.3048 e
* vol *          0.0005806 e
* fa * f          0.001905 e
* fric *          0.5          1. e
* grav *          1.          -1. e
* hd * f          0.04925 e
* icflg * f          0 e
* nff * f          1 e
* alp *          0. e
* vl *          10.06          10.06 e
* vv *          10.09          10.06 e
* tl * f          498.3 e
* tv * f          544.3 e
* p * f          5.59974e+06 e
* pa * f          0. e
*****
*          type          num          id          ctitle
tee          15          15          $15$ fw tee
*          jcell          nodes          ichf          cost          epsw
          1          0          0          0.          4.57e-5
*          iconcl          ncell1          jun1          jun2          ipow
          0          1          15          16          0
*          radin1          th1          hout11          houtv1          tout11
2.56800e+00  1.00000e-01          0.          0.          3.00000e+02
*          toutv1          pwin1          pwoff1          rpwmx1          pwsc11
          0.          0.          0.          0.          0.

```

```

3.00000e+02      0.      0.      0.      1.
*      iconc2      ncell2      jun3      ipow2
      0      1      115      0
*      radin2      th2      houtl2      houtv2      toutl2
2.56800e+00      1.00000e-01      0.      0.      3.00000e+02
*      toutv2      pwin2      pwoff2      rpwmx2      pwsc12
3.00000e+02      0.      0.      0.      1.
*      +      +      +      +      +
* dx * f      1.1887 e
* vol * f      0.05726 e
* fa * f      0.04817 e
* fric * f      0. e
* grav * f      0. e
* hd * f      0.24765 e
* icflg * f      0 e
* nff * f      1 e
* alp * f      0. e
* vl *      4.453      4.054 e
* vv *      4.452      4.053 e
* tl * f      498.4 e
* tv * f      545.6 e
* p * f      5.71361e+06 e
* pa * f      0. e
*      +      +      +      +
* dx *      0.3048 e
* vol *      0.0005806 e
* fa * f      0.001905 e
* fric *      0.5      1. e
* grav *      1.      -1. e
* hd * f      0.04925 e
* icflg * f      0 e
* nff * f      1 e
* alp *      0. e
* vl *      10.10      10.10 e
* vv *      10.12      10.10 e
* tl * f      498.3 e
* tv * f      544.3 e
* p * f      5.59984e+06 e
* pa * f      0. e
*****
*      type      num      id      ctitle
tee      16      16      $16$ fw tee
*      jcell      nodes      ichf      cost      epsw
      1      0      0      0.      4.57e-5
*      iconc1      ncell1      jun1      jun2      ipow
      0      1      16      17      0
*      radin1      th1      houtl1      houtv1      toutl1
2.56800e+00      1.00000e-01      0.      0.      3.00000e+02
*      toutv1      pwin1      pwoff1      rpwmx1      pwsc11
3.00000e+02      0.      0.      0.      1.
*      iconc2      ncell2      jun3      ipow2
      0      1      116      0
*      radin2      th2      houtl2      houtv2      toutl2
2.56800e+00      1.00000e-01      0.      0.      3.00000e+02
*      toutv2      pwin2      pwoff2      rpwmx2      pwsc12
3.00000e+02      0.      0.      0.      1.
*      +      +      +      +      +
* dx * f      1.1887 e
* vol * f      0.05726 e
* fa * f      0.04817 e
* fric * f      0. e
* grav * f      0. e
* hd * f      0.24765 e
* icflg * f      0 e
* nff * f      1 e
* alp * f      0. e
* vl *      4.054      3.653 e
* vv *      4.053      3.652 e
* tl * f      498.4 e
* tv * f      545.6 e
* p * f      5.71452e+06 e

```

```

* pa * f 0. e
* + + + +
* dx * 0.3048 e
* vol * 0.0005806 e
* fa * f 0.001905 e
* fric * 0.5 1. e
* grav * 1. -1. e
* hd * f 0.04925 e
* icflg * f 0 e
* nff * f 1 e
* alp * 0. e
* vl * 10.13 10.13 e
* vv * 10.16 10.14 e
* tl * f 498.3 e
* tv * f 544.3 e
* p * f 5.59994e+06 e
* pa * f 0. e
*****
* type num id ctitle
tee 17 17 $17$ fw tee
* jcell nodes ichf cost epsw
1 0 0 0. 4.57e-5
* iconcl ncell1 jun1 jun2 ipow
0 1 17 18 0
* radin1 th1 hout11 houtv1 tout11
2.56800e+00 1.00000e-01 0. 0. 3.00000e+02
* toutv1 pwin1 pwoff1 rpwmx1 pwsc11
3.00000e+02 0. 0. 0. 1.
* iconc2 ncell2 jun3 ipow2
0 1 117 0
* radin2 th2 hout12 houtv2 tout12
2.56800e+00 1.00000e-01 0. 0. 3.00000e+02
* toutv2 pwin2 pwoff2 rpwmx2 pwsc12
3.00000e+02 0. 0. 0. 1.
* + + + +
* dx * f 1.1887 e
* vol * f 0.05726 e
* fa * f 0.04817 e
* fric * f 0. e
* grav * f 0. e
* hd * f 0.24765 e
* icflg * f 0 e
* nff * f 1 e
* alp * f 0. e
* vl * 3.653 3.251 e
* vv * 3.652 3.250 e
* tl * f 498.4 e
* tv * f 545.6 e
* p * f 5.71538e+06 e
* pa * f 0. e
* + + + +
* dx * 0.3048 e
* vol * 0.0005806 e
* fa * f 0.001905 e
* fric * 0.5 1. e
* grav * 1. -1. e
* hd * f 0.04925 e
* icflg * f 0 e
* nff * f 1 e
* alp * 0. e
* vl * 10.17 10.17 e
* vv * 10.19 10.17 e
* tl * f 498.3 e
* tv * f 544.3 e
* p * f 5.60004e+06 e
* pa * f 0. e
*****
* type num id ctitle
tee 18 18 $18$ fw tee
* jcell nodes ichf cost epsw
1 0 0 0. 4.57e-5

```



```

*      iconc1      ncell1      jun1      jun2      ipow
*      0          1          18          19          0
*      radin1      th1      hout11      houtv1      tout11
*      2.56800e+00  1.00000e-01  0.      0.      3.00000e+02
*      toutv1      pwin1      pwoff1      rpwmx1      pwsc11
*      3.00000e+02  0.      0.      0.      1.
*      iconc2      ncell2      jun3      ipow2
*      0          1          118          0
*      radin2      th2      hout12      houtv2      tout12
*      2.56800e+00  1.00000e-01  0.      0.      3.00000e+02
*      toutv2      pwin2      pwoff2      rpwmx2      pwsc12
*      3.00000e+02  0.      0.      0.      1.
*      +          +          +          +          +
*      dx * f      1.1887 e
*      vol * f      0.05726 e
*      fa * f      0.04817 e
*      fric * f      0. e
*      grav * f      0. e
*      hd * f      0.24765 e
*      icflg *f      0 e
*      nff * f      1 e
*      alp * f      0. e
*      vl *        3.251      2.848 e
*      vv *        3.250      2.847 e
*      tl * f      498.4 e
*      tv * f      545.6 e
*      p * f      5.71618e+06 e
*      pa * f      0. e
*      +          +          +          +          +
*      dx *        0.3048 e
*      vol *      0.0005806 e
*      fa * f      0.001905 e
*      fric *      0.5      1. e
*      grav *      1.      -1. e
*      hd * f      0.04925 e
*      icflg *f      0 e
*      nff * f      1 e
*      alp *      0. e
*      vl *      10.20      10.20 e
*      vv *      10.23      10.20 e
*      tl * f      498.3 e
*      tv * f      544.3 e
*      p * f      5.60013e+06 e
*      pa * f      0. e
*****
*      type      num      id      ctitle
tee      19      19      $19$ fw tee
*      jcell      nodes      ichf      cost      epsw
*      1          0          0          0.      4.57e-5
*      iconc1      ncell1      jun1      jun2      ipow
*      0          1          19      20      0
*      radin1      th1      hout11      houtv1      tout11
*      2.56800e+00  1.00000e-01  0.      0.      3.00000e+02
*      toutv1      pwin1      pwoff1      rpwmx1      pwsc11
*      3.00000e+02  0.      0.      0.      1.
*      iconc2      ncell2      jun3      ipow2
*      0          1          119          0
*      radin2      th2      hout12      houtv2      tout12
*      2.56800e+00  1.00000e-01  0.      0.      3.00000e+02
*      toutv2      pwin2      pwoff2      rpwmx2      pwsc12
*      3.00000e+02  0.      0.      0.      1.
*      +          +          +          +          +
*      dx * f      1.1887 e
*      vol * f      0.05726 e
*      fa * f      0.04817 e
*      fric * f      0. e
*      grav * f      0. e
*      hd * f      0.24765 e
*      icflg *f      0 e
*      nff * f      1 e
*      alp * f      0. e

```

```

* vl      *          2.848          2.443 e
* vv      *          2.847          2.442 e
* tl      * f          498.4 e
* tv      * f          545.6 e
* p        * f 5.71692e+06 e
* pa      * f          0. e
*          +          +          +          +
* dx      *          0.3048 e
* vol     *          0.0005806 e
* fa      * f          0.001905 e
* fric    *          0.5          1. e
* grav    *          1.          -1. e
* hd      * f          0.04925 e
* icflg   * f          0 e
* nff     * f          1 e
* alp     *          0. e
* vl      *          10.23          10.23 e
* vv      *          10.26          10.23 e
* tl      * f          498.3 e
* tv      * f          544.3 e
* p        * f 5.60021e+06 e
* pa      * f          0. e
*****
*          type          num          id          ctitle
tee          20          20          $20$ fw tee
*          jcell          nodes          ichf          cost          epsw
          1          0          0          0          4.57e-5
*          iconcl          ncell1          jun1          jun2          ipow
          0          1          20          21          0
*          radin1          th1          houtl1          houtv1          toutl1
2.56800e+00  1.00000e-01          0.          0.          3.00000e+02
*          toutv1          pwin1          pwoff1          rpwmx1          pwsc11
3.00000e+02          0.          0.          0.          1.
*          iconc2          ncell2          jun3          ipow2
          0          1          120          0
*          radin2          th2          houtl2          houtv2          toutl2
2.56800e+00  1.00000e-01          0.          0.          3.00000e+02
*          toutv2          pwin2          pwoff2          rpwmx2          pwsc12
3.00000e+02          0.          0.          0.          1.
*          +          +          +          +          +
* dx      * f          1.1887 e
* vol     * f          0.05726 e
* fa      * f          0.04817 e
* fric    * f          0. e
* grav    * f          0. e
* hd      * f          0.24765 e
* icflg   * f          0 e
* nff     * f          1 e
* alp     * f          0. e
* vl      *          2.443          2.038 e
* vv      *          2.442          2.037 e
* tl      * f          498.4 e
* tv      * f          545.6 e
* p        * f 5.71758e+06 e
* pa      * f          0. e
*          +          +          +          +
* dx      *          0.3048 e
* vol     *          0.0005806 e
* fa      * f          0.001905 e
* fric    *          0.5          1. e
* grav    *          1.          -1. e
* hd      * f          0.04925 e
* icflg   * f          0 e
* nff     * f          1 e
* alp     *          0. e
* vl      *          10.25          10.25 e
* vv      *          10.28          10.26 e
* tl      * f          498.3 e
* tv      * f          544.3 e
* p        * f 5.60028e+06 e
* pa      * f          0. e

```

```

*****
*          type          num          id          ctitle
tee          21          21          $21$ fw tee
*          jcell          nodes          ichf          cost          epsw
*          1          0          0          0.          4.57e-5
*          iconc1          ncell1          jun1          jun2          ipow
*          0          1          21          22          0
*          radin1          th1          hout11          houtv1          tout11
2.56800e+00  1.00000e-01          0.          0.          3.00000e+02
*          toutv1          pwin1          pwoff1          rpwmx1          pwsc11
3.00000e+02          0.          0.          0.          1.
*          iconc2          ncell2          jun3          ipow2
*          0          1          121          0
*          radin2          th2          hout12          houtv2          tout12
2.56800e+00  1.00000e-01          0.          0.          3.00000e+02
*          toutv2          pwin2          pwoff2          rpwmx2          pwsc12
3.00000e+02          0.          0.          0.          1.
*          +          +          +          +          +
* dx * f          1.1887 e
* vol * f          0.05726 e
* fa * f          0.04817 e
* fric * f          0. e
* grav * f          0. e
* hd * f          0.24765 e
* icflg *f          0 e
* nff * f          1 e
* alp * f          0. e
* vl *          2.038          1.631 e
* vv *          2.037          1.631 e
* tl * f          498.4 e
* tv * f          545.6 e
* p * f          5.71816e+06 e
* pa * f          0. e
*          +          +          +          +
* dx *          0.3048 e
* vol *          0.0005806 e
* fa * f          0.001905 e
* fric *          0.5          1. e
* grav *          1.          -1. e
* hd * f          0.04925 e
* icflg *f          0 e
* nff * f          1 e
* alp *          0. e
* vl *          10.28          10.28 e
* vv *          10.31          10.28 e
* tl * f          498.3 e
* tv * f          544.3 e
* p * f          5.60034e+06 e
* pa * f          0. e
*****
*          type          num          id          ctitle
tee          22          22          $22$ fw tee
*          jcell          nodes          ichf          cost          epsw
*          1          0          0          0.          4.57e-5
*          iconc1          ncell1          jun1          jun2          ipow
*          0          1          22          23          0
*          radin1          th1          hout11          houtv1          tout11
2.56800e+00  1.00000e-01          0.          0.          3.00000e+02
*          toutv1          pwin1          pwoff1          rpwmx1          pwsc11
3.00000e+02          0.          0.          0.          1.
*          iconc2          ncell2          jun3          ipow2
*          0          1          122          0
*          radin2          th2          hout12          houtv2          tout12
2.56800e+00  1.00000e-01          0.          0.          3.00000e+02
*          toutv2          pwin2          pwoff2          rpwmx2          pwsc12
3.00000e+02          0.          0.          0.          1.
*          +          +          +          +          +
* dx * f          1.1887 e
* vol * f          0.05726 e
* fa * f          0.04817 e
* fric * f          0. e

```

```

* grav * f 0. e
* hd * f 0.24765 e
* icflg * f 0 e
* nff * f 1 e
* alp * f 0. e
* vl * 1.631 1.224 e
* vv * 1.631 1.224 e
* tl * f 498.4 e
* tv * f 545.6 e
* p * f 5.71864e+06 e
* pa * f 0. e
* + + + + +
* dx * 0.3048 e
* vol * 0.0005806 e
* fa * f 0.001905 e
* fric * 0.5 1. e
* grav * 1. -1. e
* hd * f 0.04925 e
* icflg * f 0 e
* nff * f 1 e
* alp * 0. e
* vl * 10.30 10.30 e
* vv * 10.32 10.30 e
* tl * f 498.3 e
* tv * f 544.3 e
* p * f 5.60040e+06 e
* pa * f 0. e
*****
* type num id ctitle
tee 23 23 $23$ fw tee
* jcell nodes ichf cost epsw
1 0 0 0. 4.57e-5
* iconcl ncell1 jun1 jun2 ipow
0 1 23 24 0
* radin1 th1 hout11 houtv1 tout11
2.56800e+00 1.00000e-01 0. 0. 3.00000e+02
* toutv1 pwin1 pwoff1 rpwmx1 pwsc11
3.00000e+02 0. 0. 0. 1.
* iconc2 ncell2 jun3 ipow2
0 1 123 0
* radin2 th2 hout12 houtv2 tout12
2.56800e+00 1.00000e-01 0. 0. 3.00000e+02
* toutv2 pwin2 pwoff2 rpwmx2 pwsc12
3.00000e+02 0. 0. 0. 1.
* + + + + +
* dx * f 1.1887 e
* vol * f 0.05726 e
* fa * f 0.04817 e
* fric * f 0. e
* grav * f 0. e
* hd * f 0.24765 e
* icflg * f 0 e
* nff * f 1 e
* alp * f 0. e
* vl * 1.224 0.8165 e
* vv * 1.224 0.8160 e
* tl * f 498.4 e
* tv * f 545.6 e
* p * f 5.71901e+06 e
* pa * f 0. e
* + + + + +
* dx * 0.3048 e
* vol * 0.0005806 e
* fa * f 0.001905 e
* fric * 0.5 1. e
* grav * 1. -1. e
* hd * f 0.04925 e
* icflg * f 0 e
* nff * f 1 e
* alp * 0. e
* vl * 10.31 10.31 e

```

```

* vv      *      10.34      10.31 e
* tl      * f      498.3 e
* tv      * f      544.3 e
* p       * f      5.60044e+06 e
* pa      * f      0. e
*****
*          type          num          id          ctitle
tee          24          24          $24$ fw tee
*          jcell          nodes          ichf          cost          epsw
*          1          0          0          0.          4.57e-5
*          iconcl          ncell1          jun1          jun2          ipow
*          0          1          24          25          0
*          radin1          th1          hout11          houtv1          tout11
*          2.56800e+00      1.00000e-01      0.          0.          3.00000e+02
*          toutv1          pwin1          pwoff1          rpwmx1          pwsc11
*          3.00000e+02      0.          0.          0.          1.
*          iconc2          ncell2          jun3          ipow2
*          0          1          124          0
*          radin2          th2          hout12          houtv2          tout12
*          2.56800e+00      1.00000e-01      0.          0.          3.00000e+02
*          toutv2          pwin2          pwoff2          rpwmx2          pwsc12
*          3.00000e+02      0.          0.          0.          1.
*          +          +          +          +          +
* dx      * f      1.1887 e
* vol     * f      0.05726 e
* fa      * f      0.04817 e
* fric    * f      0. e
* grav    * f      0. e
* hd      * f      0.24765 e
* icflg   * f      0 e
* nff     * f      1 e
* alp     * f      0. e
* vl      *      0.8165      0.4084 e
* vv      *      0.8160      0.4080 e
* tl      * f      498.4 e
* tv      * f      545.6 e
* p       * f      5.71927e+06 e
* pa      * f      0. e
*          +          +          +          +
* dx      *      0.3048 e
* vol     *      0.0005806 e
* fa      * f      0.001905 e
* fric    *      0.5      1. e
* grav    *      1.      -1. e
* hd      * f      0.04925 e
* icflg   * f      0 e
* nff     * f      1 e
* alp     *      0. e
* vl      *      10.32      10.32 e
* vv      *      10.35      10.32 e
* tl      * f      498.3 e
* tv      * f      544.3 e
* p       * f      5.60047e+06 e
* pa      * f      0. e
*****
*          type          num          id          ctitle
tee          25          25          $25$ fw tee
*          jcell          nodes          ichf          cost          epsw
*          1          0          0          0.          4.57e-5
*          iconcl          ncell1          jun1          jun2          ipow
*          0          1          25          26          0
*          radin1          th1          hout11          houtv1          tout11
*          2.56800e+00      1.00000e-01      0.          0.          3.00000e+02
*          toutv1          pwin1          pwoff1          rpwmx1          pwsc11
*          3.00000e+02      0.          0.          0.          1.
*          iconc2          ncell2          jun3          ipow2
*          0          1          125          0
*          radin2          th2          hout12          houtv2          tout12
*          2.56800e+00      1.00000e-01      0.          0.          3.00000e+02
*          toutv2          pwin2          pwoff2          rpwmx2          pwsc12
*          3.00000e+02      0.          0.          0.          1.

```

```

*      +      +      +      +      +
* dx * f      1.1887 e
* vol * f      0.05726 e
* fa * f      0.04817 e
* fric * f      0. e
* grav * f      0. e
* hd * f      0.24765 e
* icflg *f      0 e
* nff * f      1 e
* alp * f      0. e
* vl *      0.4084      0. e
* vv *      0.4080      0. e
* tl * f      498.4 e
* tv * f      545.6 e
* p * f      5.71941e+06 e
* pa * f      0. e
*      +      +      +      +      +
* dx *      0.3048 e
* vol *      0.0005806 e
* fa * f      0.001905 e
* fric *      0.5      1. e
* grav *      1.      -1. e
* hd * f      0.04925 e
* icflg *f      0 e
* nff * f      1 e
* alp *      0. e
* vl *      10.33      10.33 e
* vv *      10.35      10.33 e
* tl * f      498.3 e
* tv * f      544.3 e
* p * f      5.60048e+06 e
* pa * f      0. e
*****
*      type      num      id      ctitle
tee      26      26      $26$ fw tee
*      jcell      nodes      ichf      cost      epsw
      1      0      0      0.      4.57e-5
*      iconcl      ncell1      jun1      jun2      ipow
      0      1      26      27      0
*      radin1      th1      hout11      houtv1      tout11
2.56800e+00      1.00000e-01      0.      0.      3.00000e+02
*      toutv1      pwin1      pwoff1      rpwmx1      pwsc11
3.00000e+02      0.      0.      0.      1.
*      iconc2      ncell2      jun3      ipow2
      0      1      126      0
*      radin2      th2      hout12      houtv2      tout12
2.56800e+00      1.00000e-01      0.      0.      3.00000e+02
*      toutv2      pwin2      pwoff2      rpwmx2      pwsc12
3.00000e+02      0.      0.      0.      1.
*      +      +      +      +      +
* dx * f      1.1887 e
* vol * f      0.05726 e
* fa * f      0.04817 e
* fric * f      0. e
* grav * f      0. e
* hd * f      0.24765 e
* icflg *f      0 e
* nff * f      1 e
* alp * f      0. e
* vl *      0.      -0.4084 e
* vv *      0.      -0.4080 e
* tl * f      498.4 e
* tv * f      545.6 e
* p * f      5.71941e+06 e
* pa * f      0. e
*      +      +      +      +      +
* dx *      0.3048 e
* vol *      0.0005806 e
* fa * f      0.001905 e
* fric *      0.5      1. e
* grav *      1.      -1. e

```

```

* hd * f 0.04925 e
* icflg * f 0 e
* nff * f 1 e
* alp * 0. e
* vl * 10.33 10.33 e
* vv * 10.35 10.33 e
* tl * f 498.3 e
* tv * f 544.3 e
* p * f 5.60048e+06 e
* pa * f 0. e
*****

```

```

* type num id ctitle
tee 27 27 $27$ fw tee
* jcell nodes ichf cost epsw
1 0 0 4.57e-5
* iconcl ncell1 jun1 jun2 ipow
0 1 27 28 0
* radin1 th1 houtl1 houtv1 toutl1
2.56800e+00 1.00000e-01 0. 0. 3.00000e+02
* toutv1 pwin1 pwoff1 rpwmx1 pwsc11
3.00000e+02 0. 0. 0. 1.
* iconc2 ncell2 jun3 ipow2
0 1 127 0
* radin2 th2 houtl2 houtv2 toutl2
2.56800e+00 1.00000e-01 0. 0. 3.00000e+02
* toutv2 pwin2 pwoff2 rpwmx2 pwsc12
3.00000e+02 0. 0. 0. 1.
* + + + + +
* dx * f 1.1887 e
* vol * f 0.05726 e
* fa * f 0.04817 e
* fric * f 0. e
* grav * f 0. e
* hd * f 0.24765 e
* icflg * f 0 e
* nff * f 1 e
* alp * f 0. e
* vl * -0.4084 -0.8165 e
* vv * -0.4080 -0.8160 e
* tl * f 498.4 e
* tv * f 545.6 e
* p * f 5.71927e+06 e
* pa * f 0. e
* + + + + +
* dx * 0.3048 e
* vol * 0.0005806 e
* fa * f 0.001905 e
* fric * 0.5 1. e
* grav * 1. -1. e
* hd * f 0.04925 e
* icflg * f 0 e
* nff * f 1 e
* alp * 0. e
* vl * 10.32 10.32 e
* vv * 10.35 10.32 e
* tl * f 498.3 e
* tv * f 544.3 e
* p * f 5.60047e+06 e
* pa * f 0. e
*****

```

```

* type num id ctitle
tee 28 28 $28$ fw tee
* jcell nodes ichf cost epsw
1 0 0 4.57e-5
* iconcl ncell1 jun1 jun2 ipow
0 1 28 29 0
* radin1 th1 houtl1 houtv1 toutl1
2.56800e+00 1.00000e-01 0. 0. 3.00000e+02
* toutv1 pwin1 pwoff1 rpwmx1 pwsc11
3.00000e+02 0. 0. 0. 1.
* iconc2 ncell2 jun3 ipow2

```

```

*          0          1          128          0          toutl2
*      radin2      th2      houtl2      houtv2      3.00000e+02
* 2.56800e+00 1.00000e-01      0.      0.
*      toutv2      pwin2      pwoff2      rpwmx2      pwsc12
* 3.00000e+02      0.      0.      0.      1.
*
* + + + + +
* dx * f      1.1887 e
* vol * f      0.05726 e
* fa * f      0.04817 e
* fric * f      0. e
* grav * f      0. e
* hd * f      0.24765 e
* icflg * f      0 e
* nff * f      1 e
* alp * f      0. e
* vl *      -0.8165      -1.224 e
* vv *      -0.8160      -1.224 e
* tl * f      498.4 e
* tv * f      545.6 e
* p * f      5.71901e+06 e
* pa * f      0. e
*
* + + + + +
* dx *      0.3048 e
* vol *      0.0005806 e
* fa * f      0.001905 e
* fric *      0.5      1. e
* grav *      1.      -1. e
* hd * f      0.04925 e
* icflg * f      0 e
* nff * f      1 e
* alp *      0. e
* vl *      10.31      10.31 e
* vv *      10.34      10.31 e
* tl * f      498.3 e
* tv * f      544.3 e
* p * f      5.60044e+06 e
* pa * f      0. e
*****
*          type          num          id          ctitle
tee          29          29          $29$ fw tee
*          jcell          nodes          ichf          cost          epsw
*          1          0          0          0.          4.57e-5
*          iconc1          ncell1          jun1          jun2          ipow
*          0          1          29          30          0
*          radin1          th1          houtl1          houtv1          toutl1
* 2.56800e+00 1.00000e-01      0.      0.      3.00000e+02
*      toutv1          pwin1          pwoff1          rpwmx1          pwsc11
* 3.00000e+02      0.      0.      0.      1.
*          iconc2          ncell2          jun3          ipow2
*          0          1          129          0
*          radin2          th2          houtl2          houtv2          toutl2
* 2.56800e+00 1.00000e-01      0.      0.      3.00000e+02
*      toutv2          pwin2          pwoff2          rpwmx2          pwsc12
* 3.00000e+02      0.      0.      0.      1.
*
* + + + + +
* dx * f      1.1887 e
* vol * f      0.05726 e
* fa * f      0.04817 e
* fric * f      0. e
* grav * f      0. e
* hd * f      0.24765 e
* icflg * f      0 e
* nff * f      1 e
* alp * f      0. e
* vl *      -1.224      -1.631 e
* vv *      -1.224      -1.631 e
* tl * f      498.4 e
* tv * f      545.6 e
* p * f      5.71864e+06 e
* pa * f      0. e
*
* + + + + +

```



```

* dx * 0.3048 e
* vol * 0.0005806 e
* fa * f 0.001905 e
* fric * 0.5 1. e
* grav * 1. -1. e
* hd * f 0.04925 e
* icflg * f 0 e
* nff * f 1 e
* alp * 0. e
* vl * 10.30 10.30 e
* vv * 10.32 10.30 e
* tl * f 498.3 e
* tv * f 544.3 e
* p * f 5.60040e+06 e
* pa * f 0. e
*****

```

```

* type num id ctitle
tee 30 30 $30$ fw tee
* jcell nodes ichf cost epsw
1 0 0 0. 4.57e-5
* iconcl ncell1 jun1 jun2 ipow
0 1 30 31 0
* radin1 th1 hout11 houtv1 tout11
2.56800e+00 1.00000e-01 0. 0. 3.00000e+02
* toutv1 pwin1 pwoff1 rpwm1 pwsc11
3.00000e+02 0. 0. 0. 1.
* iconc2 ncell2 jun3 ipow2
0 1 130 0
* radin2 th2 hout12 houtv2 tout12
2.56800e+00 1.00000e-01 0. 0. 3.00000e+02
* toutv2 pwin2 pwoff2 rpwm2 pwsc12
3.00000e+02 0. 0. 0. 1.
* + + + + +

```

```

* dx * f 1.1887 e
* vol * f 0.05726 e
* fa * f 0.04817 e
* fric * f 0. e
* grav * f 0. e
* hd * f 0.24765 e
* icflg * f 0 e
* nff * f 1 e
* alp * f 0. e
* vl * -1.631 -2.038 e
* vv * -1.631 -2.037 e
* tl * f 498.4 e
* tv * f 545.6 e
* p * f 5.71816e+06 e
* pa * f 0. e
* + + + + +

```

```

* dx * 0.3048 e
* vol * 0.0005806 e
* fa * f 0.001905 e
* fric * 0.5 1. e
* grav * 1. -1. e
* hd * f 0.04925 e
* icflg * f 0 e
* nff * f 1 e
* alp * 0. e
* vl * 10.28 10.28 e
* vv * 10.31 10.28 e
* tl * f 498.3 e
* tv * f 544.3 e
* p * f 5.60034e+06 e
* pa * f 0. e
*****

```

```

* type num id ctitle
tee 31 31 $31$ fw tee
* jcell nodes ichf cost epsw
1 0 0 0. 4.57e-5
* iconcl ncell1 jun1 jun2 ipow
0 1 31 32 0

```

```

*      radin1      th1      houtl1      houtv1      toutl1
2.56800e+00 1.00000e-01      0.      0. 3.00000e+02
*      toutv1      pwin1      pwoff1      rpwmx1      pwsc11
3.00000e+02      0.      0.      0.      1.
*      iconc2      ncell2      jun3      ipow2
0      1      131      0
*      radin2      th2      houtl2      houtv2      toutl2
2.56800e+00 1.00000e-01      0.      0. 3.00000e+02
*      toutv2      pwin2      pwoff2      rpwmx2      pwsc12
3.00000e+02      0.      0.      0.      1.
*      +      +      +      +
* dx * f      1.1887 e
* vol * f      0.05726 e
* fa * f      0.04817 e
* fric * f      0. e
* grav * f      0. e
* hd * f      0.24765 e
* icflg * f      0 e
* nff * f      1 e
* alp * f      0. e
* vl *      -2.038      -2.443 e
* vv *      -2.037      -2.442 e
* tl * f      498.4 e
* tv * f      545.6 e
* p * f      5.71758e+06 e
* pa * f      0. e
*      +      +      +      +
* dx *      0.3048 e
* vol *      0.0005806 e
* fa * f      0.001905 e
* fric *      0.5      1. e
* grav *      1.      -1. e
* hd * f      0.04925 e
* icflg * f      0 e
* nff * f      1 e
* alp *      0. e
* vl *      10.25      10.25 e
* vv *      10.28      10.26 e
* tl * f      498.3 e
* tv * f      544.3 e
* p * f      5.60028e+06 e
* pa * f      0. e
*****
*      type      num      id      ctitle
tee      32      32      $32$ fw tee
*      jcell      nodes      ichf      cost      epsw
1      0      0      0.      4.57e-5
*      iconc1      ncell1      jun1      jun2      ipow
0      1      32      33      0
*      radin1      th1      houtl1      houtv1      toutl1
2.56800e+00 1.00000e-01      0.      0. 3.00000e+02
*      toutv1      pwin1      pwoff1      rpwmx1      pwsc11
3.00000e+02      0.      0.      0.      1.
*      iconc2      ncell2      jun3      ipow2
0      1      132      0
*      radin2      th2      houtl2      houtv2      toutl2
2.56800e+00 1.00000e-01      0.      0. 3.00000e+02
*      toutv2      pwin2      pwoff2      rpwmx2      pwsc12
3.00000e+02      0.      0.      0.      1.
*      +      +      +      +
* dx * f      1.1887 e
* vol * f      0.05726 e
* fa * f      0.04817 e
* fric * f      0. e
* grav * f      0. e
* hd * f      0.24765 e
* icflg * f      0 e
* nff * f      1 e
* alp * f      0. e
* vl *      -2.443      -2.848 e
* vv *      -2.442      -2.847 e

```

```

*   tl   * f      498.4 e
*   tv   * f      545.6 e
*   p     * f  5.71692e+06 e
*   pa    * f      0. e
*   +     +     +     +     +
*   dx    *      0.3048 e
*   vol   *      0.0005806 e
*   fa    * f      0.001905 e
*   fric  *      0.5      1. e
*   grav  *      1.      -1. e
*   hd    * f      0.04925 e
*   icflg *f      0 e
*   nff   * f      1 e
*   alp   *      0. e
*   vl    *      10.23      10.23 e
*   vv    *      10.26      10.23 e
*   tl    * f      498.3 e
*   tv    * f      544.3 e
*   p     * f  5.60021e+06 e
*   pa    * f      0. e
*****
*           type          num          id          ctitle
tee          33          33          $33$ fw tee
*   jcell      nodes      ichf      cost      epsw
*   1          0          0          0.      4.57e-5
*   iconcl     ncell1     jun1      jun2      ipow
*   0          1          33          34          0
*   radin1     th1        hout1l   houtv1   tout1l
*   2.56800e+00 1.00000e-01 0.      0.      3.00000e+02
*   toutv1     pwin1     pwoff1  rpwmx1  pwsc1l
*   3.00000e+02 0.      0.      0.      1.
*   iconc2     ncell2     jun3      ipow2
*   0          1          133         0
*   radin2     th2        houtl2   houtv2   toutl2
*   2.56800e+00 1.00000e-01 0.      0.      3.00000e+02
*   toutv2     pwin2     pwoff2  rpwmx2  pwsc12
*   3.00000e+02 0.      0.      0.      1.
*   +     +     +     +     +
*   dx    * f      1.1887 e
*   vol   * f      0.05726 e
*   fa    * f      0.04817 e
*   fric  * f      0. e
*   grav  * f      0. e
*   hd    * f      0.24765 e
*   icflg *f      0 e
*   nff   * f      1 e
*   alp   * f      0. e
*   vl    *      -2.848      -3.251 e
*   vv    *      -2.847      -3.250 e
*   tl    * f      498.4 e
*   tv    * f      545.6 e
*   p     * f  5.71618e+06 e
*   pa    * f      0. e
*   +     +     +     +     +
*   dx    *      0.3048 e
*   vol   *      0.0005806 e
*   fa    * f      0.001905 e
*   fric  *      0.5      1. e
*   grav  *      1.      -1. e
*   hd    * f      0.04925 e
*   icflg *f      0 e
*   nff   * f      1 e
*   alp   *      0. e
*   vl    *      10.20      10.20 e
*   vv    *      10.23      10.20 e
*   tl    * f      498.3 e
*   tv    * f      544.3 e
*   p     * f  5.60013e+06 e
*   pa    * f      0. e
*****
*           type          num          id          ctitle

```

```

tee          34          34      $34$ fw tee
*      jcell      nodes      ichf      cost      epsw
*          1          0          0          0.          4.57e-5
*      iconcl      ncell1      jun1      jun2      ipow
*          0          1          34          35          0
*      radin1      th1      houtl1      houtv1      toutl1
* 2.56800e+00  1.00000e-01      0.          0.      3.00000e+02
*      toutv1      pwin1      pwoff1      rpwmx1      pwsc11
* 3.00000e+02      0.          0.          0.          1.
*      iconc2      ncell2      jun3      ipow2
*          0          1          134          0
*      radin2      th2      houtl2      houtv2      toutl2
* 2.56800e+00  1.00000e-01      0.          0.      3.00000e+02
*      toutv2      pwin2      pwoff2      rpwmx2      pwsc12
* 3.00000e+02      0.          0.          0.          1.
*      +          +          +          +          +
* dx * f      1.1887 e
* vol * f      0.05726 e
* fa * f      0.04817 e
* fric * f      0. e
* grav * f      0. e
* hd * f      0.24765 e
* icflg * f      0 e
* nff * f      1 e
* alp * f      0. e
* vl *      -3.251      -3.653 e
* vv *      -3.250      -3.652 e
* tl * f      498.4 e
* tv * f      545.6 e
* p * f      5.71538e+06 e
* pa * f      0. e
*      +          +          +          +          +
* dx *      0.3048 e
* vol *      0.0005806 e
* fa * f      0.001905 e
* fric *      0.5      1. e
* grav *      1.      -1. e
* hd * f      0.04925 e
* icflg * f      0 e
* nff * f      1 e
* alp *      0. e
* vl *      10.17      10.17 e
* vv *      10.19      10.17 e
* tl * f      498.3 e
* tv * f      544.3 e
* p * f      5.60004e+06 e
* pa * f      0. e
*****
*      type      num      id      ctitle
tee          35          35      $35$ fw tee
*      jcell      nodes      ichf      cost      epsw
*          1          0          0          0.          4.57e-5
*      iconcl      ncell1      jun1      jun2      ipow
*          0          1          35          36          0
*      radin1      th1      houtl1      houtv1      toutl1
* 2.56800e+00  1.00000e-01      0.          0.      3.00000e+02
*      toutv1      pwin1      pwoff1      rpwmx1      pwsc11
* 3.00000e+02      0.          0.          0.          1.
*      iconc2      ncell2      jun3      ipow2
*          0          1          135          0
*      radin2      th2      houtl2      houtv2      toutl2
* 2.56800e+00  1.00000e-01      0.          0.      3.00000e+02
*      toutv2      pwin2      pwoff2      rpwmx2      pwsc12
* 3.00000e+02      0.          0.          0.          1.
*      +          +          +          +          +
* dx * f      1.1887 e
* vol * f      0.05726 e
* fa * f      0.04817 e
* fric * f      0. e
* grav * f      0. e
* hd * f      0.24765 e

```

```

* icflg *f          0 e
* nff *f          1 e
* alp *f          0. e
* vl *          -3.653      -4.054 e
* vv *          -3.652      -4.053 e
* tl *f          498.4 e
* tv *f          545.6 e
* p *f  5.71452e+06 e
* pa *f          0. e
* + + + +
* dx *          0.3048 e
* vol *          0.0005806 e
* fa *f          0.001905 e
* fric *          0.5      1. e
* grav *          1.      -1. e
* hd *f          0.04925 e
* icflg *f          0 e
* nff *f          1 e
* alp *          0. e
* vl *          10.13      10.13 e
* vv *          10.16      10.14 e
* tl *f          498.3 e
* tv *f          544.3 e
* p *f  5.59994e+06 e
* pa *f          0. e
*****
*          type          num          id          ctitle
tee          36          36          $36$ fw tee
*          jcell          nodes          ichf          cost          epsw
          1          0          0          0.          4.57e-5
*          iconcl          ncell1          jun1          jun2          ipow
          0          1          36          37          0
*          radin1          th1          hout11          houtv1          tout11
2.56800e+00  1.00000e-01          0.          0.          3.00000e+02
*          toutv1          pwin1          pwoff1          rpwmx1          pwsc11
3.00000e+02          0.          0.          0.          1.
*          iconc2          ncell2          jun3          ipow2
          0          1          136          0
*          radin2          th2          hout12          houtv2          tout12
2.56800e+00  1.00000e-01          0.          0.          3.00000e+02
*          toutv2          pwin2          pwoff2          rpwmx2          pwsc12
3.00000e+02          0.          0.          0.          1.
* + + + +
* dx *f          1.1887 e
* vol *f          0.05726 e
* fa *f          0.04817 e
* fric *f          0. e
* grav *f          0. e
* hd *f          0.24765 e
* icflg *f          0 e
* nff *f          1 e
* alp *f          0. e
* vl *          -4.054      -4.453 e
* vv *          -4.053      -4.452 e
* tl *f          498.4 e
* tv *f          545.5 e
* p *f  5.71361e+06 e
* pa *f          0. e
* + + + +
* dx *          0.3048 e
* vol *          0.0005806 e
* fa *f          0.001905 e
* fric *          0.5      1. e
* grav *          1.      -1. e
* hd *f          0.04925 e
* icflg *f          0 e
* nff *f          1 e
* alp *          0. e
* vl *          10.10      10.10 e
* vv *          10.12      10.10 e
* tl *f          498.3 e

```

```

* tv * f 544.3 e
* p * f 5.59984e+06 e
* pa * f 0. e
*****
* type num id ctitle
tee 37 37 $37$ fw tee
* jcell nodes ichf cost epsw
1 0 0 0. 4.57e-5
* iconcl ncell1 jun1 jun2 ipow
0 1 37 38 0
* radin1 th1 houtl1 houtv1 toutl1
2.56800e+00 1.00000e-01 0. 0. 3.00000e+02
* toutv1 pwin1 pwoff1 rpwmx1 pwsc11
3.00000e+02 0. 0. 0. 1.
* iconc2 ncell2 jun3 ipow2
0 1 137 0
* radin2 th2 houtl2 houtv2 toutl2
2.56800e+00 1.00000e-01 0. 0. 3.00000e+02
* toutv2 pwin2 pwoff2 rpwmx2 pwsc12
3.00000e+02 0. 0. 0. 1.
* + + + + +
* dx * f 1.1887 e
* vol * f 0.05726 e
* fa * f 0.04817 e
* fric * f 0. e
* grav * f 0. e
* hd * f 0.24765 e
* icflg * f 0 e
* nff * f 1 e
* alp * f 0. e
* vl * -4.453 -4.851 e
* vv * -4.452 -4.850 e
* tl * f 498.4 e
* tv * f 545.5 e
* p * f 5.71268e+06 e
* pa * f 0. e
* + + + + +
* dx * 0.3048 e
* vol * 0.0005806 e
* fa * f 0.001905 e
* fric * 0.5 1. e
* grav * 1. -1. e
* hd * f 0.04925 e
* icflg * f 0 e
* nff * f 1 e
* alp * 0. e
* vl * 10.06 10.06 e
* vv * 10.09 10.06 e
* tl * f 498.3 e
* tv * f 544.3 e
* p * f 5.59974e+06 e
* pa * f 0. e
*****
* type num id ctitle
tee 38 38 $38$ fw tee
* jcell nodes ichf cost epsw
1 0 0 0. 4.57e-5
* iconcl ncell1 jun1 jun2 ipow
0 1 38 39 0
* radin1 th1 houtl1 houtv1 toutl1
2.56800e+00 1.00000e-01 0. 0. 3.00000e+02
* toutv1 pwin1 pwoff1 rpwmx1 pwsc11
3.00000e+02 0. 0. 0. 1.
* iconc2 ncell2 jun3 ipow2
0 1 138 0
* radin2 th2 houtl2 houtv2 toutl2
2.56800e+00 1.00000e-01 0. 0. 3.00000e+02
* toutv2 pwin2 pwoff2 rpwmx2 pwsc12
3.00000e+02 0. 0. 0. 1.
* + + + + +
* dx * f 1.1887 e

```

```

* vol * f      0.05726 e
* fa  * f      0.04817 e
* fric * f      0. e
* grav * f      0. e
* hd  * f      0.24765 e
* icflg *f      0 e
* nff  * f      1 e
* alp  * f      0. e
* vl  *      -4.851      -5.247 e
* vv  *      -4.850      -5.246 e
* tl  * f      498.4 e
* tv  * f      545.5 e
* p   * f      5.71171e+06 e
* pa  * f      0. e
*      +      +      +      +
* dx  *      0.3048 e
* vol  *      0.0005806 e
* fa  * f      0.001905 e
* fric *      0.5      1. e
* grav *      1.      -1. e
* hd  * f      0.04925 e
* icflg *f      0 e
* nff  * f      1 e
* alp  *      0. e
* vl  *      10.02      10.02 e
* vv  *      10.05      10.02 e
* tl  * f      498.3 e
* tv  * f      544.3 e
* p   * f      5.59963e+06 e
* pa  * f      0. e
*****
*      type      num      id      ctitle
tee      39      39      $39$ fw tee
*      jcell      nodes      ichf      cost      epsw
*      1      0      0      0.      4.57e-5
*      iconcl      ncell1      jun1      jun2      ipow
*      0      1      39      40      0
*      radin1      th1      hout11      houtv1      tout11
*      2.56800e+00      1.00000e-01      0.      0.      3.00000e+02
*      toutv1      pwin1      pwoff1      rpwmx1      pwscl1
*      3.00000e+02      0.      0.      0.      1.
*      iconc2      ncell2      jun3      ipow2
*      0      1      139      0
*      radin2      th2      hout12      houtv2      tout12
*      2.56800e+00      1.00000e-01      0.      0.      3.00000e+02
*      toutv2      pwin2      pwoff2      rpwmx2      pwscl2
*      3.00000e+02      0.      0.      0.      1.
*      +      +      +      +      +
* dx  * f      1.1887 e
* vol  * f      0.05726 e
* fa  * f      0.04817 e
* fric * f      0. e
* grav * f      0. e
* hd  * f      0.24765 e
* icflg *f      0 e
* nff  * f      1 e
* alp  * f      0. e
* vl  *      -5.247      -5.642 e
* vv  *      -5.246      -5.641 e
* tl  * f      498.4 e
* tv  * f      545.5 e
* p   * f      5.71074e+06 e
* pa  * f      0. e
*      +      +      +      +
* dx  *      0.3048 e
* vol  *      0.0005806 e
* fa  * f      0.001905 e
* fric *      0.5      1. e
* grav *      1.      -1. e
* hd  * f      0.04925 e
* icflg *f      0 e

```

```

* nff * f 1 e
* alp * 0. e
* vl * 9.978 9.979 e
* vv * 10.01 9.983 e
* tl * f 498.3 e
* tv * f 544.3 e
* p * f 5.59953e+06 e
* pa * f 0. e
*****
* type num id ctitle
tee 40 40 $40$ fw tee
* jcell nodes ichf cost epsw
1 0 0 0. 4.57e-5
* iconcl ncell1 jun1 jun2 ipow
0 1 40 41 0
* radin1 th1 hout11 houtv1 tout11
2.56800e+00 1.00000e-01 0. 0. 3.00000e+02
* toutv1 pwin1 pwoff1 rpwmx1 pwsc11
3.00000e+02 0. 0. 0. 1.
* iconc2 ncell2 jun3 ipow2
0 1 140 0
* radin2 th2 hout12 houtv2 tout12
2.56800e+00 1.00000e-01 0. 0. 3.00000e+02
* toutv2 pwin2 pwoff2 rpwmx2 pwsc12
3.00000e+02 0. 0. 0. 1.
* + + + + +
* dx * f 1.1887 e
* vol * f 0.05726 e
* fa * f 0.04817 e
* fric * f 0. e
* grav * f 0. e
* hd * f 0.24765 e
* icflg * f 0 e
* nff * f 1 e
* alp * f 0. e
* vl * -5.642 -6.035 e
* vv * -5.641 -6.036 e
* tl * f 498.4 e
* tv * f 545.5 e
* p * f 5.70975e+06 e
* pa * f 0. e
* + + + + +
* dx * 0.3048 e
* vol * 0.0005806 e
* fa * f 0.001905 e
* fric * 0.5 1. e
* grav * 1. -1. e
* hd * f 0.04925 e
* icflg * f 0 e
* nff * f 1 e
* alp * 0. e
* vl * 9.938 9.939 e
* vv * 9.966 9.942 e
* tl * f 498.3 e
* tv * f 544.3 e
* p * f 5.59942e+06 e
* pa * f 0. e
*****
* type num id ctitle
fill 900 900 $900$ primary system fill
* jun1 ifty ioff
900 2 0
* twtold rfmxc concin felv
0. 1.e+6 0. 0.
* dxin volin alpin vlin tlin
0.3556 0.3667 0. 0. 596.3
* pin pain flowin vvin tvin
15.5132e+06 0. 3747.4 0. 618.0
*****
* type num id ctitle
pipe 901 901 $901$ primary tube inlet

```



```

*      ncells      nodes      jun1      jun2      epsw
*      8          0          900      901      4.57e-5
*      ichf      iconc      iacc      ipow      npipes
*      1          0          0          0          1
*      radin      th      houtl      houtv      toutl
* 2.56800e+00  1.00000e-01  0.          0.          3.00000e+02
*      toutv      powin      powoff      rpowmx      powscl
* 3.00000e+02      0.          0.          0.          1.
*      +          +          +          +          +          +
* dx *          0.3556      0.9271 r6      1.2827 e
* vol *          0.3667      0.9559 r6      1.3226 e
* fa * f          1.0311 e
* fric * f          0. e
* grav * f          1. e
* hd * f          0.019685 e
* icflg *f          0 e
* nff * f          1 e
* alp * f          0. e
* vl *          5.425      5.394      5.357      5.307      5.263 s
* vl *          5.220      5.181      5.144      5.109 e
* vv *          5.425      5.399      5.360      5.312      5.268 s
* vv *          5.225      5.186      5.149      5.114 e
*      +          +          +          +          +
* tl *          595.2      593.4      591.1      588.9      586.6 s
* tl *          584.3      582.0      579.8 e
* tv *          619.1      619.5      619.0      618.9      618.7 s
* tv *          618.6      618.5      618.4 e
* p *          15.7409e+06  15.7288e+06  15.7080e+06  15.6840e+06  15.6600e+06 s
* p *          15.6361e+06  15.6122e+06  15.5883e+06 e
* pa * f          0. e
*****
*      type      num      id      ctitle
pipe          902      902      $902$ primary tube bend
*      ncells      nodes      jun1      jun2      epsw
*      1          0          901      902      4.57e-5
*      ichf      iconc      iacc      ipow      npipes
*      1          0          0          0          1
*      radin      th      houtl      houtv      toutl
* 2.56800e+00  1.00000e-01  0.          0.          3.00000e+02
*      toutv      powin      powoff      rpowmx      powscl
* 3.00000e+02      0.          0.          0.          1.
*      +          +          +          +          +          +
* dx * f          2.2678 e
* vol * f          2.3383 e
* fa * f          1.0311 e
* fric * f          0. e
* grav *          1.          -1. e
* hd * f          0.019685 e
* icflg *f          0 e
* nff * f          1 e
* alp *          0. e
* vl *          5.109      5.045 e
* vv *          5.114      5.047 e
*      +          +          +          +          +
* tl *          575.5 e
* tv *          618.2 e
* p *          15.5552e+06 e
* pa * f          0. e
*****
*      type      num      id      ctitle
pipe          903      903      $903$ primary tube outlet
*      ncells      nodes      jun1      jun2      epsw
*      8          0          902      903      4.57e-5
*      ichf      iconc      iacc      ipow      npipes
*      1          0          0          0          1
*      radin      th      houtl      houtv      toutl
* 2.56800e+00  1.00000e-01  0.          0.          3.00000e+02
*      toutv      powin      powoff      rpowmx      powscl
* 3.00000e+02      0.          0.          0.          1.
*      +          +          +          +          +          +
* dx * r6          1.2827      0.9271      0.3556 e

```

```

* vol * r6      1.3226      0.9559      0.3667 e
* fa * f      1.0311 e
* fric * f      0. e
* grav * f      -1. e
* hd * f      0.019685 e
* icflg * f      0 e
* nff * f      1 e
* alp * f      0. e
* vl *      5.045      5.018      4.993      4.971      4.951s
* vl *      4.933      4.917      4.905      4.895 e
* vv *      5.047      5.020      4.996      4.973      4.953s
* vv *      4.935      4.919      4.907      4.897 e
* +      +      +      +      +
* tl *      573.6      571.9      570.4      568.9      567.7 s
* tl *      566.5      565.6      564.9 e
* tv *      618.2      618.1      618.1      618.1      618.0 s
* tv *      618.0      618.0      618.0 e
* p *      15.5475e+06      15.5421e+06      15.5367e+06      15.5315e+06      15.5263e+06 s
* p *      15.5212e+06      15.5169e+06      15.5145e+06 e
* pa * f      0. e
*****
*      type      num      id      ctitle
break      904      904      $904$ pressure boundary
*      jun1      ibty      isat      ioff
      903      0      0      1
*      dxin      volin      alpin      tin      pin
      0.3556      0.3667      0.      596.3      15.5132e+06
*      pain      concin      rbmx      poff      belv
      0.      0.      0.      0.      0.
*****
*      type      num      id      ctitle
htstr      9010      9010      $9010$ ht surface at tube inlet
*      nzhtstr      ittc      hscyl      ichf
      8      0      0      0
*      nopowr      plane      liqlev      iaxcnd
      1      3      0      0
*      nmwrx      nfcil      nfci      hdri      hdro
      0      0      0      0.019685      0.04224
*      width
      236.555
*      nhot      nodes      irftr      nzmax      irftr2
      0      3      0      8      0
*      dtxht(1)      dtxht(2)      dznht      hgapo
      1000.      1000.      1000.      1000.
*      +      +      +      +      +
*idbcin* f      2 e
*idbcon* f      2 e
*      hcomin      hcelii      hcelji      hcelki
      901      1      0      0 e
      901      2      0      0 e
      901      3      0      0 e
      901      4      0      0 e
      901      5      0      0 e
      901      6      0      0 e
      901      7      0      0 e
      901      8      0      0 e
*      hcomon      hcelio      hceljo      hcelko
      2      1      0      0 e
      2      2      0      0 e
      2      3      0      0 e
      2      4      0      0 e
      2      5      0      0 e
      2      6      0      0 e
      2      7      0      0 e
      2      8      0      0 e
* dhtstrz*      0.3556      0.9271 r6      1.2827 e
* rdx *      1. e
* radrd*      0.      0.000635      0.00127 e
* matrd* f      12 e
* nfax * f      0 e
* rftn *      584.31      572.24      560.05      587.89      581.77s

```

```

* rftn *          575.62          586.05          580.40          574.72          583.91s
* rftn *          578.40          572.85          581.63          576.13          570.60s
* rftn *          579.44          574.04          568.61          577.28          572.00s
* rftn *          566.69          575.18          570.04          564.87 e
*****
*          type          num          id          ctitle
htstr          9020          9020          $9020$ ht surface at tube bend area
*          nzhtstr          ittc          hscyl          ichf
          1          0          0          0
*          nopowr          plane          liqlev          iaxcnd
          1          3          0          0
*          nmwrwx          nfci          nfcil          hdri          hdro
          0          0          0          0.019685          0.00893
*          width
          236.555
*          nhot          nodes          irftr          nzmax          irftr2
          0          3          0          8          0
*          dtxht(1)          dtxht(2)          dznht          hgapo
          1000.          1000.          1000.          1000.
*          +          +          +          +          +
*idbcin* f          2 e
*idbcon* f          2 e
*          hcomin          hcelii          hcelji          hcelki
          902          1          0          0 e
*          hcomon          hcelio          hceljo          hcelko
          2          9          0          0 e
*dhtstrz*          2.2678 e
* rdx *          1. e
* radrd*          0.          0.000635          0.00127 e
* matrd* f          12 e
* nfax * f          0 e
* rftn *          570.44          564.81          559.16 e
*****
*          type          num          id          ctitle
htstr          9030          9030          $9030$ ht surface at tube outlet
*          nzhtstr          ittc          hscyl          ichf
          8          0          0          0
*          nopowr          plane          liqlev          iaxcnd
          1          3          0          0
*          nmwrwx          nfci          nfcil          hdri          hdro
          0          0          0          0.019685          0.04224
*          width
          236.555
*          nhot          nodes          irftr          nzmax          irftr2
          0          3          0          8          0
*          dtxht(1)          dtxht(2)          dznht          hgapo
          1000.          1000.          1000.          1000.
*          +          +          +          +          +
*idbcin* f          2 e
*idbcon* f          2 e
*          hcomin          hcelii          hcelji          hcelki
          903          1          0          0 e
          903          2          0          0 e
          903          3          0          0 e
          903          4          0          0 e
          903          5          0          0 e
          903          6          0          0 e
          903          7          0          0 e
          903          8          0          0 e
*          hcomon          hcelio          hceljo          hcelko
          2          8          0          0 e
          2          7          0          0 e
          2          6          0          0 e
          2          5          0          0 e
          2          4          0          0 e
          2          3          0          0 e
          2          2          0          0 e
          2          1          0          0 e
*dhtstrz* r6          1.2827          0.9271          0.3556 e
* rdx *          1. e
* radrd*          0.          0.000635          0.00127 e

```

```

* matrd* f          12 e
* nfax * f          0 e
* rftn *          569.79          565.55          561.28          568.44          564.57s
* rftn *          560.69          567.20          563.68          560.16          566.06s
* rftn *          562.86          559.65          565.06          562.19          559.30s
* rftn *          564.07          561.41          558.75          563.11          560.38s
* rftn *          557.64          559.87          554.31          548.72 e
*****
end
*
*****
*
*               time step data
*
*
*      dtmin      dtmax      tend      trwfp
*      .00001      .01      10.      10.
*
*      edint      gfint      dmpint      sedint
*      2.      0.01      20.      1.e6
*      -1.0

```

**APPENDIX B**  
**TRAC-M Assessment of GE Vessel Blowdown Tests**



# **TRAC-M Assessment of PWR Steam and Feedwater Line Breaks: GE Vessel Blowdown Tests**

**Submitted to:**

**The United States Nuclear Regulatory Commission  
Office of Nuclear Regulatory Research  
Division of Systems Analysis and Regulatory Effectiveness  
Safety Margins and System Analysis Branch**

*Prepared by:  
Birol Aktas*

*Reviewed by:  
Dan Prelewicz*

*Information Systems Laboratories, Inc.  
Nuclear Systems Analysis Division*

*January 2003*

*Under Contract No. NRC-04-02-054*

*ISL-NSAD-NRC-TR-03-04*





## TABLE OF CONTENTS

1. INTRODUCTION .....	1
2. DESCRIPTION OF THE GE LEVEL SWELL TEST FACILITY .....	1
3. DESCRIPTION OF THE TRAC-M MODEL .....	3
4. RESULTS OF TEST 1004-3 .....	4
5. RESULTS OF TEST 5801-15 .....	8
6. CONCLUSIONS .....	9
7. REFERENCES .....	10
APPENDIX.. SUPPLEMENTAL PLOTS .....	11

## LIST OF FIGURES

1. Schematic and nodalization for GE level swell Test 1004-3 .....	2
2. Schematic and nodalization for GE level swell Test 5801-15 .....	3
3. Void fraction at 6 ft elevation (node 3) of Test 1004-3 .....	4
4. Void fraction at 12 ft elevation (node 6) of Test 1004-3 .....	5
5. Void fraction profiles at 10, 40, 100, and 160 seconds of Test 1004-3 .....	5
6. Void fractions of Nodes 5 and 6 of Test 1004-3 (simulated without the level tracking method) .....	6
7. Void fractions of Nodes 5 and 6 of Test 1004-3 (simulated with the level tracking method) .....	6
8. Liquid and gas velocities at Face 21 of Test 1004-3 .....	7
9. Interfacial drag coefficient at Face 21 of Test 1004-3 .....	7
10. Predicted void fractions for nodes 3, 4, and 6 of Test 5801-15 .....	8
11. Void fraction profiles at 2, 5, 10, and 20 seconds of Test 5801-15 .....	8
A-1. Flow regimes across nodes 5 and 6 of Test 1004-3 (simulated without the level tracking method) ..	11
A-2. Flow regimes across nodes 5 and 6 of Test 1004-3 (simulated with the level tracking method) ..	11
A-3. Interfacial Mass Exchange across nodes 5 and 6 of Test 1004-3 (simulated without the level tracking method) .....	12
A-4. Interfacial Mass Exchange across nodes 5 and 6 of Test 1004-3 (simulated with the level tracking method) .....	12
A-5. Flow regimes across nodes 4 and 5 of Test 5801-15 (simulated without the level tracking method) ..	13
A-6. Flow regimes across nodes 4 and 5 of Test 5801-15 (simulated with the level tracking method) ..	13
A-7. Interfacial Mass Exchange across nodes 4 and 5 of Test 5801-15 (simulated without the level tracking method) .....	14
A-8. Interfacial Mass Exchange across nodes 4 and 5 of Test 5801-15 (simulated with the level tracking method) .....	14

## 1. INTRODUCTION

Two-phase mixture level swell is one of the governing phenomena that is critical to making accurate predictions of post-accident conditions. A series of tests were conducted by the General Electric (GE) Company in the '80s to establish a data base from which analytical models could be developed and verified. These tests were used widely in the assessment of the thermal-hydraulic codes including the ones that had been developed and maintained by the US NRC (i.e. RELAP5 and TRAC-BF1).

The following exercise assesses the ability of the US NRC Consolidated Code (a.k.a. TRAC-M) to simulate the one-foot and four-foot diameter vessel GE level swell tests.

## 2. DESCRIPTION OF THE GE LEVEL SWELL TEST FACILITY

The one-foot facility consisted of a 12-inch, Schedule 80 carbon steel pipe, flanged at the center, with standard pipe end caps for the top and bottom. The vessel was 14 ft long and had an approximate volume of 10 ft<sup>3</sup>. It was connected to a suppression pool at atmospheric conditions via a blowdown line containing an orifice. The orifice helped to control the blowdown flow rate and vary the depressurization rate. The vessel was insulated to minimize heat losses to the surroundings. Five immersible heaters 1-inch in diameter and 2 ft long were used for heating the water.

Initially, the vessel was filled with water. Using the immersible heaters at the bottom of the vessel, the water was boiled for half an hour to liberate the dissolved gases in the water and fill up the empty space above the water level with steam. The vessel was then sealed and heated until the desired initial conditions were obtained, i.e. 1000 psi and 545°F. Once the desired initial conditions were reached, the heaters were turned off and the fluid was allowed to settle. Before the test was initiated, the water level was located at 10.4 ft.

The test was initiated by opening a valve in the blowdown line. The system pressure was measured using a pressure transducer at the top of the vessel. Measurements made during the transient also included differential pressure measurements over 2-ft intervals along the vessel. The “measured” axial pressure gradient is mainly due to the density head since within a few seconds from the initiation of the blowdown transient, the spatial and temporal acceleration effects become negligible.

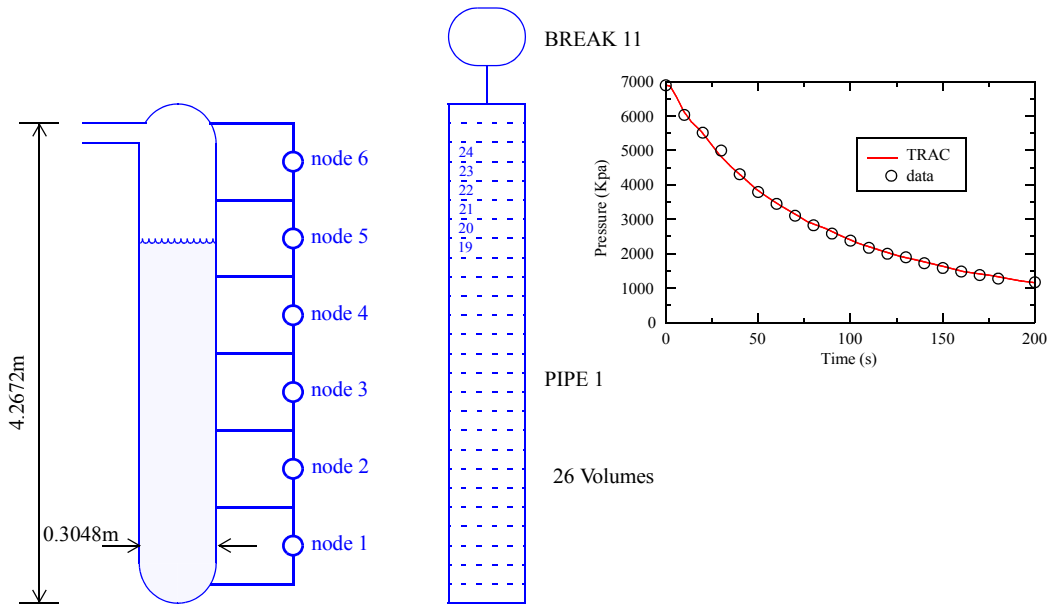


FIGURE 1. Schematic and nodalization for GE level swell Test 1004-3

Over each interval where the measured differential pressures were measured, a void fraction was calculated assuming a uniform nodal density and thermodynamic properties of the liquid and vapor phases.

$$\alpha_i = \frac{\rho_i - \rho_f}{\rho_g - \rho_f}$$

where

$\alpha_i$  = Average void fraction in  $i$ th node.

$\rho_i$  = Average mixture density in  $i$ th node.

$\rho_f$  = Liquid density in  $i$ th node.

$\rho_g$  = Vapor density in  $i$ th node.

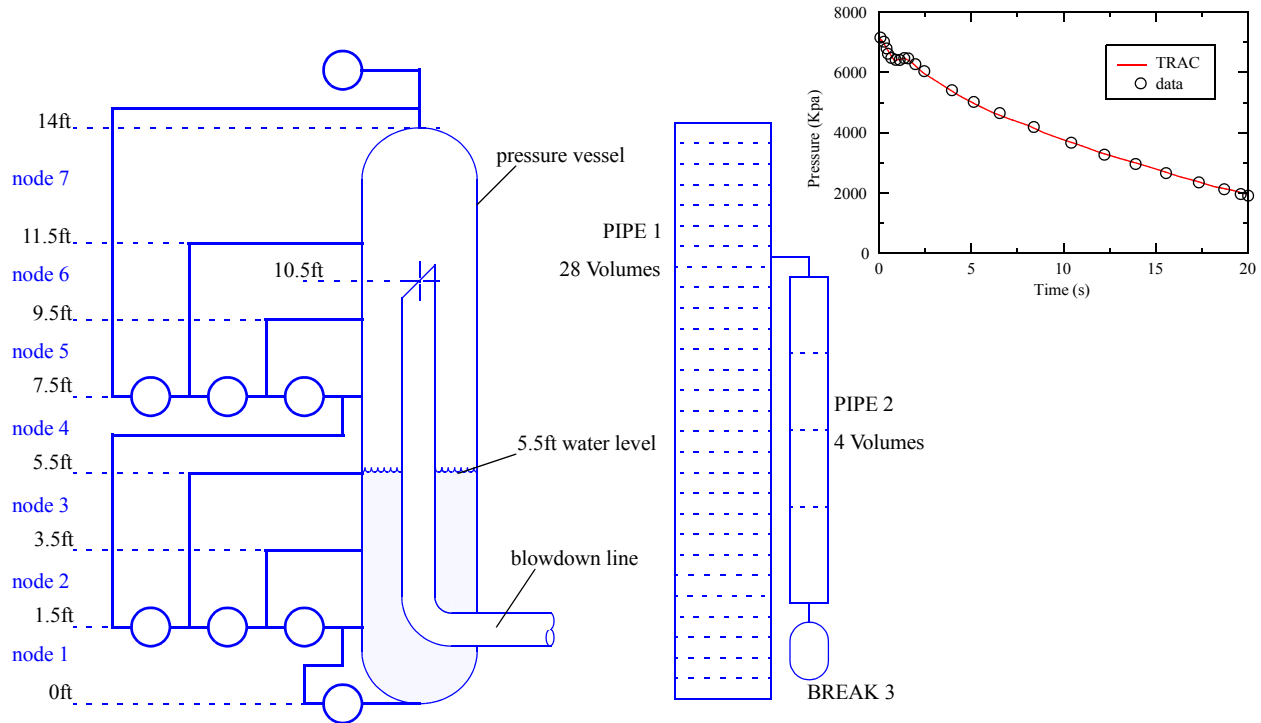


FIGURE 2. Schematic and nodalization for GE level swell Test 5801-15

The four-foot facility consisted of a vessel, 47-in in diameter and 14 ft long, which was constructed from a 1-in thick carbon steel plate. The vessel contained a free volume of 160 ft<sup>3</sup> and it was insulated using a 2-in thick asbestos insulation.

The test procedure and void fraction measurements were similar to those discussed above for the one-foot blowdown vessel. Initially, the water level was located at 5.5 ft from the bottom of vessel.

### 3. DESCRIPTION OF THE TRAC-M MODEL

The vessel of Test 1004-3 is modeled using a TRAC-M pipe component that consists of 26 equal height and volume cells (shown in Figure 1) while the vessel of Test 5801-15 is modeled using a TRAC-M pipe component that consists of 28 equal height and volume cells (shown in Figure 2). The blowdown pipe in both tests is not modeled in TRAC-M simulations and the blowdown transient is simulated using a BREAK component with a pressure vs. time table.

#### 4. RESULTS OF TEST 1004-3

A pressure vs. time plot in Figure 1 verifies that the system pressure is properly imposed as a boundary condition at the blowdown line exit, by comparing it to the measure pressure. As described in the facility description, the void fraction distribution is available across six nodes where the differential pressures are measured. It is important to note that these “nodal” void fractions can not be compared directly to the void fractions of the 26 computational volumes in the TRAC model. Therefore, the void fractions predicted by TRAC-M for the computational volumes are reduced by a volume-weighted averaging across each of the original six nodes to allow a useful comparison. The following equation describes the volume-weighted averaging used for the reduction of the void fractions from a “fine distribution” to the measured “nodal distribution”

$$\alpha_i = \frac{\sum_{j \in i} \alpha_j \text{Vol}_j}{\sum \text{Vol}_j}$$

where  $i = 1, 2, \dots, 6$  and  $j = 1, 2, \dots, 26$  for the one-foot vessel model, and  $i = 1, 2, \dots, 7$  and  $j = 1, 2, \dots, 28$  for the four-foot vessel model.

In Figure 3 and Figure 4, the volume-weighted averages of void fractions (predicted by TRAC-M) across cells that correspond to nodes 3 and 6 are compared to the “measured” void fractions of the same nodes. During the blowdown, the two-phase mixture level remains well above node 3 and the fluid across

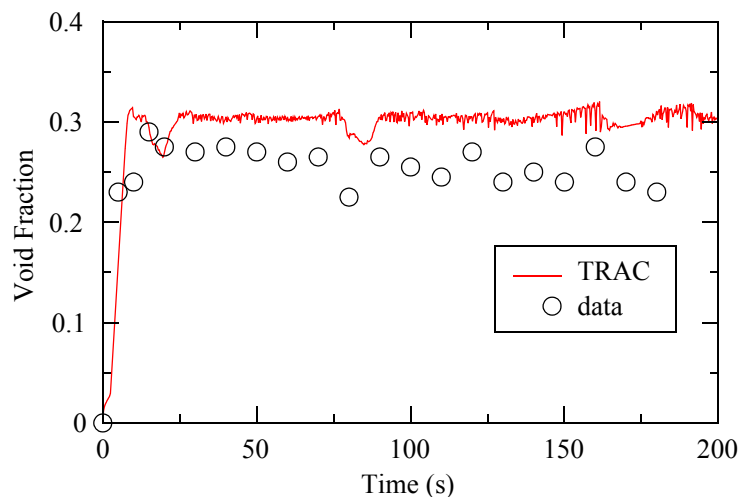


FIGURE 3. Void fraction at 6 ft elevation (node 3) of Test 1004-3

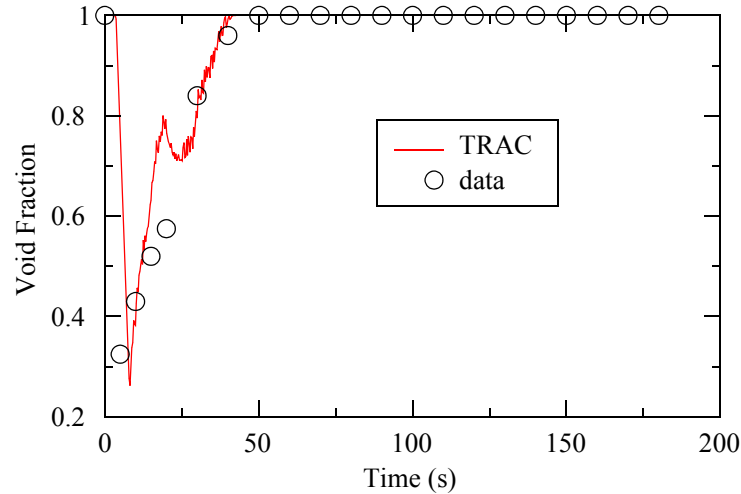


FIGURE 4. Void fraction at 12 ft elevation (node 6) of Test 1004-3

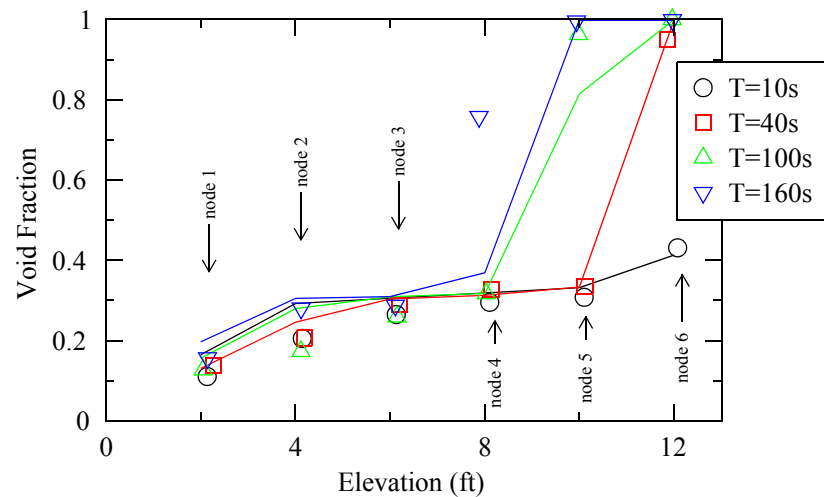


FIGURE 5. Void fraction profiles at 10, 40, 100, and 160 seconds of Test 1004-3

this node changes from single-phase liquid to a two-phase mixture of steam and liquid water as it boils. Figure 3 demonstrates that this behavior is predicted well by TRAC-M. However, a visible difference between the “measured” and “predicted” nodal void fractions deserves attention as it may be a sign for troubles in the phase exchange terms or the interfacial drag term of TRAC-M’s field equations. While the differences early in the transient are more likely due to the phase exchange terms, the differences late in the transient are due to the interfacial drag term. The mixture level, initially in node 5, swells into node 6 as the pressure decreases. The “predicted” void fraction for node 6 shown in Figure 4 confirms this expected behavior. As further seen in Figure 4, the mixture level collapses back to node 5 later as the steam escapes from the two-phase mixture. The progression of the mixture level during the transient can also be seen in Figure 5 which shows the snap shot profiles of the nodal void fractions at 10, 40, 100, and 160 seconds into the blowdown transient. The symbols in Figure 5 point to the measured nodal void fractions while the

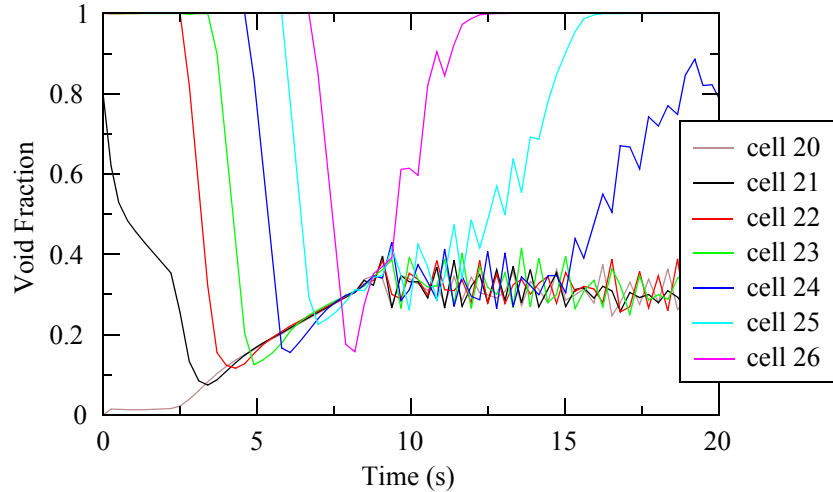


FIGURE 6. Void fractions of Nodes 5 and 6 of Test 1004-3 (simulated without the level tracking method)

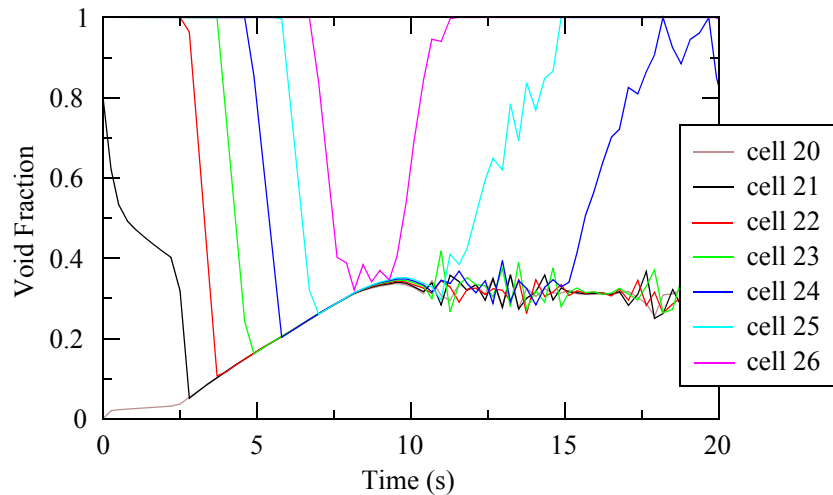


FIGURE 7. Void fractions of Nodes 5 and 6 of Test 1004-3 (simulated with the level tracking method)

curves represent the instantaneous profiles of predicted nodal void fractions at any given time. The differences in the “predicted” and “measured” void fractions for nodes 4 and 5 in Figure 5 indicate that TRAC-M fails to predict the collapse of the mixture level after 100 seconds into the transient.

While it is important to compare the predicted and measured “nodal” void fractions to assess TRAC-M’s ability to simulate the GE level swell tests, the comparison of these “averaged” void fractions does not provide an insight to the code calculations at the desired level. The void fractions of computational cells that make up nodes 5 (partially) and 6 are shown in Figure 6 and Figure 7. The simulation which produced the void fractions in Figure 7 was assisted by the level tracking method. A comparison of the two figures demonstrates that the code can handle better the sharp changes in void fraction as the mixture level crosses the cell boundaries when the level tracking method is activated. At the same time, the



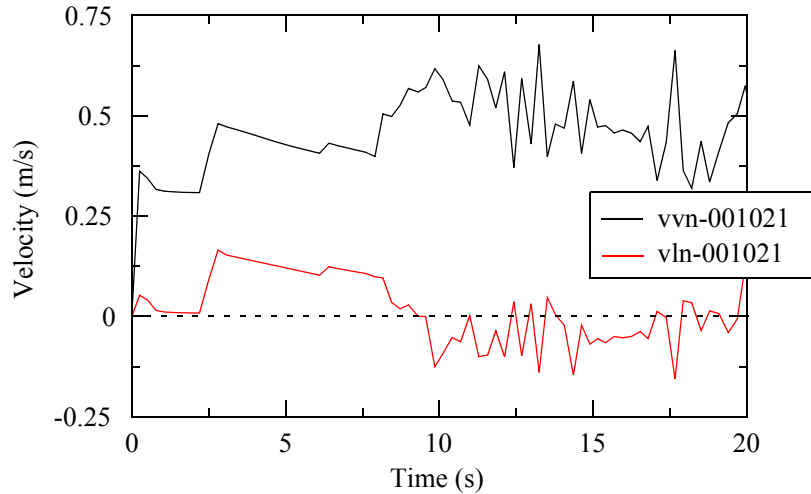


FIGURE 8. Liquid and gas velocities at Face 21 of Test 1004-3

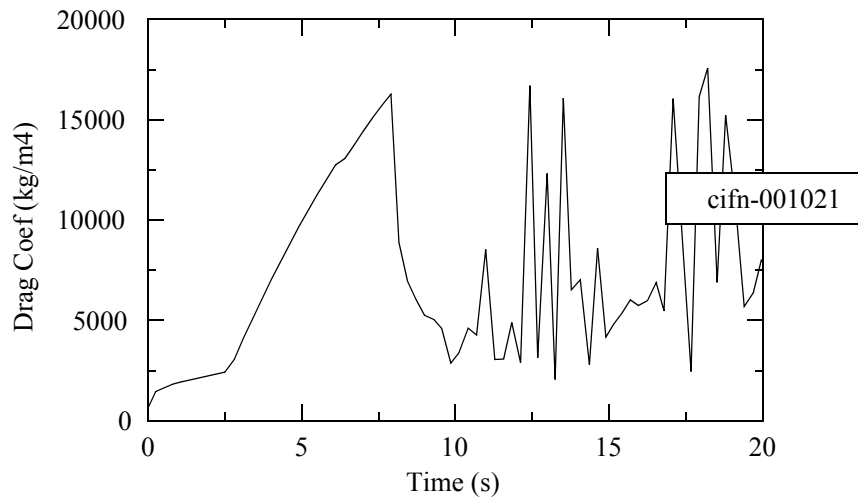


FIGURE 9. Interfacial drag coefficient at Face 21 of Test 1004-3

void fractions in both figures suffer from small oscillations after 10 seconds into the transient which can be considered as “numerical noise.” As a result of the decreasing drag between the two fields, the uplift of the liquid field (by the steam escaping into the void above the mixture level) can no longer be sustained at approximately 10 seconds and a reversal in liquid velocities is observed. Figure 8 shows the liquid and gas velocities at cell face 21. In Figure 9, a discontinuous change in the interfacial drag between the two fields follows the change of direction by the liquid field. Similar discontinuities in the interfacial drag coefficient are observed in Figure 9 as there are more reversals of the liquid field velocity shown in Figure 8. These discontinuities are the cause of “numerical noise” in void fraction predictions seen in Figure 6 and Figure 7. Clearly, there seems to be a need for a better way to evaluate the interfacial drag in TRAC-M when there are velocity reversals in a flow.

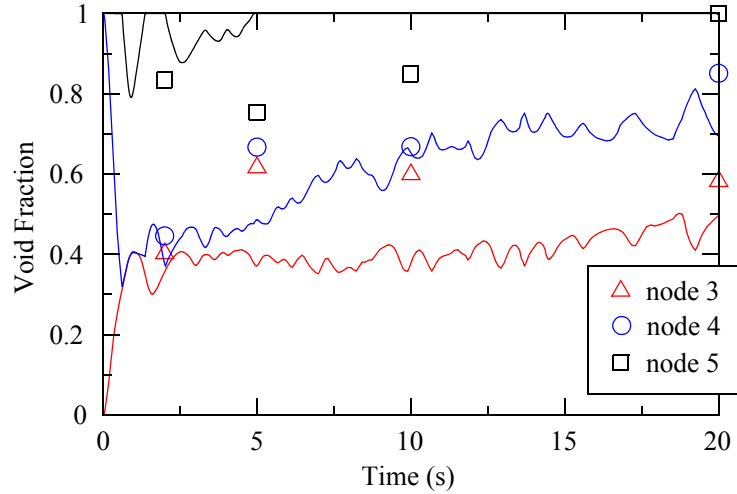


FIGURE 10. Predicted void fractions for nodes 3, 4, and 6 of Test 5801-15

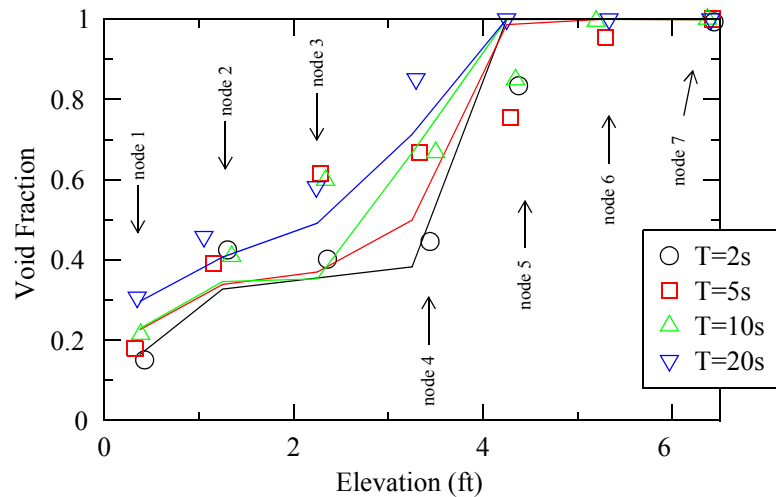


FIGURE 11. Void fraction profiles at 2, 5, 10, and 20 seconds of Test 5801-15

## 5. RESULTS OF TEST 5801-15

The results obtained for the four-foot vessel test indicate similar failures of TRAC-M. Figure 10 shows the “predicted” void fractions of nodes 3, 4, and 5 that indicate an initial swell and a later slow collapse of the two-phase mixture level. The mixture level reaches briefly into node 6 in the first 5 seconds of the transient. Figure 11 compares the instantaneous profiles of the “predicted” nodal void fractions to the “measured” nodal void fractions at 2, 5, 10, and 20 seconds into the blowdown transient. The measured void fractions in both Figure 10 and Figure 11 reveal a “frothier” profile than the profile which TRAC-M predicts during the first 10 seconds of the transient. The closeness of the predicted profile to the measured data at 20 seconds indicates that the nodal void fractions predicted by TRAC-M approaches to the measured

void fractions as the transient progresses. The differences between the predicted and measured void fractions are significant and the reasons behind them deserve an investigation.

## 6. CONCLUSIONS

The GE vessel blowdown experiments (Tests 1004-3 and 5801-15) were simulated with TRAC-M. The code predictions were compared against the available data in order to assess TRAC-M's ability to simulate these blowdown transients with a focus on two-phase mixture swell. The only available data for these tests are the nodal void fractions which were calculated from the differential pressure measurements. This study compares these nodal void fractions to the "predicted" void fractions by TRAC-M. Here, it is assumed that the "measured" differential pressures are mainly due to the density head since the spatial and temporal acceleration effects become negligible within a few seconds of the transient.

TRAC-M captured the progression of the mixture level swell successfully for both tests. However, a noticeable error was observed in the void fractions it predicted for the two-phase mixture, warranting a study to determine its cause.

The presence of water levels in vertical flows poses certain difficulties to the solution of field equations. Unless handled with proper care, these difficulties can plague the solution of TRAC-M. When a two-phase water level is present in a computational volume, the use of an average void fraction for a computational volume is inadequate. A volume that contains a water level indeed has two sub-volumes separated by the surface of the water level and each of these sub-volumes has its own distinct flow topology. There is usually dispersed-droplets above the level and bubbles below. Since the outcome of closure models strongly depends on the flow regime and the flow regime is described as a function of the void fraction, an accurate description of these divided computational volumes require that separate void fractions be assigned to each sub-volume. Not only must the void fractions must be known for the sub-volumes but also the size of each sub-volume and its rate of change. A level tracking method in TRAC-M provides this additional information for the code to modify its method of solution to account for the presence of water levels.<sup>3</sup> In Figures 6 and 7, a comparison of the void fractions demonstrates that the sharp changes in void fraction can be handled more accurately with the aid of a level tracking method as a water level crosses the cell boundaries. The mixture void fraction increases as the water level drops in the test vessel. The solution without the level tracking shows void fraction depressions during this phase and it is less stable during the next phase when the swelling occurs (in Figure 6). The level tracking aids the solution by primarily allowing the flow regime transition directly from pure bubbly-slug flow to pure annular mist and vice versa

without any interpolation between the two flow regimes (see Figures A-1 to A-8). While the accuracy of TRAC-M solution without the aid of a level tracking is sufficiently accurate for these swell tests, its accuracy is improved visibly with the level tracking method.

The simulations of these tests also revealed that the interfacial drag coefficient suffered from discontinuous changes following flow reversals. It seems possible to improve the quality of simulations by revisiting the procedures that evaluate the interfacial drag coefficient in the wake of flow reversals.

## 7. REFERENCES

1. Sozzi, G. L., "Level Swell and Void Fraction Measurements during Vessel Blowdown Experiments," 6, Hemisphere Publishing, New York (1992) 167-211
2. Kuo, H., "Level Tracking Model," Developmental Assessment of RELAP5/MOD3.1.2, Idaho National Engineering Laboratory (1995)
3. Aktas, B., "A Level Tracking Method for TRAC-M," ISL/NSAD-NRC-01-005 (December 2001)

## APPENDIX. SUPPLEMENTAL PLOTS

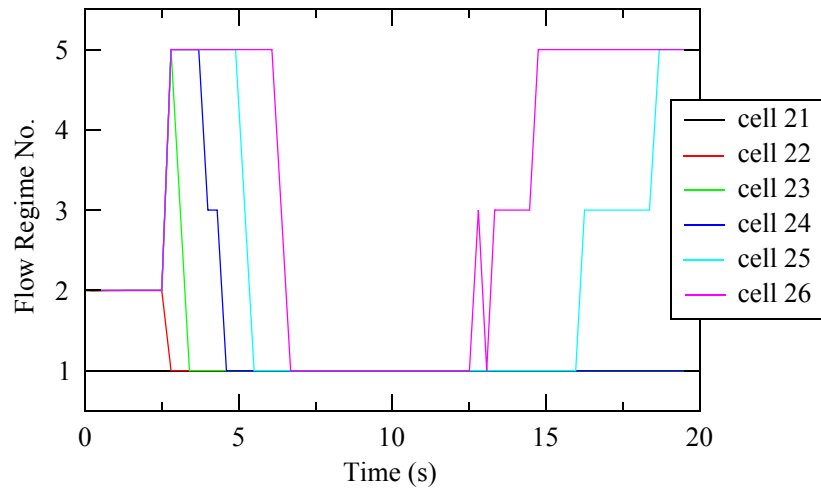


FIGURE A-1. Flow regimes across nodes 5 and 6 of Test 1004-3 (simulated without the level tracking method)

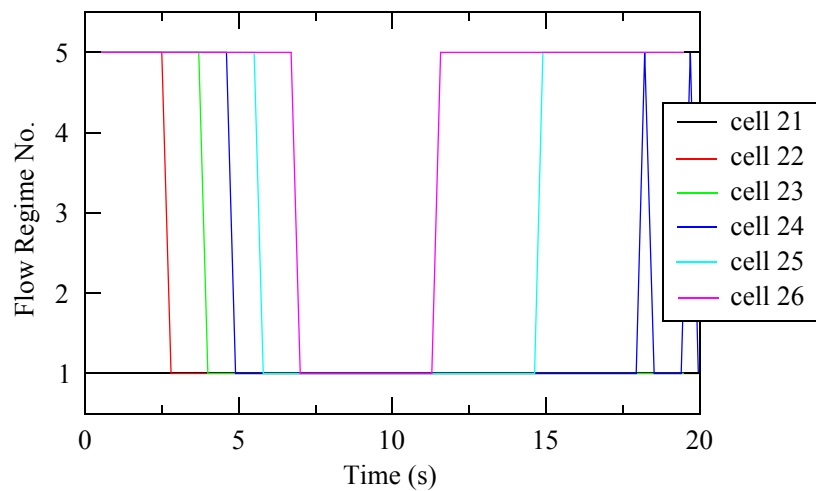


FIGURE A-2. Flow regimes across nodes 5 and 6 of Test 1004-3 (simulated with the level tracking method)

REGNM	Description
1.0	pure bubbly-slug flow. Values between 1.0 and 2.0 signify flow becoming horizontally stratified from the bubbly-slug regime.
3.0	"pure" transition flow. Values between 3.0 and 4.0 signify flow becoming horizontally stratified from the transition regime.
5.0	pure annular-mist flow. Values between 5.0 and 6.0 signify flow becoming horizontally stratified from the annular-mist regime.
-1.0	an indication of an error.

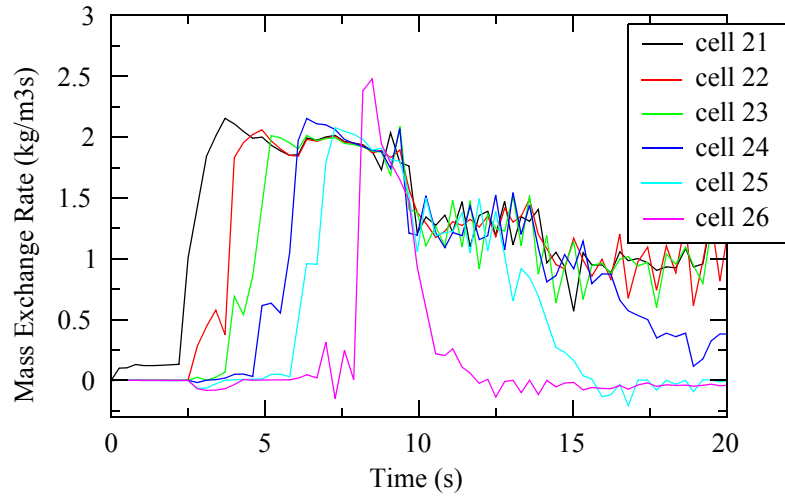


FIGURE A-3. Interfacial Mass Exchange across nodes 5 and 6 of Test 1004-3 (simulated without the level tracking method)

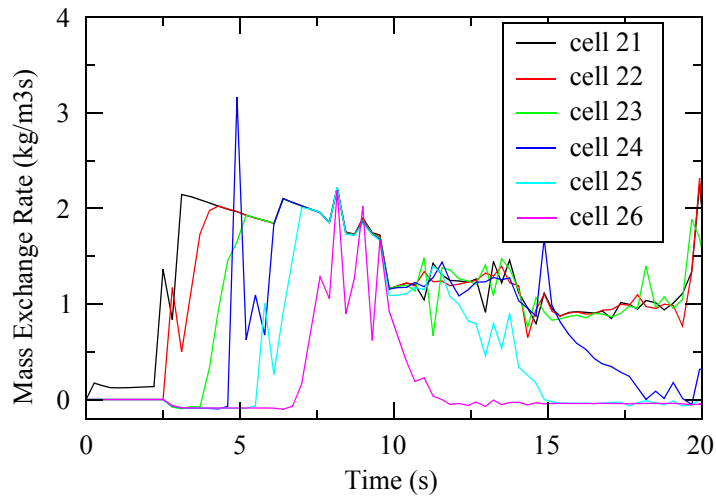


FIGURE A-4. Interfacial Mass Exchange across nodes 5 and 6 of Test 1004-3 (simulated with the level tracking method)

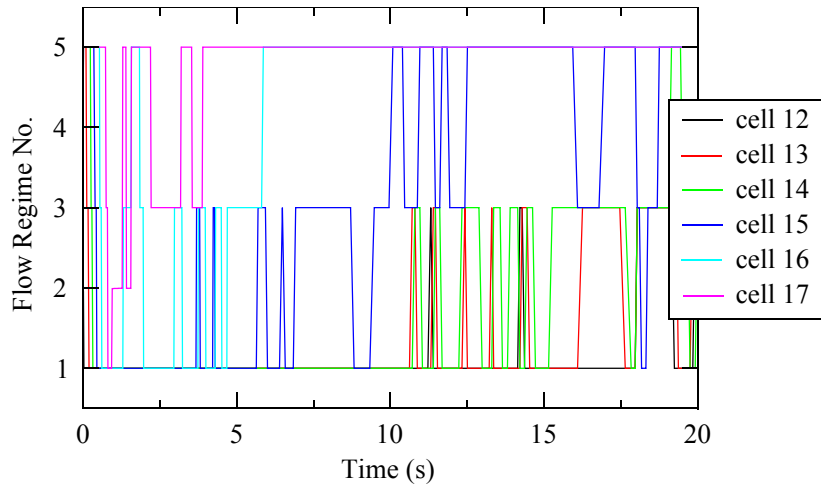


FIGURE A-5. Flow regimes across nodes 4 and 5 of Test 5801-15 (simulated without the level tracking method)

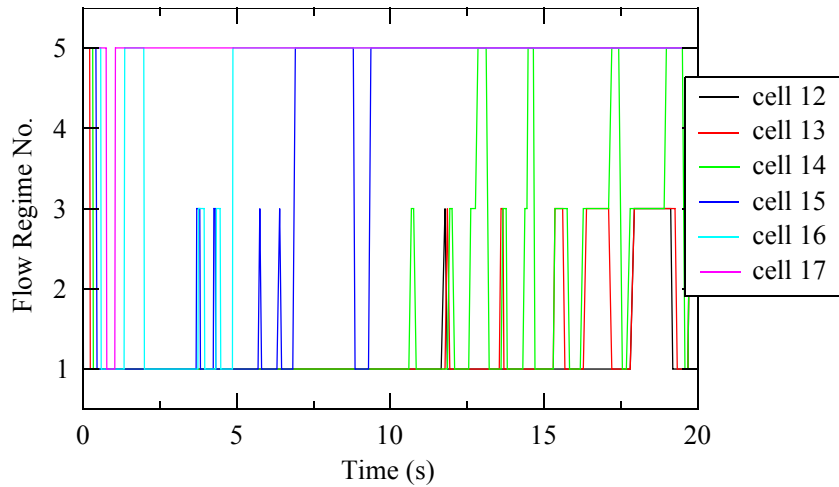


FIGURE A-6. Flow regimes across nodes 4 and 5 of Test 5801-15 (simulated with the level tracking method)

REGNM	Description
1.0	pure bubbly-slug flow. Values between 1.0 and 2.0 signify flow becoming horizontally stratified from the bubbly-slug regime.
3.0	"pure" transition flow. Values between 3.0 and 4.0 signify flow becoming horizontally stratified from the transition regime.
5.0	pure annular-mist flow. Values between 5.0 and 6.0 signify flow becoming horizontally stratified from the annular-mist regime.
-1.0	an indication of an error.

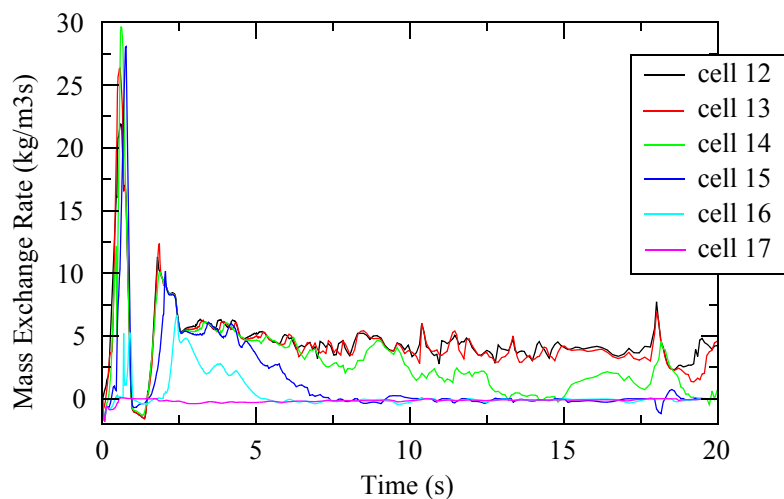


FIGURE A-7. Interfacial Mass Exchange across nodes 4 and 5 of Test 5801-15 (simulated without the level tracking method)

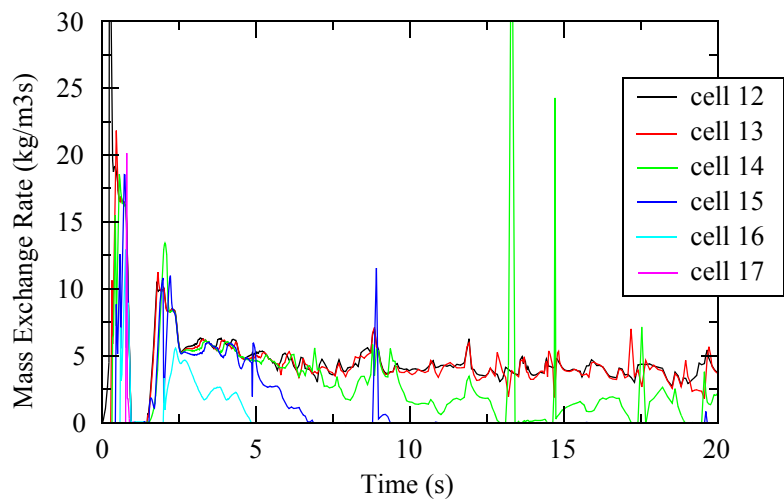


FIGURE A-8. Interfacial Mass Exchange across nodes 4 and 5 of Test 5801-15 (simulated with the level tracking method)



**APPENDIX C**  
**TRAC-M Simulations of Westinghouse MB-2 Tests**



# TRAC-M Simulations of MB-2 Steam Line Breaks

Task Order No. 7, Task 2

Submitted to:  
The United States Nuclear Regulatory Commission  
Office of Nuclear Regulatory Research  
Division of Systems Analysis and Regulatory Effectiveness  
Safety Margins and System Analysis Branch

Prepared by:  
Robert Beaton and C. Don Fletcher

Reviewed by:  
Dan Prelewicz

Information Systems Laboratories, Inc.  
Nuclear Systems Analysis Division  
March 2003

Under Contract No. NRC-04-02-054  
ISL-NSAD-TR-03-09



## Table of Contents

<b>TABLE OF CONTENTS .....</b>	<b>2</b>
<b>LIST OF FIGURES.....</b>	<b>2</b>
<b>1.0 INTRODUCTION.....</b>	<b>4</b>
<b>2.0 DESCRIPTION OF THE MB-2 TEST FACILITY.....</b>	<b>4</b>
<b>3.0 DESCRIPTION OF THE TRAC-M MODEL.....</b>	<b>9</b>
3.1 COMPARISON TO HOT FULL POWER CONDITIONS (TEST 1712).....	11
<b>4.0 STEAM LINE BREAK TRANSIENTS .....</b>	<b>21</b>
4.1 TEST 2013.....	21
4.2 TEST 2029.....	35
<b>5.0 SUMMARY/CONCLUSIONS.....</b>	<b>49</b>
<b>6.0 REFERENCES.....</b>	<b>49</b>
<b>7.0 ATTACHED FILES .....</b>	<b>49</b>
<b>8.0 PROBLEMS ENCOUNTERED .....</b>	<b>51</b>

## List of Figures

FIGURE 2.0-1: <i>MODEL BOILER 2 ELEVATION AND CROSS SECTION THROUGH TUBE BUNDLE .....</i>	<i>5</i>
FIGURE 2.0-2: <i>MODEL BOILER 2 BUNDLE CROSS SECTION .....</i>	<i>6</i>
FIGURE 2.0-3: <i>MODEL BOILER 2 UPPER SHELL REGION .....</i>	<i>7</i>
FIGURE 2.0-4: <i>SECONDARY SIDE PRESSURE TAPS WITHIN TUBE BUNDLE .....</i>	<i>8</i>
FIGURE 3.1-1: <i>FULL POWER PRIMARY PRESSURES .....</i>	<i>12</i>
FIGURE 3.1-2: <i>FULL POWER PRIMARY TEMPERATURES .....</i>	<i>12</i>
FIGURE 3.1-3: <i>FULL POWER PRIMARY TEMPERATURE -VS- ELEVATION.....</i>	<i>13</i>
FIGURE 3.1-4: <i>FULL POWER PRIMARY MASS FLOW .....</i>	<i>13</i>
FIGURE 3.1-5: <i>FULL POWER SECONDARY PRESSURE .....</i>	<i>14</i>
FIGURE 3.1-6: <i>FULL POWER FEEDWATER FLOW .....</i>	<i>15</i>
FIGURE 3.1-7: <i>FULL POWER NARROW RANGE WATER LEVEL.....</i>	<i>15</i>
FIGURE 3.1-8: <i>FULL POWER PRESSURE DIFFERENTIAL BETWEEN PRESSURE TAPS P01 AND P02 .....</i>	<i>16</i>
FIGURE 3.1-9: <i>FULL POWER PRESSURE DIFFERENTIAL BETWEEN PRESSURE TAPS P02 AND P03 .....</i>	<i>17</i>
FIGURE 3.1-10: <i>FULL POWER PRESSURE DIFFERENTIAL BETWEEN PRESSURE TAPS P03 AND P08 .....</i>	<i>17</i>
FIGURE 3.1-11: <i>FULL POWER PRESSURE DIFFERENTIAL BETWEEN PRESSURE TAPS P08 AND P09 .....</i>	<i>18</i>
FIGURE 3.1-12: <i>FULL POWER PRESSURE DIFFERENTIAL BETWEEN PRESSURE TAPS P09 AND P04 .....</i>	<i>18</i>
FIGURE 3.1-13: <i>FULL POWER PRESSURE DIFFERENTIAL BETWEEN PRESSURE TAPS P04 AND P05 .....</i>	<i>19</i>
FIGURE 3.1-14: <i>FULL POWER PRESSURE DIFFERENTIAL BETWEEN PRESSURE TAPS P05 AND P06 .....</i>	<i>19</i>
FIGURE 3.1-15: <i>FULL POWER PRESSURE DIFFERENTIAL BETWEEN PRESSURE TAPS P06 AND P07 .....</i>	<i>20</i>
FIGURE 3.1-16: <i>FULL POWER PRESSURE DIFFERENTIAL BETWEEN TAPS P01 AND P07 (TOTAL BUNDLE <math>\Delta P</math>) ....</i>	<i>20</i>
FIGURE 4.1-1: <i>TEST 2013 PRIMARY SIDE PRESSURES.....</i>	<i>22</i>
FIGURE 4.1-2: <i>TEST 2013 PRIMARY SIDE TEMPERATURES.....</i>	<i>23</i>
FIGURE 4.1-3: <i>TEST 2013 PRIMARY TEMPERATURE IN U-TUBES AT 100 SECONDS.....</i>	<i>23</i>
FIGURE 4.1-4: <i>TEST 2013 PRIMARY SIDE MASS FLOW.....</i>	<i>24</i>
FIGURE 4.1-5: <i>TEST 2013 SECONDARY SIDE PRESSURE.....</i>	<i>26</i>
FIGURE 4.1-6: <i>TEST 2013 BREAK FLOW .....</i>	<i>26</i>

FIGURE 4.1-7: <i>TEST 2013 FEEDWATER FLOW</i> .....	27
FIGURE 4.1-8: <i>TEST 2013 NARROW RANGE WATER LEVEL</i> .....	27
FIGURE 4.1-9: <i>TEST 2013 LOWER DOWNCOMER TEMPERATURE</i> .....	28
FIGURE 4.1-10: <i>TEST 2013 PRESSURE DIFFERENTIAL BETWEEN PRESSURE TAPS P01 AND P02</i> .....	28
FIGURE 4.1-11: <i>TEST 2013 PRESSURE DIFFERENTIAL BETWEEN PRESSURE TAPS P02 AND P03</i> .....	29
FIGURE 4.1-12: <i>TEST 2013 PRESSURE DIFFERENTIAL BETWEEN PRESSURE TAPS P03 AND P08</i> .....	29
FIGURE 4.1-13: <i>TEST 2013 PRESSURE DIFFERENTIAL BETWEEN PRESSURE TAPS P08 AND P09</i> .....	30
FIGURE 4.1-14: <i>TEST 2013 PRESSURE DIFFERENTIAL BETWEEN PRESSURE TAPS P09 AND P04</i> .....	30
FIGURE 4.1-15: <i>TEST 2013 PRESSURE DIFFERENTIAL BETWEEN PRESSURE TAPS P04 AND P05</i> .....	31
FIGURE 4.1-16: <i>TEST 2013 PRESSURE DIFFERENTIAL BETWEEN PRESSURE TAPS P05 AND P06</i> .....	31
FIGURE 4.1-17: <i>TEST 2013 PRESSURE DIFFERENTIAL BETWEEN PRESSURE TAPS P06 AND P07</i> .....	32
FIGURE 4.1-18: <i>TEST 2013 PRESSURE DIFFERENTIAL BETWEEN PRESSURE TAPS P01 AND P07</i> .....	32
FIGURE 4.1-19: <i>TEST 2013 PRESSURE DROP ACROSS THE TUBE SUPPORT PLATES</i> .....	33
FIGURE 4.1-20: <i>TEST 2013 PRESSURE DROP ACROSS THE TUBE SUPPORT PLATES</i> .....	33
FIGURE 4.1-21: <i>TEST 2013 PRESSURE DROP ACROSS THE TUBE SUPPORT PLATES</i> .....	34
FIGURE 4.1-22: <i>TEST 2013 PRESSURE DROP ACROSS THE TUBE SUPPORT PLATES</i> .....	34
FIGURE 4.2-1: <i>TEST 2029 PRIMARY SIDE PRESSURES</i> .....	36
FIGURE 4.2-2: <i>TEST 2029 PRIMARY SIDE TEMPERATURES</i> .....	37
FIGURE 4.2-3: <i>TEST 2029 PRIMARY TEMPERATURE IN U-TUBES AT 500 SECONDS</i> .....	37
FIGURE 4.2-4: <i>TEST 2029 PRIMARY SIDE MASS FLOW</i> .....	38
FIGURE 4.2-5: <i>TEST 2029 SECONDARY SIDE PRESSURE</i> .....	39
FIGURE 4.2-6: <i>TEST 2029 STEAM LINE BREAK FLOW</i> .....	39
FIGURE 4.2-7: <i>TEST 2029 STEAM GENERATOR TUBE RUPTURE FLOW</i> .....	40
FIGURE 4.2-8: <i>TEST 2029 FEEDWATER FLOW</i> .....	40
FIGURE 4.2-9: <i>TEST 2029 NARROW RANGE WATER LEVEL</i> .....	41
FIGURE 4.2-10: <i>TEST 2029 LOWER DOWNCOMER TEMPERATURE</i> .....	41
FIGURE 4.2-11: <i>TEST 2029 PRESSURE DIFFERENTIAL BETWEEN PRESSURE TAPS P01 AND P02</i> .....	42
FIGURE 4.2-12: <i>TEST 2029 PRESSURE DIFFERENTIAL BETWEEN PRESSURE TAPS P02 AND P03</i> .....	42
FIGURE 4.2-13: <i>TEST 2029 PRESSURE DIFFERENTIAL BETWEEN PRESSURE TAPS P03 AND P08</i> .....	43
FIGURE 4.2-14: <i>TEST 2029 PRESSURE DIFFERENTIAL BETWEEN PRESSURE TAPS P08 AND P09</i> .....	43
FIGURE 4.2-15: <i>TEST 2029 PRESSURE DIFFERENTIAL BETWEEN PRESSURE TAPS P09 AND P04</i> .....	44
FIGURE 4.2-16: <i>TEST 2029 PRESSURE DIFFERENTIAL BETWEEN PRESSURE TAPS P04 AND P05</i> .....	44
FIGURE 4.2-17: <i>TEST 2029 PRESSURE DIFFERENTIAL BETWEEN PRESSURE TAPS P05 AND P06</i> .....	45
FIGURE 4.2-18: <i>TEST 2029 PRESSURE DIFFERENTIAL BETWEEN PRESSURE TAPS P06 AND P07</i> .....	45
FIGURE 4.2-19: <i>TEST 2029 PRESSURE DIFFERENTIAL BETWEEN PRESSURE TAPS P01 AND P07</i> .....	46
FIGURE 4.2-20: <i>TEST 2029 PRESSURE DROP ACROSS THE TUBE SUPPORT PLATES</i> .....	47
FIGURE 4.2-21: <i>TEST 2029 PRESSURE DROP ACROSS THE TUBE SUPPORT PLATES</i> .....	47
FIGURE 4.2-22: <i>TEST 2029 PRESSURE DROP ACROSS THE TUBE SUPPORT PLATES</i> .....	48
FIGURE 4.2-23: <i>TEST 2029 PRESSURE DROP ACROSS THE TUBE SUPPORT PLATES</i> .....	48

## 1.0 Introduction

As part of the TRAC-M developmental assessment, TRAC-M calculations have been compared to two MB-2 steam line break tests. The objective of these code to data comparisons is to demonstrate success of the TRAC-M code consolidation effort. The specific area of comparison is thermal and hydraulic loads on steam generator internals (i.e., tube support plates, primary tubes) during steamline breaks. TRAC-M version 31050 was used. The TRAC-M input model was developed based on an existing RELAP5 model of the MB-2 facility.

## 2.0 Description of the MB-2 Test Facility

The Model Boiler No. 2 (MB-2) is an approximately 0.8 percent power-scaled model of the Westinghouse Model F steam generator, a feeding-type unit. It was designed to be geometrically and thermal-hydraulically similar to the Model F in important areas. The MB-2 steam generator is shown in Figure 2.0-1 through Figure 2.0-4.

The primary loop is a closed pressurized water loop, consisting of a 10 MW natural-gas-fired heater, a pump, a pressurizer, a flow control valve and a 54 tube steam generator. The 54 U-tubes were placed in a shroud as shown in Figure 2.0-2. The tubes are arranged in four columns with 13 rows and are about 23 feet tall. At full capacity conditions (100% power) the tubes can transfer 6.67 MW from the primary water (at 2250 psia) to the secondary water at (1000 psia).

Feedwater is mixed with separated water in one of two downcomer pipes and enters the bundle secondary just above the tube sheet. As it flows upward through the boiler it becomes a two phase mixture, leaves the top of the bundle, and is forced through a cone into a riser. At the top of the riser, a centrifugal separator removes the water and returns it to the downcomer. Steam, with some entrained water, then enters a single-tier vane type separator to remove the remaining moisture. The exit steam is essentially dry. The moisture is collected in a 'disengagement tank' to facilitate a moisture flow rate measurement and then returns to the downcomer where it mixes with fluid from the feedwater line. Further information relating to the MB-2 test facility can be found in References 1 and 2.

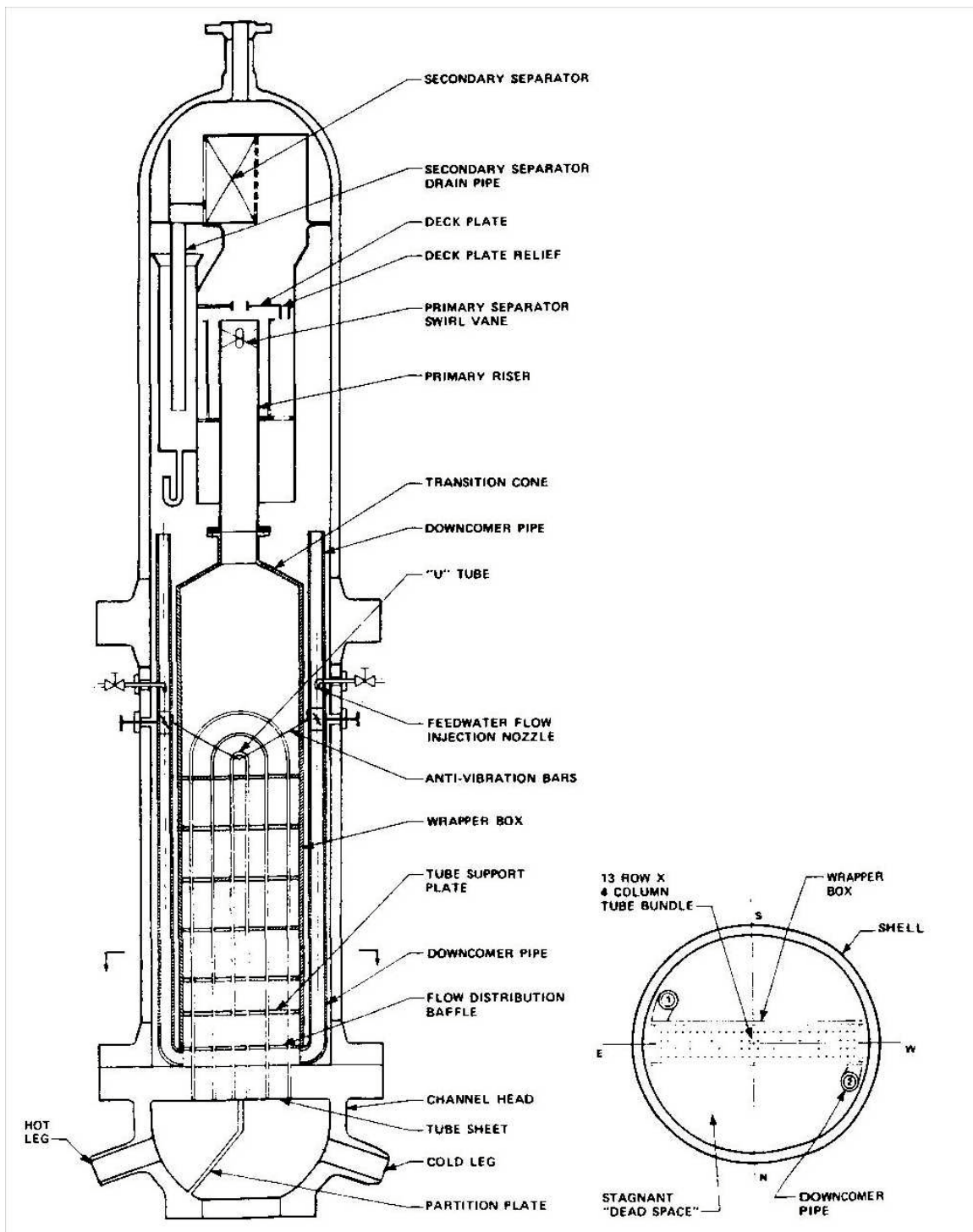


**Figure 2.0-1: Model Boiler 2 Elevation and Cross Section Through Tube Bundle**



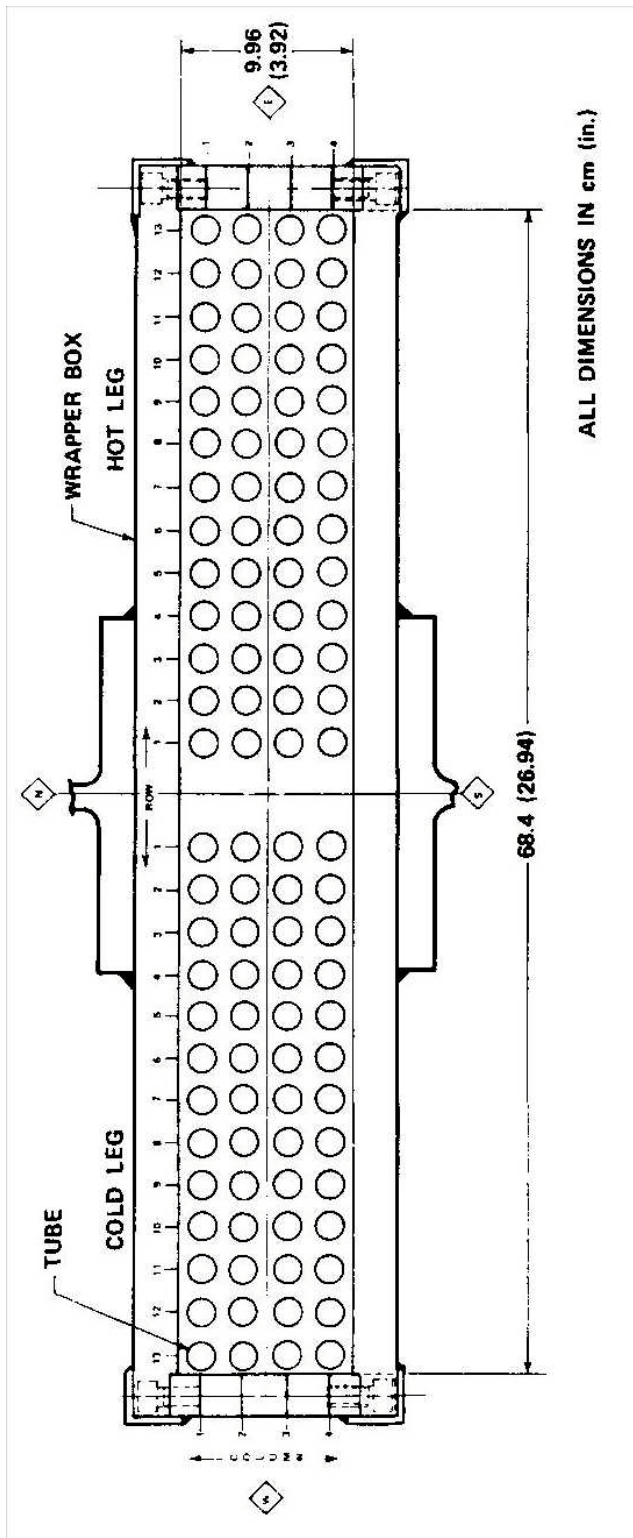


**Figure 2.0-2:** *Model Boiler 2 Bundle Cross Section*

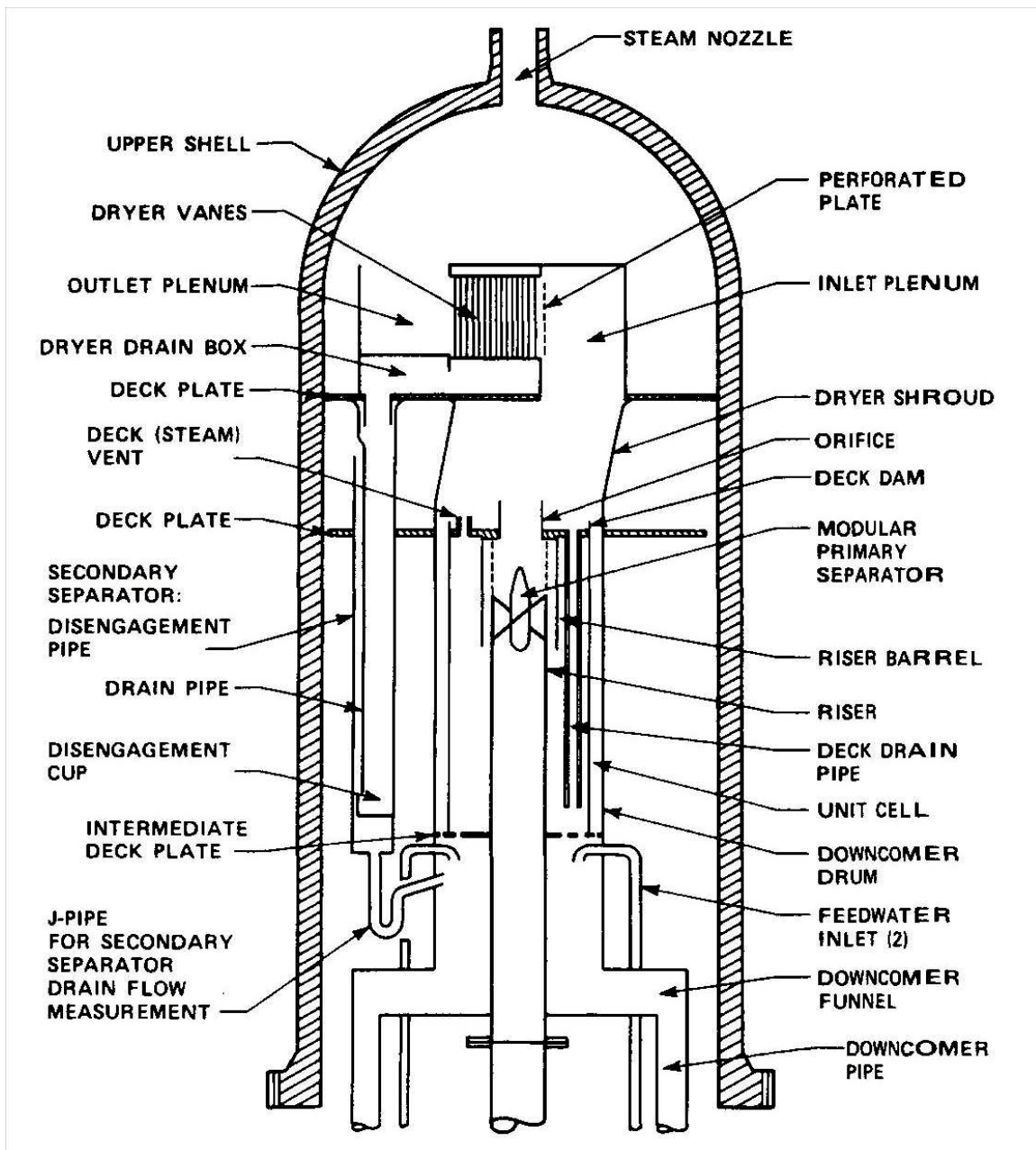


**Figure 2.0-3: Model Boiler 2 Upper Shell Region**

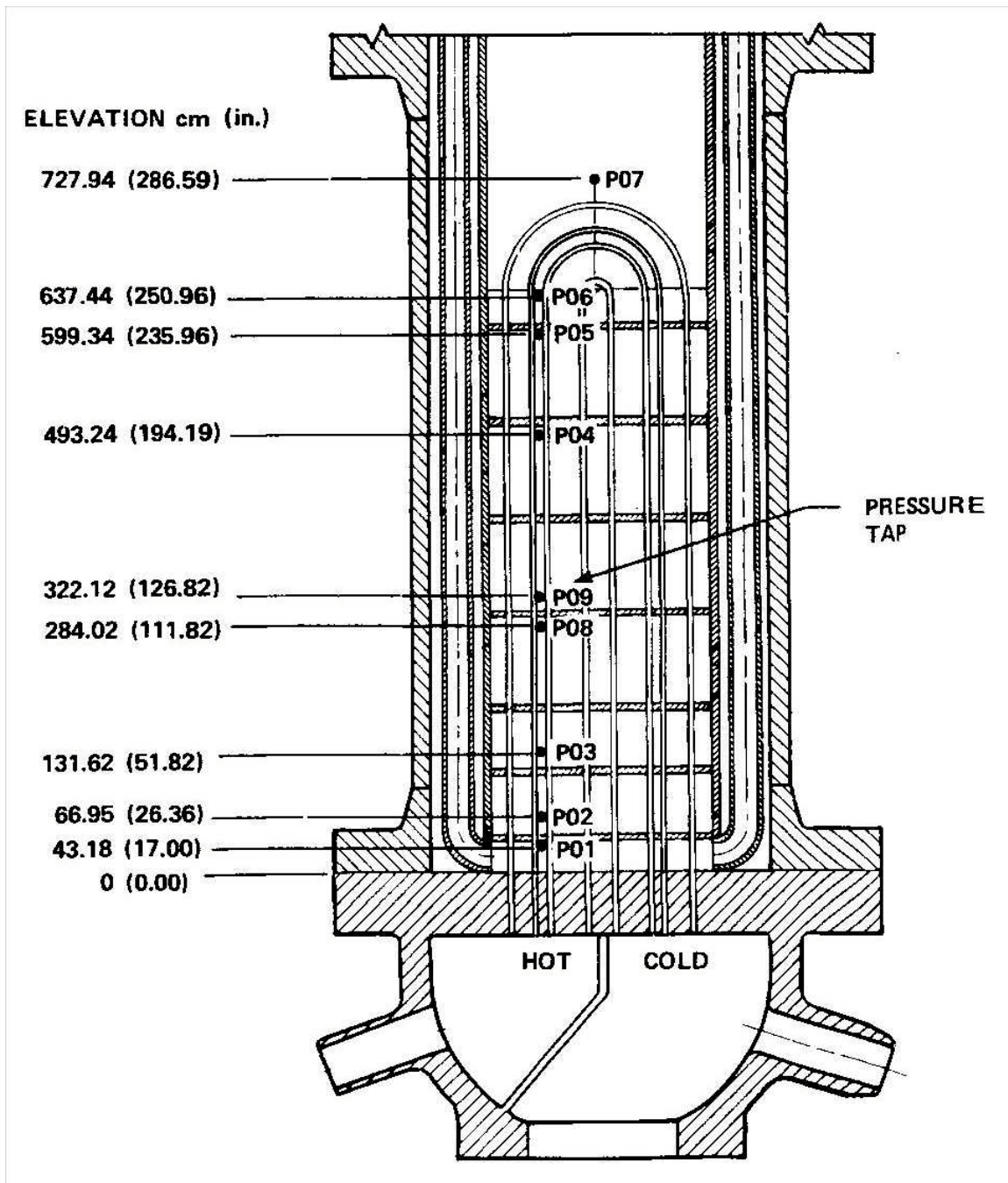


**Figure 2.0-4:** *Secondary Side Pressure Taps Within Tube Bundle*

### 3.0 Description of the TRAC-M Model

The only available model of the MB-2 was a RELAP5 model which was previously used for RELAP5 assessment. This model (Reference 3) is used as the starting point for this analysis. In general, the conversion from RELAP5 to TRAC-M is a straightforward process and many input values are used directly. A noding diagram of the TRAC-M model is shown as Figure 3.0-1. RELAP5 annulus components were replaced with TRAC-M pipe components. The separator (SEPD) component in TRAC-M is not recommended (according to Reference 4), so a TRAC-M TEE component was used. The flow areas of the return junctions were modified so that the flow velocity would allow the steam bubbles to flow up and the liquid to flow back down to the downcomer. All NAMELIST variables are the default values except as shown below.

- ◆ `iadded = 20`, option that adds a numerical-solution status parameter message to the TRCMSG and TTY files. The status parameters are written every 20<sup>th</sup> timestep. This option does not affect the calculation.
- ◆ `icflow = 2`, choked flow model option is turned on at cell edges indicated in the component input. Choking is turned on only at the break valve (set on valve component 238).
- ◆ `ielv = 1`, cell centered elevations are entered in the input (rather than gravity terms).
- ◆ `ikfac = 1`, option that specifies K factors are entered in the input (rather than additive loss coefficients).
- ◆ `usesjc = 3`, option which allows the use of side junctions. This allows multiple connections to a single component.

Since the TRAC-M model will be used to determine tube support plate pressure drops, the secondary boiler region was renodalized so that there is a hydraulic volume between each tube support plate. The original RELAP5 model included only 4 cells adjacent to the tubes. The TRAC-M model includes nine cells adjacent to the tubes. The loss coefficients at the tube support plates and flow distribution baffle were obtained from Appendix A of Reference 2. Detailed calculation of the renodalization can be found in Attachment A to this document.

The dead space (See Figure 2.0-1) was modeled in TRAC as a pipe with a FILL component at each end. The dead space is the volume outside of the tube bundle and inside the outer shell. It is connected to the secondary side through heat structures. For the hot full power initialization, this was set to the desired temperature and pressure with no flow from the FILL components to the dead space volume. For the two transient runs, the pressure was set as a boundary condition. Reference 2, page 3-13 lists instruments P-14 and P-99 as the pressure in the dead space, however, these data channels were not available for the tests of interest. During the steam line break transients, the MB-2 dead space was allowed to depressurize in parallel with the MB-2 test section to prevent rupture or collapse of the test section (Reference 2, page 5-111). To accomplish this without the addition of a significant control scheme, a BREAK component was connected to the dead space and the pressure was forced to the experimental data for the secondary side pressure.

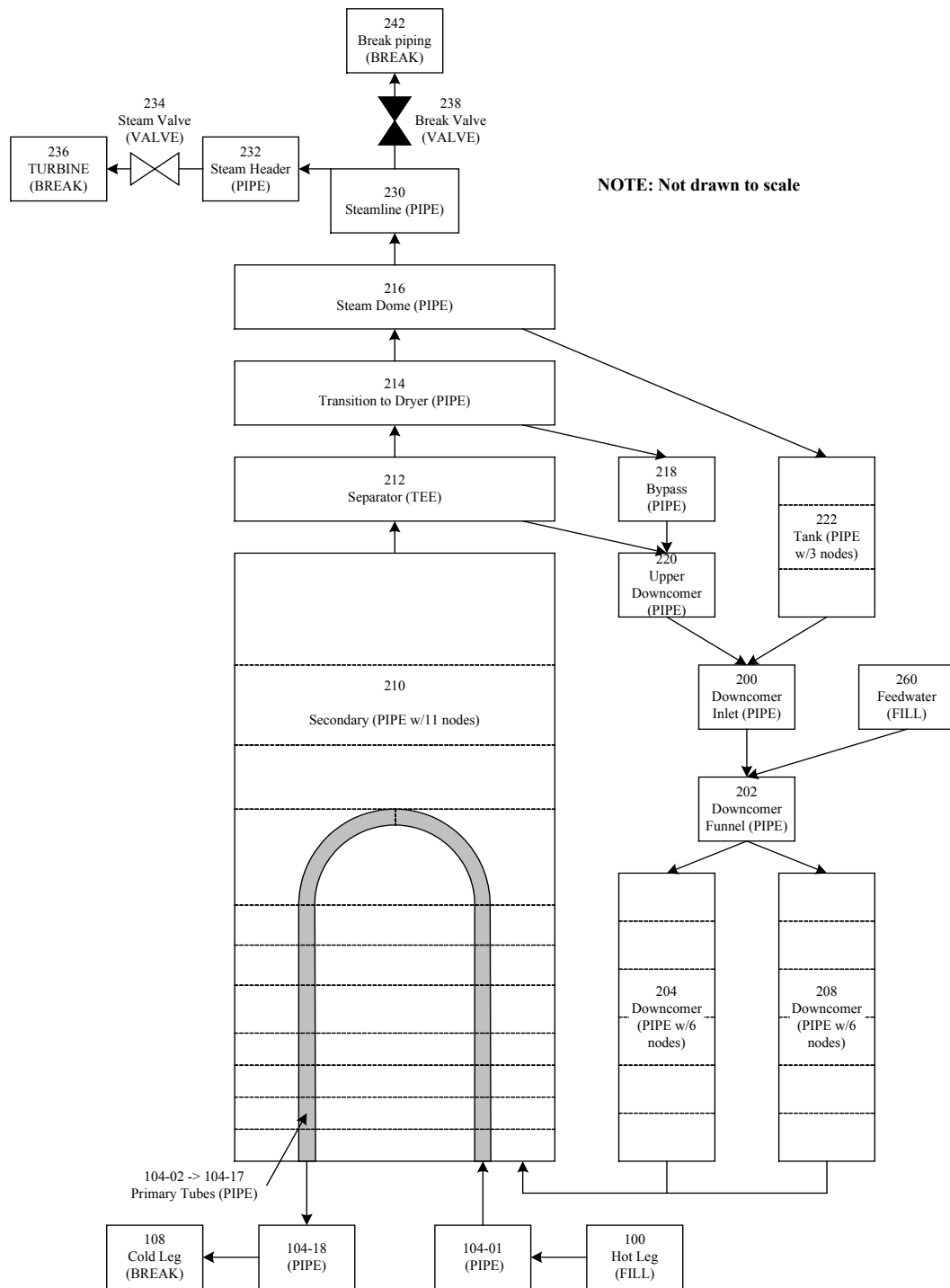


**Figure 3.0-1: TRAC-M Noding Diagram of the MB-2 Facility**

### 3.1 Comparison to Hot Full Power Conditions (Test 1712)

Once the model was converted from RELAP5 to TRAC-M, it was initialized to a hot full power steady state condition. This was done to assure that the SG is modeled correctly, particularly the separator. A null transient was run to assure the model would hold the steady conditions. This null transient run was compared to data from test 1712. While this test is a loss of feedwater flow test, the initial part (approximately the first 40 seconds) represents hot full power initial conditions. Results from this comparison show that the model is holding a quasi-steady state and predicting thermal hydraulic conditions reasonably well. Table 3.1-1 compares experimental data to TRAC-M for some key parameters.

The boundary conditions input on the primary side of the model include cold leg pressure, primary mass flow rate and hot leg temperature. Note that in this null transient all of these parameters are held at fixed values obtained from the experimental data. Figures 3.1-1 through 3.1-4 show the primary system response. Note that the TRAC-M parameter as well as experimental data channel are typically shown on the figures. The energy removal rate on the secondary side of the steam generator tube bundle can be shown by plotting the primary side fluid temperature as it flows up and down inside the U-tubes. As seen in Figure 3.1-3, the TRAC-M model is calculating the temperature profile very well, which shows that the calculated heat transfer is accurate. Data for the temperature versus elevation plot was taken using all available data channels in the primary tubes (Reference 2, page 3-2).

**Table 3.1-1: Steady State Conditions for Hot Full Power Test 1712 (at 40 seconds).**

Parameter	Desired Value (Data Channel)	TRAC-M Value (parameter)
Hot leg temperature*	618°F (T-1150)	618°F (tln-104001)
Cold leg temperature	562°F (T-1250)	565°F (tln-104018)
Cold leg pressure*	2200 psia (P-13)	2209 psia (pn-104018)
Primary mass flow*	91.5 lbm/s (WF109)	91.5 lbm/s (rmvm-104001)
Feedwater flow*	8.8 lbm/s (WF201A)	8.8 lbm/s (rmvm-202004)
Secondary pressure	995 psia (P-91)	997 psia (pn-230001)
Narrow range water level	439 in (WL9368)	443 in (cb11)
Secondary side total bundle pressure drop	5.6 psid (DPT-0107)	6.1 psid (cb1107)

\* - Set as boundary condition

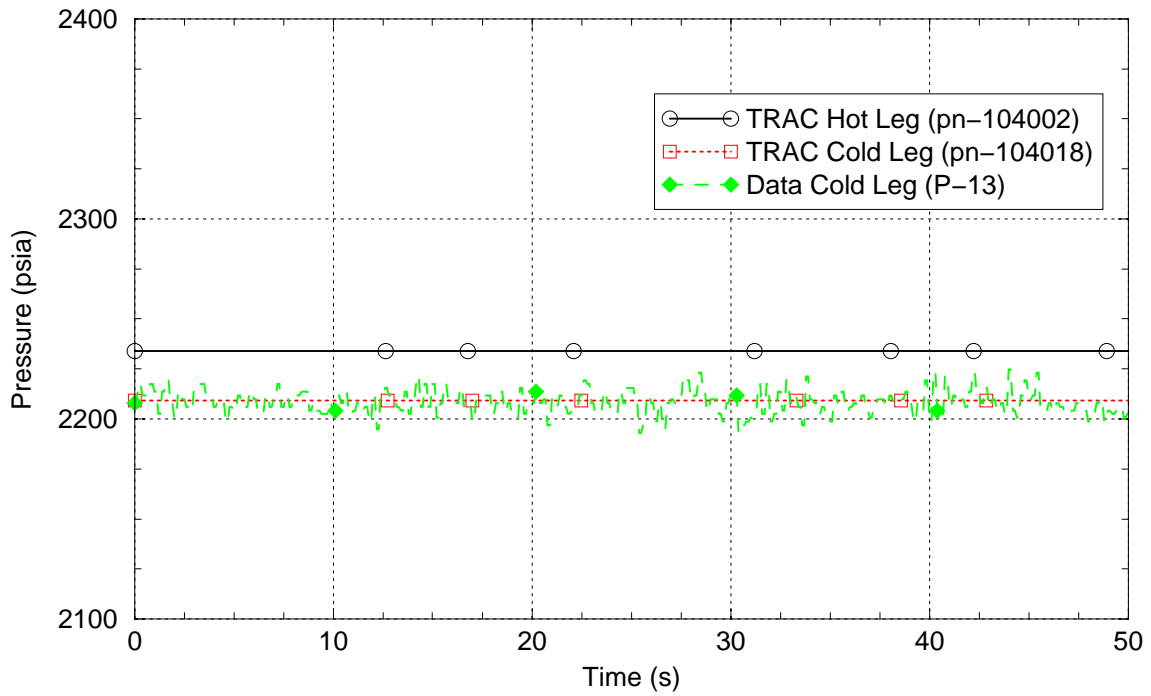


**Figure 3.1-1:** *Full Power Primary Pressures*

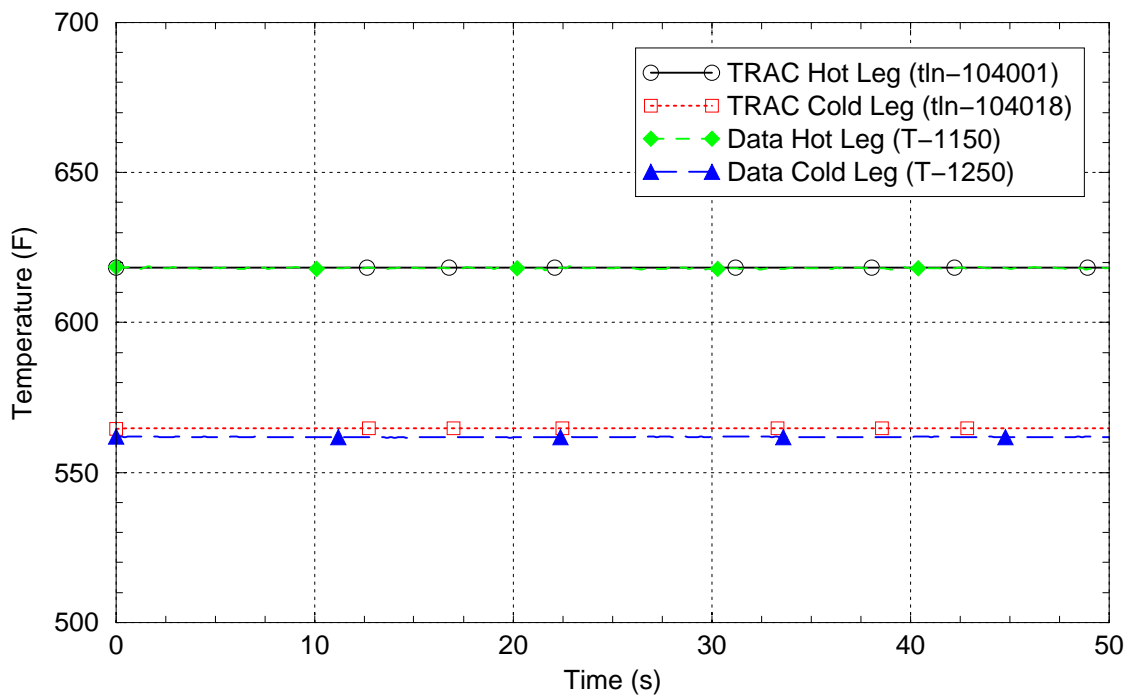


**Figure 3.1-2:** *Full Power Primary Temperatures*

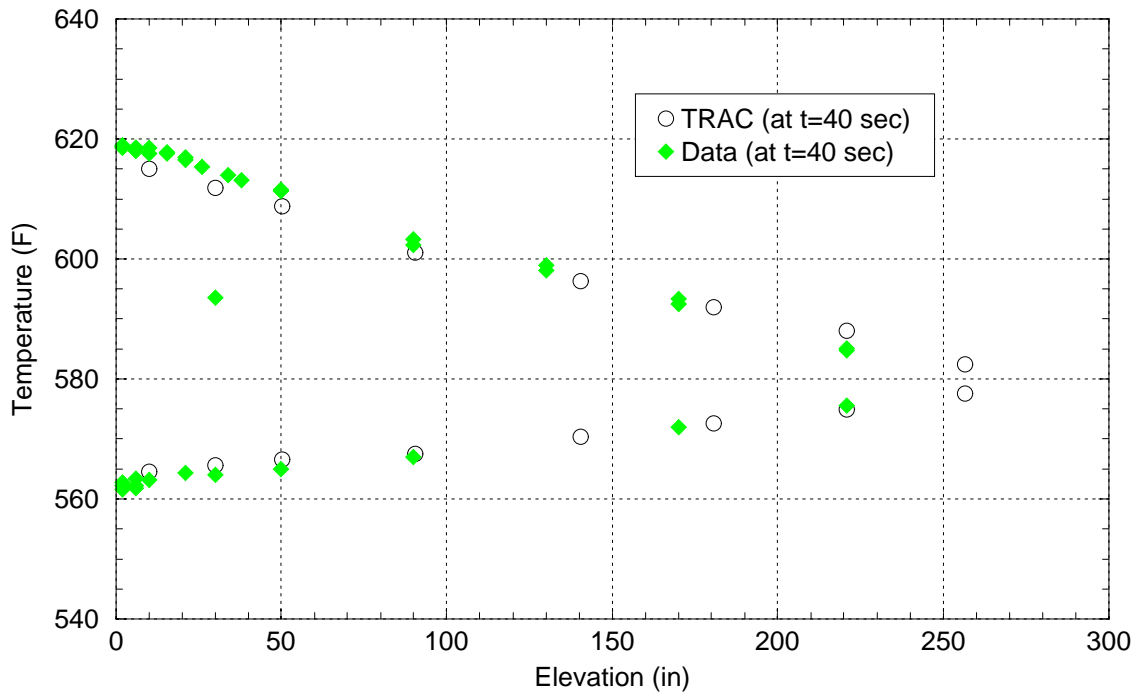


**Figure 3.1-3:** *Full Power Primary Temperature -vs- Elevation*

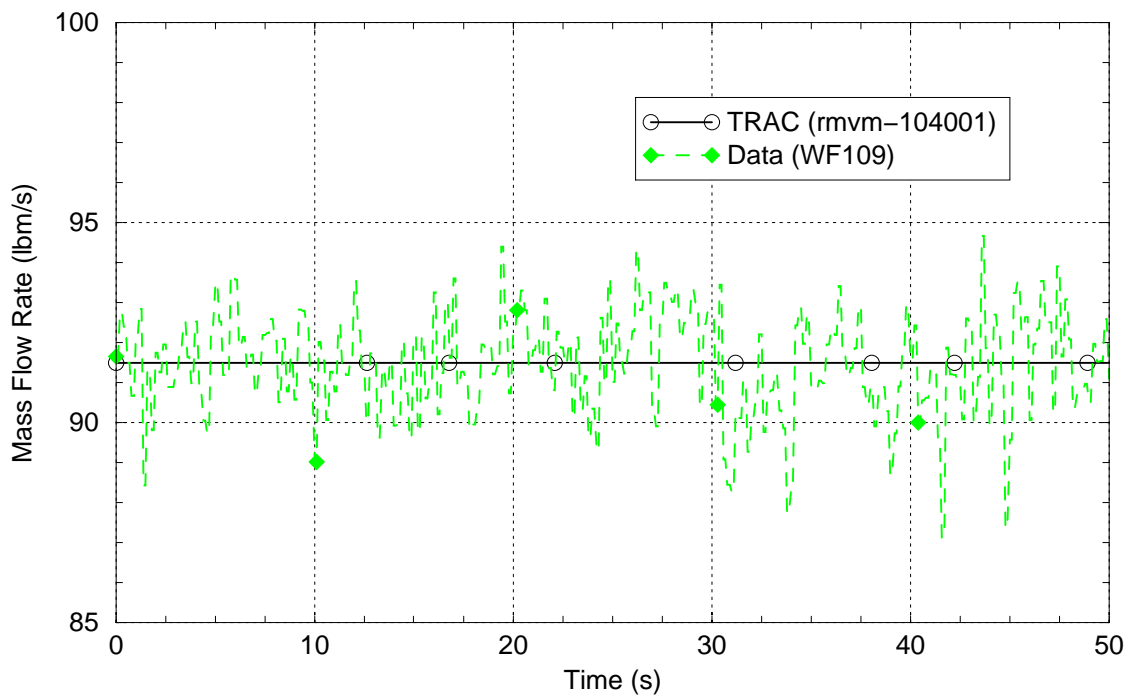


**Figure 3.1-4:** *Full Power Primary Mass Flow*

The secondary side boundary conditions include feedwater pressure, temperature and flow rate as well as steam dome pressure. As with the primary side, the boundary



conditions are held at fixed values. Plots of the secondary side response are shown in Figure 3.1-5 through Figure 3.1-16. Since the steam dome pressure is maintained with a check valve, the steam dome pressure exhibits small oscillations as the check valve opens/closes. While these pressure oscillations are small, they have a greater effect on the water level. The check valve control of pressure and a fixed feedwater flow rate result in the narrow range water level oscillations as seen in Figure 3.1-7. The water level is also slightly higher than the experimental data. The use of control systems to maintain steam dome pressure and feedwater flow rate could eliminate these oscillations and result in the water level being driven to the desired setpoint. However, the current model was judged to be adequate for this assessment, which employs MB-2 hot zero power experiments.

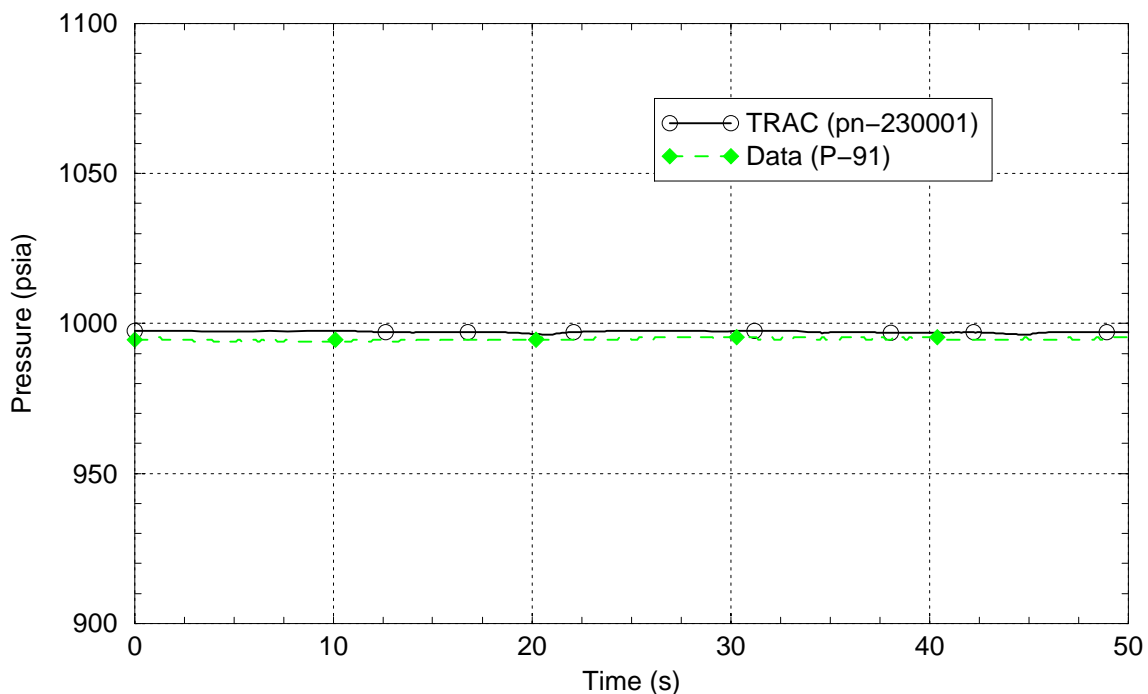


**Figure 3.1-5:** *Full Power Secondary Pressure*

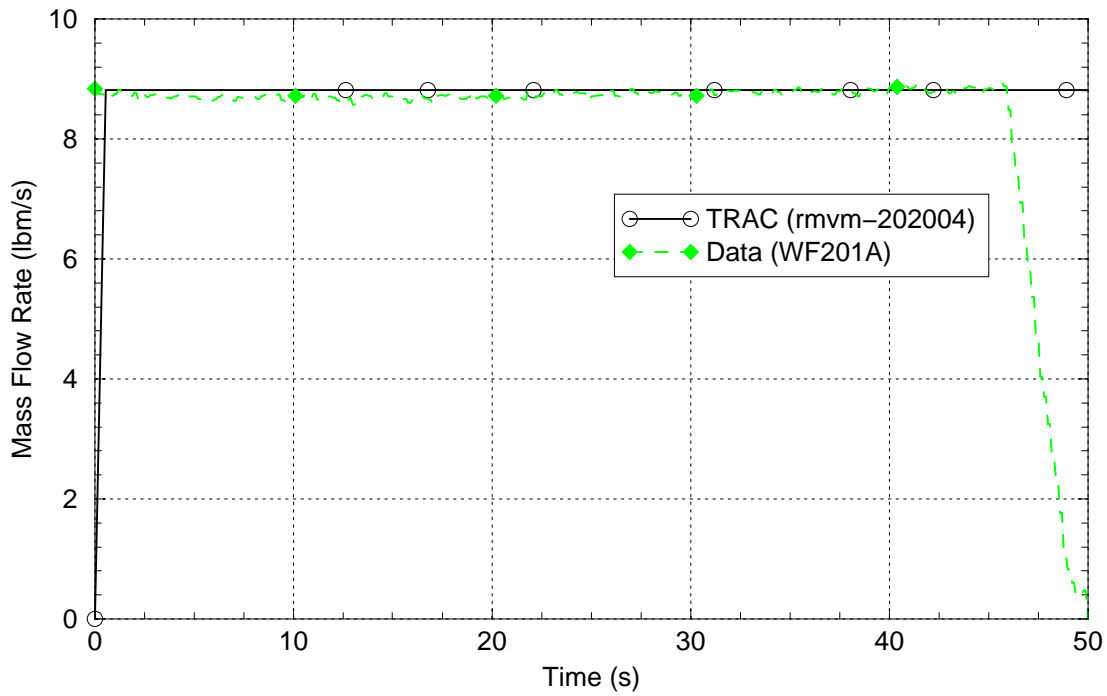


**Figure 3.1-6:** *Full Power Feedwater Flow*

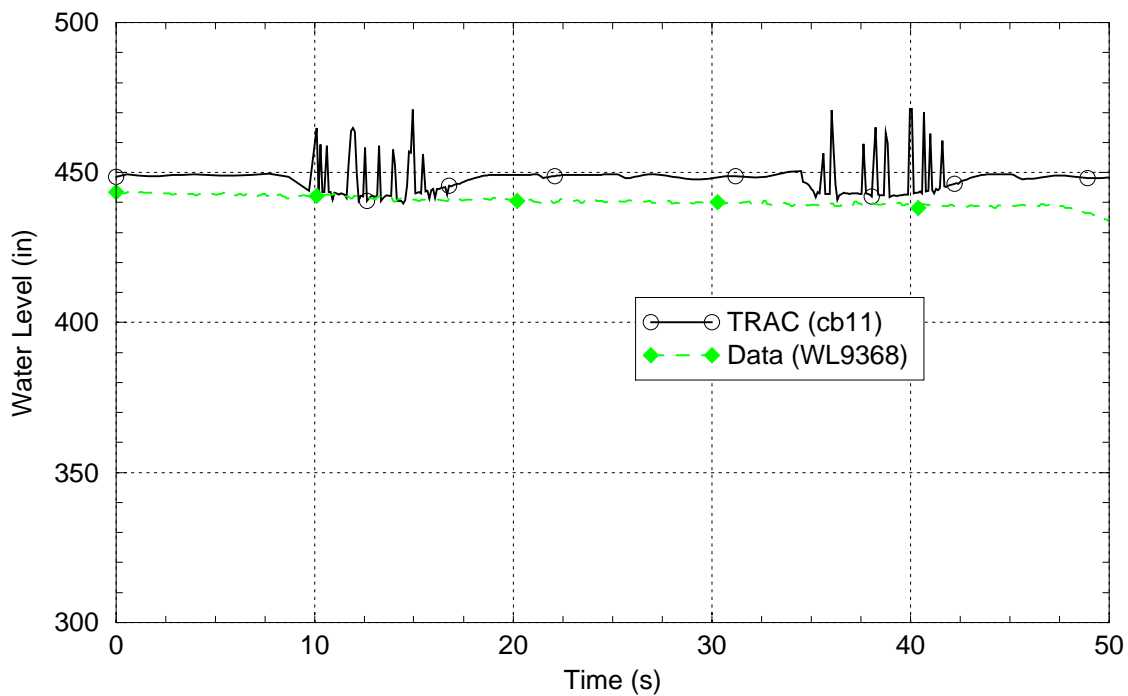


**Figure 3.1-7:** *Full Power Narrow Range Water Level*

In order to compute pressure drops between the experimental pressure taps, the TRAC-M pressure must be known at the elevation of a given pressure tap. Since the

TRAC-M pressure is only known at node centers, the pressure at tap locations must be determined based on node centers plus (or minus) elevation head and a frictional term. These calculations are described in Attachment B and are implemented in TRAC-M using control blocks. Similar calculations are performed to obtain the pressure drops across the tube support plates.

Figure 3.1-8 through Figure 3.1-16 compare differential pressure measurements in the secondary bundle region. For locations of pressure taps, see Figure 2.0-4. In general, the TRAC-M calculated  $\Delta P$ s are higher than the experimental data (DPT-0102, DPT-0203, DPT-0904, DPT-0405, and DPT-0506). One of the TRAC-M computed  $\Delta P$ s is lower (DPT-0607) and two agree with the data (DPT-0308 and DPT-0809). The pressure drops which are too high are generally within about 25% and the total TRAC-M  $\Delta P$  (DPT-0107) is just a little high (about 10%). The pressure drops are based on the K factors applied to the tube support plate junctions that were taken directly from Appendix A of Reference 2. The comparison of TRAC-M calculated  $\Delta P$ s to the data is judged to be acceptable.

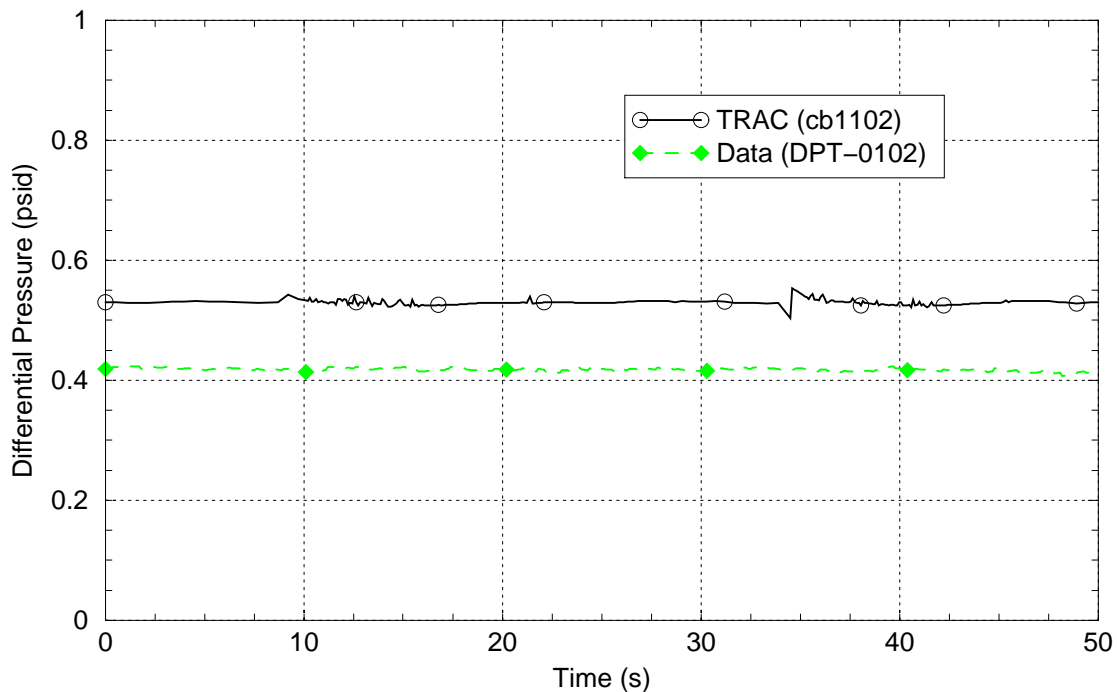


**Figure 3.1-8:** Full Power Pressure Differential between Pressure Taps P01 and P02

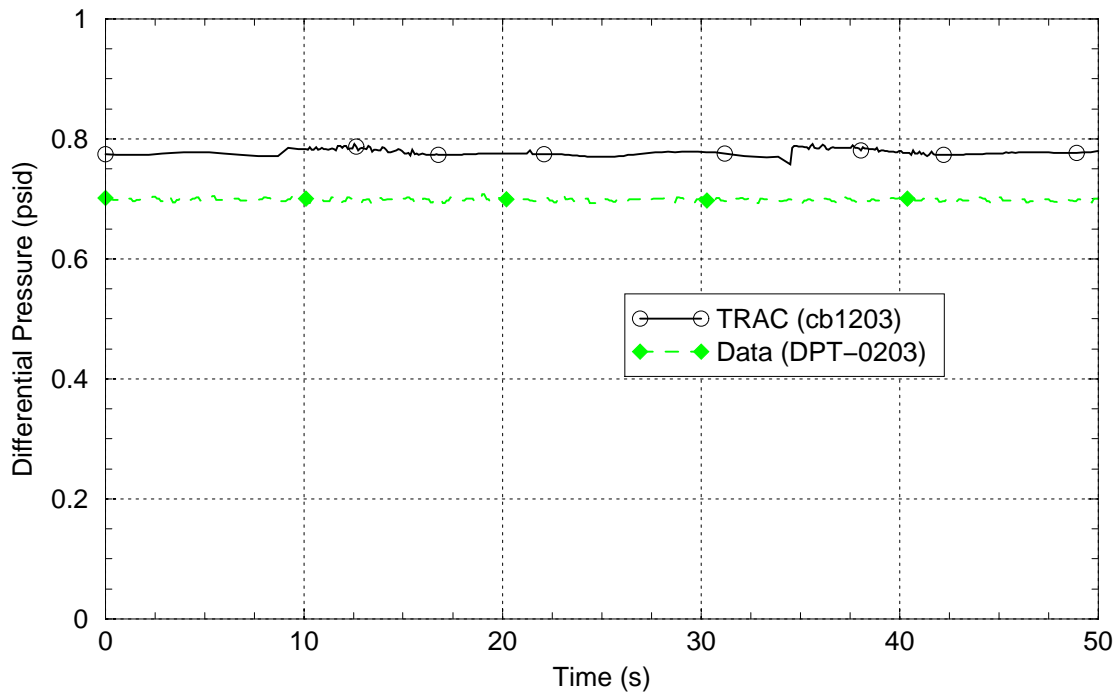


**Figure 3.1-9:** Full Power Pressure Differential between Pressure Taps P02 and P03

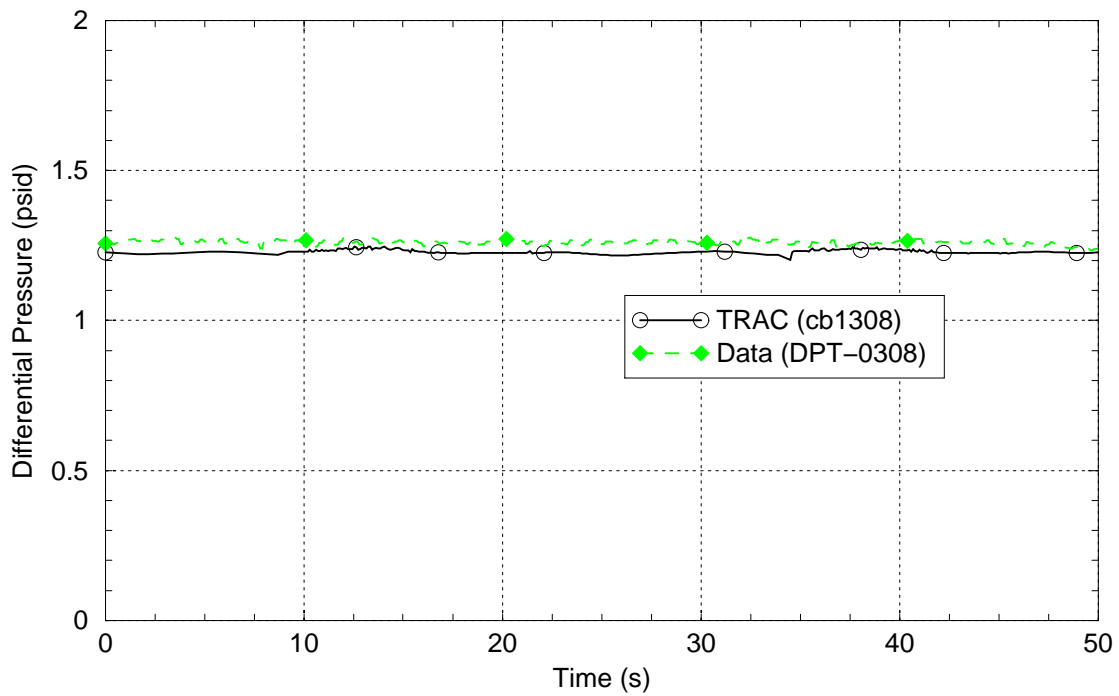


**Figure 3.1-10:** Full Power Pressure Differential between Pressure Taps P03 and P08

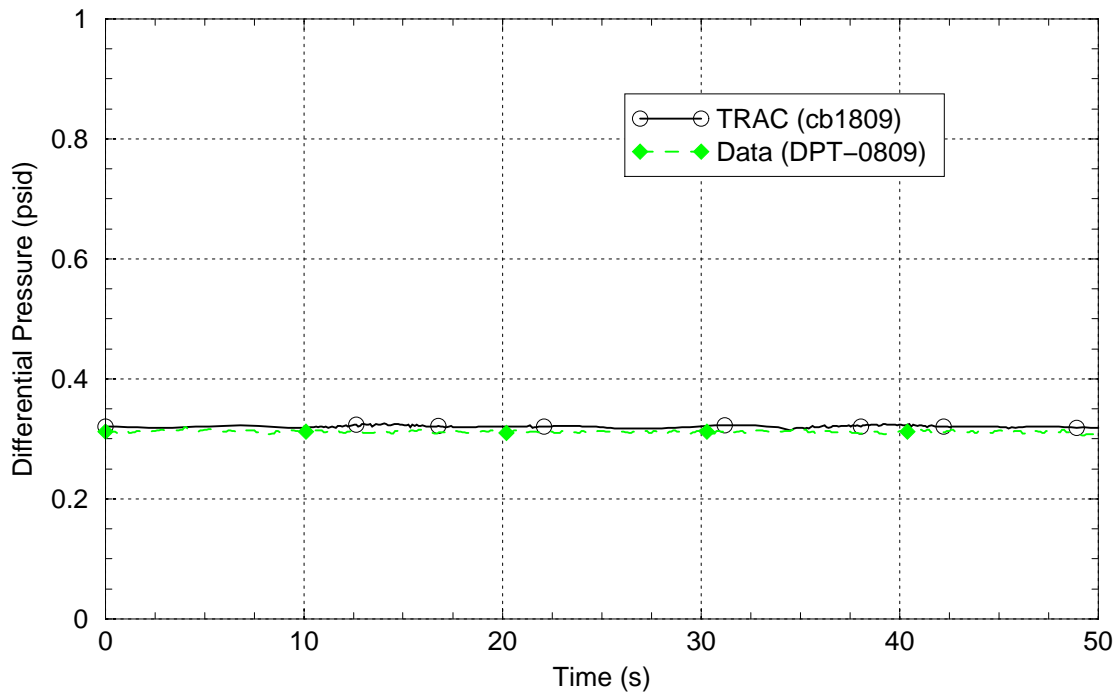


**Figure 3.1-11:** Full Power Pressure Differential between Pressure Taps P08 and P09

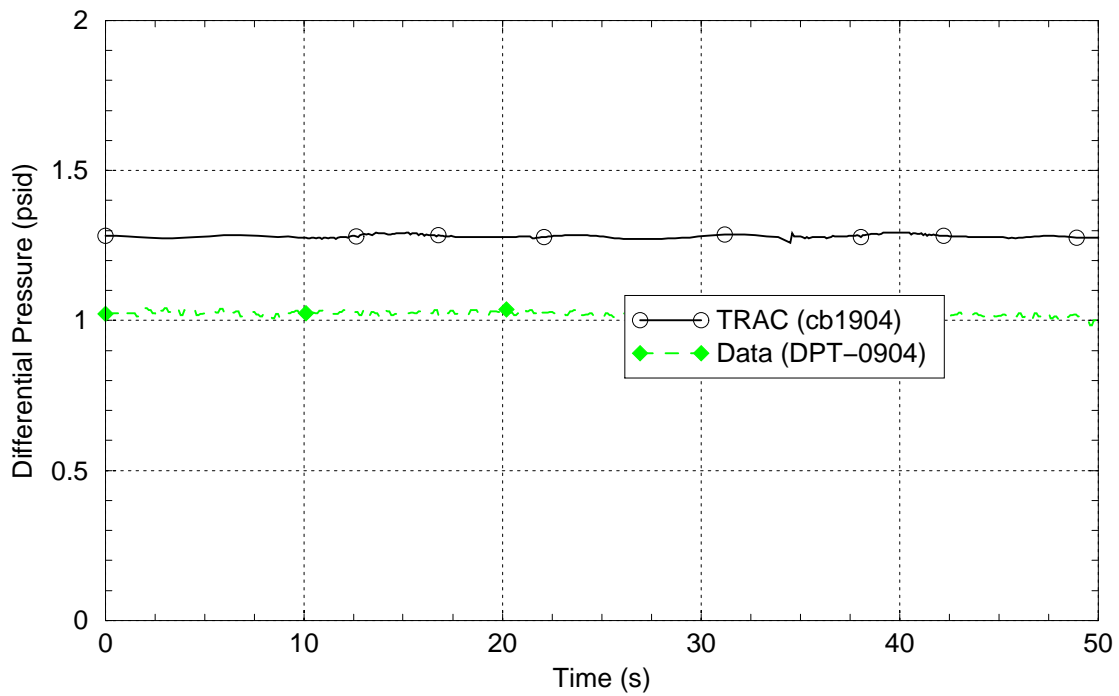


**Figure 3.1-12:** Full Power Pressure Differential between Pressure Taps P09 and P04

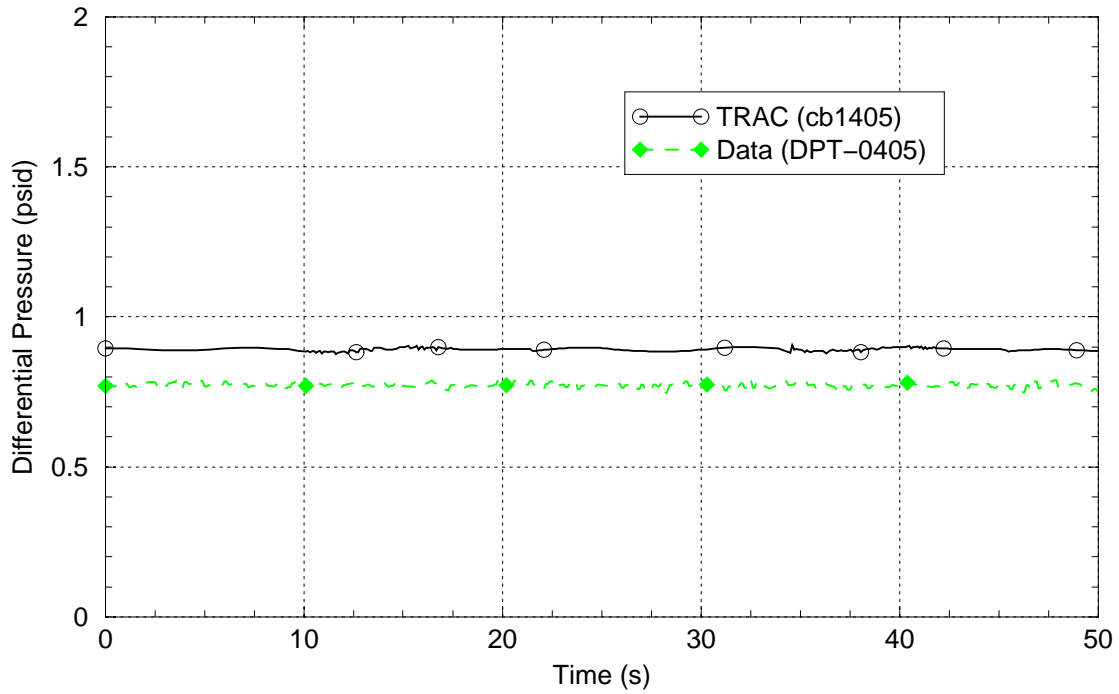


**Figure 3.1-13:** Full Power Pressure Differential between Pressure Taps P04 and P05

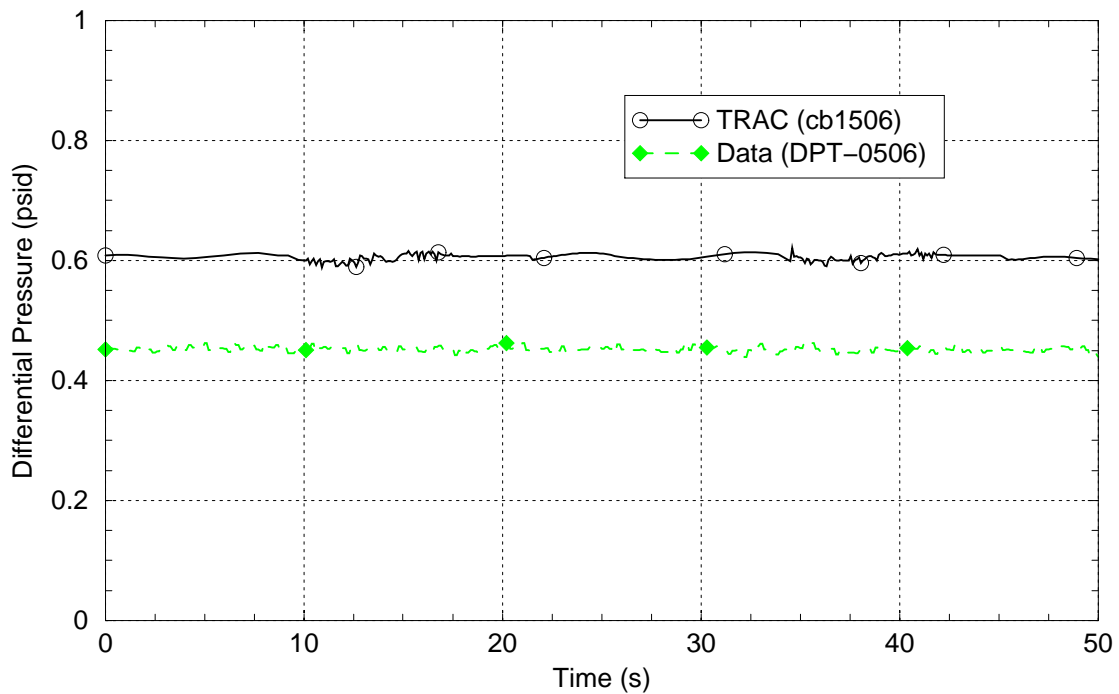


**Figure 3.1-14:** Full Power Pressure Differential between Pressure Taps P05 and P06

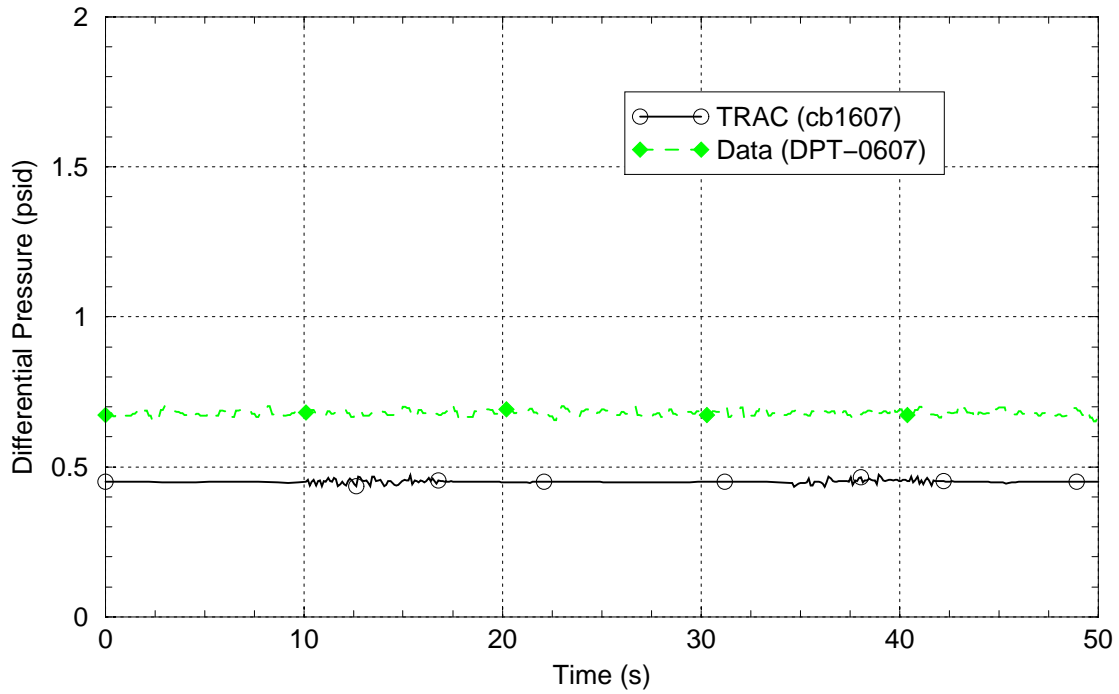


**Figure 3.1-15:** Full Power Pressure Differential between Pressure Taps P06 and P07

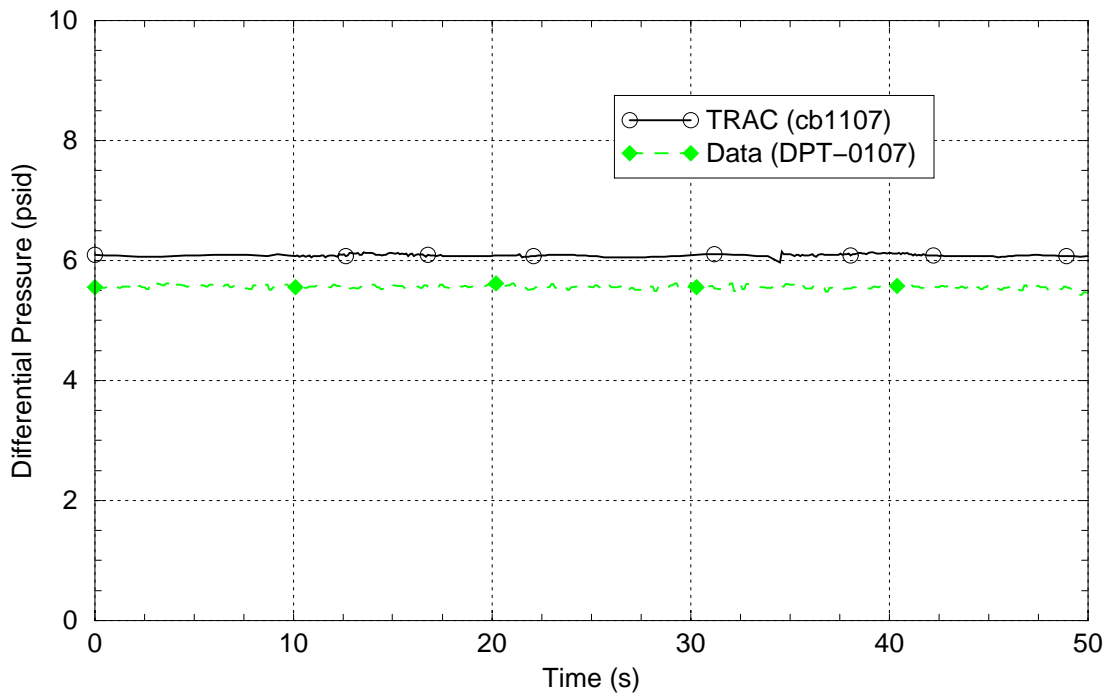


**Figure 3.1-16:** Full Power Pressure Differential between Taps P01 and P07 (total bundle  $\Delta P$ )

## 4.0 Steam Line Break Transients

Steam line break tests were performed to determine the heat transfer and fluid behavior of the steam generator during steam line breaks from hot standby conditions. Two of these tests were used for this assessment, and they are described in more detail in Sections 4.1 and 4.2 below.

### 4.1 Test 2013

Test 2013 is a 100 percent steam line break from hot standby conditions. The test was simulated using a 1.35 inch throat diameter representing the SG flow limiter installed in the 3.0 inch steam line. The initial steady conditions prior to the steam line break are summarized in Table 4.1-1. These conditions were taken from experimental data obtained from the USNRC Data Bank (Reference 5). The boundary conditions were input into the TRAC-M model and the initial temperatures of all nodes were adjusted. Then, a steady state run was made to assure that the model was at the desired initial conditions.

**Table 4.1-1:** *Initial/Boundary Conditions for Steam Line Break Test 2013*

Parameter	Data Channel	Value
Hot leg temperature	T-1150	559.4°F (566.2 K)
Cold leg pressure	P-13	2051.3 psia (14.143 MPa)
Primary mass flow	WF109	91.5 lbm/s (41.5 kg/s)
Feedwater flow	WF299	0.254 lbm/s (0.115 kg/s)
Feedwater pressure	P-299	1595.4 psia (11.0 MPa)
Feedwater temperature	T-299	96.5°F (309.0 K)
Secondary pressure	P-91	1101.0 psia (7.591 MPa)
Break downstream pressure	PT-215	14.4 psia (0.0993 MPa)

The break valve was added to the TRAC-M model as VALVE component 238 along with a BREAK component (see Figure 3.0-1). Since the flow out of the break will be initially choked, choking was turned on at the break valve. In the test facility, the break does not go to the atmosphere, but rather to a series of piping/separators to allow measurement of flow. Therefore, the downstream pressure in the BREAK component was set to follow the downstream pressure in the experiment.

For test 2013, the system was held in a steady manner for 60 seconds at which point the break valve was opened. Figures 4.1-1 through 4.1-4 show the primary system response. The calculated primary side pressure (cold leg), temperature (hot leg), and mass flow rates were specified as boundary conditions and agree with the measured values as expected. Note that while the experimental hot leg temperature varies slightly, it was set at a constant value in the TRAC-M model for the entire transient.



Temperatures throughout the U-tubes are computed by TRAC-M and are in good agreement with the experimental data. Figure 4.1-3 shows the temperature distribution throughout the U-tubes at 100 seconds (around the time when the difference between the hot and cold leg temperature is at its maximum). Figure 4.1-4 shows the primary mass flow which was set as a boundary condition. Note that the data was very "noisy" and the input to TRAC-M used a smoothed fit of this data.

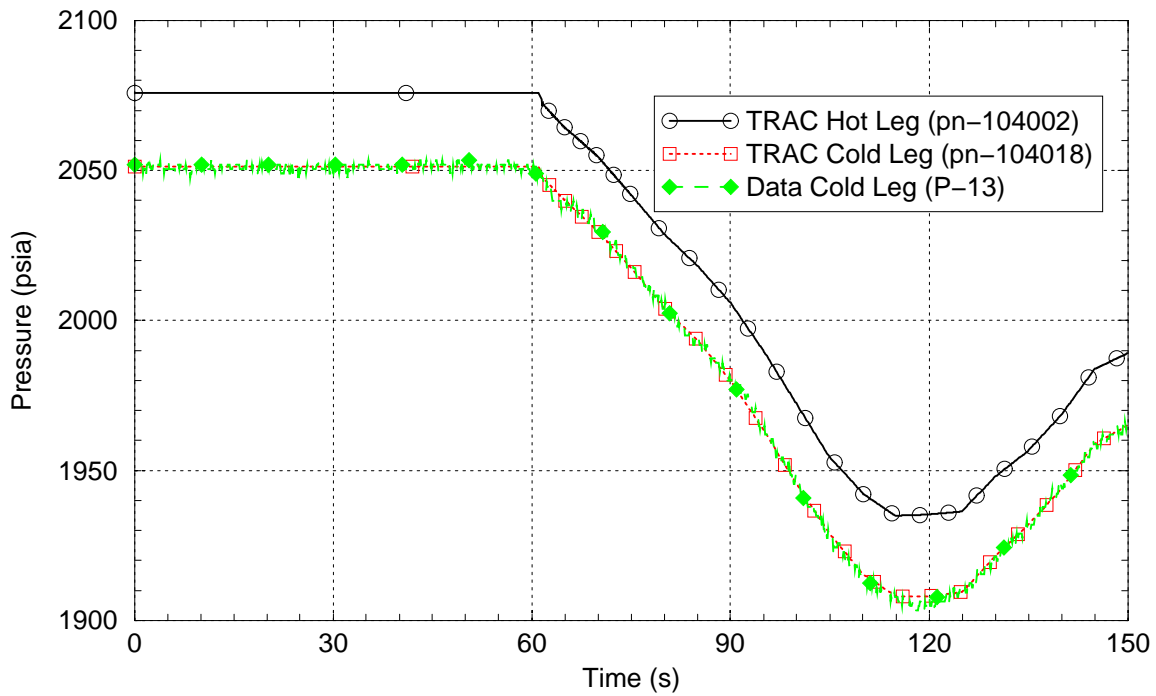


**Figure 4.1-1:** *Test 2013 Primary Side Pressures*

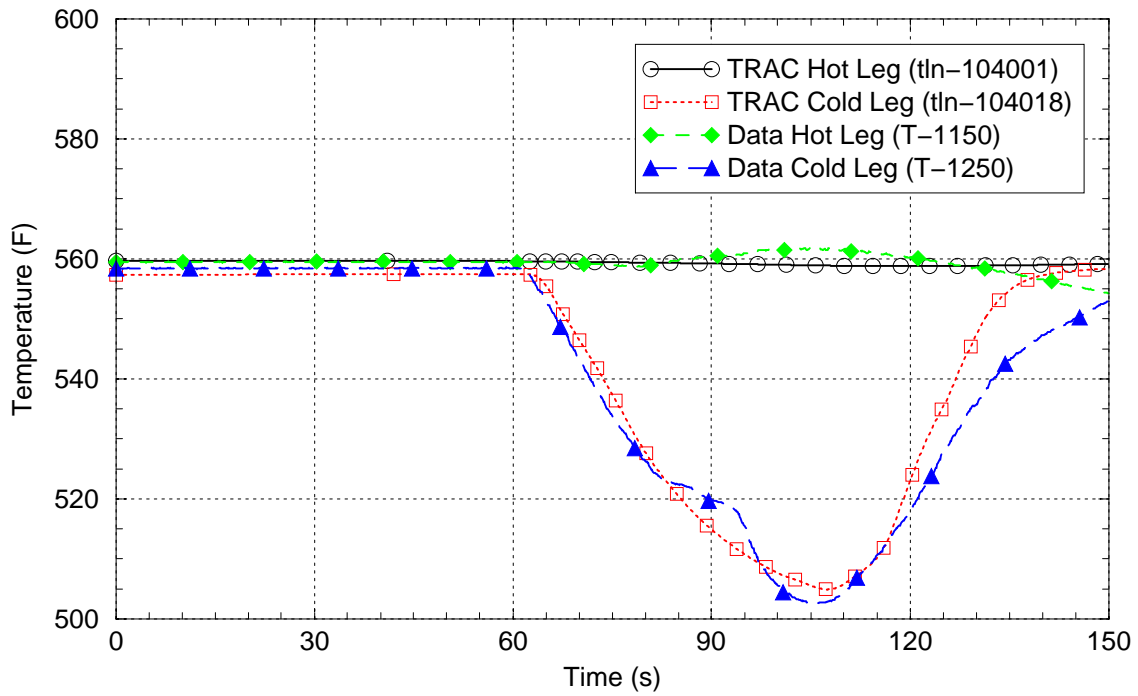


**Figure 4.1-2:** Test 2013 Primary Side Temperatures

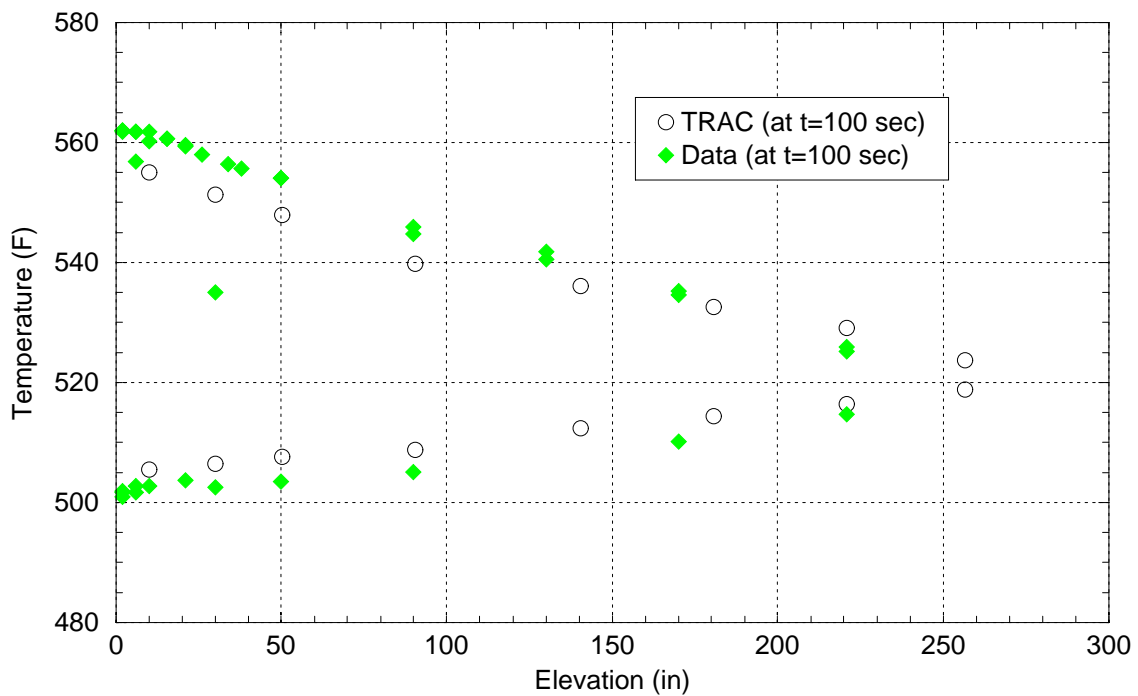


**Figure 4.1-3:** Test 2013 Primary Temperature in U-tubes at 100 seconds

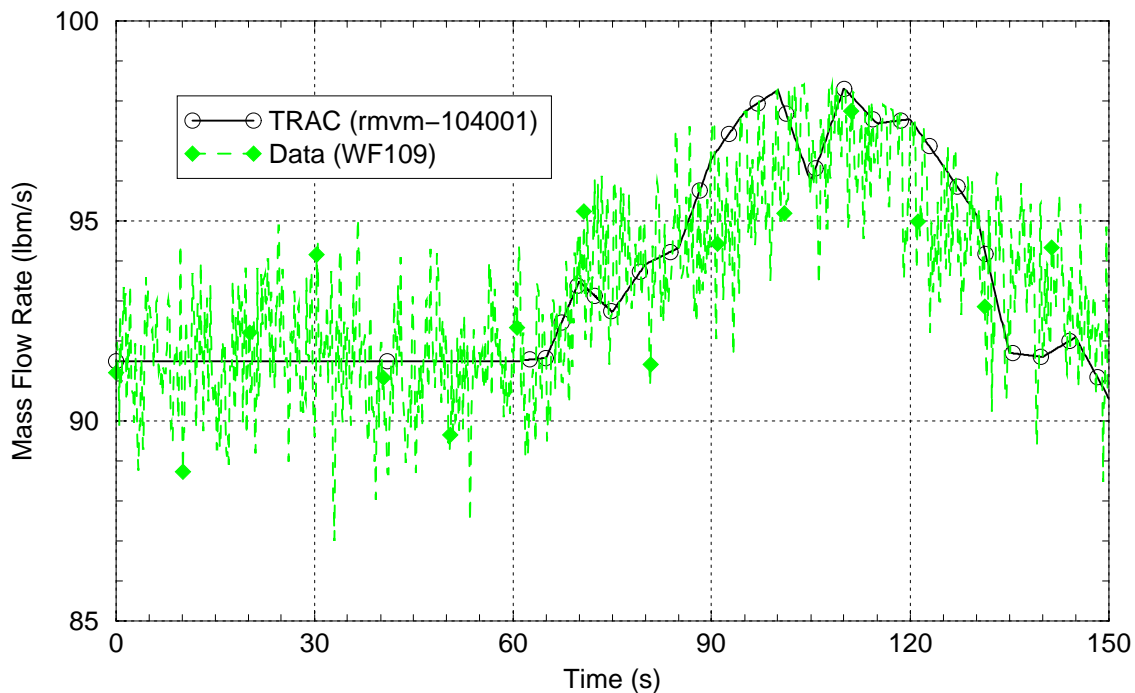


**Figure 4.1-4:** *Test 2013 Primary Side Mass Flow*

Figures 4.1-5 through 4.1-18 show the secondary side response to steam line break test 2013. The secondary side pressure is in very good agreement up to 90 seconds as seen in Figure 4.1-5.

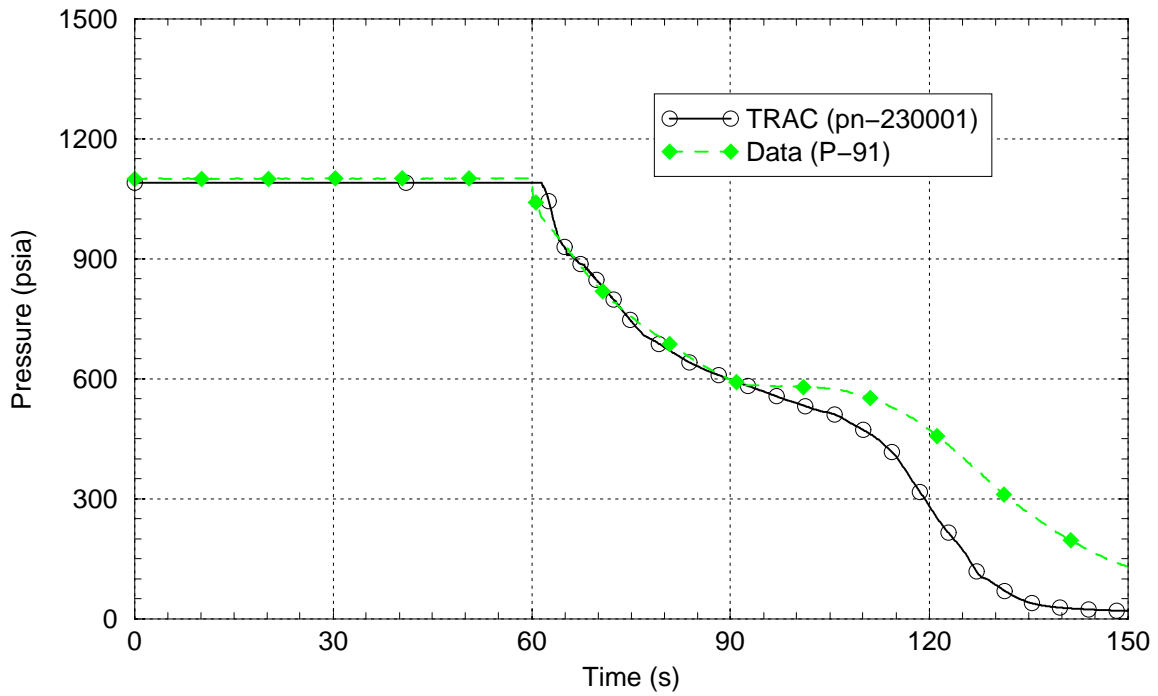
The break flow is measured in the test with data channel WF216, which is believed to be only the steam portion of the break flow. Both the TRAC-M vapor break flow (rvmf-238001) and total break flow (rmvm-238001) rates are shown in Figure 4.1-6. The calculated break steam flow rate agrees very well with the test data (Figure 4.1-6). The test data does not include similar transient response data for the break liquid flow rate. However, a rudimentary comparison of calculated and measured total break flow rate can be made. Catch tank data for the test indicates that 410 lbm of liquid exited the break during the first 30 seconds after the break opened (Reference 2, page 9-38), for an implied average liquid break flow rate of 13.7 lbm/s over that period. If one adds this average liquid flow rate to the approximately 13 lbm/s break steam flow rate during the period, the implied total break flow rate in the test data is about 26.7 lbm/s over the first 30 seconds. A comparison of this average total break flow rate against the calculated break flow rate in Figure 4.1-6 indicates a relatively good agreement between the total average calculated and measured break flow rates. Therefore, the calculated and measured liquid break flow rates appear to be in fair agreement.

Figure 4.1-7 shows the feedwater flow rate (which was set as a boundary condition). Reference 2 states that feedwater flow was terminated at 70 seconds, however, the experimental data (channel WF299) shows some small flow from 70 to 150 seconds. This small flow was used in the TRAC-M model.

The calculated and measured downcomer water level responses are compared in Figure 4.1-8. When the break opens, the test data shows a very rapid level spike to a high value. The calculated data also displays an increase during this period, but the peak level is much lower than seen in the data. The conclusion is that when the break opens in the test liquid is drawn much higher upward into the downcomer than seen in the calculation. Liquid drawn upward in this way can easily find its way to the break in a manner which circumvents the separation processes.

The effects of this early downcomer behavior difference are seen in the boiler-side differential pressure comparisons in Figures 4.1-10, -11, -13, -14, -15 and -17. In the test, when the break opens water flows downward in the boiler and upward into the downcomer. This is evidenced by the early decline in the differential pressures in the test data. In the calculation, the reversal of flow from the boiler into the downcomer is not seen and as a result the differential pressures decline only moderately. The calculated response of the differential pressure from P01 to P02 at the bottom of the boiler (Figure 4.1-10) clearly shows that when the break opens the flow is upward (i.e., not backward into the downcomer) over the first 30 seconds after the break. The differential pressure increases when the liquid flows upward because of the friction drop created by the upward flow through the restriction at that location. The calculated differential pressure responses therefore portray a situation where flow is always upward in the boiler and the slow decay of the differential pressures simply represents a downward progression of the voiding process. On the other hand, the measured differential pressure responses portray a process where water is first drawn upward into the downcomer. Later, at about 90 seconds, the column of water in the downcomer can no longer be supported by the upward flow to the break. At that time the water level in the downcomer falls (Figure 4.1-8) and the measured boiler differential pressures rise as that water re-enters the boiler.

Figure 4.1-9 shows the lower downcomer temperatures. After 110 seconds, the TRAC-M calculated lower downcomer temperature begins to drop significantly lower than the experimental data. This drop is due to the TRAC-M calculated lower secondary side pressure.



**Figure 4.1-5:** *Test 2013 Secondary Side Pressure*

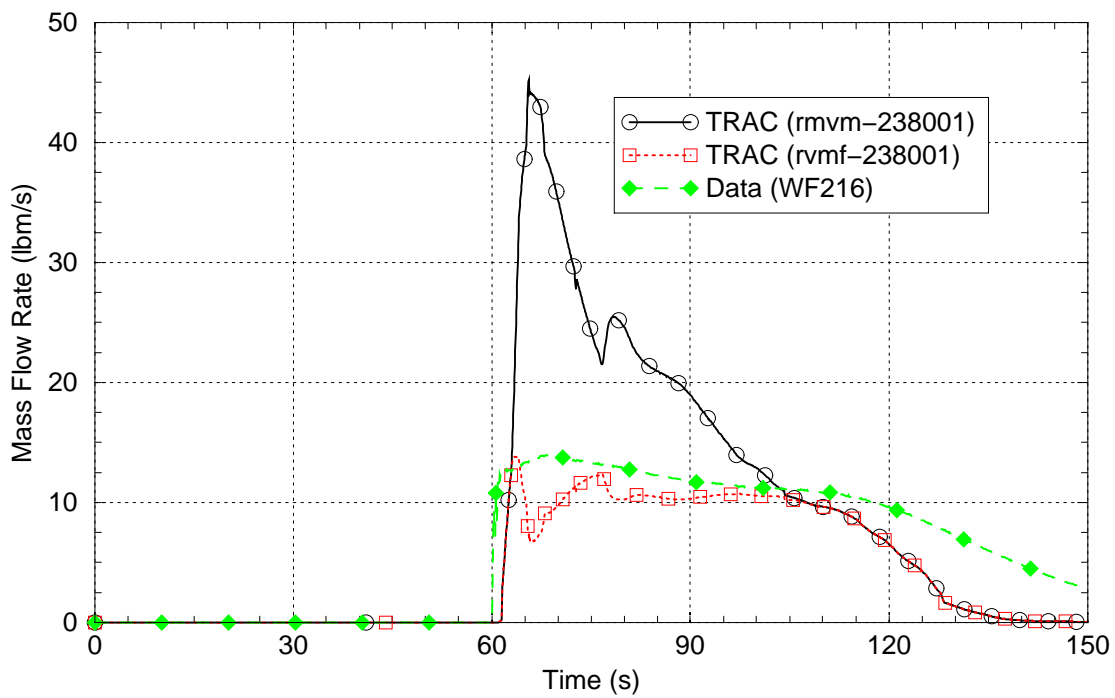


**Figure 4.1-6:** *Test 2013 Break Flow*

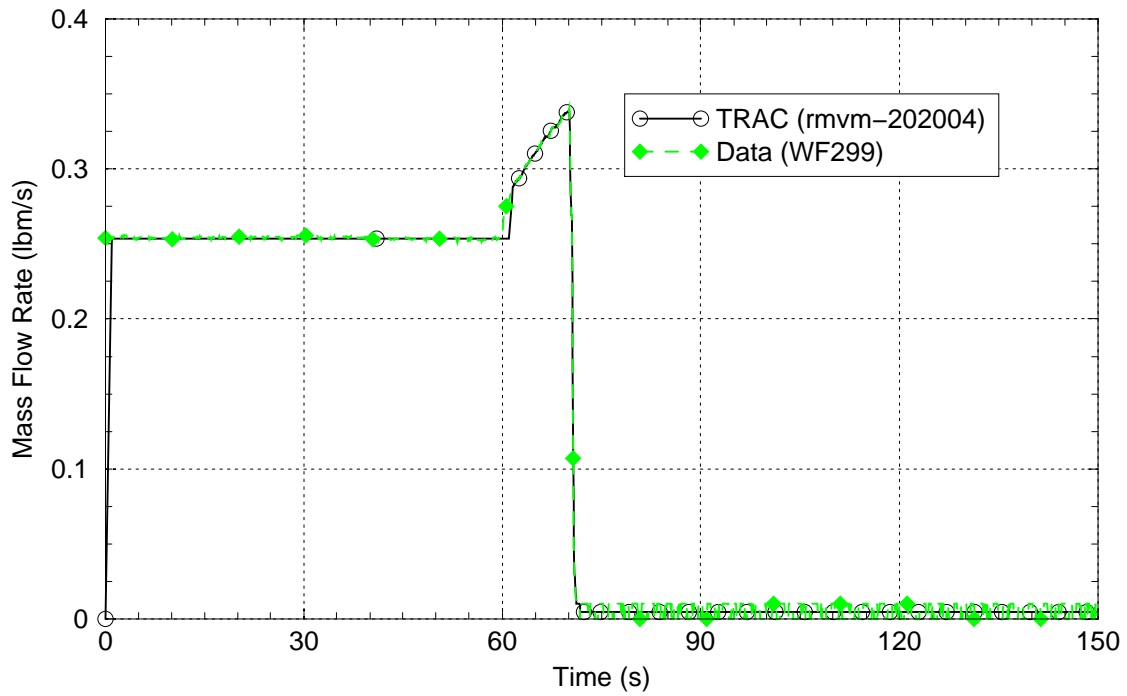


**Figure 4.1-7:** *Test 2013 Feedwater Flow*

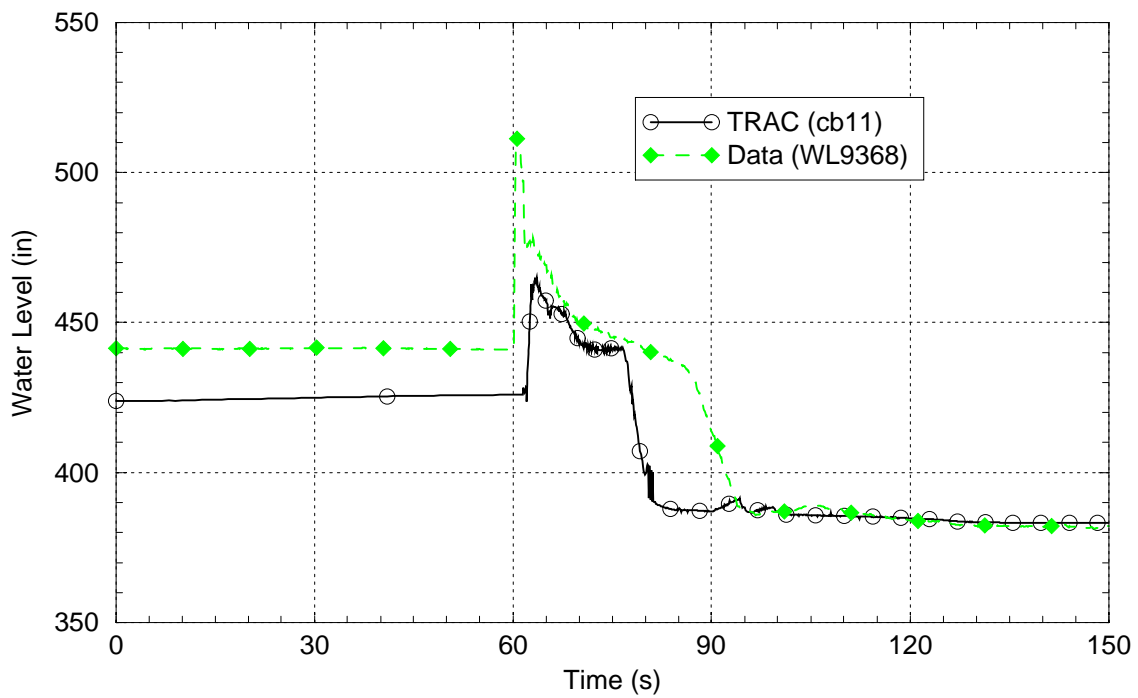


**Figure 4.1-8:** *Test 2013 Narrow Range Water Level*

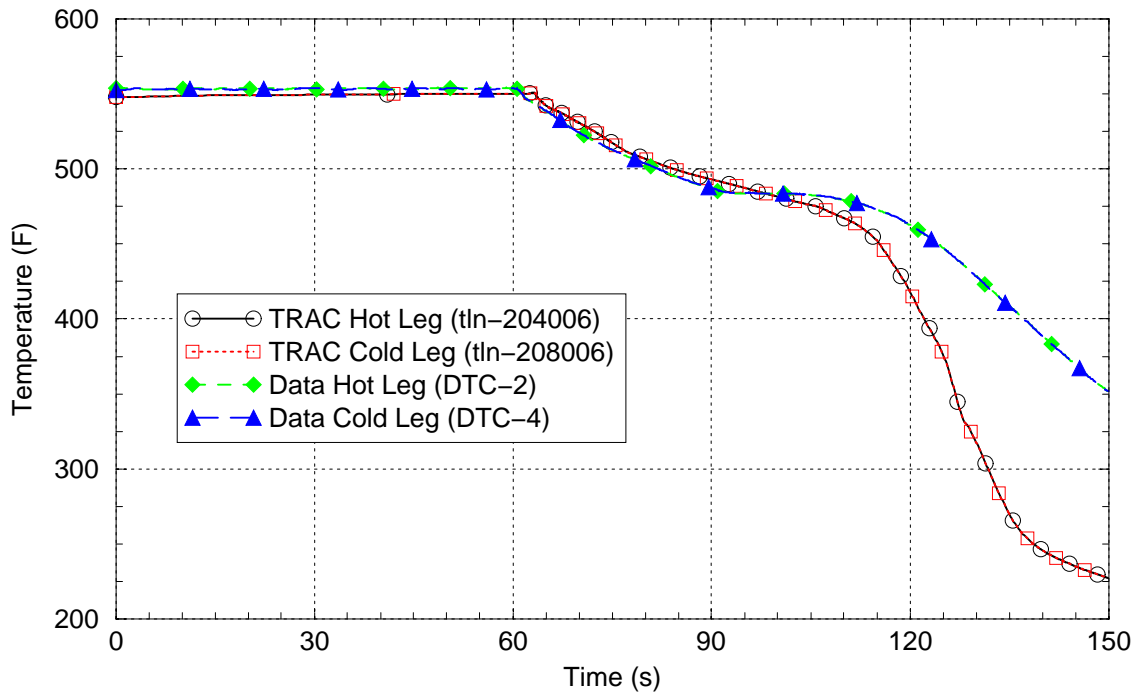


**Figure 4.1-9:** *Test 2013 Lower Downcomer Temperature*

Figures 4.1-10 through 4.1-18 show differential pressure comparisons in the secondary side tube region. Note that not all data channels are available in every test (i.e., data channel DPT-0308 is not available in test 2013).

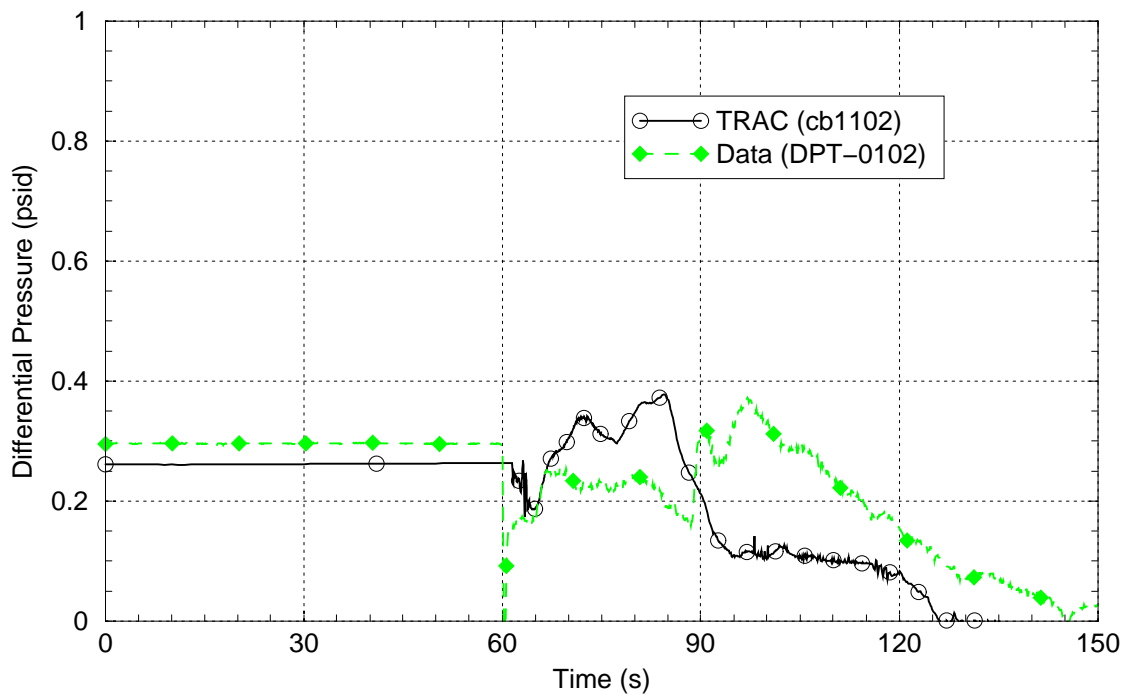


**Figure 4.1-10:** *Test 2013 Pressure differential between pressure taps P01 and P02*

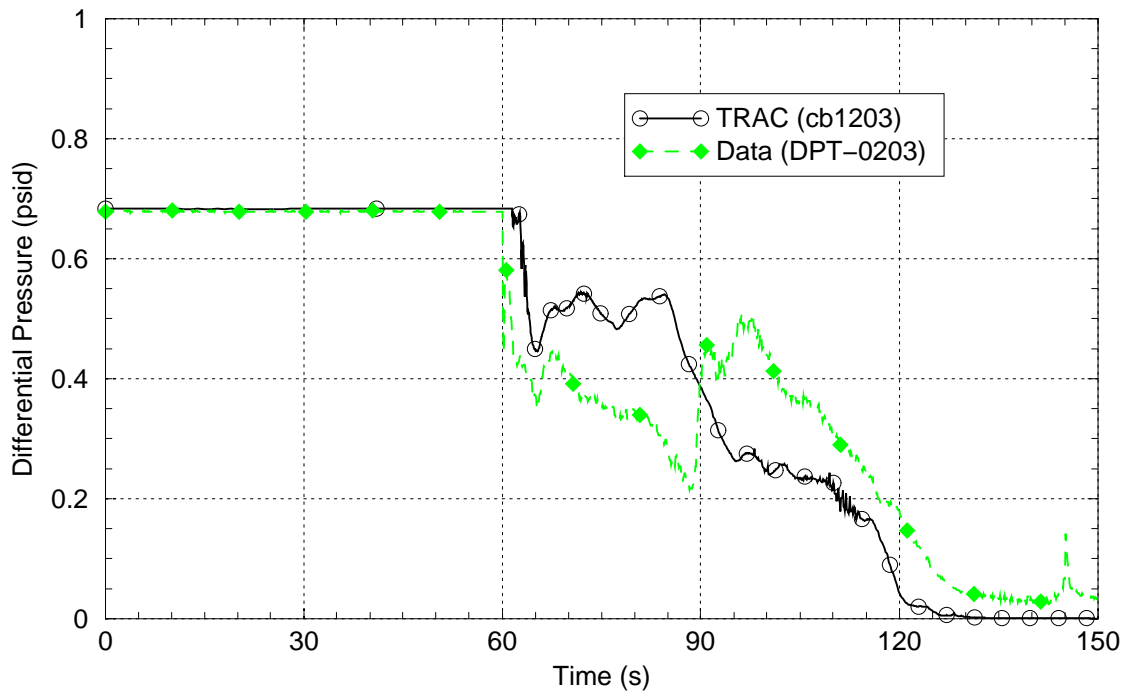


**Figure 4.1-11:** Test 2013 Pressure differential between pressure taps P02 and P03

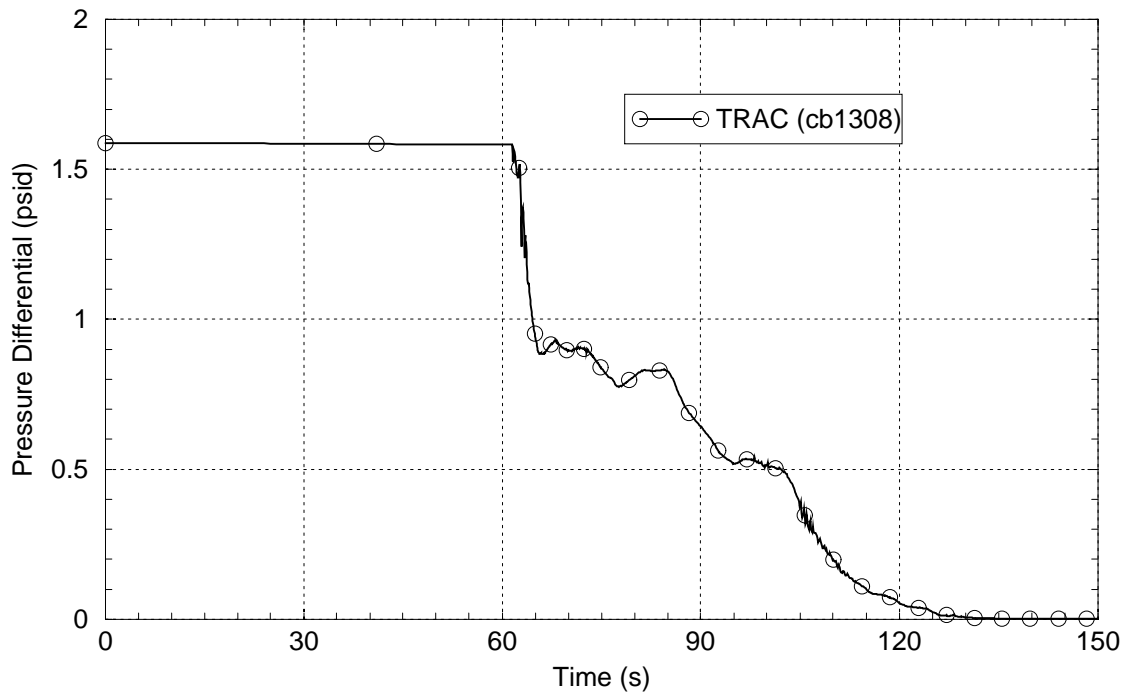


**Figure 4.1-12:** Test 2013 Pressure differential between pressure taps P03 and P08



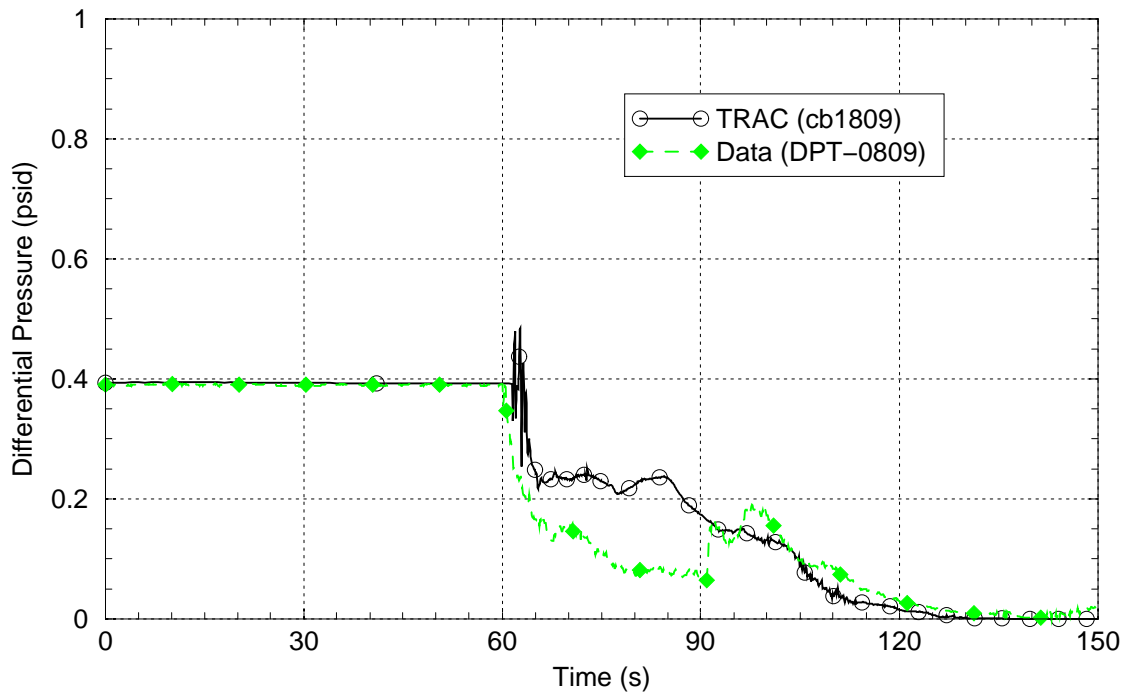


**Figure 4.1-13:** Test 2013 Pressure differential between pressure taps P08 and P09

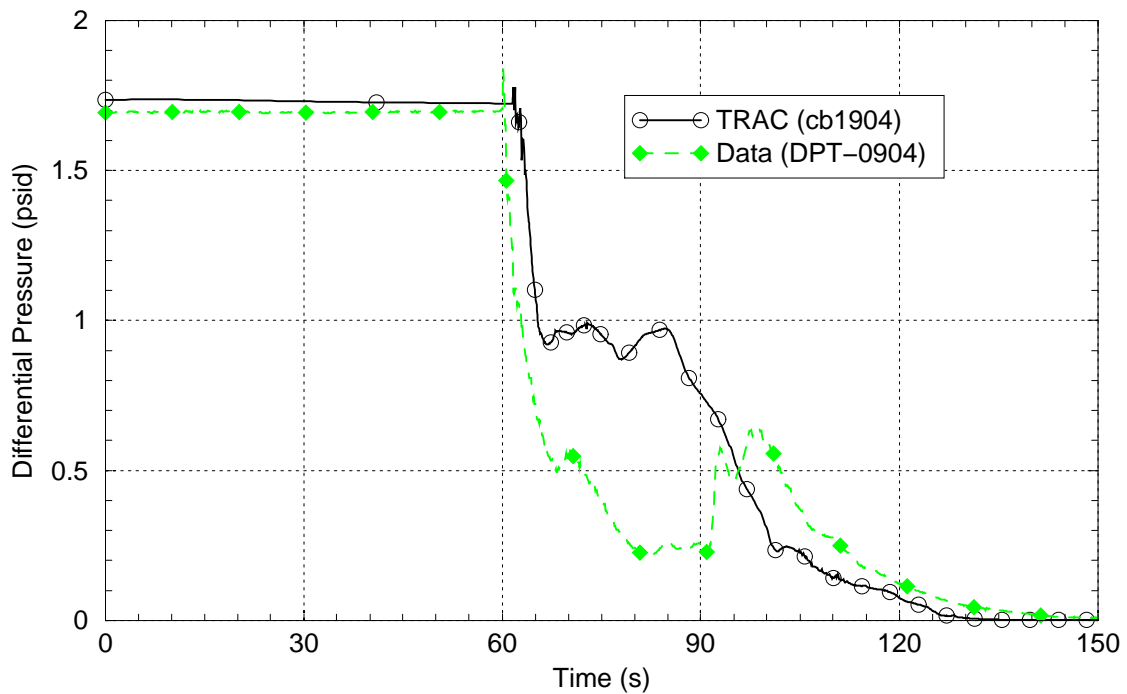


**Figure 4.1-14:** Test 2013 Pressure differential between pressure taps P09 and P04

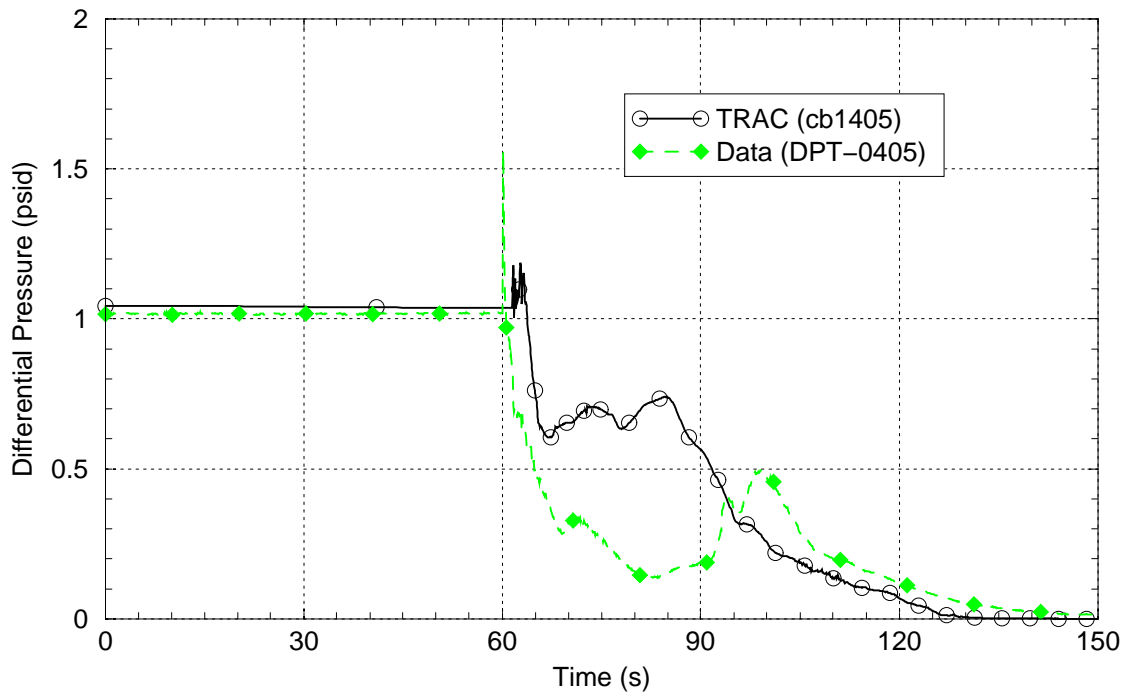


**Figure 4.1-15:** Test 2013 Pressure differential between pressure taps P04 and P05

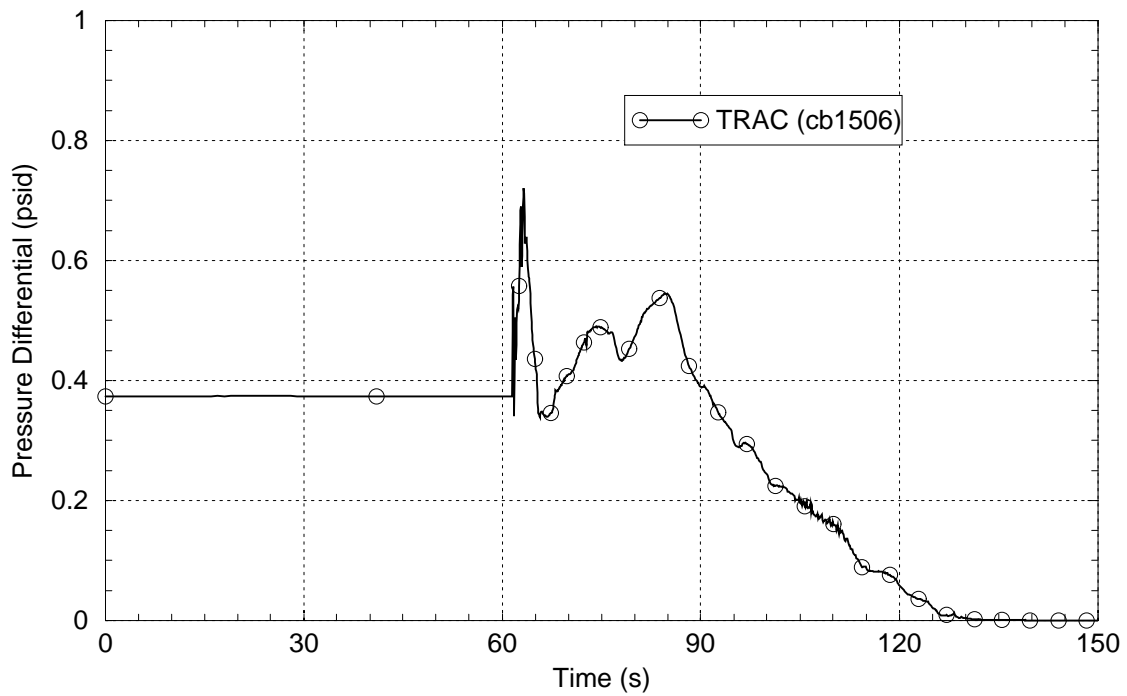


**Figure 4.1-16:** Test 2013 Pressure differential between pressure taps P05 and P06

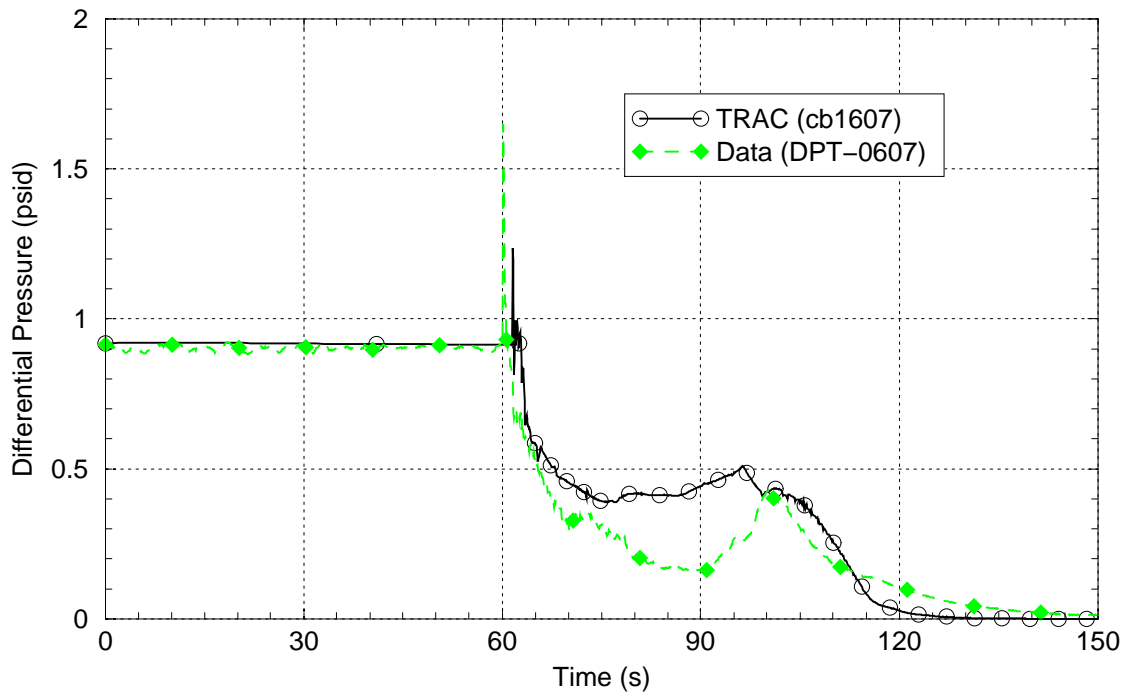


**Figure 4.1-17:** Test 2013 Pressure differential between pressure taps P06 and P07

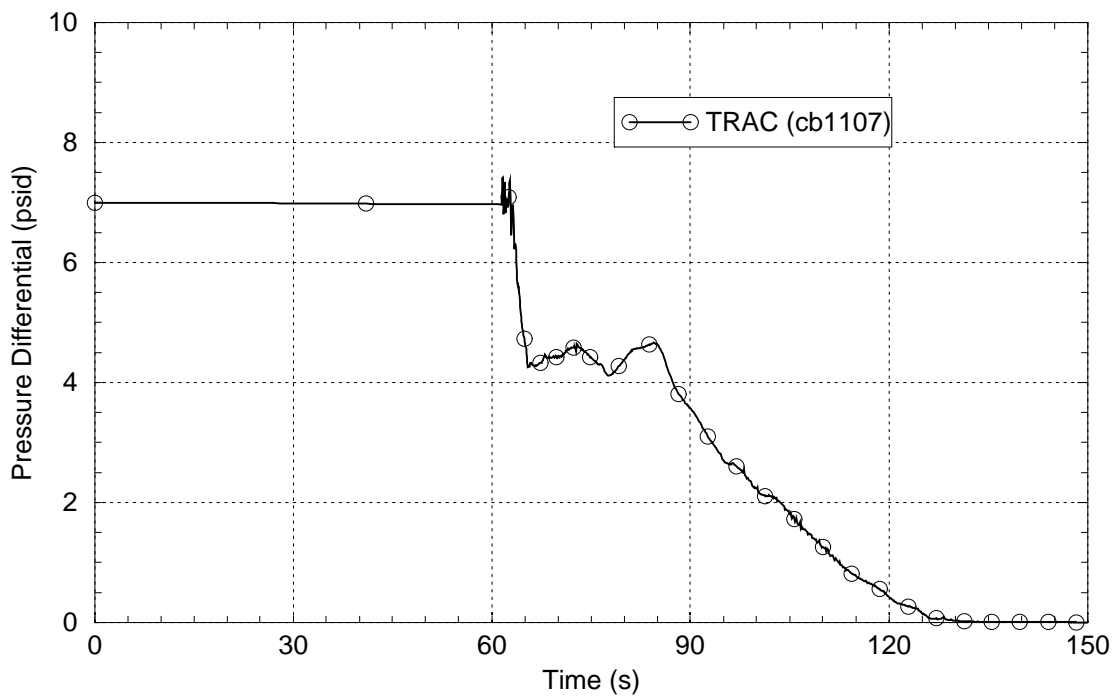


**Figure 4.1-18:** Test 2013 Pressure differential between pressure taps P01 and P07

Figures 4.1-19 through 4.1-22 show the TRAC calculated pressure drop across the tube support plates and flow distribution baffle. There is no experimental data to compare these values with, so they are shown for informational purposes only.

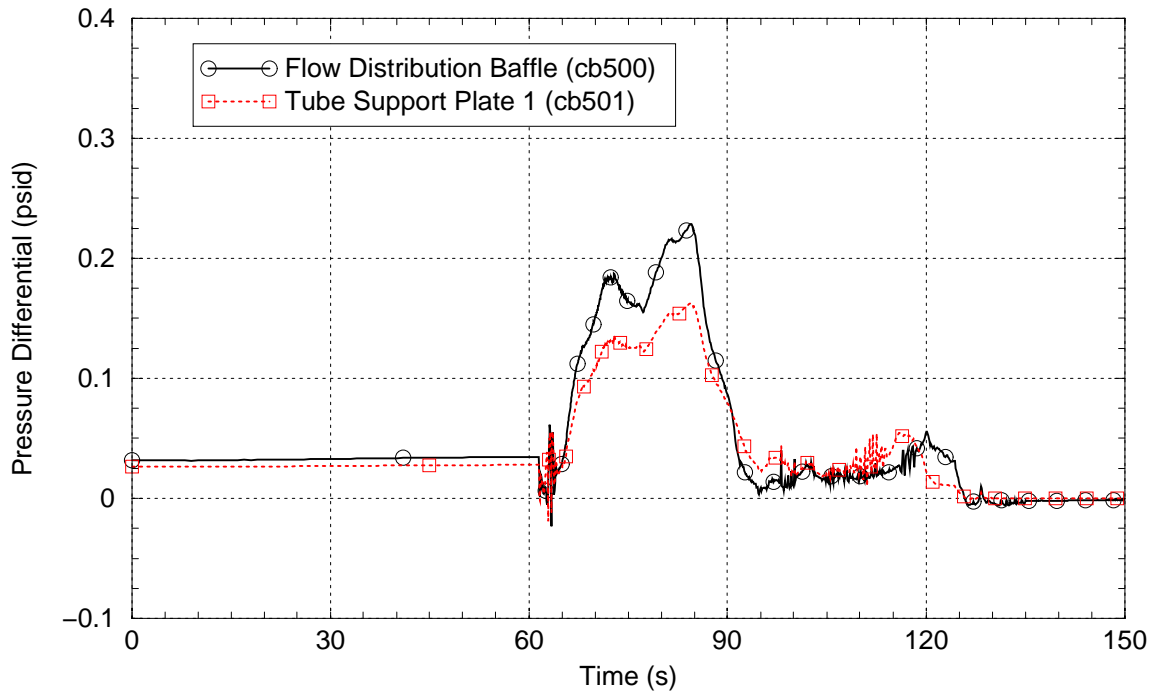


**Figure 4.1-19:** Test 2013 Pressure Drop Across the Tube Support Plates

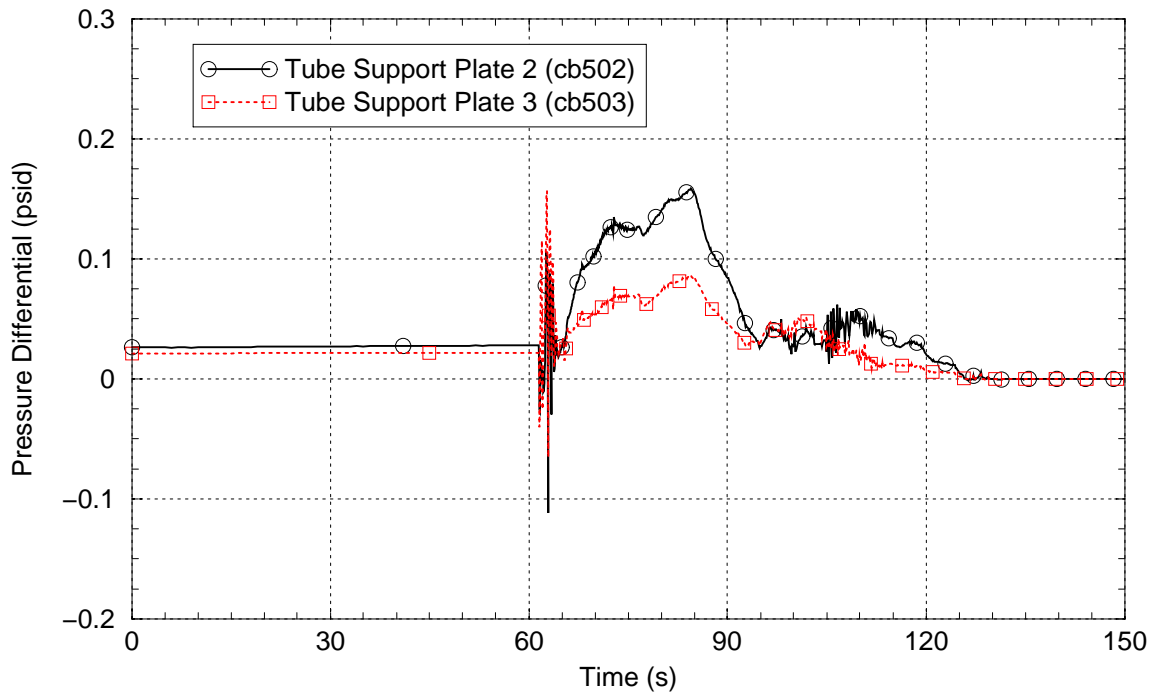


**Figure 4.1-20:** Test 2013 Pressure Drop Across the Tube Support Plates

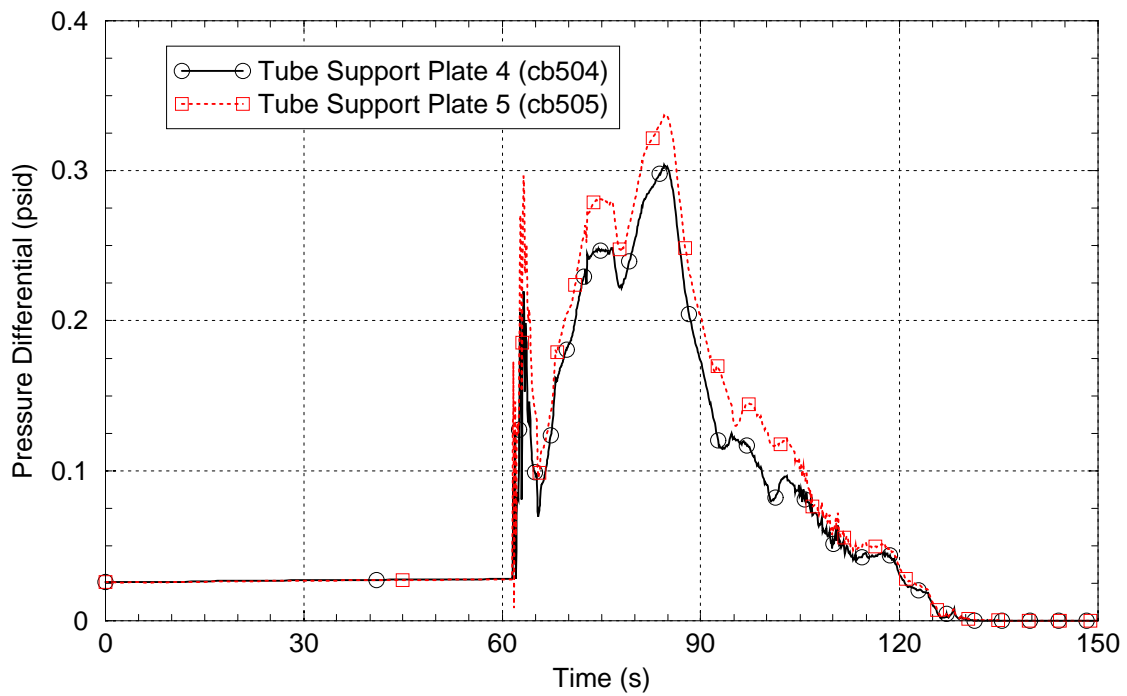


**Figure 4.1-21:** *Test 2013 Pressure Drop Across the Tube Support Plates*

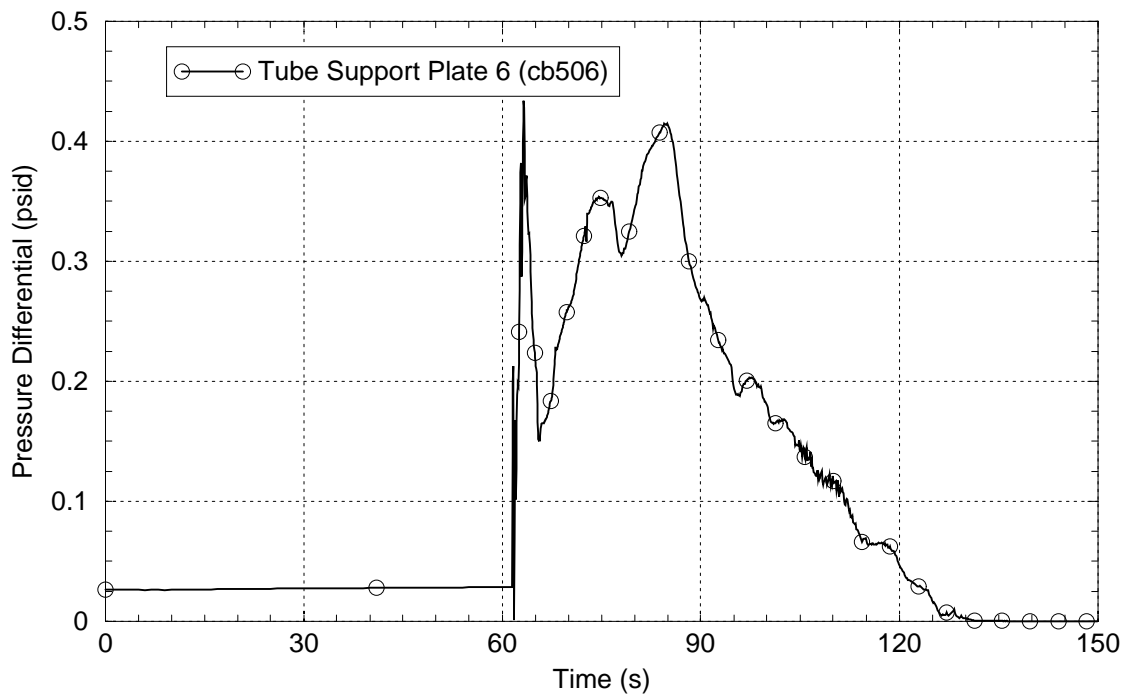


**Figure 4.1-22:** *Test 2013 Pressure Drop Across the Tube Support Plates*

The conclusion is that the calculated differential pressures well represent the processes observed in the calculation, but that the reversal of flow and rise in downcomer level seen in the test are not present in the calculation. A possible explanation for this discrepancy is that the model does not adequately represent the relative flow losses through the separator and downcomer paths to the steam dome (i.e., the model may have too little loss in the separator region or too much loss in the downcomer region). Additional evaluation and model improvement in this regard was beyond the scope of this task.

## 4.2 Test 2029

Test 2029 is an 8 percent steam line break with a steam generator tube rupture from approximately 4% power. This test was simulated using a 0.386 inch diameter sharp-edge orifice installed at the MB-2 steam exit nozzle. The initial steady conditions prior to the break are summarized in Table 4.2-1. These conditions were taken from experimental data obtained from the USNRC Data Bank (Reference 5).

**Table 4.2-1: Initial/Boundary Conditions for Steam Line Break Test 2029**

Parameter	Data Channel	Value
Hot leg temperature	T-1150	580.4°F (577.8 K)
Cold leg pressure	P-13	1845.0 psia (12.72 MPa)
Primary mass flow	WF109	5.29 lbm/s (2.4 kg/s)
Feedwater flow	WF299	0.316 lbm/s (0.1435 kg/s)
Feedwater pressure	P-299	1595.4 psia (11.0 MPa)
Feedwater temperature	T-299	106.1°F (314.3 K)
Secondary pressure	P-91	1002.0 psia (6.908 MPa)

The steam line break is simulated as in test 2013 with the flow area and hydraulic diameter changed to the appropriate values. The steam generator tube rupture is simulated in the experimental facility by adding a pipe to the hot leg of the primary loop. This pipe allows water to be passed to the secondary side inside the wrapper box. The SGTR break element penetrated both the lower shell and the wrapper box at an elevation of 282 inches, which is approximately 5.5 inches above the top of the tube bundle. This was simulated in TRAC-M with a FILL component connected to the secondary side. Flow parameters were obtained from experimental data channels as follows; mass flow (WF150), temperature (T-1150) and pressure (P-13).

For test 2029, the system was held in a steady manner for 60 seconds at which point the break valve was opened and the steam generator tube rupture flow was started. Figures 4.2-1 through 4.2-4 show the primary system response. The calculated primary

side pressure (cold leg), temperature (hot leg), and mass flow rates were specified as boundary conditions and agree with experimental data as expected. The cold leg temperature matches very well until 700 seconds at which point, the data levels off while TRAC-M continues the cooldown. Figure 4.2-3 shows the temperature distribution throughout the U-tubes at 500 seconds (an arbitrary point in time where the temperature difference between the hot and cold legs is a maximum).

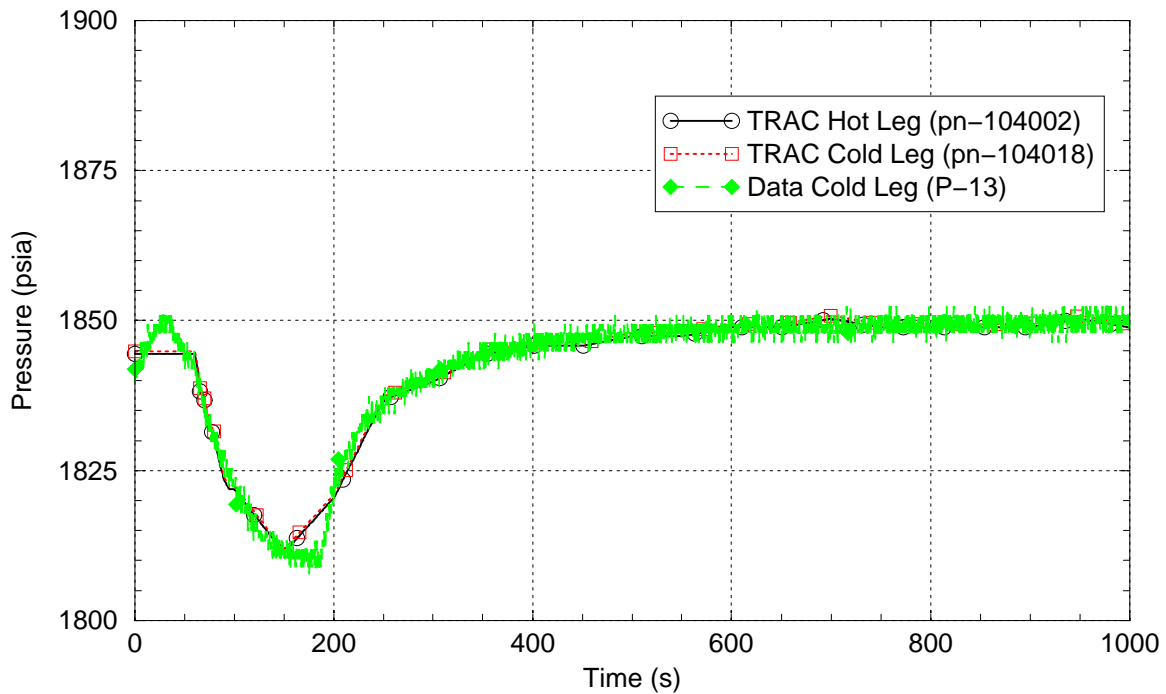


**Figure 4.2-1:** *Test 2029 Primary Side Pressures*

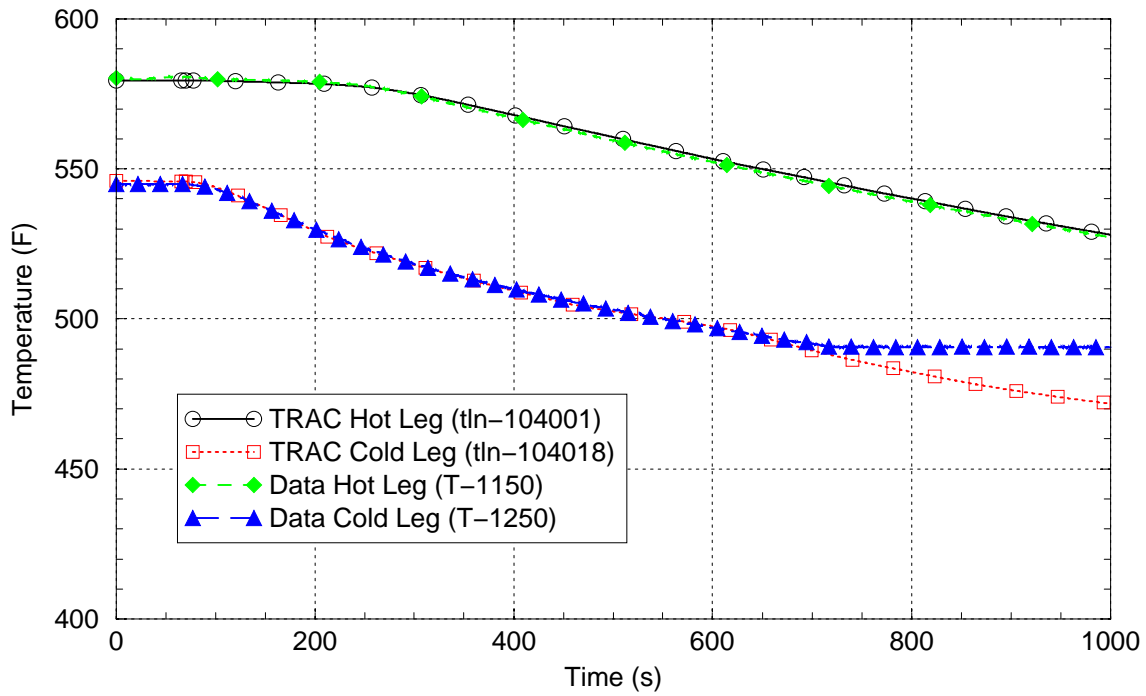


**Figure 4.2-2:** Test 2029 Primary Side Temperatures

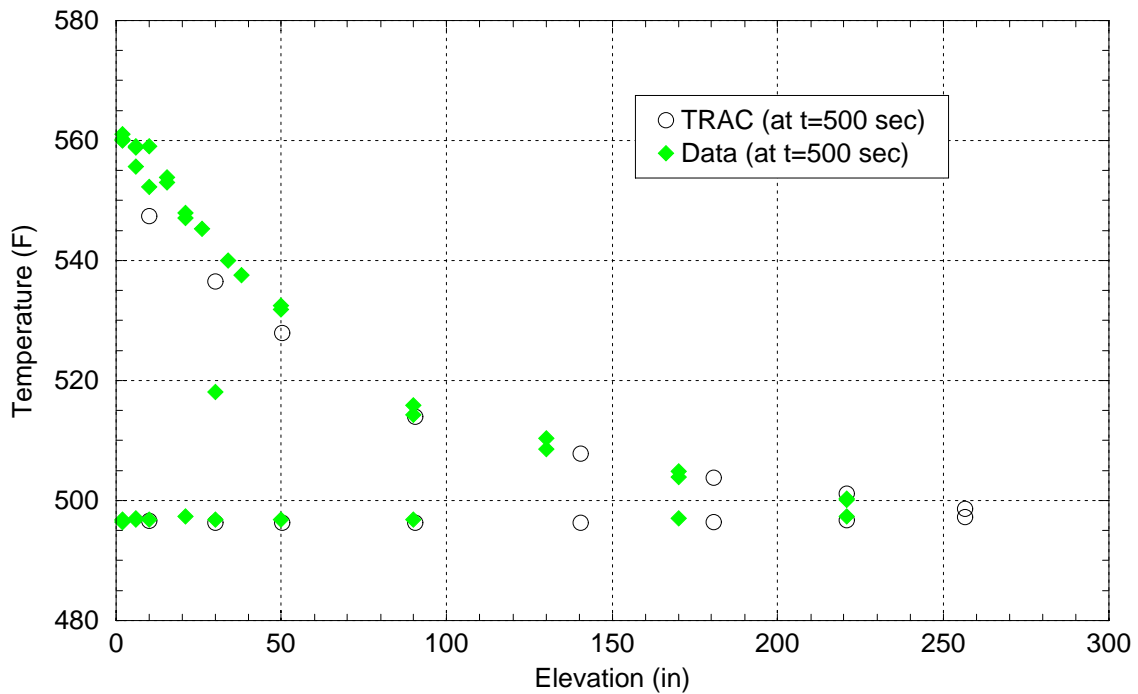


**Figure 4.2-3:** Test 2029 Primary Temperature in U-tubes at 500 seconds



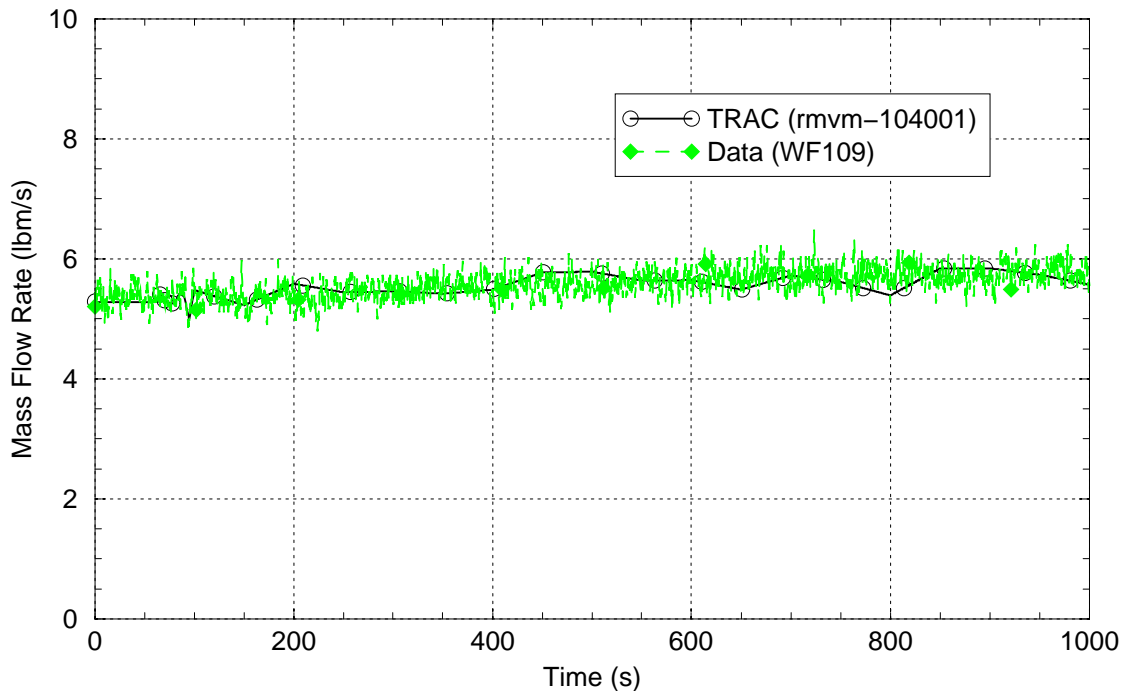


**Figure 4.2-4:** *Test 2029 Primary Side Mass Flow*

Figures 4.2-5 through 4.1-19 show the secondary side response for test 2029. The secondary side pressure (Figure 4.2-5) is predicted very well by TRAC-M. As with test 2013, the break flow measurement in the experiment (WF216) is believed to be just the steam flow. The break flow comparison in Figure 4.2-6 shows more break flow in the TRAC-M calculation. Figure 4.2-7 shows the steam generator tube rupture flow. This was set as a boundary condition in the calculation, and agrees with experimental data as expected. Figure 4.2-8 shows the feedwater flow rate (which was set as a boundary condition). Reference 2 states that feedwater flow was terminated at 60 seconds, however, the experimental data (channel WF299) shows some small flow from 60 to 1,000 seconds. This small flow was used in the TRAC-M model. Figure 4.2-9 shows the narrow range water level. In this experiment, the TRAC-M calculated water level is higher than the experimental data and does not swell as much as the experiment after the break is opened. Since a fixed value of feedwater is used (for the initial 60 seconds), the system model determines the water level. As noted in Section 3, a control system could be used to adjust the water level to the desired value; however, the feedwater flow may no longer match the experimental data. The water level in the experimental data drops faster than the TRAC-M calculation, and levels off at a lower value than TRAC-M. Figure 4.2-10 shows the lower downcomer temperatures which are in good agreement.

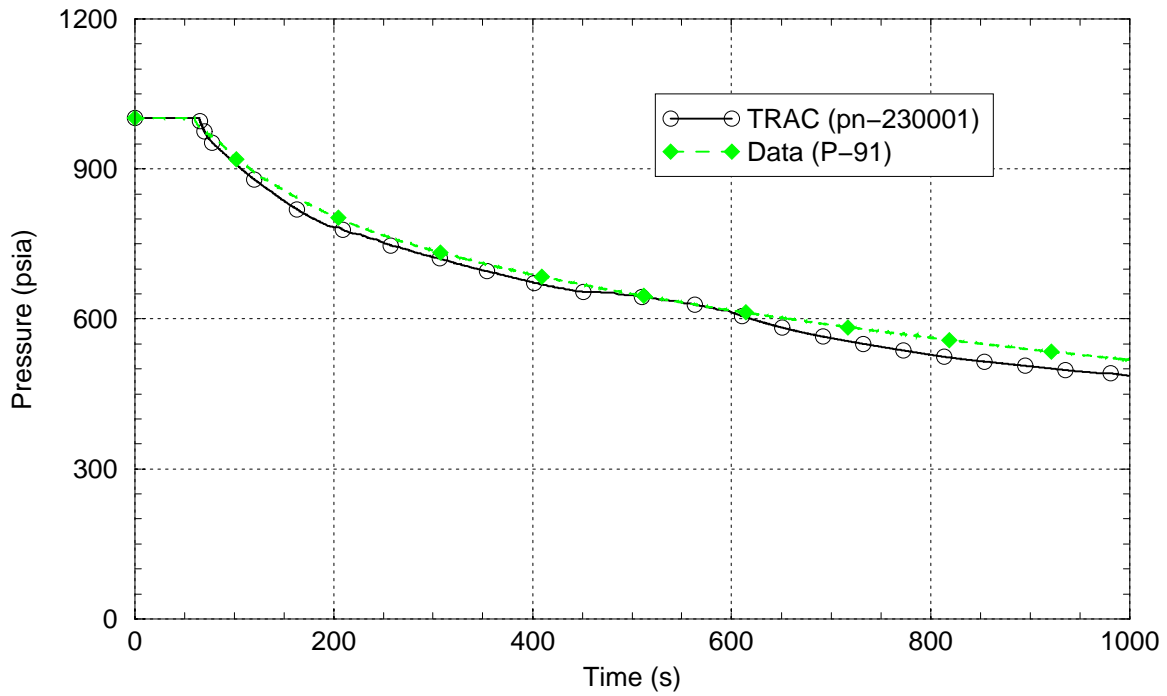


**Figure 4.2-5:** *Test 2029 Secondary Side Pressure*

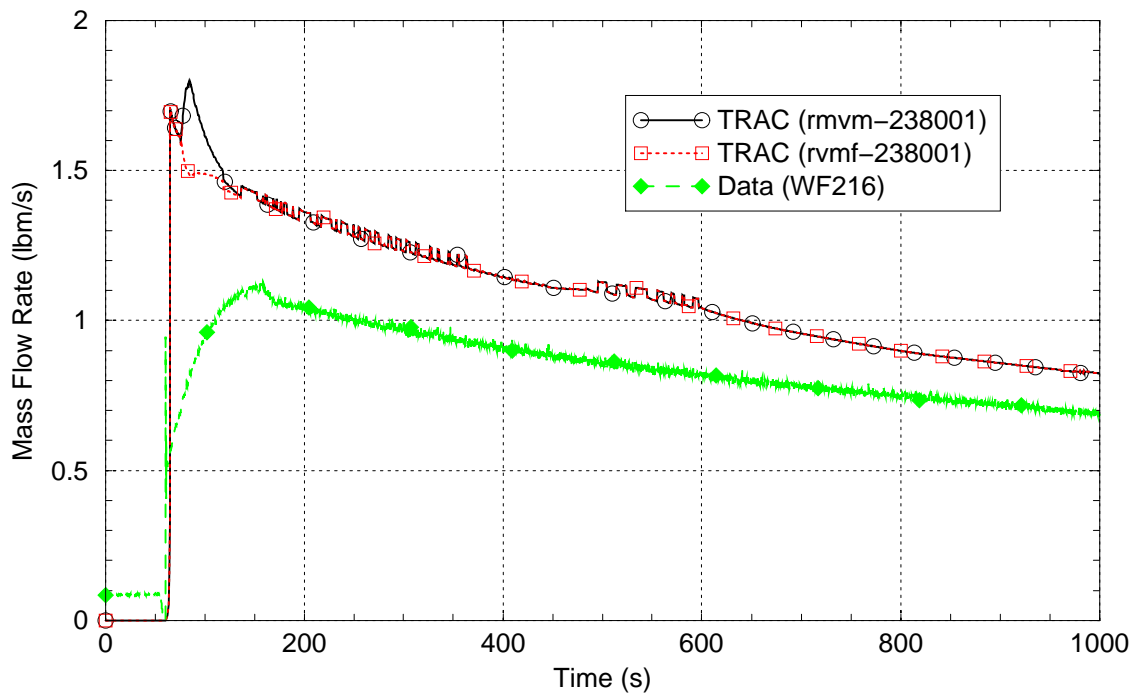


**Figure 4.2-6:** *Test 2029 Steam Line Break Flow*

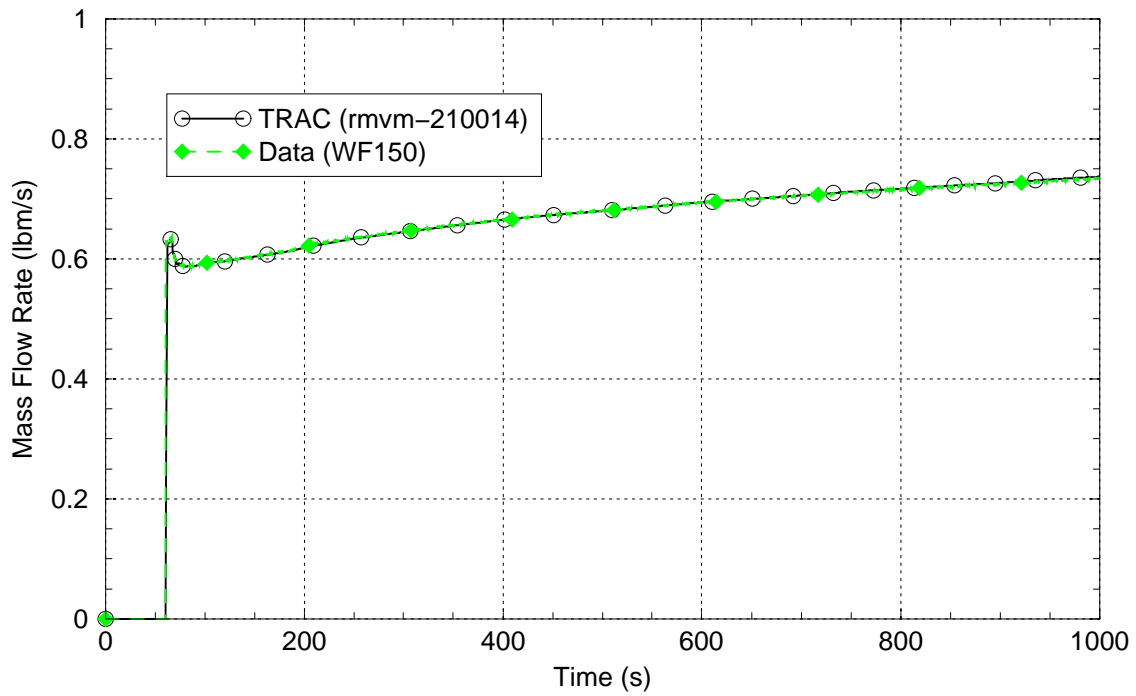


**Figure 4.2-7:** *Test 2029 Steam Generator Tube Rupture Flow*

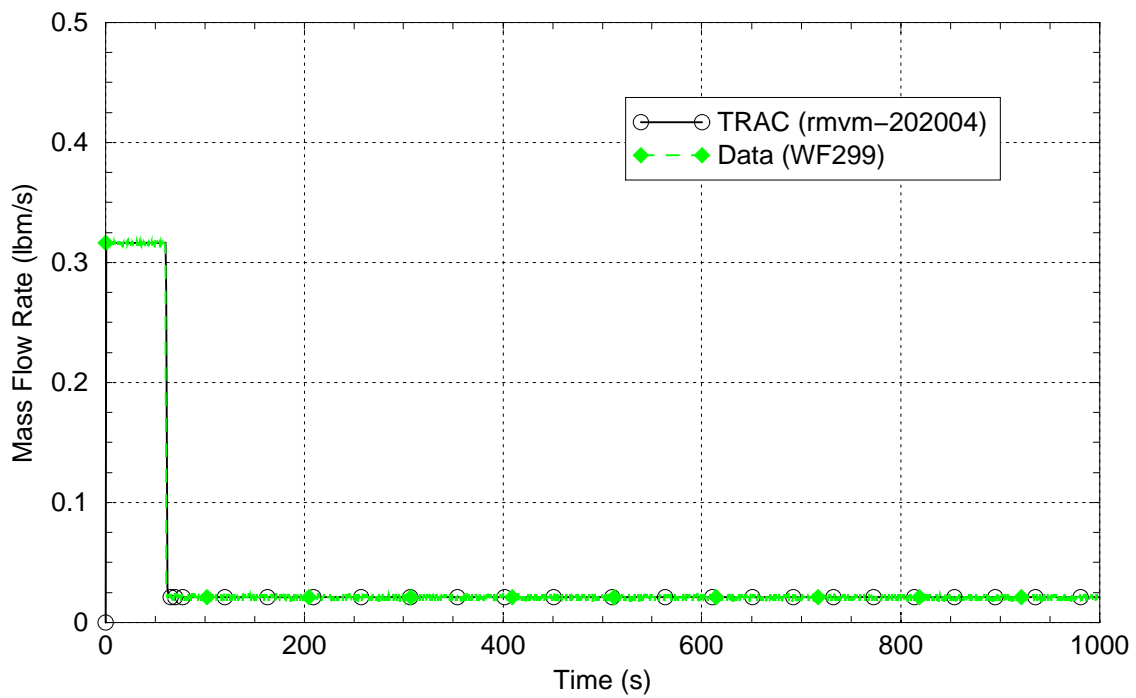


**Figure 4.2-8:** *Test 2029 Feedwater Flow*

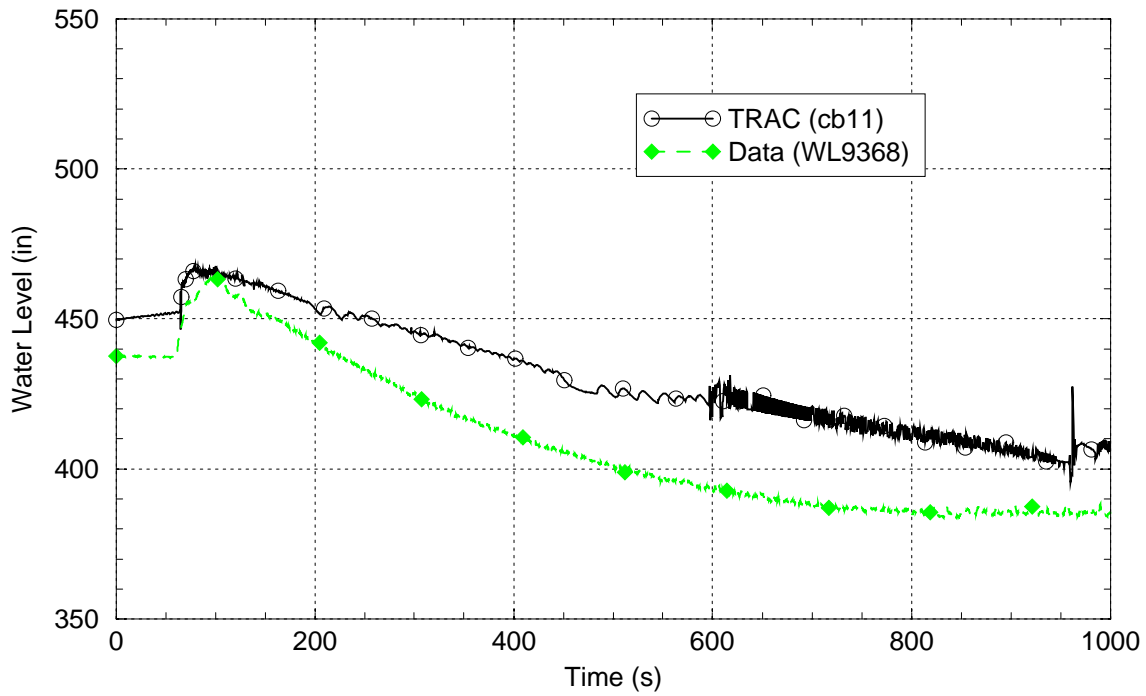


**Figure 4.2-9:** *Test 2029 Narrow Range Water Level*

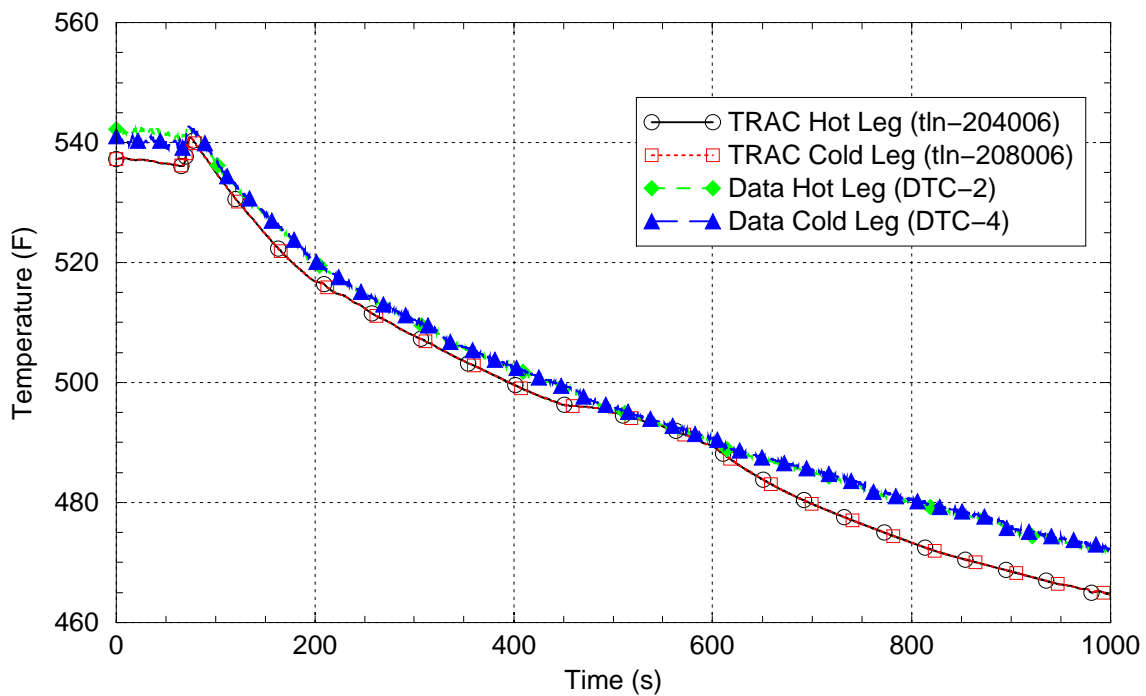


**Figure 4.2-10:** *Test 2029 Lower Downcomer Temperature*

Figures 4.2-11 through 4.2-19 show differential pressure comparisons in the secondary side tube region.

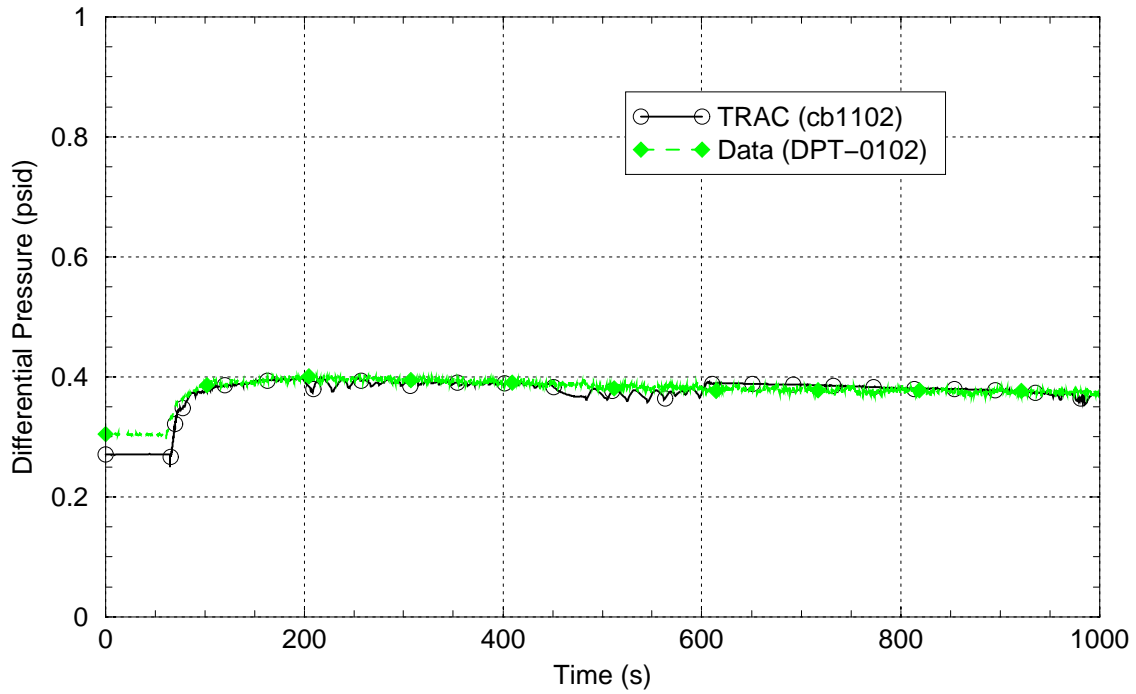


**Figure 4.2-11:** Test 2029 Pressure differential between pressure taps P01 and P02

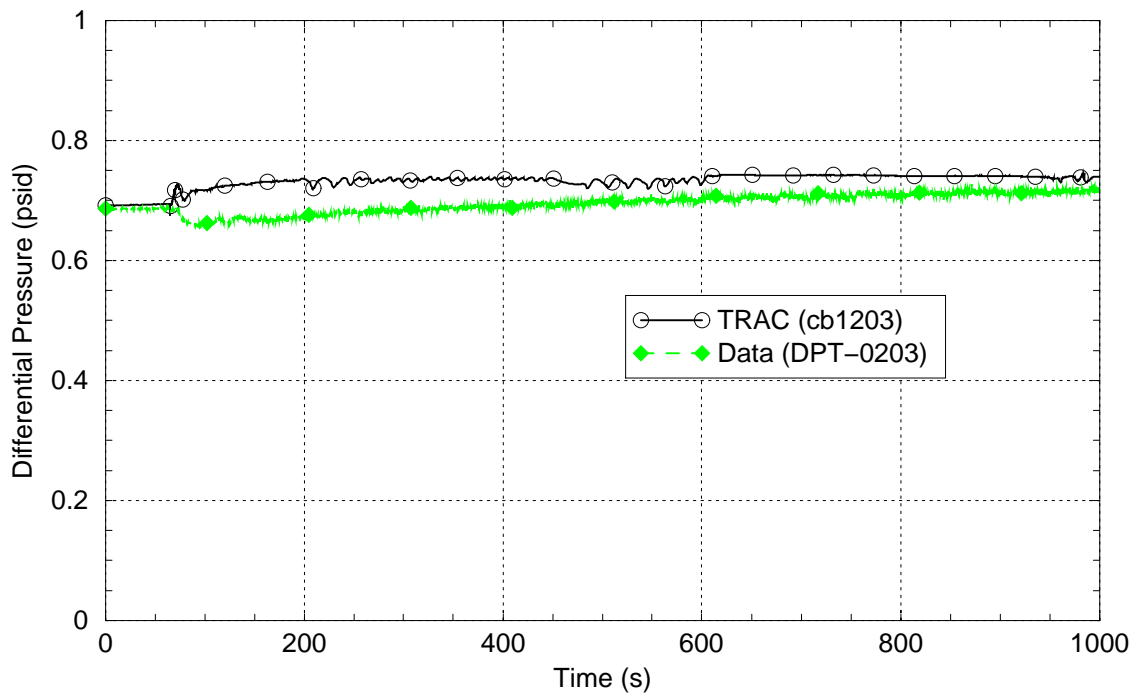


**Figure 4.2-12:** Test 2029 Pressure differential between pressure taps P02 and P03

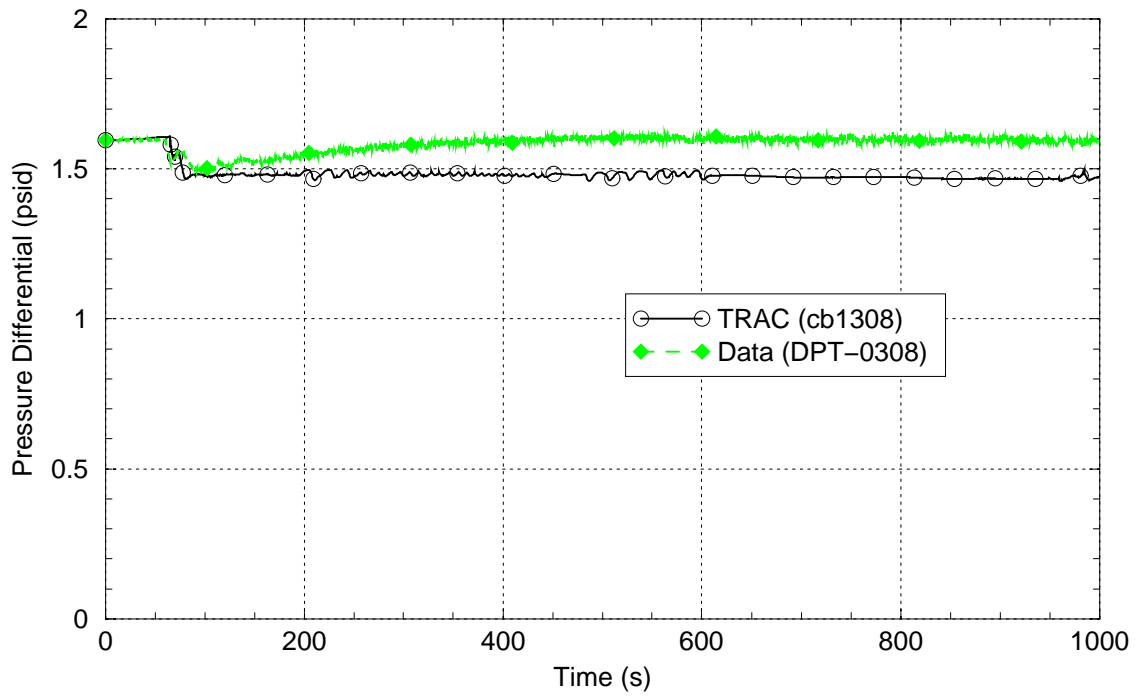


**Figure 4.2-13:** Test 2029 Pressure differential between pressure taps P03 and P08

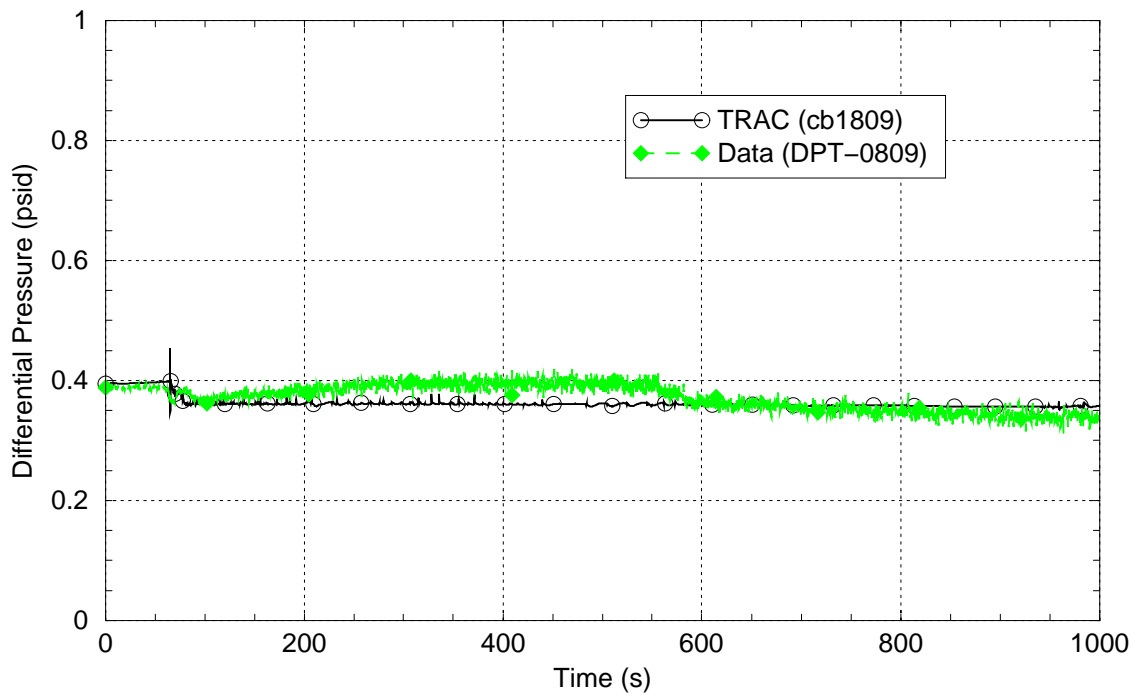


**Figure 4.2-14:** Test 2029 Pressure differential between pressure taps P08 and P09

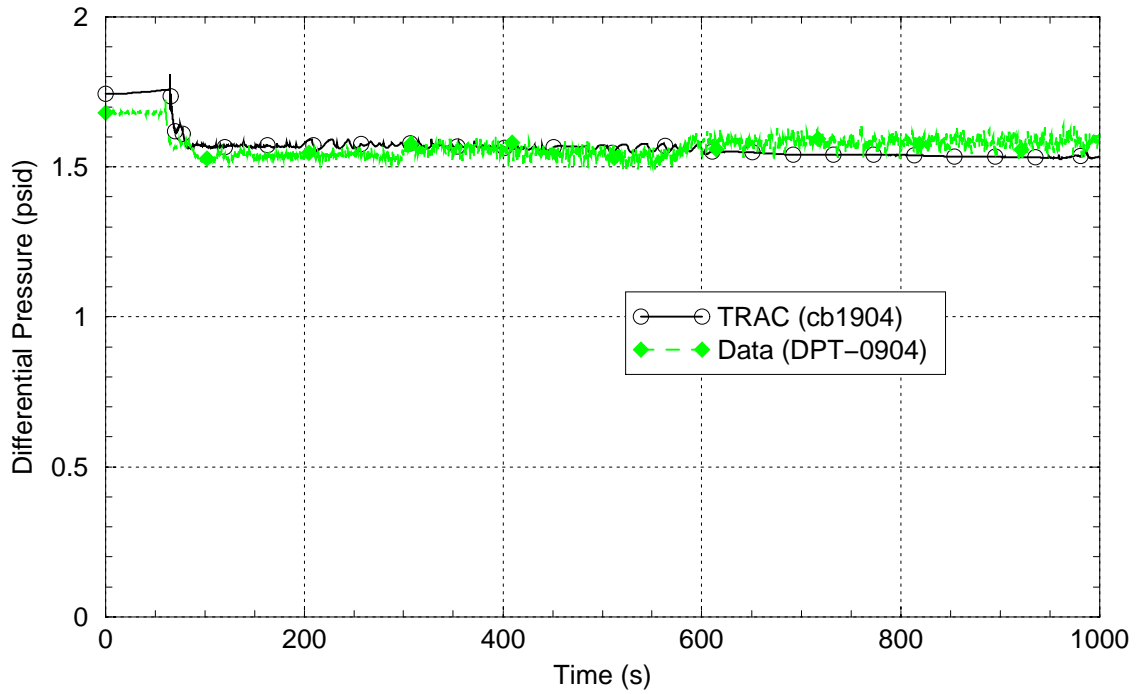


**Figure 4.2-15:** Test 2029 Pressure differential between pressure taps P09 and P04

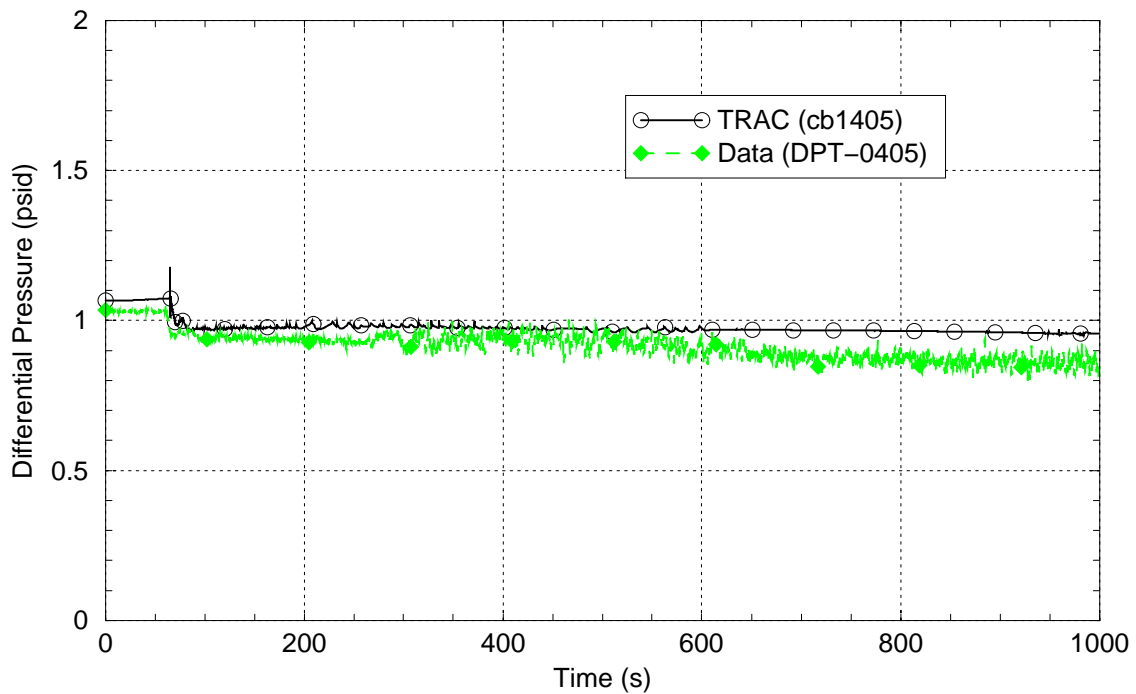


**Figure 4.2-16:** Test 2029 Pressure differential between pressure taps P04 and P05

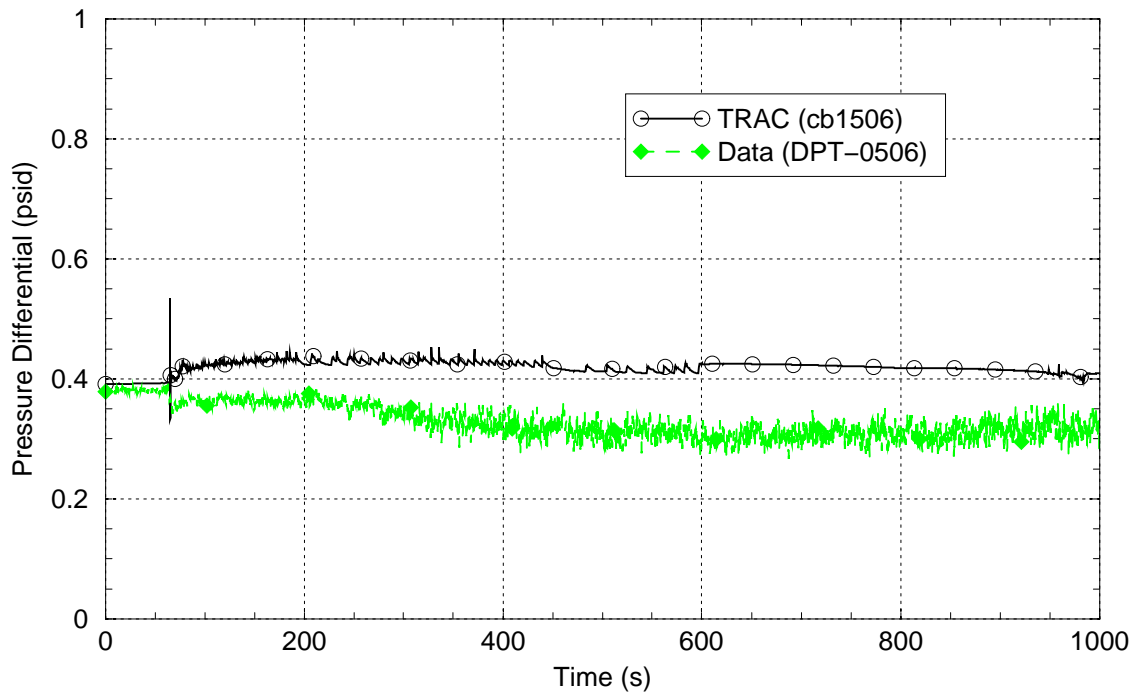


**Figure 4.2-17:** Test 2029 Pressure differential between pressure taps P05 and P06

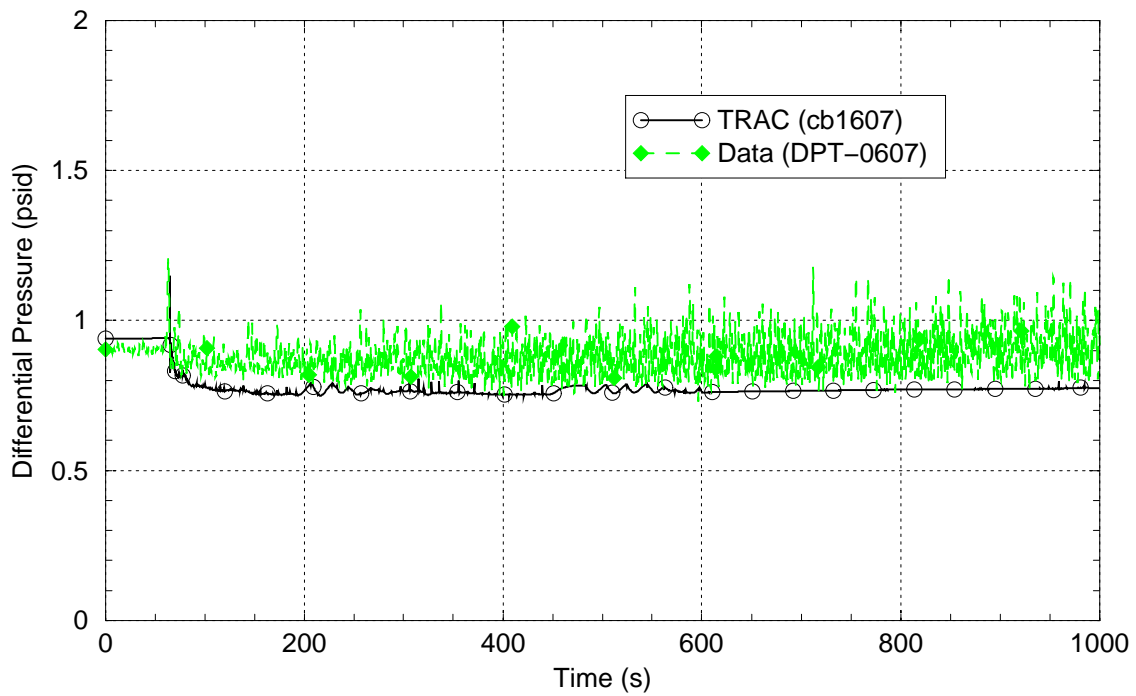


**Figure 4.2-18:** Test 2029 Pressure differential between pressure taps P06 and P07



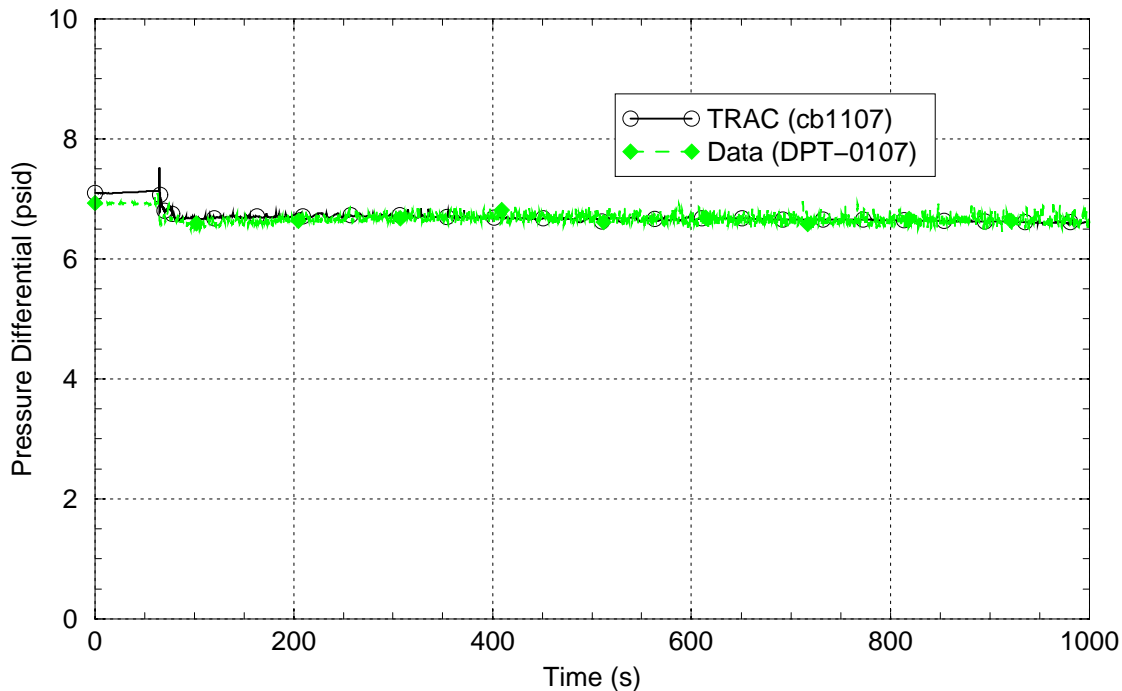


**Figure 4.2-19:** *Test 2029 Pressure differential between pressure taps P01 and P07*

The above figures show that deviations between the calculated and measured responses of many secondary side parameters begin at about 600 seconds. The source of the deviations was traced to the behavior in the TRAC-M downcomer component into which feedwater is injected (PIPE 202, see Figure 3.0-1). Prior to 600 seconds, PIPE 202 is generally water-filled, but minor voiding (around 2%) is seen throughout the lower downcomer region. Those voids are slowly reduced (due to flow from the broken steam generator tube and feedwater injection) and at 600 seconds the lower downcomer regions becomes water-filled. After 600 seconds, a small (around 1%) but steady void fraction appears in PIPE 202. Condensation of this steam void, in the presence of the cold feedwater injection causes the noisy calculated level behavior seen in Figure 4.2-9. The condensation in the calculation lowers the primary system pressure (Figure 4.2-5), the steam line break flow rate (Figure 4.2-6) and the secondary side temperatures (Figure 4.2-10). Further evaluation of these deviations and possible model corrections to remedy them was considered to be beyond the scope of this analysis. The deviations are not seen to have a major impact on the major parameters of interest, the secondary side differential pressures (Figures 4.2-11 through 4.2-19), which show good agreement.

Figures 4.2-20 through 4.2-23 show the TRAC calculated pressure drop across the tube support plates and flow distribution baffle. There is no experimental data to compare these values with, so they are shown for informational purposes only.

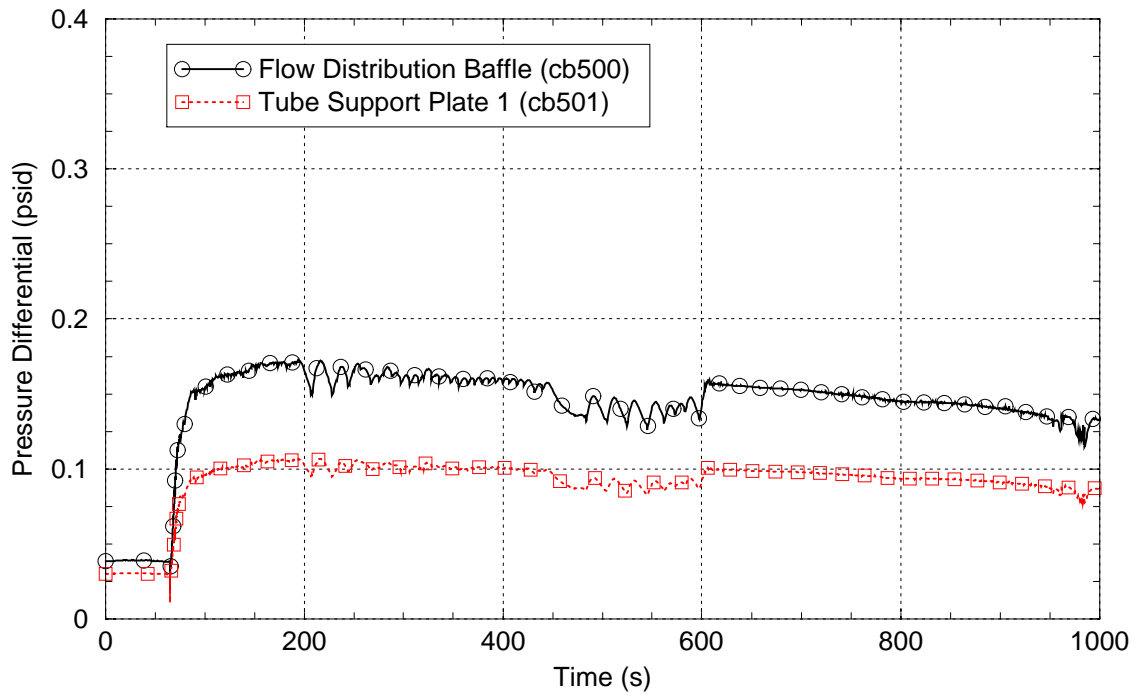


**Figure 4.2-20:** Test 2029 Pressure Drop Across the Tube Support Plates

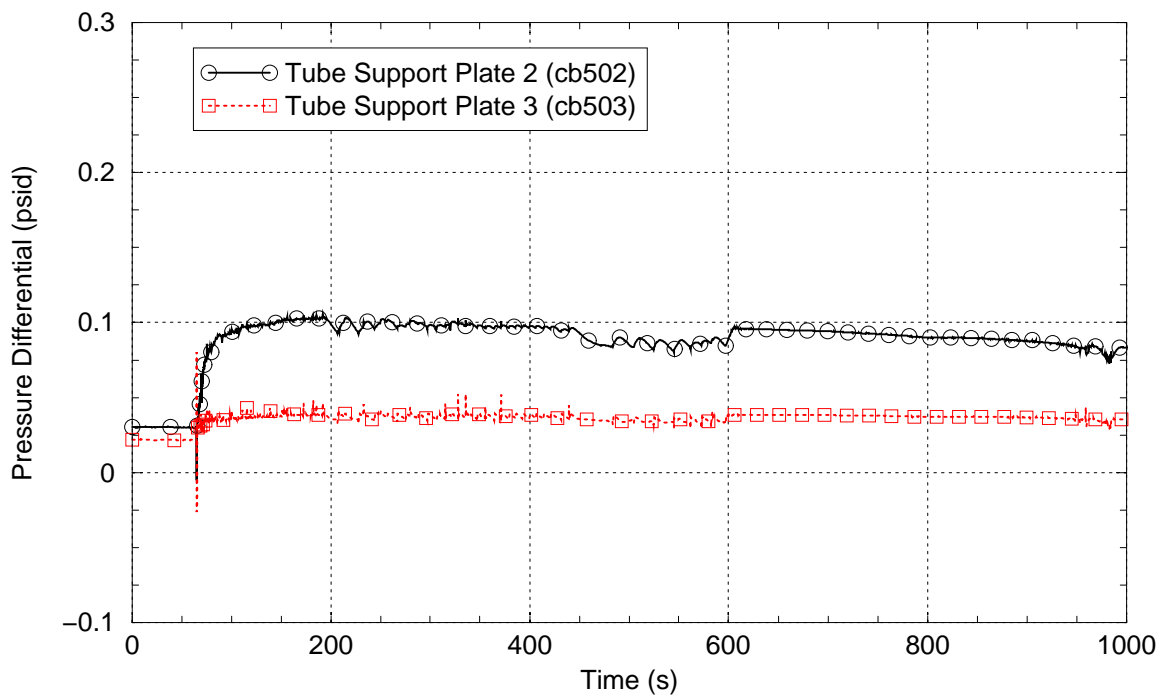


**Figure 4.2-21:** Test 2029 Pressure Drop Across the Tube Support Plates

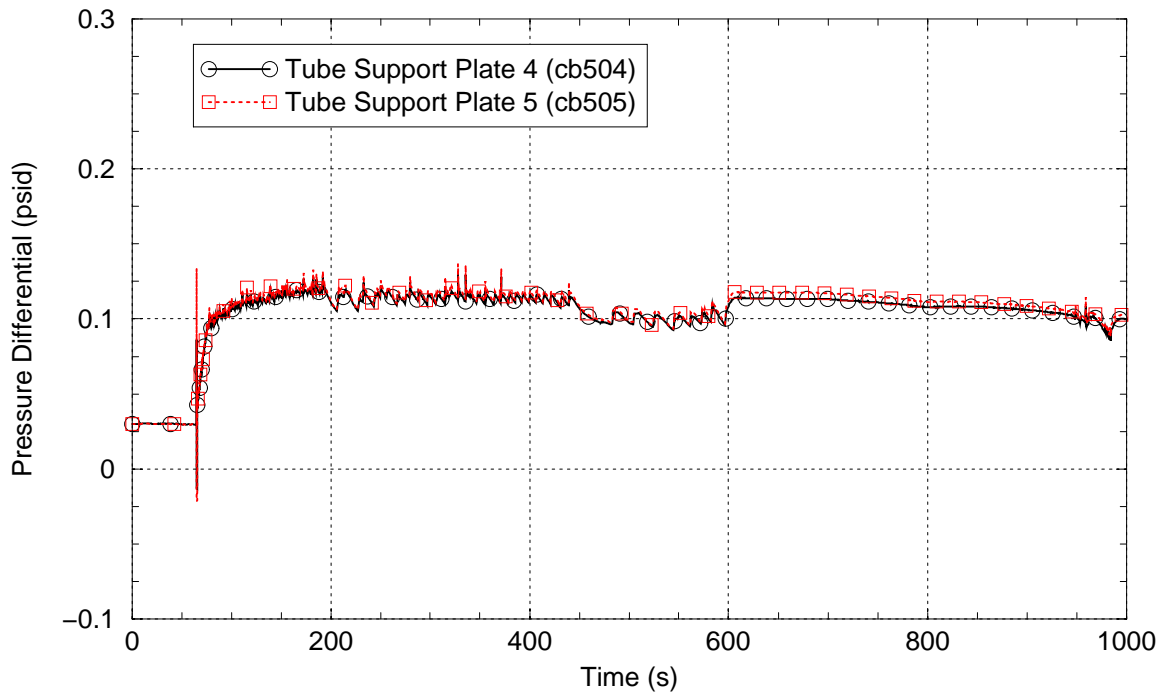


**Figure 4.2-22:** Test 2029 Pressure Drop Across the Tube Support Plates

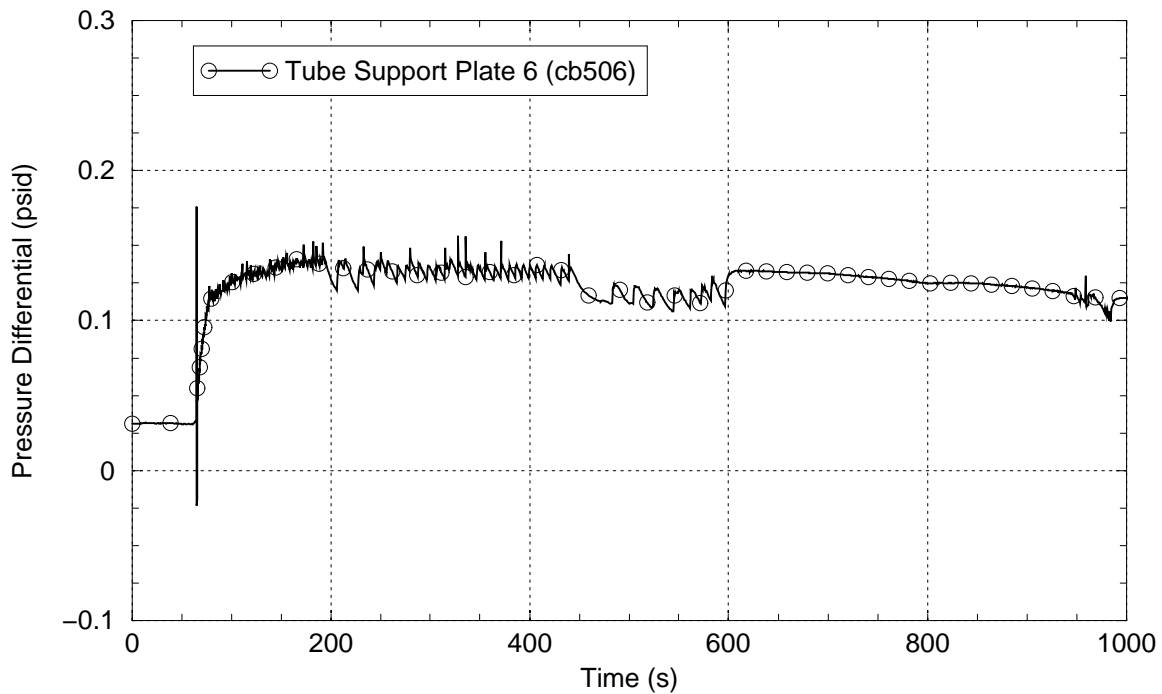


**Figure 4.2-23:** Test 2029 Pressure Drop Across the Tube Support Plates

## 5.0 Summary/Conclusions

A TRAC-M model of the MB-2 test facility was developed based on an existing RELAP5 model. Comparing the TRAC-M calculations to experimental data for several transients shows that TRAC-M does a reasonable job predicting the overall system response, indicating that TRAC-M is acceptable for analysis of steam line break events from hot zero power.

In the tests examined, the differential pressure across the support plates did not exhibit the large increases typical of main steam line breaks and the code correctly predicted this behavior. Since the differential pressure did not change significantly, this test is not well suited for determining the ability of TRAC-M to predict transient differential pressure loadings. The prediction of initial pressure differences could be improved by further refinement of the relative flow losses in the separator and downcomer paths to the steam dome should greater precision be required.

## 6.0 References

- 1) M.Y. Young, K. Takeuchi, O.J. Mendler, G.W. Hopkins, *"Prototypical Steam Generator (MB-2) Transient Testing Program, Task Plan/Scaling Report"*, NUREG/CR-3661, Published March 1984.
- 2) M.Y. Young, K. Takeuchi, O.J. Mendler, *"Loss of Feed Flow, Steam Generator Tube Rupture and Steam Line Break Thermohydraulic Experiments (MB-2 Steam Generator Transient Response Test Program)"*, NUREG/CR-4751, Published October 1986.
- 3) R. W. Shumway, *"Assessment of RELAP5/MOD3.2 Steam Generator Heat Transfer"*, Idaho National Engineering Laboratory, R5M3DA-015, February 1995.
- 4) TRAC-M users Manual
- 5) NRC Data Bank Data for MB-2 Tests 1712, 2013 and 2029.

## 7.0 Attached Files

All files used in this analysis are included on the attached CD-ROM(s). A summary of what is included is presented below:

Directory	File(s)	Description
AV1712	av.pl case1712.txt fig1712.txt path1712.txt	Perl script which runs TRAC-M and makes plots along with associated script inputs for test 1712

Directory	File(s)	Description
AV2013	av.pl case2013.txt fig2013.txt path2013.txt	Perl script which runs TRAC-M and makes plots along with associated script inputs for test 2013
AV2029	av.pl case2029.txt fig2029.txt path2029.txt	Perl script which runs TRAC-M and makes plots along with associated script inputs for test 2029
HFP	MB2_1712_00.inp MB2_1712_01.inp	TRAC-M input files for MB-2 test 1712 including steady state and transient.
HFP/Fig1712	1712SS.PDF 1712TR.PDF	Various plots generated during steady state and transient runs for test 1712
HFP/Out1712/V31050	* Numerous *	TRAC-M output files from test 1712
HZP	MB2_2013_00.inp MB2_2013_01.inp MB2_2029_00.inp MB2_2029_01.inp	TRAC-M input files for MB-2 tests 2013 and 2029 including steady state and transient for each test.
HZP/Fig2013	2013SS.PDF 2013TR.PDF	Various plots generated during steady state and transient runs for test 2013
HZP/Fig2029	2029SS.PDF 2029TR.PDF	Various plots generated during steady state and transient runs for test 2029
HFP/Out2013/V31050	* Numerous *	TRAC-M output files from test 2013
HFP/Out2029/V31050	* Numerous *	TRAC-M output files from test 2029
Report	Attachment_A.doc Attachment_A.mcd Attachment_A.pdf Attachment_B.doc Attachment_B.mcd Attachment_B.pdf MB2 final report.doc MB2 final report.pdf	This report and associated attachments in Microsoft Word format as well as Adobe PDF format. Attachments A and B in Mathcad 11 format.
Report/Figures	* Numerous *	Figures for main report in EPS and JPG format.

Directory	File(s)	Description
Report/Scripts	* Numerous *	XMGR5/AcGrace plot scripts used to generate figures for main report

## 8.0 Problems encountered

Several difficulties were encountered while developing the TRAC-M input and running the code. These are summarized below.

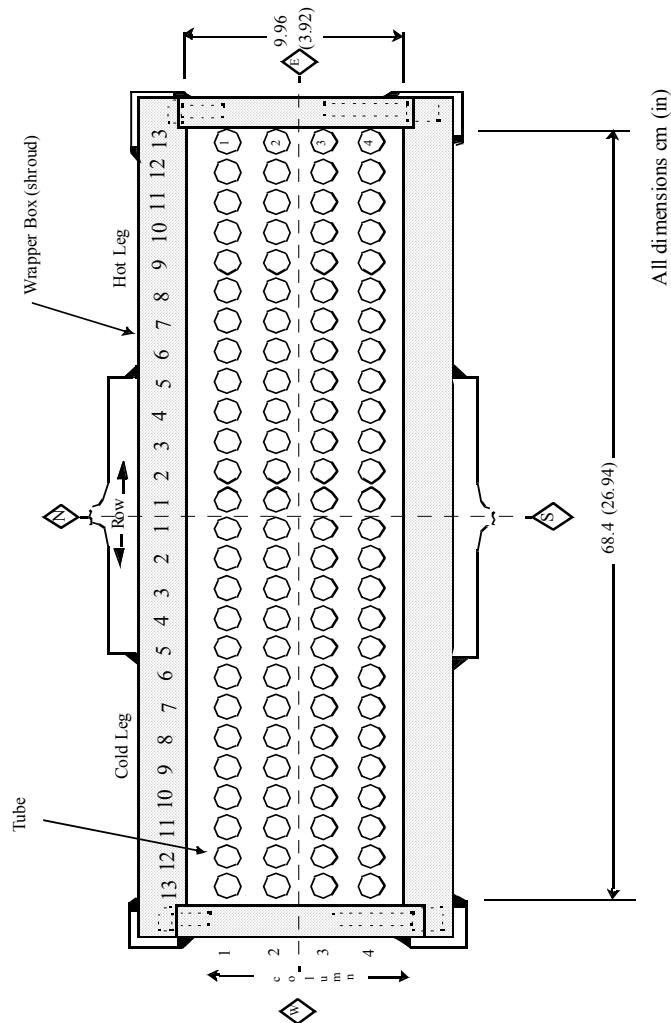
- ◆ Namelist variable "IKFAC" was originally left at the default value of 0 (additive loss coefficients input); however, when the RELAP5 model was converted, K factors were input. This led to unrealistic pressure drops throughout the model. Namelist variable was changed to 1 to allow the input of K factors.
- ◆ Found problems with the AV script not running restarts. This was related to the AV script expecting a TRAC-M TPR file, when in fact, the restart input was an ASCII text file. This problem was reported to the NRC. The AV script was modified to use ASCII text restart inputs. Also, when using the AV "update" mode to rerun a restart (transient), the AV script did not copy the results into the appropriate directory and just left them in the working directory.
- ◆ In tuning the separator (TEE component) the return junction flow area was varied. By making small changes to this value, the code running time went from several hours to several minutes.
- ◆ By default, TRAC-M only allows choking at junctions connected directly to a BREAK component. So, the piping downstream of the break was not modeled (as in the RELAP5 model).
- ◆ In setting up the break valve (VALVE component 238), the area is input three times (once on card 13, and twice on card 25). When changing the break flow area between tests the flow area was originally only changed on card 25, which resulted in incorrect break flow.
- ◆ When setting up the model, an input error was made wherein a wrong hydrodynamic component number was specified as connecting to the face of a heat structure. That wrong component did not have a cell corresponding to the cell number requested in the heat structure input. This input error lead to a code execution failure with insufficient information to permit a user to uncover the source of the failure. A user problem report will be submitted suggesting that better input error checking and reporting is needed to allow users to diagnose this input error.
- ◆ There is no way to determine if flow is choked/unchoked. An output parameter should be available to monitor whether the flow is choked.

## **ATTACHMENT A**

**ATTACHMENT A**  
**to ISL-NSAD-TR-03-09**

The following calculations document the re-nodalization of the secondary side boiler region in the MB-2 TRAC-M model. The RELAP5 model which is being converted to TRAC-M uses only 4 nodes in this region. Since the TRAC-M model will be used to compute tube support plate (TSP) pressure drops, the number of nodes will be increased to coincide with the TSPs. Information relating to dimensions (flow areas, heights, etc.) are found in NUREG/CR-4751, *Loss of Feed Flow, Steam Generator Tube Rupture and Steam Line Break Thermohydraulic Experiments (MB-2 Steam Generator Transient Response Test Program)*, published October 1986.

**MB-2 Bundle Cross Section**





**ATTACHMENT A  
to ISL-NSAD-TR-03-09**

Calculate parameters for TRAC-M component 210

$$W := 26.94 \text{ in}$$

$$L := 3.92 \text{ in}$$

$$\text{Open\_Area} := L \cdot W$$

$$\text{Open\_Area} = 0.068132 \text{ m}^2$$

Tube dimensions

$$\text{OD} := 0.6875 \text{ in}$$

$$\text{Area\_Tube} := \pi \cdot \frac{\text{OD}^2}{4}$$

$$\text{Area\_Tube} = 2.394985 \times 10^{-4} \text{ m}^2$$

$$\text{Total\_Tube\_Area} := 104 \cdot \text{Area\_Tube}$$

$$\text{Total\_Tube\_Area} = 0.024908 \text{ m}^2$$

$$\text{Flow\_Area} := \text{Open\_Area} - \text{Total\_Tube\_Area}$$

$$\text{Flow\_Area} = 0.043224 \text{ m}^2$$

Flow Distribution Baffle

$$\text{FB}_{\text{height}} := 0.75 \text{ in}$$

$$\text{FB}_{\text{flowarea}} := 20.88 \text{ in}^2$$

$$\text{FB}_{\text{flowarea}} = 0.01347 \text{ m}^2$$

$$\text{FB}_{\text{fluidvolume}} := \text{FB}_{\text{height}} \cdot \text{FB}_{\text{flowarea}}$$

$$\text{FB}_{\text{fluidvolume}} = 2.566214 \times 10^{-4} \text{ m}^3$$

$$K_{\text{FB}} := 11.0 \quad K \text{ is based on open flow area of } 4.322\text{e-}02 \text{ m}^2$$

Tube Support Plates

$$\text{TSP}_{\text{height}} := 0.75 \text{ in}$$

NUREG/CR-4751 gives the height of the flow distribution baffle, but not the tube support plates, so the tube support plates were assumed to be the same height.

**ATTACHMENT A  
to ISL-NSAD-TR-03-09**

**TSP 1**

$K_{TSP1} := 5.0$       All K factors for the tube support plates are based on the open flow area of  $4.322e-02 \text{ m}^2$

$$TSP1_{flowarea} := 27.31 \cdot \text{in}^2$$

$$TSP1_{flowarea} = 0.017619 \text{ m}^2$$

$$TSP1_{fluidvolume} := TSP1_{flowarea} \cdot TSP_{height}$$

$$TSP1_{fluidvolume} = 3.35648 \times 10^{-4} \text{ m}^3$$

**TSP 2**       $K_{TSP2} := 5.0$

$$TSP2_{flowarea} := 27.31 \cdot \text{in}^2$$

$$TSP2_{flowarea} = 0.017619 \text{ m}^2$$

$$TSP2_{fluidvolume} := TSP2_{flowarea} \cdot TSP_{height}$$

$$TSP2_{fluidvolume} = 3.35648 \times 10^{-4} \text{ m}^3$$

**TSP 3**       $K_{TSP3} := 0.85$

$$TSP3_{flowarea} := 36.51 \cdot \text{in}^2$$

$$TSP3_{flowarea} = 0.023555 \text{ m}^2$$

$$TSP3_{fluidvolume} := TSP3_{flowarea} \cdot TSP_{height}$$

$$TSP3_{fluidvolume} = 4.487188 \times 10^{-4} \text{ m}^3$$

**TSP 4**       $K_{TSP4} := 5.0$

$$TSP4_{flowarea} := 27.31 \cdot \text{in}^2$$

$$TSP4_{flowarea} = 0.017619 \text{ m}^2$$

$$TSP4_{fluidvolume} := TSP4_{flowarea} \cdot TSP_{height}$$

$$TSP4_{fluidvolume} = 3.35648 \times 10^{-4} \text{ m}^3$$

**TSP 5**       $K_{TSP5} := 5.0$

$$TSP5_{flowarea} := 27.31 \cdot \text{in}^2$$

$$TSP5_{flowarea} = 0.017619 \text{ m}^2$$

$$TSP5_{fluidvolume} := TSP5_{flowarea} \cdot TSP_{height}$$

$$TSP5_{fluidvolume} = 3.35648 \times 10^{-4} \text{ m}^3$$

**TSP 6**       $K_{TSP6} := 5.4$

$$TSP6_{flowarea} := 26.91 \cdot \text{in}^2$$

$$TSP6_{flowarea} = 0.017361 \text{ m}^2$$

$$TSP6_{fluidvolume} := TSP6_{flowarea} \cdot TSP_{height}$$

$$TSP6_{fluidvolume} = 3.307319 \times 10^{-4} \text{ m}^3$$

**ATTACHMENT A  
to ISL-NSAD-TR-03-09**

Each node consists of the open area volume + 1/2 of the fluid volume in the adjacent TSP (or flow baffle)

**Node 1**

$$H_{\text{volume1}} := 20 \cdot \text{in}$$

$$H_{\text{volume1}} = 0.508\text{m} \quad \text{DX}$$

$$h_1 := 20 \cdot \text{in} - \frac{0.75 \cdot \text{in}}{2}$$

$$h_1 = 0.498475\text{m}$$

$$v_1 := h_1 \cdot \text{Flow\_Area}$$

$$v_1 = 0.021546\text{m}^3$$

$$V_{\text{volume1}} := v_1 + \frac{1}{2} \cdot \text{FB}_{\text{fluidvolume}}$$

$$V_{\text{volume1}} = 0.021674\text{m}^3 \quad \text{VOL}$$

$$A_{\text{volume1}} := \frac{V_{\text{volume1}}}{H_{\text{volume1}}}$$

$$A_{\text{volume1}} = 0.042666\text{m}^2$$

$$\text{Elev}_1 := \frac{H_{\text{volume1}}}{2}$$

$$\text{Elev}_1 = 0.254\text{m} \quad \text{Cell center elevation (ELEV)}$$

**Node 2**

$$H_{\text{volume2}} := 40.16 \text{ in} - 20 \cdot \text{in}$$

$$H_{\text{volume2}} = 0.512064\text{m} \quad \text{DX}$$

$$h_2 := H_{\text{volume2}} - \frac{1}{2} \cdot \text{FB}_{\text{height}} - \frac{1}{2} \cdot \text{TSP}_{\text{height}}$$

$$h_2 = 0.493014\text{m}$$

$$v_2 := h_2 \cdot \text{Flow\_Area}$$

$$v_2 = 0.02131\text{m}^3$$

$$V_{\text{volume2}} := v_2 + \frac{1}{2} \cdot \text{FB}_{\text{fluidvolume}} + \frac{1}{2} \cdot \text{TSP1}_{\text{fluidvolume}}$$

$$V_{\text{volume2}} = 0.021606\text{m}^3 \quad \text{VOL}$$

$$A_{\text{volume2}} := \frac{V_{\text{volume2}}}{H_{\text{volume2}}}$$

$$A_{\text{volume2}} = 0.042194\text{m}^2$$

$$\text{Elev}_2 := \text{Elev}_1 + \frac{H_{\text{volume1}}}{2} + \frac{H_{\text{volume2}}}{2}$$

$$\text{Elev}_2 = 0.764032\text{m} \quad \text{ELEV}$$

**ATTACHMENT A  
to ISL-NSAD-TR-03-09**

**Node 3**

$$H_{\text{volume3}} := 60.32 \text{ in} - 40.16 \text{ in}$$

$$H_{\text{volume3}} = 0.512064 \text{ m}$$

DX

$$h_3 := H_{\text{volume3}} - \frac{1}{2} \cdot \text{TSP}_{\text{height}} - \frac{1}{2} \cdot \text{TSP}_{\text{height}}$$

$$h_3 = 0.493014 \text{ m}$$

$$v_3 := h_3 \cdot \text{Flow\_Area}$$

$$v_3 = 0.02131 \text{ m}^3$$

$$V_{\text{volume3}} := v_3 + \frac{1}{2} \cdot \text{TSP1}_{\text{fluidvolume}} + \frac{1}{2} \cdot \text{TSP2}_{\text{fluidvolume}}$$

$$V_{\text{volume3}} = 0.021646 \text{ m}^3$$

VOL

$$A_{\text{volume3}} := \frac{V_{\text{volume3}}}{H_{\text{volume3}}}$$

$$A_{\text{volume3}} = 0.042272 \text{ m}^2$$

$$\text{Elev}_3 := \text{Elev}_2 + \frac{H_{\text{volume2}}}{2} + \frac{H_{\text{volume3}}}{2}$$

$$\text{Elev}_3 = 1.276096 \text{ m}$$

ELEV

**Node 4**

$$H_{\text{volume4}} := 120.48 \text{ in} - 60.32 \text{ in}$$

$$H_{\text{volume4}} = 1.528064 \text{ m}$$

DX

$$h_4 := H_{\text{volume4}} - \frac{1}{2} \cdot \text{TSP}_{\text{height}} - \frac{1}{2} \cdot \text{TSP}_{\text{height}}$$

$$h_4 = 1.509014 \text{ m}$$

$$v_4 := h_4 \cdot \text{Flow\_Area}$$

$$v_4 = 0.065226 \text{ m}^3$$

$$V_{\text{volume4}} := v_4 + \frac{1}{2} \cdot \text{TSP2}_{\text{fluidvolume}} + \frac{1}{2} \cdot \text{TSP3}_{\text{fluidvolume}}$$

$$V_{\text{volume4}} = 0.065618 \text{ m}^3$$

VOL

$$A_{\text{volume4}} := \frac{V_{\text{volume4}}}{H_{\text{volume4}}}$$

$$A_{\text{volume4}} = 0.042942 \text{ m}^2$$

$$\text{Elev}_4 := \text{Elev}_3 + \frac{H_{\text{volume3}}}{2} + \frac{H_{\text{volume4}}}{2}$$

$$\text{Elev}_4 = 2.29616 \text{ m}$$

ELEV

**ATTACHMENT A  
to ISL-NSAD-TR-03-09**

**Node 5**

$$H_{\text{volume5}} := 160.64 \text{ in} - 120.48 \text{ in}$$

$$H_{\text{volume5}} = 1.020064 \text{ m}$$

**DX**

$$h_5 := H_{\text{volume5}} - \frac{1}{2} \cdot \text{TSP}_{\text{height}} - \frac{1}{2} \cdot \text{TSP}_{\text{height}}$$

$$h_5 = 1.001014 \text{ m}$$

$$v_5 := h_5 \cdot \text{Flow\_Area}$$

$$v_5 = 0.043268 \text{ m}^3$$

$$V_{\text{volume5}} := v_5 + \frac{1}{2} \cdot \text{TSP}_{\text{fluidvolume}} + \frac{1}{2} \cdot \text{TSP}_{\text{fluidvolume}}$$

$$V_{\text{volume5}} = 0.04366 \text{ m}^3$$

**VOL**

$$A_{\text{volume5}} := \frac{V_{\text{volume5}}}{H_{\text{volume5}}}$$

$$A_{\text{volume5}} = 0.042801 \text{ m}^2$$

$$\text{Elev}_5 := \text{Elev}_4 + \frac{H_{\text{volume4}}}{2} + \frac{H_{\text{volume5}}}{2}$$

$$\text{Elev}_5 = 3.570224 \text{ m}$$

**ELEV**

**Node 6**

$$H_{\text{volume6}} := 200.80 \text{ in} - 160.64 \text{ in}$$

$$H_{\text{volume6}} = 1.020064 \text{ m}$$

**DX**

$$h_6 := H_{\text{volume6}} - \frac{1}{2} \cdot \text{TSP}_{\text{height}} - \frac{1}{2} \cdot \text{TSP}_{\text{height}}$$

$$h_6 = 1.001014 \text{ m}$$

$$v_6 := h_6 \cdot \text{Flow\_Area}$$

$$v_6 = 0.043268 \text{ m}^3$$

$$V_{\text{volume6}} := v_6 + \frac{1}{2} \cdot \text{TSP}_{\text{fluidvolume}} + \frac{1}{2} \cdot \text{TSP}_{\text{fluidvolume}}$$

$$V_{\text{volume6}} = 0.043604 \text{ m}^3$$

**VOL**

$$A_{\text{volume6}} := \frac{V_{\text{volume6}}}{H_{\text{volume6}}}$$

$$A_{\text{volume6}} = 0.042746 \text{ m}^2$$

$$\text{Elev}_6 := \text{Elev}_5 + \frac{H_{\text{volume5}}}{2} + \frac{H_{\text{volume6}}}{2}$$

$$\text{Elev}_6 = 4.590288 \text{ m}$$

**ELEV**

**ATTACHMENT A  
to ISL-NSAD-TR-03-09**

**Node 7**

$$H_{\text{volume7}} := 240.94 \text{ in} - 200.80 \text{ in}$$

$$H_{\text{volume7}} = 1.019556 \text{ m}$$

**DX**

$$h_7 := H_{\text{volume7}} - \frac{1}{2} \cdot \text{TSP}_{\text{height}} - \frac{1}{2} \cdot \text{TSP}_{\text{height}}$$

$$h_7 = 1.000506 \text{ m}$$

$$v_7 := h_7 \cdot \text{Flow\_Area}$$

$$v_7 = 0.043246 \text{ m}^3$$

$$V_{\text{volume7}} := v_7 + \frac{1}{2} \cdot \text{TSP5}_{\text{fluidvolume}} + \frac{1}{2} \cdot \text{TSP6}_{\text{fluidvolume}}$$

$$V_{\text{volume7}} = 0.04358 \text{ m}^3$$

**VOL**

$$A_{\text{volume7}} := \frac{V_{\text{volume7}}}{H_{\text{volume7}}}$$

$$A_{\text{volume7}} = 0.042743 \text{ m}^2$$

$$\text{Elev}_7 := \text{Elev}_6 + \frac{H_{\text{volume6}}}{2} + \frac{H_{\text{volume7}}}{2}$$

$$\text{Elev}_7 = 5.61 \text{ m}$$

**ELEV**

Compute Hydarulic diameter based on  $4 \cdot \text{Flow Area} / \text{Wetted Perimeter}$ , and will apply to nodes 1 - > 7

$$\text{Perimeter} := 2 \cdot (L + W) + 104 \pi \cdot \text{OD}$$

$$\text{Perimeter} = 7.273134 \text{ m}$$

$$\text{HD} := \frac{4 \cdot \text{Flow\_Area}}{\text{Perimeter}}$$

$$\text{HD} = 0.023772 \text{ m}$$

**Node 8**

**ATTACHMENT A  
to ISL-NSAD-TR-03-09**

$$V_{\text{volume8}} := 1.387 \text{ft}^3$$

$$V_{\text{volume8}} = 0.039275 \text{m}^3$$

$$H_{\text{volume8}} := 276.25 \text{in} - 240.96 \text{in}$$

$$H_{\text{volume8}} = 0.896366 \text{m}$$

$$A_{\text{volume8}} := \frac{V_{\text{volume8}}}{H_{\text{volume8}}}$$

$$A_{\text{volume8}} = 0.043816 \text{m}^2$$

$$\text{Elev8} := \text{Elev7} + \frac{H_{\text{volume7}}}{2} + \frac{H_{\text{volume8}}}{2}$$

$$\text{Elev8} = 6.568059 \text{m}$$

Hydraulic diameter of node 8 will be calculated as  $4 \cdot \text{volume} / \text{wetted surface area}$

$$A_{\text{wall}} := (L + W) \cdot 2 \cdot H_{\text{volume8}}$$

$$A_{\text{wall}} = 1.405222 \text{m}^2$$

$$H_{\text{straight}} := 263.27 \text{in} - 240.94 \text{in}$$

$$H_{\text{straight}} = 0.567182 \text{m}$$

$$A_{\text{straight}} := H_{\text{straight}} \cdot \pi \cdot \text{OD} \cdot 10^4$$

$$A_{\text{straight}} = 3.236027 \text{m}^2$$

Surface area of the curved portion of the tubes is calculated as follows:

Surface Area for a given tube =  $2 \cdot \pi^2 \cdot R \cdot \text{Tube OD}$

$$R_1 := 1.22 \text{in}$$

$$R_2 := 2.2 \text{in}$$

$$R_3 := 3.18 \text{in}$$

$$R_4 := 4.16 \text{in}$$

$$R_5 := 5.14 \text{in}$$

$$R_6 := 6.12 \text{in}$$

$$R_7 := 7.1 \text{in}$$

$$R_8 := 8.08 \text{in}$$

$$R_9 := 9.06 \text{in}$$

$$R_{10} := 10.04 \text{in}$$

$$R_{11} := 11.02 \text{in}$$

$$R_{12} := 12.0 \text{in}$$

$$R_{13} := 12.98 \text{in}$$

$$S_1 := 2 \cdot \pi^2 \cdot R_1 \cdot \text{OD}$$

$$S_2 := 2 \cdot \pi^2 \cdot R_2 \cdot \text{OD}$$

$$S_3 := 2 \cdot \pi^2 \cdot R_3 \cdot \text{OD}$$

$$S_4 := 2 \cdot \pi^2 \cdot R_4 \cdot \text{OD}$$

$$S_5 := 2 \cdot \pi^2 \cdot R_5 \cdot \text{OD}$$

$$S_6 := 2 \cdot \pi^2 \cdot R_6 \cdot \text{OD}$$

$$S_7 := 2 \cdot \pi^2 \cdot R_7 \cdot \text{OD}$$

$$S_8 := 2 \cdot \pi^2 \cdot R_8 \cdot \text{OD}$$

$$S_9 := 2 \cdot \pi^2 \cdot R_9 \cdot \text{OD}$$

$$S_{10} := 2 \cdot \pi^2 \cdot R_{10} \cdot \text{OD}$$

$$S_{11} := 2 \cdot \pi^2 \cdot R_{11} \cdot \text{OD}$$

$$S_{12} := 2 \cdot \pi^2 \cdot R_{12} \cdot \text{OD}$$

$$S_{13} := 2 \cdot \pi^2 \cdot R_{13} \cdot \text{OD}$$

$$\text{CurvedSurfacearea} := (S_1 + S_2 + S_3 + S_4 + S_5 + S_6 + S_7 + S_8 + S_9 + S_{10} + S_{11} + S_{12} + S_{13}) \cdot 4$$

**ATTACHMENT A  
to ISL-NSAD-TR-03-09**

$$\text{CurvedSurfacearea} = 3.232448\text{m}^2$$

$$\text{Totalsurfacearea} := \text{CurvedSurfacearea} + A_{\text{straight}}$$

$$\text{Totalsurfacearea} = 6.468475\text{m}^2$$

$$\text{HD}_8 := \frac{4 \cdot V_{\text{volume8}}}{\text{Totalsurfacearea}}$$

$$\text{HD}_8 = 0.024287\text{m}$$

### Node 9

This node will stop at elevation 7.979 m (the same as the original node 5)

$$H_{\text{volume9}} := 7.979\text{m} - \text{Elev}_8 - \frac{H_{\text{volume8}}}{2}$$

$$H_{\text{volume9}} = 0.962758\text{m} \quad \text{DX}$$

$$\text{Elev}_9 := \text{Elev}_8 + \frac{H_{\text{volume8}}}{2} + \frac{H_{\text{volume9}}}{2}$$

$$\text{Elev}_9 = 7.497621\text{m} \quad \text{ELEV}$$

$$A_{\text{volume9}} := \text{Open\_Area}$$

$$A_{\text{volume9}} = 0.068132\text{m}^2$$

$$V_{\text{volume9}} := A_{\text{volume9}} \cdot H_{\text{volume9}}$$

$$V_{\text{volume9}} = 0.065595\text{m}^3 \quad \text{VOL}$$

$$\text{HD}_9 := \frac{4 \cdot A_{\text{volume9}}}{(L + W) \cdot 2}$$

$$\text{HD}_9 = 0.173841\text{m} \quad \text{HD}$$

Junction area between node 8 and 9

$$\text{Area}_{8\_9} := 105.60\text{in}^2$$

$$\text{Area}_{8\_9} = 0.068129\text{m}^2$$

Renodalization of the primary tubes (TRAC-M pipe component 104) to be consistent with the revised secondary side



**ATTACHMENT A**  
**to ISL-NSAD-TR-03-09**

Component 104 originally had 10 nodes (inlet, 8 for the tubes and an outlet). The inlet and outlet will remain the same.

**Tube thickness**

$$\text{thickness} := 0.04 \text{ in}$$

$$\text{ID} := \text{OD} - 2 \cdot \text{thickness} \quad \text{ID} = 0.015431 \text{ m}$$

$$\text{Pri\_Flow\_Area} := \frac{\pi}{4} \cdot \text{ID}^2 \cdot 52$$

$$\text{Pri\_Flow\_Area} = 9.724185 \times 10^{-3} \text{ m}^2$$

**Compute heights**

**Total TRAC-M Height**

$$\text{H}_{\text{pri2}} := \text{H}_{\text{volume1}}$$

$$\text{H}_{\text{pri2}} = 0.508 \text{ m}$$

$$\text{TRAC\_H}_{\text{total}} := 1.797 \text{ m} \cdot 4$$

$$\text{H}_{\text{pri3}} := \text{H}_{\text{volume2}}$$

$$\text{H}_{\text{pri3}} = 0.512064 \text{ m}$$

$$\text{TRAC\_H}_{\text{total}} = 7.188 \text{ m}$$

$$\text{H}_{\text{pri4}} := \text{H}_{\text{volume3}}$$

$$\text{H}_{\text{pri4}} = 0.512064 \text{ m}$$

$$\text{H}_{\text{pri5}} := \text{H}_{\text{volume4}}$$

$$\text{H}_{\text{pri5}} = 1.528064 \text{ m}$$

$$\text{H}_{\text{pri6}} := \text{H}_{\text{volume5}}$$

$$\text{H}_{\text{pri6}} = 1.020064 \text{ m}$$

$$\text{H}_{\text{pri7}} := \text{H}_{\text{volume6}}$$

$$\text{H}_{\text{pri7}} = 1.020064 \text{ m}$$

$$\text{H}_{\text{pri8}} := \text{H}_{\text{volume7}}$$

$$\text{H}_{\text{pri8}} = 1.019556 \text{ m}$$

$$\text{H}_{\text{subtotal}} := \text{H}_{\text{pri2}} + \text{H}_{\text{pri3}} + \text{H}_{\text{pri4}} + \text{H}_{\text{pri5}} + \text{H}_{\text{pri6}} + \text{H}_{\text{pri7}} + \text{H}_{\text{pri8}}$$

$$\text{H}_{\text{subtotal}} = 6.119876 \text{ m}$$

$$\text{H}_{\text{pri9}} := \text{TRAC\_H}_{\text{total}} - \text{H}_{\text{subtotal}}$$

$$\text{H}_{\text{pri9}} = 1.068124 \text{ m}$$

**Compute volume**

**ATTACHMENT A  
to ISL-NSAD-TR-03-09**

$V_{pri2} := H_{pri2} \cdot Pri\_Flow\_Area$	$V_{pri2} = 4.939886 \times 10^{-3} m^3$
$V_{pri3} := H_{pri3} \cdot Pri\_Flow\_Area$	$V_{pri3} = 4.979405 \times 10^{-3} m^3$
$V_{pri4} := H_{pri4} \cdot Pri\_Flow\_Area$	$V_{pri4} = 4.979405 \times 10^{-3} m^3$
$V_{pri5} := H_{pri5} \cdot Pri\_Flow\_Area$	$V_{pri5} = 0.014859 m^3$
$V_{pri6} := H_{pri6} \cdot Pri\_Flow\_Area$	$V_{pri6} = 9.919291 \times 10^{-3} m^3$
$V_{pri7} := H_{pri7} \cdot Pri\_Flow\_Area$	$V_{pri7} = 9.919291 \times 10^{-3} m^3$
$V_{pri8} := H_{pri8} \cdot Pri\_Flow\_Area$	$V_{pri8} = 9.914351 \times 10^{-3} m^3$
$V_{pri9} := H_{pri9} \cdot Pri\_Flow\_Area$	$V_{pri9} = 0.010387 m^3$

**Total tube volume**

$$V_{tot} := (V_{pri2} + V_{pri3} + V_{pri4} + V_{pri5} + V_{pri6} + V_{pri7} + V_{pri8} + V_{pri9}) \cdot 2$$

$$V_{tot} = 0.139795 m^3$$

$$TRAC\_V_{tot} := 0.017469 m^3 \cdot 8$$

$$TRAC\_V_{tot} = 0.139752 m^3$$

$$Error := \frac{TRAC\_V_{tot} - V_{tot}}{TRAC\_V_{tot}} \cdot 100$$

$$Error = -0.030688$$

# **ATTACHMENT B**

**ATTACHMENT B**  
**to ISL-NSAD-TR-03-09**

The pressure taps in the MB-2 test facility are not located at the TRAC-M cell center elevations, so the pressures cannot be directly compared. In order to make comparisons, the TRAC-M cell center pressure will be adjusted to account for the difference in elevation between the tap and cell-center.

Define some useful constants

$$g_c := 32.217 \frac{\text{lb} \cdot \text{ft}}{\text{lbf} \cdot \text{sec}^2} \quad g := 32.217 \frac{\text{ft}}{\text{sec}^2}$$

Using pressure tap P01 as an example:

$$P01_{\text{elevation}} := 17 \cdot \text{in}$$

The closest TRAC-M cell center is component 210, node 1

$$TRAC01_{\text{elevation}} := 0.254 \text{ m} \quad TRAC01_{\text{elevation}} = 10 \text{ in}$$

The TRAC-M pressure at the data P01<sub>elevation</sub> can be computed based on the following:  
TRAC-M P01 = Cell Center (at 10") Pressure +  $\rho \cdot g \cdot h$  +  $f \cdot L/D \cdot \rho \cdot V^2 / 2g$   
where the elevation and friction terms will be computed for both the liquid and vapor phases.

The wall surface roughness is input to TRAC-M as 4.572e-5 m

$$\text{Rough} := 4.572 \cdot 10^{-5} \cdot \text{m}$$

The hydraulic diameter of the boiler region is 2.3772e-2 m

$$HD := 2.3772 \cdot 10^{-2} \cdot \text{m}$$

Assuming the flow will be completely turbulent, from CRANE, page A-24, the friction factor (f) is 0.014

$$\frac{\text{Rough}}{HD} = 0.0019 \quad f := 0.022$$

Compute elevation difference

$$DH := P01_{\text{elevation}} - TRAC01_{\text{elevation}}$$

$$DH = 0.1778 \text{ m} \quad DH = 7 \text{ in}$$

**ATTACHMENT B  
to ISL-NSAD-TR-03-09**

Define gravity term multiplier for conversion into psi

$$P01_{gravity} := 1 \cdot \frac{\text{kg}}{\text{m}^3} \cdot \frac{\text{g}}{\text{g}_c} \cdot -DH$$

$$P01_{gravity} = -2.5289 \times 10^{-4} \frac{\text{lbf}}{\text{in}^2}$$

Define friction term multiplier for conversion into psi

$$P01_{friction} := \frac{f \cdot \frac{-DH}{HD} \cdot 1 \cdot \frac{\text{kg}}{\text{m}^3} \cdot \left(1 \cdot \frac{\text{m}}{\text{sec}}\right)^2}{2}$$

$$P01_{friction} = -1.2204 \times 10^{-5} \frac{\text{lbf}}{\text{in}^2}$$

Define pressure multiplier for conversion into psi

$$P := 1 \cdot \text{Pa}$$

$$P = 1.4504 \times 10^{-4} \frac{\text{lbf}}{\text{in}^2}$$

TRAC-M pressure at 17" (psi) =

$$\begin{aligned} & \text{pn-210001} * 1.4504\text{e-4} \\ & - \rho_V (\text{kg/m}^3) * 2.5289\text{e-4} * \alpha_{210001} \\ & - \rho_l (\text{kg/m}^3) * 2.5289\text{e-4} * (1-\alpha_{210001}) \\ & - \rho_V (\text{kg/m}^3) * V_V^2 (\text{m/s})^2 * 1.2204\text{e-5} * \alpha_{210001} \\ & - \rho_l (\text{kg/m}^3) * V_l^2 (\text{m/s})^2 * 1.2204\text{e-5} * (1-\alpha_{210001}) \end{aligned}$$

The above assumes that the flow is positive upwards. If the flow is reversed, the gravity term will remain unchanged, however, the friction term will change signs. In order to account for this, the velocity squared term will be entered into TRAC-M controls as (velocity \* ABS(velocity)).

**ATTACHMENT B**  
**to ISL-NSAD-TR-03-09**

The above can be repeated for P02

$$P02_{\text{elevation}} := 26.36 \text{ in}$$

$$TRAC02_{\text{elevation}} := 0.76403 \text{ m}$$

$$DH2 := P02_{\text{elevation}} - TRAC02_{\text{elevation}}$$

$$DH2 = -0.0945 \text{ m}$$

$$DH2 = -3.7199 \text{ in}$$

Define gravity term multiplier for conversion into psi

$$P02_{\text{gravity}} := 1 \cdot \frac{\text{kg}}{\text{m}^3} \cdot \frac{\text{g}}{\text{g}_c} \cdot DH2$$

$$P02_{\text{gravity}} = 1.3439 \times 10^{-4} \frac{\text{lbf}}{\text{in}^2}$$

Define friction term multiplier for conversion into psi

$$P02_{\text{friction}} := \frac{f \cdot \frac{-DH2}{HD} \cdot 1 \cdot \frac{\text{kg}}{\text{m}^3} \cdot \left(1 \cdot \frac{\text{m}}{\text{sec}}\right)^2}{2}$$

$$P02_{\text{friction}} = 6.4854 \times 10^{-6} \frac{\text{lbf}}{\text{in}^2}$$

TRAC-M pressure at 26.36" (psi) =

$$\begin{aligned} & \text{pn-210002} * 1.4504\text{e-4} \\ & + \rho_V (\text{kg/m}^3) * 1.3439\text{e-4} * \alpha_{210002} \\ & + \rho_l (\text{kg/m}^3) * 1.3439\text{e-4} * (1 - \alpha_{210002}) \\ & + \rho_V (\text{kg/m}^3) * V_V^2 (\text{m/s})^2 * 6.4854\text{e-6} * \alpha_{210002} \\ & + \rho_l (\text{kg/m}^3) * V_l^2 (\text{m/s})^2 * 6.4854\text{e-6} * (1 - \alpha_{210002}) \end{aligned}$$

**ATTACHMENT B  
to ISL-NSAD-TR-03-09**

The above can be repeated for P03

$$P03_{\text{elevation}} := 51.82 \text{ in}$$

$$TRAC03_{\text{elevation}} := 1.2761 \text{ m}$$

$$DH3 := P03_{\text{elevation}} - TRAC03_{\text{elevation}}$$

$$DH3 = 0.0401 \text{ m}$$

$$DH3 = 1.5798 \text{ in}$$

Define gravity term multiplier for conversion into psi

$$P03_{\text{gravity}} := 1 \cdot \frac{\text{kg}}{\text{m}^3} \cdot \frac{\text{g}}{\text{g}_c} \cdot DH3$$

$$P03_{\text{gravity}} = -5.7075 \times 10^{-5} \frac{\text{lbf}}{\text{in}^2}$$

Define friction term multiplier for conversion into psi

$$P03_{\text{friction}} := \frac{f \cdot \frac{-DH3}{HD} \cdot 1 \cdot \frac{\text{kg}}{\text{m}^3} \cdot \left(1 \cdot \frac{\text{m}}{\text{sec}}\right)^2}{2}$$

$$P03_{\text{friction}} = -2.7543 \times 10^{-6} \frac{\text{lbf}}{\text{in}^2}$$

TRAC-M pressure at 51.82" (psi) =

$$pn-210003 * 1.4504e-4$$

$$- \rho_V (\text{kg/m}^3) * 5.7075e-5 * \alpha_{210003}$$

$$- \rho_l (\text{kg/m}^3) * 5.7075e-5 * (1 - \alpha_{210003})$$

$$- \rho_V (\text{kg/m}^3) * V_V^2 (\text{m/s})^2 * 2.7543e-6 * \alpha_{210003}$$

$$- \rho_l (\text{kg/m}^3) * V_l^2 (\text{m/s})^2 * 2.7543e-6 * (1 - \alpha_{210003})$$

**ATTACHMENT B**  
**to ISL-NSAD-TR-03-09**

The above can be repeated for P08

Note the pressure tap numbers are not in numerical order as they go up the secondary. In this case, P08 is near TRAC-M cell 210 node 4.

$$P08_{\text{elevation}} := 111.82 \text{ in}$$

$$TRAC04_{\text{elevation}} := 2.2962 \text{ m}$$

$$DH4 := P08_{\text{elevation}} - TRAC04_{\text{elevation}}$$

$$DH4 = 0.544 \text{ m}$$

$$DH4 = 21.4184 \text{ in}$$

Define gravity term multiplier for conversion into psi

$$P08_{\text{gravity}} := 1 \cdot \frac{\text{kg}}{\text{m}^3} \cdot \frac{\text{g}}{\text{g}_c} \cdot DH4$$

$$P08_{\text{gravity}} = -7.7379 \times 10^{-4} \frac{\text{lbf}}{\text{in}^2}$$

Define friction term multiplier for conversion into psi

$$P08_{\text{friction}} := \frac{f \cdot \frac{-DH4}{HD} \cdot 1 \cdot \frac{\text{kg}}{\text{m}^3} \cdot \left(1 \cdot \frac{\text{m}}{\text{sec}}\right)^2}{2}$$

$$P08_{\text{friction}} = -3.7341 \times 10^{-5} \frac{\text{lbf}}{\text{in}^2}$$

TRAC-M pressure at 111.82" (psi) =

$$pn-210004 * 1.4504e-4$$

$$- \rho_V (\text{kg/m}^3) * 7.7379e-4 * \alpha_{210004}$$

$$- \rho_L (\text{kg/m}^3) * 7.7379e-4 * (1 - \alpha_{210004})$$

$$- \rho_V (\text{kg/m}^3) * V_V^2 (\text{m/s})^2 * 3.7341e-5 * \alpha_{210004}$$

$$- \rho_L (\text{kg/m}^3) * V_L^2 (\text{m/s})^2 * 3.7341e-5 * (1 - \alpha_{210004})$$



**ATTACHMENT B  
to ISL-NSAD-TR-03-09**

The above can be repeated for P09

$$P09_{\text{elevation}} := 126.82 \text{ in}$$

$$TRAC05_{\text{elevation}} := 3.5702 \text{ m}$$

$$DH5 := P09_{\text{elevation}} - TRAC05_{\text{elevation}}$$

$$DH5 = -0.349 \text{ m}$$

$$DH5 = -13.739 \text{ in}$$

Define gravity term multiplier for conversion into psi

$$P09_{\text{gravity}} := 1 \cdot \frac{\text{kg}}{\text{m}^3} \cdot \frac{\text{g}}{\text{g}_c} \cdot DH5$$

$$P09_{\text{gravity}} = 4.9635 \times 10^{-4} \frac{\text{lbf}}{\text{in}^2}$$

Define friction term multiplier for conversion into psi

$$P09_{\text{friction}} := \frac{f \cdot \frac{-DH5}{HD} \cdot 1 \cdot \frac{\text{kg}}{\text{m}^3} \cdot \left(1 \cdot \frac{\text{m}}{\text{sec}}\right)^2}{2}$$

$$P09_{\text{friction}} = 2.3953 \times 10^{-5} \frac{\text{lbf}}{\text{in}^2}$$

TRAC-M pressure at 126.82" (psi) =

$$\begin{aligned} & pn-210005 * 1.4504e-4 \\ & + \rho_v (\text{kg/m}^3) * 4.9635e-4 * \alpha_{210005} \\ & + \rho_l (\text{kg/m}^3) * 4.9635e-4 * (1-\alpha_{210005}) \\ & + \rho_v (\text{kg/m}^3) * V_v^2 (\text{m/s})^2 * 2.3953e-5 * \alpha_{210005} \\ & + \rho_l (\text{kg/m}^3) * V_l^2 (\text{m/s})^2 * 2.3953e-5 * (1-\alpha_{210005}) \end{aligned}$$

**ATTACHMENT B  
to ISL-NSAD-TR-03-09**

The above can be repeated for P04

$$P04_{\text{elevation}} := 194.19 \text{ in}$$

$$TRAC06_{\text{elevation}} := 4.5903 \text{ m}$$

$$DH6 := P04_{\text{elevation}} - TRAC06_{\text{elevation}}$$

$$DH6 = 0.3421 \text{ m}$$

$$DH6 = 13.4695 \text{ in}$$

Define gravity term multiplier for conversion into psi

$$P04_{\text{gravity}} := 1 \cdot \frac{\text{kg}}{\text{m}^3} \cdot \frac{\text{g}}{\text{g}_c} \cdot DH6$$

$$P04_{\text{gravity}} = -4.8662 \times 10^{-4} \frac{\text{lbf}}{\text{in}^2}$$

Define friction term multiplier for conversion into psi

$$P04_{\text{friction}} := \frac{f \cdot \frac{-DH6}{HD} \cdot 1 \cdot \frac{\text{kg}}{\text{m}^3} \cdot \left(1 \cdot \frac{\text{m}}{\text{sec}}\right)^2}{2}$$

$$P04_{\text{friction}} = -2.3483 \times 10^{-5} \frac{\text{lbf}}{\text{in}^2}$$

TRAC-M pressure at 194.19" (psi) =

$$pn-210006 * 1.4504e-4$$

$$- \rho_V (\text{kg/m}^3) * 4.8662e-4 * \alpha_{210006}$$

$$- \rho_l (\text{kg/m}^3) * 4.8662e-4 * (1 - \alpha_{210006})$$

$$- \rho_V (\text{kg/m}^3) * V_V^2 (\text{m/s})^2 * 2.3483e-5 * \alpha_{210006}$$

$$- \rho_l (\text{kg/m}^3) * V_l^2 (\text{m/s})^2 * 2.3483e-5 * (1 - \alpha_{210006})$$

**ATTACHMENT B  
to ISL-NSAD-TR-03-09**

The above can be repeated for P05

$$P05_{\text{elevation}} := 235.96 \text{ in}$$

$$TRAC07_{\text{elevation}} := 5.6101 \text{ m}$$

$$DH7 := P05_{\text{elevation}} - TRAC07_{\text{elevation}}$$

$$DH7 = 0.3833 \text{ m}$$

$$DH7 = 15.0899 \text{ in}$$

Define gravity term multiplier for conversion into psi

$$P05_{\text{gravity}} := 1 \cdot \frac{\text{kg}}{\text{m}^3} \cdot \frac{\text{g}}{\text{g}_c} \cdot DH7$$

$$P05_{\text{gravity}} = -5.4516 \times 10^{-4} \frac{\text{lbf}}{\text{in}^2}$$

Define friction term multiplier for conversion into psi

$$P05_{\text{friction}} := \frac{f \cdot \frac{-DH7}{HD} \cdot 1 \cdot \frac{\text{kg}}{\text{m}^3} \cdot \left(1 \cdot \frac{\text{m}}{\text{sec}}\right)^2}{2}$$

$$P05_{\text{friction}} = -2.6308 \times 10^{-5} \frac{\text{lbf}}{\text{in}^2}$$

TRAC-M pressure at 235.96" (psi) =

$$pn-210007 * 1.4504e-4$$

$$- \rho_v (\text{kg/m}^3) * 5.4516e-4 * \alpha_{210007}$$

$$- \rho_l (\text{kg/m}^3) * 5.4516e-4 * (1 - \alpha_{210007})$$

$$- \rho_v (\text{kg/m}^3) * V_v^2 (\text{m/s})^2 * 2.6308e-5 * \alpha_{210007}$$

$$- \rho_l (\text{kg/m}^3) * V_l^2 (\text{m/s})^2 * 2.6308e-5 * (1 - \alpha_{210007})$$

**ATTACHMENT B  
to ISL-NSAD-TR-03-09**

The above can be repeated for P06

$$P06_{\text{elevation}} := 250.96 \text{ in}$$

$$TRAC08_{\text{elevation}} := 6.5681 \text{ m}$$

$$DH8 := P06_{\text{elevation}} - TRAC08_{\text{elevation}}$$

$$DH8 = -0.1937 \text{ m}$$

$$DH8 = -7.6266 \text{ in}$$

Define gravity term multiplier for conversion into psi

$$P06_{\text{gravity}} := 1 \cdot \frac{\text{kg}}{\text{m}^3} \cdot \frac{\text{g}}{\text{g}_c} \cdot DH8$$

$$P06_{\text{gravity}} = 2.7553 \times 10^{-4} \frac{\text{lbf}}{\text{in}^2}$$

Define friction term multiplier for conversion into psi

$$P06_{\text{friction}} := \frac{f \cdot \frac{-DH8}{HD} \cdot 1 \cdot \frac{\text{kg}}{\text{m}^3} \cdot \left(1 \cdot \frac{\text{m}}{\text{sec}}\right)^2}{2}$$

$$P06_{\text{friction}} = 1.3296 \times 10^{-5} \frac{\text{lbf}}{\text{in}^2}$$

TRAC-M pressure at 250.96" (psi) =

$$\begin{aligned} & pn-210008 * 1.4504e-4 \\ & + \rho_v (\text{kg/m}^3) * 2.7553e-4 * \alpha_{210008} \\ & + \rho_l (\text{kg/m}^3) * 2.7553e-4 * (1-\alpha_{210008}) \\ & + \rho_v (\text{kg/m}^3) * V_v^2 (\text{m/s})^2 * 1.3296e-5 * \alpha_{210008} \\ & + \rho_l (\text{kg/m}^3) * V_l^2 (\text{m/s})^2 * 1.3296e-5 * (1-\alpha_{210008}) \end{aligned}$$

**ATTACHMENT B  
to ISL-NSAD-TR-03-09**

Pressure at tap P07 is above the tubes, therefore, the hydraulic diameter is different than at the other pressure tap locations

The hydraulic diameter of the boiler region is 2.3772e-2 m

$$HD := 1.7782 \times 10^{-1} \cdot m$$

Assuming the flow will be completely turbulent, from CRANE, page A-24, the friction factor (f) is 0.014

$$\frac{Rough}{HD} = 0.00026 \quad f := 0.014$$

$$P07_{elevation} := 286.59 \text{ in}$$

TRAC-M cell 9 is closer to pressure tap P07, however, cell 9 is the volume surrounding the tubes. Since the pressure tap is in the open area above the tubes, cell 10 was chosen as the starting point.

$$TRAC10_{elevation} := 8.534 \text{ m}$$

$$DH10 := P07_{elevation} - TRAC10_{elevation}$$

$$DH10 = -1.2546 \text{ m}$$

$$DH10 = -49.3943 \text{ in}$$

Define gravity term multiplier for conversion into psi

$$P07_{gravity} := 1 \cdot \frac{kg}{m^3} \cdot \frac{g}{g_c} \cdot DH10$$

$$P07_{gravity} = 1.7845 \times 10^{-3} \frac{lbf}{in^2}$$

Define friction term multiplier for conversion into psi

$$P10_{friction} := \frac{f \cdot \frac{-DH10}{HD} \cdot 1 \cdot \frac{kg}{m^3} \cdot \left(1 \cdot \frac{m}{sec}\right)^2}{2}$$

$$P10_{friction} = 7.1632 \times 10^{-6} \frac{lbf}{in^2}$$

**ATTACHMENT B**  
**to ISL-NSAD-TR-03-09**

TRAC-M pressure at 286.59" (psi) =

$$\begin{aligned} & \text{pn-210010} * 1.4504\text{e-}4 \\ & + \rho_V (\text{kg/m}^3) * 1.7845\text{e-}3 * \alpha_{210010} \\ & + \rho_I (\text{kg/m}^3) * 1.7845\text{e-}3 * (1-\alpha_{210010}) \\ & + \rho_V (\text{kg/m}^3) * V_V^2 (\text{m/s})^2 * 7.1632\text{e-}6 * \alpha_{210010} \\ & + \rho_I (\text{kg/m}^3) * V_I^2 (\text{m/s})^2 * 7.1632\text{e-}6 * (1-\alpha_{210010}) \end{aligned}$$

**ATTACHMENT B**  
**to ISL-NSAD-TR-03-09**

A Summary of TRAC-M control blocks for computing pressure at each pressure tap is shown below.

<b>Pressure Tap</b>	<b>TRAC-M Control Block</b>
P01	-0034
P02	-0054
P03	-0074
P08	-0094
P09	-0114
P04	-0134
P05	-0154
P06	-0174
P07	-0194

A summary of TRAC-M control block used for computing pressure differential is shown below.

<b>Data DPressure</b>	<b>TRAC-M Control Block</b>
DPT-0102	-1102
DPT-0203	-1203
DPT-0308	-1308
DPT-0809	-1809
DPT-0904	-1904
DPT-0405	-1405
DPT-0506	-1506
DPT-0607	-1607
DPT-0107	-1107

**ATTACHMENT B**  
**to ISL-NSAD-TR-03-09**

Computation of tube support plate pressure drops is accomplished in a manner similar to the above computations. The difference is that the elevation term has changed from "node center to pressure tap" to "node center to top/bottom of each tube support plate". These elevation changes will effect the multipliers used in the gravity and friction terms. The elevations and associated gravity and friction multipliers are summarized below.

		Elevation (in)	TRAC Cell	TRAC Elevation (m)	TRAC Elevation (in)	Elevation difference (in)	Gravity term multiplier	Friction term multiplier
FDB	Bottom	19.625	1	0.2540	10.000	9.625	-3.4772E-04	-1.6780E-05
	Top	20.375	2	0.7640	30.080	-9.705	3.5061E-04	1.6920E-05
TSP 1	Bottom	39.785	2	0.7640	30.080	9.705	-3.5062E-04	-1.6920E-05
	Top	40.535	3	1.2761	50.240	-9.705	3.5062E-04	1.6920E-05
TSP 2	Bottom	59.945	3	1.2761	50.240	9.705	-3.5061E-04	-1.6919E-05
	Top	60.695	4	2.2962	90.402	-29.707	1.0732E-03	5.1790E-05
TSP 3	Bottom	120.105	4	2.2962	90.402	29.703	-1.0731E-03	-5.1785E-05
	Top	120.855	5	3.5702	140.559	-19.704	7.1185E-04	3.4352E-05
TSP 4	Bottom	160.265	5	3.5702	140.559	19.706	-7.1192E-04	-3.4355E-05
	Top	161.015	6	4.5903	180.720	-19.705	7.1190E-04	3.4355E-05
TSP 5	Bottom	200.425	6	4.5903	180.720	19.705	-7.1187E-04	-3.4353E-05
	Top	201.175	7	5.6101	220.870	-19.695	7.1152E-04	3.4336E-05
TSP 6	Bottom	240.565	7	5.6101	220.870	19.695	-7.1152E-04	-3.4336E-05
	Top	241.315	8	6.5681	258.587	-17.272	6.2397E-04	3.0111E-05



**ATTACHMENT B**  
**to ISL-NSAD-TR-03-09**

A summary of TRAC-M control block used for computing pressure at top/bottom of the tube support plates is shown below.

<b>Pressure at</b>	<b>TRAC-M Control Block</b>
Bottom of Flow Distribution Baffle	-0214
Top of Flow Distribution Baffle	-0234
Bottom of TSP 1	-0254
Top of TSP 1	-0274
Bottom of TSP 2	-0294
Top of TSP 2	-0314
Bottom of TSP 3	-0334
Top of TSP 3	-0354
Bottom of TSP 4	-0374
Top of TSP 4	-0394
Bottom of TSP 5	-0414
Top of TSP 5	-0434
Bottom of TSP 6	-0454
Top of TSP 6	-0474

A summary of TRAC-M control blocks used for computing tube support plate pressure drops is shown below.

<b><math>\Delta P</math></b>	<b>TRAC-M Control Block</b>
Flow Distribution Baffle	-0500
Tube Support Plate 1	-0501
Tube Support Plate 2	-0502
Tube Support Plate 3	-0503
Tube Support Plate 4	-0504
Tube Support Plate 5	-0505
Tube Support Plate 6	-0506